SUOMEN GEODEETTISEN LAITOKSEN JULKAISUJA
VERÖFFENTLICHUNGEN DES FINNISCHEN GEODÄTISCHEN INSTITUTES
PUBLICATIONS OF THE FINNISH GEODETIC INSTITUTE

N:o 154

LENGTH IN GEODESY – ON METROLOGICAL TRACEABILITY OF A GEOSPATIAL MEASURAND

by

Jorma Jokela

GEODEETTINEN LAITOS · GEODETISKA INSTITUTET ·

SUOMEN GEODEETTISEN LAITOKSEN JULKAISUJA
VERÖFFENTLICHUNGEN DES FINNISCHEN GEODÄTISCHEN INSTITUTES
PUBLICATIONS OF THE FINNISH GEODETIC INSTITUTE
N:o 154

LENGTH IN GEODESY – ON METROLOGICAL TRACEABILITY OF A GEOSPATIAL MEASURAND

by

Jorma Jokela

Doctoral dissertation for the degree of Doctor of Science in Technology
to be presented with due permission of the School of Engineering
for public examination and debate in Auditorium H304 at the Aalto University
School of Science (Espoo, Finland) on the 27th of October 2014 at 12 noon.

KIRKKONUMMI 2014

Supervising professor

Prof. Martin Vermeer, Aalto University, School of Engineering, Espoo, Finland

Thesis advisor

Prof. Markku Poutanen, Finnish Geodetic Institute, Kirkkonummi, Finland

Preliminary examiners

Univ.-Prof. Dr.-Ing. Otto Heunecke, Universität der Bundeswehr München, Germany

Prof. Dr. (em.) Hilmar Ingensand, Eidgenössische Technische Hochschule Zürich, Switzerland

Opponents

Prof. Dr.-Ing. Jakob Flury, Leibniz Universität Hannover, Germany

Univ.-Prof. Dr.-Ing. Otto Heunecke, Universität der Bundeswehr München, Germany

ISBN (printed): 978-951-711-309-0
ISBN (pdf): 978-951-711-310-6
ISSN: 0085-6932

Aalto University
School of Engineering

Abstract

Author
Jorma Jokela

Name of the doctoral dissertation
Length in Geodesy – On Metrological Traceability of a Geospatial Measurand

Unit Department of Real Estate, Planning and Geoinformatics

Publisher Finnish Geodetic Institute

Series Publications of the Finnish Geodetic Institute

Field of research Geodesy

Manuscript submitted 3 September 2013 **Date of defense** 27 October 2014

Permission to publish granted 26 May 2014 **Language** English

Monograph

Abstract

The metre is one of the base units in the International System of Units (SI). The traceability chain connects length measurements to the definition of the metre. Metrological institutes implement this with sequential measurements ranging from the realization of the metre using internationally recommended procedures to practical length or distance measurements with high-precision electro-optical or mechanical instruments. Estimating the uncertainty of measurement at every stage in the traceability chain is an essential part of the measurement result and its usability. This publication examines the traceability of a geospatial measurand, a length used in geodesy, beginning with lengths of 1-m-long quartz gauge blocks and ending with terrestrial distance measurements of up to 1 km or more.

The Finnish Geodetic Institute (FGI) started measuring geodetic standard baselines with the Väisälä interference comparator in 1947. Based on the author's 25 years of experience, this publication includes the most detailed description of the interference measurement method to date. New results and inspiring experiences are presented from five Väisälä baseline measurements. Especially interesting is the FGI's 864-m Nummela Standard Baseline, recognized as a world-class measurement standard due to its extreme accuracy and stability. In addition, a few alternative standard baseline designs are presented.

From standard baselines, the FGI transfers the traceable scale to other geodetic baselines or test fields using calibrated, high-precision electro-optical distance measurement instruments as transfer standards. Using the calibrated objects, the traceable scale is then transferred forward for the calibration of surveyors' instruments or for scientific purposes. This publication shows the capability of the method, which is not utilized elsewhere, and discusses 11 scale transfer examples of it to seven baselines or test fields. The influence of atmospheric conditions is a major source of uncertainty of measurement, and it is discussed in detail in connection with a few cases. The traceable scale transfer service of the FGI has become internationally in demand, and it makes a remarkable contribution to the ongoing European research and development projects in length metrology. Most baselines that we have measured are alive and well, and interest in them is growing.

The latest measurements with the Väisälä interference comparator at standard baselines produced total expanded uncertainties ranging from 0.04 mm to 0.14 mm for baseline section lengths between 5 m and 864 m. After applying the scale transfer measurements to calibration baselines and test fields, the comparable uncertainty values were from 0.1 mm to 1.2 mm for baseline section lengths between 2 m and 1 488 m. A total expanded uncertainty of 0.5 mm/km is achievable under favourable conditions, and when the scale transfer is performed as a continuation of interference measurements at the same baseline, it is possible to reach 0.2 mm/km.

Keywords geodesy, metrology, geodetic baseline, Väisälä interference comparator, Nummela Standard Baseline, length measurement, scale transfer, calibration, EDM, traceability.

ISBN (printed) 978-951-711-309-0 **ISBN (pdf)** 978-951-711-310-6

ISSN 0085-6932

Location of publisher Kirkkonummi **Location of printing** Tampere **Year** 2014

Pages 240 **urn** http://urn.fi/URN:ISBN:978-951-711-310-6

Aalto-yliopisto
Insinööritieteiden korkeakoulu

Tiivistelmä

Tekijä
Jorma Jokela

Väitöskirjan nimi
Pituus geodesiassa – Geospatiaalisen mittaussuureen metrologisesta jäljitettävyydestä

Yksikkö Maankäyttötieteiden laitos

Julkaisija Geodeettinen laitos

Sarja Suomen Geodeettisen laitoksen julkaisuja

Tutkimusala Geodesia

Käsikirjoituksen päivämäärä 3. syyskuuta 2013 **Väitöspäivä** 27. lokakuuta 2014

Julkaisuluvan myöntämispäivä 26. toukokuuta 2014 **Kieli** Englanti

Monografia

Tiivistelmä

Metri on yksi kansainvälisen SI-yksikköjärjestelmän perusyksiköistä. Jäljitettävyysketju kytkee pituusmittaukset metrin määritelmään. Metrologia-alan laitokset toteuttavat tämän peräkkäisillä mittauksilla, alkaen metrin realisoinnista kansainvälisesti suositeltuja menetelmiä käyttäen ja päätyen käytännön pituus- tai etäisyysmittauksiin tarkoilla elektro-optisilla tai mekaanisilla mittauskojeilla. Mittausepävarmuuden arviointi jäljitettävyysketjun jokaisessa vaiheessa on olennainen osa mittaustulosta ja sen käyttökelpoisuutta. Tässä julkaisussa tutkitaan geospatiaalisen mittaussuureen, pituuden, jäljitettävyyttä erityisesti geodesiassa, alkaen metrin mittaisten kvartsimittapalojen pituuksista ja päätyen terrestrisiin etäisyydenmittauksiin kilometriin asti ja pitemmälle.

Geodeettinen laitos (GL) aloitti geodeettisten normaaliperusviivojen mittaamisen Väisälän interferenssikomparaattorilla vuonna 1947. Tämä julkaisu sisältää kirjoittajan 25 vuoden kokemukseen perustuen tähän asti yksityiskohtaisimman kuvauksen interferenssimittaus-menetelmästä. Uusia tuloksia ja innostavia kokemuksia esitetään viidestä Väisälä-perusviivan-mittauksesta. Erityisen kiinnostava on 864-metrinen Nummelan normaaliperusviiva, maailmanluokan mittanormaali äärimmäisen tarkkuutensa ja vakautensa ansiosta. Lisäksi esitellään vaihtoehtoisia perusviivamalleja.

Normaaliperusviivoilta GL siirtää jäljitettävän mittakaavan muille geodeettisille perusviivoille tai testikentille käyttämällä elektro-optisia tarkkuusetäisyysmittareita siirtonormaaleina. Kalibroituja kohteita käyttämällä jäljitettävä mittakaava siirretään edelleen mittaajien mittauskojeisiin tai tieteellisiin tarkoituksiin. Tämä julkaisu osoittaa menetelmän kyvykkyyden. Esimerkkeinä on 11 mittakaavan siirtomittausta seitsemälle perusviivalle tai testikentälle. Menetelmä ei ole käytössä muualla. Ilmakehän ominaisuuksien vaikutus on huomattava mittausepävarmuuden lähde, mitä tarkastellaan yksityiskohtaisesti muutaman esimerkkitapauksen yhteydessä. GL:n jäljitettävästä mittakaavan siirrosta on muodostunut kansainvälisesti kysytty palvelu, jolla on merkittävä asema meneillään olevissa eurooppalaisissa pituusmetrologian tutkimus- ja kehityshankkeissa. Useimmat mittaamamme kohteet voivat hyvin, ja kiinnostus perusviivoja kohtaan on kasvussa.

Viimeisimpien Väisälän interferenssikomparaattorilla tehtyjen normaaliperusviivojen mittausten laajennetut kokonaisepävarmuudet ovat 0.04 mm:stä 0.14 mm:iin perusviivajaksoille 5 m:stä 864 m:iin. Kalibrointiperusviivoille ja testikentille tehtyjen mittakaavan siirtojen vastaavat mittaus-epävarmuudet ovat 0.1 mm:stä 1.2 mm:iin perusviivajaksoille 2 m:stä 1 488 m:iin. Suotuisissa olosuhteissa on mahdollista päästä laajennettuun kokonaisepävarmuuteen 0.5 mm/km, ja jos mittakaavan siirto tehdään jatkona saman perusviivan interferenssimittauksille, voidaan saavuttaa 0.2 mm/km.

Avainsanat geodesia, metrologia, geodeettinen perusviiva, Väisälän interferenssikomparaattori, Nummelan normaaliperusviiva, pituusmittaus, mittakaavan siirto, kalibrointi, EDM, jäljitettävyys.

ISBN (painettu) 978-951-711-309-0 **ISBN (pdf)** 978-951-711-310-6

ISSN 0085-6932

Julkaisupaikka Kirkkonummi **Painopaikka** Tampere **Vuosi** 2014

Sivumäärä 240 **urn** http://urn.fi/URN:ISBN:978-951-711-310-6

Acknowledgements

The advances in geodetic metrology described in this thesis would not have been possible without a scientific base, which the Finnish Geodetic Institute created during the decades of triangulation for nationwide surveying and mapping. Also, our international connections in the sciences of both geodesy and metrology originated during that time. The Department of Geodesy and Geodynamics, along with its predecessors, has provided decent facilities at which to maintain and develop this fundamental research area, which is still proceeding in a vital manner. I acknowledge our former and present Directors General, Professors Juhani Kakkuri, Risto Kuittinen and Jarkko Koskinen, and my former and present Department Heads, Professors Teuvo Parm, Martin Vermeer and Markku Poutanen, for these efforts. My postgraduate studies with length metrology were originally Teuvo's proposal. I would also like to acknowledge Martin as the supervisor and Markku as the advisor for my thesis.

I acknowledge all personnel in the Department of Geodesy and Geodynamics for the cosy atmosphere that they provide. Over the years, people have always been willing to assist me in my metrological work when needed – and most people have indeed been needed every now and then. I especially thank Prof. Markku Poutanen, Mr Pasi Häkli, Mr Joel Ahola and Mr Timo Saari for performing interference observations at standard baselines with me. Smooth cooperation when making these challenging measurements has greatly contributed to our successful results. Pasi has also participated in several international scale transfer measurements with me.

Tuorla Observatory, now a division of the Department of Physics and Astronomy at the University of Turku, is maintaining premises for making quartz gauge comparisons for our interference measurements. I would like to thank Dr Aimo Niemi and Dr Kaj Wiik from the observatory for their priceless practical help in making these comparisons. At MIKES, I would like to thank Dr Antti Lassila for making arrangements for the absolute calibrations of the quartz gauges. The Department of Real Estate, Planning and Geoinformatics at the Aalto University School of Engineering, along with its predecessors, has advanced this research by allowing me to use their metrological instruments and facilities.

I wish to thank the foreign experts in our joint international endeavours, including the numerous but crucial assisting personnel in every project. This international cooperation has given me opportunities to work together with some of the world's best specialists in geodetic metrology: their names are listed in connection with the works included in this thesis.

Finally, I would like to thank the preliminary examiners of this thesis, Prof. Dr. (em.) Hilmar Ingensand and Univ.-Prof. Dr.-Ing. Otto Heunecke, for their constructive comments and recommendations, which I have tried to carefully consider in this final version.

Jorma Jokela

Author's contributions to the previously published material, which were made use of when preparing this thesis

Standard baselines

Jokela, J. and P. Häkli (2010). Interference measurements of the Nummela Standard Baseline in 2005 and 2007. Publ. of the FGI no. 144. 85 p. http://www.fgi.fi/fgi/sites/default/files/publications/fgipubl/FGI_Publ_144.pdf

Jokela wrote this publication, complemented with abundant clarifying details by Häkli, who also participated in the observation work. The publication was from the beginning designated as forming the backbone of this thesis, but in order to profit from the results, the FGI decided to publish them. The comprehensive publication of the measurement procedure includes both a description of comparisons of quartz gauges and of observations with the Väisälä interference comparator. The publication also lists the observation data and computation of the latest interference measurements and presents the resulting lengths together with the estimation of uncertainty of measurement.

Jokela, J., M. Poutanen, Zs. Németh and G. Virág (2001). Remeasurement of the Gödöllő Standard Baseline. Publ. of the FGI no. 131. 37 p.

Jokela wrote this publication, except for Chapter 8, which is based on information submitted by Németh and Virág. Jokela and Poutanen performed the interference observations, and Németh and Virág assisted. This work is a remeasurement of an existing stable Väisälä baseline that includes a simultaneous multiplication of it with high-precision EDM equipment. A Hungarian specialist, K. Szaládi, performed the EDM observations, while the other team assisted.

Jokela, J., M., Poutanen, J.Z. Zhao, W.L. Pei, Z.Y. Hu and S.S. Zhang (2000). The Chengdu Standard Baseline. Publ. of the FGI no. 130. 46 p.

Jokela wrote this publication, except Chapters 2 and 3, which are based on information submitted by Zhao, Pei, Hu and Zhang, and Section 4.2, where Poutanen and Jokela investigated the mirror surfaces. Jokela and Poutanen performed the interference and EDM observations, and the other authors assisted. Specialities of this work include a challenging baseline design and an immediate continuation of a Väisälä baseline with high-precision EDM equipment.

Jokela, J. and M. Poutanen (1998). The HUT Väisälä Baseline. In Jokela, J. and M. Poutanen (1998) The Väisälä Baselines in Finland. Publ. of the FGI no. 127, Part II, pp. 47–61.

Jokela wrote this publication. Jokela and Poutanen performed the interference observations. The publication presents examinations at a 75-m indoor baseline and introduces a developed transferring method in addition to traditional theodolite-based projections. Part I of the publication, "50 years of interference observations at the Nummela Standard Baseline", is also within the scope of this thesis, but much of the content is included in the previously listed publication by Jokela and Häkli (2010).

Scale transfer measurements

Jokela, J., P. Häkli, J. Ahola, A. Būga and R. Putrimas (2009). On traceability of long distances. Proceedings of the XIX IMEKO World Congress "Fundamental and Applied Metrology", September 6–11, 2009, Lisbon, Portugal, pp. 1882–1887, ISBN 978-963-88410-0-1.
http://www.imeko2009.it.pt/Papers/FP_100.pdf

Jokela wrote the article, and the other authors contributed to the successful performance of the reported measurement projects. Häkli presented the paper at the world congress. The paper is a summary of our recent works, written especially for an audience of specialists in metrology.

Būga, A., J. Jokela and R. Putrimas (2008). Traceability, stability and use of the Kyviškės Calibration Baseline – the first 10 years. In Cygas, D. and K.D. Froehner (Eds.) The 7th International Conference Environmental Engineering, Selected Papers, Vol. 3, p. 1274–1280. Vilnius, Lithuania, May 22–23, 2008. http://www.vgtu.lt/upload/leid_konf/buga_et_al_traceability.pdf

Jokela wrote the article, which was slightly modified after a few remarks by Būga and Putrimas. Būga presented the paper at the international congress. A repeated scale transfer measurement to a geodetic baseline and test field under varying environmental conditions is reported in the paper.

Jokela, J., P. Häkli, R. Kugler, H. Skorpil, M. Matus and M. Poutanen (2010). Calibration of the BEV Geodetic Baseline. FIG Congress 2010 "Facing the Challenges – Building the Capacity", Sydney, Australia, April 11–16, 2010. 15 p.
http://www.fig.net/pub/fig2010/papers/ts05c/ts05c_jokela_hakli_et_al_3873.pdf

Jokela wrote the article, except the Summary in German, which Kugler translated. All of the authors participated in the work as part of the European Metrology Research Programme (EMRP) Joint Research Project "Absolute Long-distance Measurement in Air". Jokela and Häkli performed the measurements upon which the paper is based. This recent scale transfer measurement establishes a new European geodetic baseline and includes an improved estimation of uncertainty of measurement. The work for this paper has received funding from the European Community's Seventh Framework Programme, ERA-NET Plus, under Grant Agreement No. 217257.

Jokela, J., F. Pollinger, N. R. Doloca and K. Meiners-Hagen (2012). A comparison of two weather data acquisition methods for the calibration of the PTB geodetic baseline. Proceedings of the XX IMEKO World Congress "Metrology for Green Growth" (paper no. TC14-O-18), September 9–14, 2012, Busan, Republic of Korea.
http://www.imeko.org/publications/wc-2012/IMEKO-WC-2012-TC14-O18.pdf

Jokela wrote the article and Pollinger added to it. All of the authors participated in the calibration measurements of the baseline. The paper treats the essential problem of obtaining weather data for the EDMs from a new point of view.

Jokela, J., P. Häkli, J. Uusitalo, J. Piironen and M. Poutanen (2009). Control Measurements between the Geodetic Observation Sites at Metsähovi. In Drewes, H. (Ed.) Geodetic Reference Frames. IAG Symposium, Munich, Germany, October 9–14, 2006. International Association of Geodesy Symposia, Vol. 134, p. 101–106. Springer, ISBN 978-3-642-00859-7.

Jokela wrote most of the article and Poutanen completed it. Häkli performed the computation for the GPS measurements. All of the authors participated in the measurements upon which the paper is based on. The paper is an example of applications of dimensional metrology in tie measurements between fundamental geodetic stations; it serves as a status report on an ongoing work.

Jokela, J., P. Häkli, M. Poutanen, U. Kallio and J. Ahola (2012). Improving length and scale traceability in local geodynamical measurements. In Kenyon, S., M. C. Pacino and U. Marti (Eds.) Proceedings of the 2009 IAG Symposium "Geodesy for Planet Earth", Buenos Aires, Argentina, August 31 – September 4, 2009. International Association of Geodesy Symposia, Vol. 136, p. 59–66. ISBN 978-3-642-20337-4.

Jokela wrote the article. Poutanen presented the paper at the symposium. Jokela, Häkli and Ahola have participated in several works utilizing geodetic length metrology and the paper is written especially for an audience of specialists in geodesy.

All scale transfer articles are peer-reviewed congress papers.

Contents

1 Introduction 1
1.1 Some definitions 1
1.1.1 Geodetic baseline 2
1.1.2 Calibrations in geodetic length metrology 3
1.2 Some history 5
1.2.1 Using the interference of white light when measuring long distances 5
1.2.2 Quartz gauges as measurement standards 6
1.2.3 Nummela and other standard baselines 8
1.2.4 Change from invar wires to EDM instruments as transfer standards 10
1.3 The present state and the scope of the thesis 12
1.3.1 Hypothesis 13
1.3.2 Väisälä baselines 13
1.3.3 Scale transfers 15
1.3.4 International and national comparisons 17
1.3.5 Length metrology for local geodynamical research 18
1.3.6 Remarks on the compilation of the thesis 19

2 Instruments, facilities and methods 21
2.1 Traceability chain of geodetic length measurements 22
2.2 Maintenance of the quartz gauge system 24
2.3 Geodetic baselines 25
2.4 Standard baselines 26
2.5 Calibrations at standard baselines 28
2.6 Calibration baselines and test fields 30
2.7 Piloting international comparisons 32
2.8 Control networks for local geodynamical research and their scale determination 34
2.9 Estimation of uncertainty of measurement 35

3 Quartz gauges as length standards 36
3.1 Review of quartz gauge systems at Tuorla Observatory 36
3.2 Comparisons at Tuorla Observatory 37
3.3 Determining the length of quartz gauge no. VIII in BTM00 41

4 Latest interference measurements at the Nummela Standard Baseline in 2005 and 2007 45
4.1 Preparing a standard baseline for interference measurements 46
4.1.1 Principle of the Väisälä interference comparator 47
4.1.2 Preparing the observation pillars for interference measurements 48
4.1.3 Precise levellings – start of the measurements 49
4.1.4 Aligning the mirrors 51
4.1.5 Setting the mirrors at correct positions in the baseline direction 53
4.1.6 Installing the transferring bars onto the observation pillars 55
4.1.7 Installations on the telescope pillar 56
4.1.8 Installations on pillars 0 and 1 59

4.2 Interference observations 59
4.2.1 Observation procedure 59
4.2.2 About the weather conditions 67
4.2.3 Personnel 68
4.3 Determination of corrections 69
4.3.1 Compensator corrections 69
4.3.2 Refraction correction 70
4.3.3 Corrections due to mirrors 75
4.3.4 Geometric corrections 75
4.3.5 Projection corrections 77
4.4 Computation of baseline lengths 84
4.4.1 Computation of the actual length of the quartz gauge 84
4.4.2 Results from interference observations done in 2005 87
4.4.3 Results from interference observations done in 2007 94
4.4.4 Final lengths 103
4.5 Estimation of uncertainty of measurement 104
4.5.1 Combined uncertainty of the lengths between the underground markers .. 104
4.5.2 Some supplementary analysis of uncertainty of measurement 107
4.6. Intermediate summary and conclusions 109

5 Chengdu Standard Baseline 112
5.1 History of the project 112
5.2 Location of the baseline 112
5.3 Baseline design 113
5.4 Interference measurements 117
5.4.1 Scale of the measurement 117
5.4.2 Mirrors and compensators 119
5.4.3 Geometrical corrections 120
5.4.4 Refraction 121
5.4.5 Interference observations 121
5.4.6 Distances between transferring bars 130
5.4.7 Distances between central benchmarks 130
5.4.8 Uncertainty of the measurement 134
5.4.9 Results from the interference measurements 136
5.5 Kern Mekometer ME5000 measurements 138
5.5.1 Measurement procedure 138
5.5.2 Calibration of the Mekometer 138
5.5.3 Refraction 138
5.5.4 Geometrical corrections 139
5.5.5 Computation 140
5.5.6 Results from the EDM 141
5.6 Comparison and combination of interference measurements and EDM 144

6 Gödöllő Standard Baseline 153
6.1 History of the baseline 153
6.2 Scale and traceability of interference measurements 153
6.2.1 Absolute calibrations of quartz gauges 153
6.2.2 Comparisons of quartz gauges 154
6.2.3 Lengths of quartz gauges at Gödöllő 155

6.3 Interference measurements 157
6.3.1 Mirrors and compensators 157
6.3.2 Geometrical corrections 158
6.3.3 Refraction 159
6.3.4 Interference observations 160
6.3.5 Projection measurements 167
6.4 Kern Mekometer ME5000 measurements 174
6.5 Results and conclusion 178

7 The HUT Väisälä Baseline 182
7.1 Baseline design 182
7.2 Measurement procedure 182
7.3 Quartz gauges 183
7.4 Light source, collimator, mirrors and compensators 184
7.5 Refraction 184
7.6 Heights 184
7.7 Interference observations 186
7.8 Replacing the traditional projection method by developing transferring methods 192
7.9 Length of the baseline 195
7.10 Uncertainty of the measurement 195
7.11 Final results 198
7.12 Conclusion regarding indoor measurements 198

8 Summary of experiences with Väisälä baseline measurements 199
8.1 Nummela Standard Baseline 199
8.1.1 True values for the scale transfer 201
8.1.2 Stability of the transfer standard 201
8.2 Experiences at the Chengdu Standard Baseline 203
8.3 Experiences at the Gödöllő Standard Baseline 204
8.4 Experiences at the HUT Väisälä Baseline 205
8.5 Traceability and uncertainty for incompatible measurement methods 206

9 Summary of scale transfer measurements 209
9.1 Kyviškės Calibration Baseline in Lithuania 211
9.2 Vääna Calibration Baseline in Estonia 213
9.3 BEV Geodetic Baseline in Innsbruck, Austria 216
9.4 PTB Geodetic Baseline in Braunschweig, Germany 217
9.5 UPV Geodetic Baseline and Test Field in Valencia, Spain 222
9.6 EDM comparisons at NMIJ and KRISS 222
9.7 Contribution of the European Metrology Research Programme 225
9.8 Some applications in local geodynamics 225

10 Concluding discussion 228

References 233

List of abbreviations

ADM	Absolute distance measurement
AIST	National Institute of Advanced Industrial Science and Technology (Japan)
APMP	Asia Pacific Metrology Programme
BEV	*Bundesamt für Eich- und Vermessungswesen* (NMI in Austria)
BIPM	*Le Bureau international des poids et mesures,* The International Bureau of Weights and Measures
BTM00	Braunschweig–Tuorla–MIKES 2000, the present quartz gauge system
CIPM	*Le Comité international des poids et mesures,* The International Committee for Weights and Measures
CMC	Calibration and Measurement Capabilities (BIPM database)
CMM	Coordinate measuring machine
CNAM	*Conservatoire national des arts et métiers* (NMI in France)
DI	Designated Institute (in metrology)
EDM	Electronic distance measurement
EMRP	European Metrology Research Programme
EURAMET e.V.	European Association of National Metrology Institutes *eintragener Verein*
FIG	*Fédération Internationale des Géomètres,* International Federation of Surveyors
FGI	Finnish Geodetic Institute
FGI-GG	Finnish Geodetic Institute, Department of Geodesy and Geodynamics
FÖMI	*Földmérési és Távérzékelési Intézet,* Institute of Geodesy, Cartography and Remote Sensing (Hungary)
GNSS	Global Navigation Satellite System
GPS	Global Positioning System
GUM	Guide to the Expression of Uncertainty in Measurement
HUT	Helsinki University of Technology (since 2010 absorbed in Aalto University)
IAG	International Association of Geodesy
IMEKO	International Measurement Confederation
ISO	International Organization for Standardization
ITRI	Industrial Technology Research Institute (Taiwan)
IUGG	International Union of Geodesy and Geodynamics
KRISS	Korea Research Institute of Standards and Science
MIKES	*Mittatekniikan keskus* (NMI in Finland)
MRA	CIPM Mutual Recognition Arrangement
NMI	National Metrology Institute
NMIJ	National Metrology Institute of Japan
NSL	National Standards Laboratory
PTB	*Physikalisch-Technische Bundesanstalt* (NMI in Germany)
SBSM	Sichuan Bureau of Surveying and Mapping
SI	*Le Système international d'unités,* The International System of Units
SLR	Satellite Laser Ranging
TC-Q	EURAMET Technical Committee for Quality
UniBW	*Universität der Bundeswehr München*
UPV	*Universidad Politécnica de Valencia*
VGTU	Vilnius Gediminas Technical University
VIM	International Vocabulary of Metrology
VLBI	Very Long Baseline Interferometry

Table of notations

a, b, c	Constants in computing temperature corrections for quartz gauges
α, β, c, d	Parameters when estimating corrections due to mirror surfaces
c_v	Coefficient in formula for temperature difference for refraction correction
B	Distance between transferring bars (in interference observations)
D	Mirror thickness
δ	Compensator glass plate thickness
e	Partial pressure of water vapour
ε	Fraction of half of wavelength in gap width determination
H, h	Height
I	"Interference observation", Distance between mirrors
k	Coverage factor, when expressing expanded uncertainty; usually $k = 2$
L	Transfer reading (in interference observations)
L_{29}	Nominal length of the principal normal, quartz gauge no. 29
L_{abs}	Measured length of a quartz gauge converted into BTM00 system
L_{calc}	Calculated length of a quartz gauge (using time series)
$L_{corr,\ 29}$	Corrected length of the principal normal, which takes into account lengthening after the reference epoch of the nominal length
L_{meas}	Measured length of a quartz gauge (using Sauna comparator)
λ	Wavelength
n	Number (of observations) or Refractive index
P	Projection, projection correction
p	Air pressure
p, q	Constants in the computation of corrected length of the principal normal
$\bar{q}$	Arithmetic mean
R	Radius of the Earth
r	Refraction correction
s	Distance or Length
$s(\bar{q})$	Experimental standard deviation of the mean
t	Temperature
$u;\ u_I, u_M, u_B$	Standard uncertainty components
u^{acc}	Accumulated uncertainty in baseline multiplication
u_c	Combined standard uncertainty
U	Expanded uncertainty
W	Weight coefficient
w	Gap width between the quartz gauge and mirror 1
X	Known distances from previous measurements
Ψ	Auxiliary term in compensator correction computation

1 Introduction

1.1 Some definitions

Metrological traceability is the *"property of a measurement result whereby the result can be related to a reference through a documented unbroken chain of calibrations, each contributing to the measurement uncertainty"* (BIPM 2008a, Section 2.41). A metrological traceability chain is a *"sequence of measurement standards and calibrations that is used to relate a measurement result to a reference"* (BIPM 2008a, Section 2.42). The measurement result can be traced to an international or national measurement standard and thereby to a measurement unit of the International System of Units (SI). For the length measurements used in geodesy, the traceability chain creates a connection from the definition of the metre to applications in surveying and mapping, with a reliable estimation of the uncertainty of measurement.

A measurand is a *"quantity intended to be measured"* (BIPM 2008a, Section 2.3). Many quantities being measured in length measurements in geodesy are not constant, but may differ from the nominal conditions of a measurand, or the ambient conditions may have an effect on the measurement event. For example, the length of a quartz gauge or the distance displayed in an electronic distance measurement (EDM) instrument are dependent on environmental conditions, and corrections are needed to determine the value of the measurand. The length between the underground benchmarks of a geodetic standard baseline is an example of a measurand, which is practically independent of environmental conditions, but the changes or deficiencies in the measurement system may still influence the measured quantity values.

A spatial measurand is a measured dimensional quantity used to produce information about location, and a geospatial measurand is related to the Earth-fixed presentation of location and the use of coordinate frames. Coordinates are not intrinsically measured, but are computed from the measured quantities. Typical measured quantities include the angle and length, the basis for all surveying. While geodetic satellite positioning is based on length measurements (accessed by the means of time difference measurements), the terrestrial methods usually also use angle measurements.

Length as a geospatial measurand is not restricted to horizontal or sloping lengths. Also, measurements of levelled height differences are basically length measurements, since they can be traced to the SI unit metre, even though the measurement system is completely different than the actual length measurements. The measurements of height differences also use angle information either indirectly by determining the direction of the local equipotential surface (in traditional and digital precise levelling) or directly by way of angle measurements (in trigonometric levelling). Length as a geospatial measurand is thereby independent of direction. It is also not restricted to artefacts, but also includes the distances between two points, if they can be

measured with an appropriate measurement system. Finally, a measurement procedure may also produce coordinates or coordinate differences, which are metrologically traceable and have estimated uncertainties and are computed from the values of measurands.

In this publication, the term “length” is often used for a measurand, though the term “distance” would also be justified. As a Finnish peculiarity, “length in geodesy” is sometimes referred to as “geodetic length”. The latter expression is unnecessary and without any metrological relevance; geodesy uses the same SI system as other length metrology. Furthermore, the term in Finnish, *geodeettinen pituus*, is identical with the translation “geodetic longitude” and thus misleading.

1.1.1 Geodetic baseline

The length of a geodetic baseline is a geospatial measurand of crucial importance. Geodesists have used geodetic baselines to determine the scale of surveying and mapping already for three centuries, since the beginning of triangulation. For measuring geodetic baselines for nationwide triangulations in the 20th century, the measurement institutes first used measurement wires and replaced them with EDM instruments in the last few decades. The regular calibrations and comparisons of these transfer standards and working standards brought metrological traceability into the measurements.

Typically, a geodetic baseline is a straight line between the end benchmarks (bolt or pillar structures), the length of which may range from several hundred metres to several kilometres. The calibrations done in indoor laboratories also utilize shorter baselines, whereas longer baselines of up to tens of kilometres were previously used for calibrating long-range EDM instruments. Absolute straightness is not always a strict requirement since the baseline in field conditions usually includes several intermediate points, which may slightly deviate from the line between the end benchmarks, and also height differences may exist along the baseline. The utilization of a baseline in a triangulation requires visual contact between the end points; the calibration measurements also require visibility between the intermediate points.

In the present applications of geodetic baselines, at the top end the calibration of high-precision EDM instruments for scale transfer is performed at a few standard baselines, and there are infrequent but continuous activities for testing and validating novel instruments. The traceability chain may also end – in addition to practical measurements with ordinary surveyors’ instruments – in local scientific applications, such as monitoring networks for local geodynamical phenomena and the stability control of large structures.

This publication deals with the traceability of terrestrial length measurements at geodetic baselines, where a special measurement procedure using the Väisälä interference comparator and quartz gauges (Väisälä 1923, 1930; Kukkamäki 1933) and a scale transfer with high-precision EDM instruments is followed. The measurements done with the Väisälä interference comparator require a special standard baseline design. The measurement

principle has already been used by the Finnish Geodetic Institute (FGI) for dozens of years, but the entire procedure involved in scale transfer and its present state have not been inclusively researched and documented in detail before. The method is rarely used in any other institute in the world, since experts in the Väisälä method nowadays are few in number. The old method has remained as a topical subject in length metrology, since more accurate terrestrial methods for taking measurements in field conditions have not been developed and the methods using satellite positioning are not capable in the metrologically interesting range of one metre to a few kilometres.

This publication is intended to enlighten the professional fields of geodesy, surveying and metrology about the interesting measurement procedure, which can be used to establish facilities for the calibration of surveying instruments and in scale transfer measurements in place of less accurate methods, which are not even metrologically traceable. Some actions have been necessary to adapt the prevailing practices to the improved guidance of estimation for the uncertainty of measurement. In general, GUM (BIPM 2008b), the guide to the expression of uncertainty in measurement, is followed in this study. The practices are now also covered by a quality management system, which is internationally approved (by the Technical Committee "Quality" of the European Association of National Metrology Institutes, EURAMET e.V. TC-Q) and continuously being improved.

1.1.2 Calibrations in geodetic length metrology

A calibration is an "*operation that, under specified conditions, in a first step, establishes a relation between the quantity values with measurement uncertainties provided by measurement standards and corresponding indications with associated measurement uncertainties and, in a second step, uses this information to establish a relation for obtaining a measurement result from an indication*" (BIPM 2008a, Section 2.39). A measurement standard is a "*realization of the definition of a given quantity, with stated quantity value and associated measurement uncertainty, used as a reference*" (BIPM 2008a, Section 5.1). The national measurement standards of the FGI in geodetic length metrology include quartz gauges, Väisälä interference comparators, standard baselines and rod comparators. The calibrations of quartz gauges, laser interferometers and auxiliary instruments establish a relationship between the measurement standards of the FGI and the primary national standards of other metrological institutes. The measurement standards of the FGI also include, in addition to the above-mentioned secondary measurement standards, reference standards, working standards and transfer standards, each of which transfers the metrological traceability of a measurement, as controlled by the calibration hierarchy. Finally, the calibrations of the final users' distance measurement instruments and levelling equipment complete the calibration and traceability chain and establish a relationship between the measurement standards and the end-product measurands to be measured.

The calibration of theodolites, geodetic angle measurement instruments, includes determining the instrument errors and accuracy of the instrument, which is essential for many industrial and engineering measurements. In practical surveying, the calibration of a theodolite may help when assessing the operating condition of the instrument, but it is of little importance from the point of view of traceability or even in the estimation of uncertainty. A proper surveying project containing angle measurements always consists of observations in a net or traverse of observation points, and single angle observations without any closure control are never used. The estimation of the uncertainty of measurement is based on the results of the adjustment computation of observations, in which the number of observations always exceeds the number of unknown parameters. The nature of the angle as a geospatial measurand is therefore completely different from the length, and omitted in this length-oriented publication.

The International Organization for Standardization (ISO) has published some international standards for the field procedures involved in testing theodolites and EDM instruments (ISO 2001, 2012a). The ISO presents both simplified and full-testing procedures together with guidance on observation arrangements, calculations and statistical analysis. By following these suggestions, the uncertainty of measurement can be estimated, mostly by analyzing the repeatability of measurements. This may be very useful for the regular quality control of operational surveying, but it does not bring traceability into the measurements. However, partly for its clarity and simplicity, the standardized method was also chosen as the basis of a pilot comparison of the calibration of EDM instruments, as presented in Sections 2.7 and 9.6.

The calibration of tacheometers, modern integrated angle and distance measurement instruments usually equipped with versatile observation processing software, is more difficult. Laboratories may calibrate the angle and distance measurement parts separately or use some combined procedures. Still, the inclusive estimation of the total uncertainty of measurement accumulating in the coordinates produced by a “total station” measurement system remains challenging. To guide this on the basic level, the ISO has also published an international standard for the calibration of tacheometers (ISO 2012b).

An adjustment computation of a geodetic network may consist of lengths only, as in trilateration networks, or of both angles and distances, as in proper triangulation networks. The computation usually is fitted with the existing coordinate frame by choosing a previously determined set of points as fixed. The computation may include geodetic baselines to bring the traceable scale into the network, as was the case in the nationwide triangulations. More often – in the lower order measurements – the metrological contribution is already hidden within the established coordinate frame; one just has to include points with known coordinates in the measurements and to take measurements using capable and calibrated instruments.

Recent activities in geodetic length metrology are focussed on what is traditionally called “short distances” in geodesy and surveying, distances from one metre to a few kilometres. They distinctly differ from other activities in length metrology, which are mostly focussed on lengths shorter than one metre and on various other dimensional quantities. The Calibration and Measurement Capabilities (CMC) database of the International Bureau of Weights and Measures (*Bureau International des Poids et Mesures,* BIPM) divides length metrology into two branches: dimensional metrology and laser frequencies. The five services of dimensional metrology are angle, complex geometry, form, linear dimensions and various dimensional. Each of them can be divided into several sub-services, just a few of which include geodesist and surveyor utensils. Official comparisons, which often are essential for showing metrological competence and entering into the CMC database, are few. The reason is that the geodetic measurements usually are outside the field of activity of the national metrology institutes. Recent international co-operation, both within the EURAMET and in some bilateral projects, is changing the situation. It is obvious that more institutes with services in geodetic metrology will be prepared to be listed in the CMC database in the future. One objective of this publication is to contribute to this work.

1.2 Some history

1.2.1 Using the interference of white light when measuring long distances

Yrjö Väisälä first introduced the principle of how to use white-light interferometry to measure distances in his doctoral thesis (Väisälä 1923). In the physical laboratory of the University of Helsinki, he scrutinized the propagation and reflections of two light beams, which travel along different paths between mirrors. Observing the interference fringes that the two light beams created, he tried to exactly determine the mutual positions of the mirrors, with the longer distance being an exact multiple of the shorter distance. Väisälä used different light sources, a collimator lens and a set of specially shaped mirrors to create and direct the light beams. He used an observation telescope to search for the interference fringes in the reflected light beams; an ocular spectroscope and glass plate compensators attached to the telescope helped in this search. The work was fundamental for the forthcoming applications in geodetic metrology.

Väisälä also wrote the first thorough description of how to use the white-light interference method for measuring geodetic baselines (Väisälä 1930); at that time, he was a professor at the University of Turku. Väisälä’s description presents the principle of the multiplication of a scale-determining distance in detail, as well as the theoretical base for the optics needed for arranging the observations. In his work, he presents the observation instruments and offers guidance on how to perform the observations and compute them. Väisälä also presents an example of a measurement up to 192 m, in which he obtained a relative uncertainty of 10^{-7}, as he had presumed. Compared with what had

previously been achieved with interferometry in laboratory conditions, the measured 192 m distance was quite long. The performance using the Väisälä interference comparator has been replicated and revised in numerous later publications.

1.2.2 Quartz gauges as measurement standards

Even with the geodetic length measurements, the length of the first traceable realized metric object is determined in an indoor laboratory, as few national metrology institutes have performed absolute calibrations of quartz gauges. Through these calibrations, the one-metre-long quartz gauges bring the traceable scale to the Väisälä interference comparator and the geodetic standard baselines. In addition to the absolute calibrations, the quartz gauge system is maintained with comparisons of quartz gauge lengths at the University of Turku. Quartz is a favourable material when measuring at the baselines in field conditions since the coefficient of thermal expansion for it is even smaller than for *invar*, the "invariant" iron-nickel alloy, which is widely used in length metrology.

T. J. Kukkamäki provided a thorough study of quartz gauges in his 1933 doctoral thesis, written under the guidance of Yrjö Väisälä. In it, Kukkamäki briefly described the production of quartz bars in Germany and the finishing of their ends in Turku, Finland, to generate quartz gauges as measurement standards. Kukkamäki explained the principle, structure and use of the special interference comparator used for the quartz gauge comparisons; also, he estimated the components of the uncertainty of measurement. With the comparator, Kukkamäki compared 18 different quartz gauges.

Based on Kukkamäki's work, three quartz gauges are placed in a horizontal position between the two vertical end planes in the comparator box. The two side gauges control the direction of the end planes, and the quartz gauge that is to be measured is placed in the middle. The scale-transferring principal normal (since 1952, quartz gauge no. 29) is usually measured first and last, while a few other quartz gauges are measured in between. The widths of the six air gaps between the quartz gauges and the end planes are the measurands. The widths can be computed by measuring the photographed interference fringes, which the light sources and the optics of the comparator create. Some corrections and adjustment calculations are needed to create a uniform quartz gauge system. The methods used to take the pictures and read the ambient temperatures have become more automatic in the last 80 years, but most of the measurement system has remained the same. Chapter 3 discusses how some of the latest measurements are processed in detail.

Kukkamäki's work includes a large study done to determine the thermal coefficients of the quartz gauges in order to model the thermal behaviour of the quartz gauges. He made the measurements in different temperatures with an interference dilatometer. He implemented other special arrangements to study the influence of varying air pressure on the quartz gauges and to determine the applicable air pressure coefficients.

Kukkamäki brought the traceability in the quartz gauge system first in comparisons between one quartz gauge, no. XV, and the Finnish metre prototype, no. V. He made this comparison using a microscope comparator. Although interference measurements were already used in metrology, the platinum-iridium standard metre prototype served as the basis for the definition of the metre until 1960, and the national prototypes helped support the definition. Instead of platinum-iridium alloy, many of the more practical works in length metrology could utilize the much cheaper invar alloy.

Absolute calibrations of the quartz gauges have been available since 1952, first at the BIPM in Sèvres, France, and since 1964 at the *Physikalisch-Technische Bundesanstalt* (PTB) in Braunschweig, Germany. Väisälä and Oterma (1967) investigated the 1 µm-level discrepancies between the French "T" (Terrien) and the German "E" (Engelhard) quartz metre systems. When applied in mapping, such a difference – and error – caused a 1 mm/km error in the scale of triangulation in Finland. Since 1967, the result provided by the PTB served as the basis for the absolute length and traceability of the quartz gauge system, now maintained at the University of Turku's Tuorla Observatory (Kukkamäki 1978). The Centre for Metrology and Accreditation (MIKES, *Mittatekniikan keskus* in Finnish) began doing absolute calibrations of quartz gauges in Finland in 2000 (Lassila et al. 2003).

The FGI has used just a few quartz gauges in its standard baseline measurements. In measurements done abroad, quartz gauges nos. VIII and XI were used in the years 1947–1969, whereas quartz gauges nos. 49 and 51 were used in the years 1964–1999. Only in Munich in the years 1958–1963 were quartz gauges nos. 31, 42 and 53 used in addition to quartz gauges nos. VIII and XI. At the Finnish standard baseline in Nummela, only quartz gauges nos. VIII and XI can be used because of the baseline design; these two quartz gauges are 0.1 mm longer than the previously mentioned quartz gauges and therefore suitable. Since 1983, only quartz gauge no. VIII has been used at the Nummela Standard Baseline because the shape of quartz gauge no. XI is slightly imperfect and inconvenient to use. The adjustment of the present quartz gauge system, BTM00, includes several absolute calibrations for less than ten quartz gauges, including all of the above-mentioned gauges except for gauge no. 31. The total number of quartz gauges in comparison with the principal normal, quartz gauge no. 29 is much larger.

The present quartz metre system, BTM00, is based on the latest absolute calibrations done at the PTB and MIKES and on the comparisons done at the Tuorla Observatory. The absolute calibrations are performed with interferometers for long gauge blocks, after making some necessary modifications due to the convex ends of the quartz gauges. The premises of MIKES were moved from Helsinki to Otaniemi, Espoo, in 2005. MIKES is performing the next absolute calibrations of quartz gauges in 2014. The purpose-built comparator intended for comparing the quartz gauges is still in use at the University of Turku's Tuorla Observatory.

1.2.3 Nummela and other standard baselines

Still 50 years ago, field baselines measured with invar wires determined the scale of the first-order horizontal geodetic network in which the baselines were placed. The invar wires were calibrated either in laboratory conditions or in more field-like conditions. The latter conditions prevailed at the Nummela Standard Baseline, where the FGI had been calibrating the 24-m invar wires using the Väisälä interference comparator since the establishment of the baseline in 1933. Work on the Finnish first-order triangulation began already in 1919, and before 1933 a baseline in Santahamina, Helsinki, was being used to determine the scale of the triangulation network. The international compatibility of the fundamental measurements was ensured through comparisons with the invar wires used in other countries. In 1947, the FGI measured the entire 864-m Nummela Standard Baseline with the Väisälä interference comparator, in addition to conducting the invar wire measurements, and the history of the Nummela Standard Baseline began. Since then, the baseline has served in the calibrations of invar wires and high-precision EDM instruments and transferred the traceable scale further in national and international applications.

Honkasalo (1950) documented the first interference measurements done at the Nummela Standard Baseline in autumn 1947. The preceding measurements in 1941 and 1946 consisted of invar wire measurements, in which the invar wires were concurrently standardized with the Väisälä interference comparator; the wire comparisons with a quartz gauge and the baseline measurements with the wires were made in turns. The comparator was installed in a special unheated building next to the baseline. Honkasalo's work also includes the determination of the temperature coefficients of invar wires; in April and June 1946, and in June 1949, the lengths of the invar wires were compared with the 24-m length of the interference comparator in different temperatures. The determination of the entire baseline length using invar wires was continued in 1947, 1951 and 1952, each time with concurrent calibrations of the invar wires, as documented in detail by Honkasalo. Also, the determination of the length of the entire baseline with interference measurements was documented in 1947 – preparations, performance and computations; it was quite detailed and was mainly followed in later measurements.

Kukkamäki (1978) listed the results of the next interference measurements of the entire baseline performed in 1952, 1955, 1958, 1961, 1968 and 1975. The measurements performed in 1952 were connected with the international measurements of several invar wires, organized by the BIPM. The next measurements were performed mostly for national purposes: to maintain the national measurement standard and to transfer the scale with invar wires to other calibration baselines (Santahamina, Niinisalo) and to the 16 field baselines of the Finnish first-order triangulation.

Kääriäinen et al. (1992) presented the interference measurements for the Nummela Standard Baseline performed in 1977, 1983, 1984 and 1991, and Jokela and Poutanen (1998, 5–43) presented the measurements performed in

1996. The latest measurements, performed in 2005 and 2007, have been documented by Jokela and Häkli (2010) and they are also included in Chapter 4 of this thesis. The four latest measurements (done in 1996, 2005, 2007, and, to be computed when the new quartz gauge lengths are available, in 2013) provide a firm backbone for the contemporary scale transfer measurements. The principle and performance of the measurements have now remained about the same for nearly a century, and most of the original observation instruments are still in use at the FGI.

Since the 1960s, geodesists and surveyors also calibrated EDM instruments at special calibration baselines, which were traceably measured using invar wires. The calibrated EDM instruments transferred the scale further to lower-order triangulation networks and local measurements. Since the 1970s, geodesists have used high-precision EDM instruments to establish calibration baselines for lower-order EDM instruments. The correctness of the scale is usually ensured by calibrating the modulation frequency of the high-precision EDM instrument. In this way, the traceability chain is not as clear as in a proper scale transfer from a standard baseline, which the FGI started in the 1980s.

In another study, Kukkamäki (1978) briefly discusses several interference measurements that the FGI performed at standard baselines abroad in the years 1953–1976, and he gives a list of references to essential publications about them. The lengths of these baselines range from 432 m to 576 m, except in Munich, where the metres are equal to those at Nummela: 864 m. Using the improved quartz gauge system, after making a new adjustment, Kukkamäki also presents slightly corrected lengths for all of the baselines.

Kukkamäki (1969) wrote another detailed description of interference observations at a geodetic standard baseline. The Ohio State University had purchased a Väisälä interference comparator to measure the 500-m-long Ohio Standard Baseline; Kukkamäki presents a 20-step observation procedure and a 22-step computation procedure on this baseline measurement. This clear documentation has served as a useful guide for later measurements, though the measurement done in Ohio was far from trouble-free. Kukkamäki also presents the formula for the refraction correction because of temperature differences, and the method for projection measurements and making necessary corrections to convert the distances between transferring bars to the distances between underground markers. At the Ohio Standard Baseline, the underground markers are placed in an open space under the observation pillars, which is different from the structure of the pillars at the Nummela Standard Baseline. The estimation of uncertainty completes the report on the measurement results.

The global interest in the standard baseline measurements done with the Väisälä interference comparator is a consequence of the official recommendations, which the General Assembly of the International Association of Geodesy (IAG) gave in a motion in 1951 (IAG 1951) and the General Assembly of the International Union of Geodesy and Geodynamics (IUGG) in a resolution in 1954 (IAG 1955). Activities for national and continental

triangulations for surveying and mapping were the most extensive at that time. By measuring Väisälä-type standard baselines in different countries, the purpose was to obtain a uniform and traceable scale for all of these activities.

The International Association of Geodesy (IAG) adopted a motion in the General Assembly in Brussels in 1951: it stated that, "*considering the high accuracy obtained in the measurement of a standard base-line in Finland with a light-interference apparatus, recommends that such bases be measured by a similar method in different countries by the interested organizations and asks the Bureau of the Association to facilitate necessary arrangements so that such bases could be used, if desired, by neighbouring countries, to compare the results obtained by this process, with those obtained by wires or tapes compared to the standards of the International Bureau of Weights and Measures*".

The International Union of Geodesy and Geophysics (IUGG) resolved in the General Assembly in Rome in 1955 that member countries should "*establish a standard base-line in each country using the Väisälä method (or similar apparatus) for assuring a uniform scale in all [triangulation] networks and for calibrating invar tapes and geodimeters*". Since then, the Väisälä interference comparators have been delivered to more than ten countries; no statistics are available about how they have been used. With its comparators, the Finnish Geodetic Institute performed nearly 40 measurements at 14 baselines in more than ten countries: in Finland (two baselines, 17 measurements, 1947–2013), in Argentina (1953), in the Netherlands (1957, 1969), in Germany (West; four measurements in 1958–1963), in Portugal (1962, 1978), in the DDR (1964), in the USA (1966), in South Africa (1976), in Spain (1978), in Hungary (1987, 1999), in China (two baselines, four measurements, 1985–1998) and in Taiwan (1993).

Some 30 years later, the importance of traditional terrestrial measurements in nationwide surveying and mapping started to fade, but since more accurate traceable methods for short distances have not been developed, the significance of the recommendations has remained in place. The significance of the Nummela Standard Baseline is warranted due to its long history, continuous maintenance, favourable measurement conditions (surroundings, ground and climate), unique measurement results, small degree of uncertainty in the measurements and extreme stability. The FGI has also succeeded in appointing skilful and responsible personnel to take care of the baseline and the projects and relations concerning it during decades.

1.2.4 Change from invar wires to EDM instruments as transfer standards

The importance of the Nummela Standard Baseline and its predecessors (comparison baselines in Santahamina until 1932 and in Nummela until 1947) was essential for determining the scale of the Finnish first-order triangulation. The invar wires, which have been used since 1923 to measure the 16 field baselines for triangulation, were calibrated at those baselines. The lengths of the

field baselines ranged from 2.6 km to 6.2 km. The last one, the Finström baseline in Åland, was measured in 1966 (Kääriäinen 1984).

The 6.0-km-long Vihti field baseline, established in 1961, was used for the calibration of tellurometers as well; these were some of the first EDM instruments. The 22.2-km-long Niinisalo calibration baseline, measured with a large set of invar wires in 1968, was built especially to calibrate long-range EDM instruments (Kiviniemi 1970). The scale of these baselines was determined using measurements with invar wires calibrated at the Nummela Standard Baseline, but the use of both the Vihti and Niinisalo baselines in calibrations for the Finnish first-order triangulation was eventually of minor importance. The numerous baselines established all over the country for the calibration of EDM instruments used in lower-order triangulations are not discussed here.

During the last years of triangulation, in addition to angle measurements, the FGI extensively performed trilateration. Distances were measured with a laser geodimeter (AGA Model 8) in northern Finland between 1971 and 1985 (Konttinen 1994). The modulation frequency of the instrument was measured twice a day, and the counter for that was compared with a quartz clock twice a year. Trilateration measurements, including geodimeter observations made at the Niinisalo calibration baseline with an extension net, and of a 913-km-long traverse (Parm 1976), were included in the final adjustment of the Finnish first-order triangulation (Jokela 1994). In general, the scale of the geodimeter observations was not traceable to the Nummela Standard Baseline. This was reasonable, since the distances measured with the geodimeter (up to 70 km) were considerably longer than what was available for calibration at Nummela or Niinisalo, and the daily frequency control was an easy method for checking the instrument.

In practice, the scale of new nationwide distance measurements, performed especially in northern Finland, has not been derived from the Nummela Standard Baseline since the 1970s. For other parts of the country, the importance of the invar wire measurements, performed during the previous 50 years at the 16 field baselines throughout the country, remained in the adjustments, which determined the scale of surveying and mapping in Finland. Only since the 1990s have new reference frames, based on completely different techniques, been introduced (yet with imperfect traceability).

Since the 1980s, national and international scale transfer measurements from the Nummela Standard Baseline have become common again, along with new high-precision, medium-range EDM instruments, such as the Kern Mekometer ME3000 and ME5000. Now the scale transfer measurements mostly serve other geodetic baselines and test fields, for which a traceable scale is desired, as well as other scientific applications.

1.3 The present state and the scope of the thesis

Since the change from terrestrial methods to satellite positioning in national and continental surveying and mapping works, concern about the metrological traceability of the measurements has not been prominent. The needs for accurate geospatial measurements have been met by the realization of global geodetic reference systems and by fitting the new measurements, performed with satellite positioning, into the new reference frames. The metrology of satellite positioning has so far been largely disregarded, and the accuracy of the reference frames and the measurements related to them has been estimated using non-standardized methods.

In local measurements, more interest in quality control has remained, though obligatory requirements to regularly calibrate instruments exist only in a few countries. This has meant that those who bother to have their EDM instruments calibrated often choose an easy and cheap frequency calibration instead of the proper calibration at a geodetic baseline. At present, requirements for quality work are increasingly being emphasized, and both public authorities and private companies in various fields of surveying and mapping have implemented quality management systems according to the international standards. These standards include a general quality management standard, ISO 9001 (ISO 2008), and a special standard, ISO/IEC 17025, for the competence of calibration laboratories (ISO 2005). The need to comply with quality policies is becoming increasingly important and growing interest is being shown in metrological skills and competence. In practice, more interest is also being shown in geodetic baselines and properly documented traceability.

The official status of the FGI in the scientific field as an institute that combines geodesy and metrology is exceptional. In many countries, the “long” (in metrology, or “short” in geodesy) distances are more or less beyond the control of metrology, and only surveying and mapping institutes are responsible for the correctness of the scale. In Finland, the existing legislation confirms the FGI is a National Standards Laboratory (NSL) of length. In the Rules of Procedures of the FGI, its activities as an NSL are appointed to the Department of Geodesy and Geodynamics (FGI-GG). Its status as a Designated Institute (DI) requires the FGI-GG to take care of the metrology of lengths in geodesy. In addition, MIKES or other National Metrology Institutes (NMI) take care of the first links in the traceability chain in terms of realizing the measurement unit, the metre. One major difference between geodetic metrology and “ordinary” metrology is that most actions of geodetic metrology are performed in authentic field conditions instead of indoor laboratories. Instead of calibrating an instrument, often it is possible to calibrate an entire measurement procedure.

Since both geodesy and metrology are global sciences in which international collaboration is essential, the special knowledge and official status of the FGI have created an extensive network of contacts. This collaboration continuously brings forth new international measurement projects. A few standard baselines have recently been re-measured using the Väisälä interference

comparator. However, it is more common, and more economical, to perform a scale transfer measurement from the Nummela Standard Baseline to an existing calibration baseline or test field using a high-precision EDM instrument as a transfer standard. The collaboration has also enabled some of the first comparisons of geodetic calibration services and tests of the capabilities of the new instruments. This thesis briefly introduces some recent research and development projects for geodetic baselines and the traceable scale transfer measurements related to them.

1.3.1 Hypothesis

The main hypothesis of this work is that by using a quartz gauge system, geodetic baselines measured using the Väisälä interference comparator and scale transfer using high-precision EDM instruments, the metrologically traceable scale can be transferred from the SI unit metre to the geodetic and surveying applications with only minor uncertainty.

1.3.2 Väisälä baselines

Any inclusive report on the present state of the Väisälä-type baselines does not exist on a global level. Some of the baselines have been reported as unusable, mostly because of expanded built-up areas or because of natural catastrophes. Many of the rest have been abandoned due to a lack of resources and use. In addition to the fundamental Nummela Standard Baseline, measurements at two other standard baselines in Hungary and China and one short, Väisälä-type indoor baseline are discussed in this thesis. The author of the thesis has made important contributions to the measurements at all of these baselines. All four represent quite different baseline designs, which require different measurement solutions.

The Nummela Standard Baseline has maintained its status as a world-class measurement standard regardless of the great change in measurement methods and instruments during the last half century. The obvious reason is that length is still a fundamental geospatial measurand, though at the moment the applications of geodetic metrology emphasize local, high-precision geodesy instead of nationwide mapping. There is also global interest in extending the traceability chain again to include longer distances, but the methods for doing this are still insufficient. In efforts to improve the present situation, recent tests in autumn 2010 using new absolute distance measurement (ADM) instruments at the Nummela Standard Baseline were promising. In this thesis, the latest measurements performed using the Väisälä interference comparator (Jokela and Häkli 2010) are included in detail in the more comprehensive Chapter 4, since such a laborious project always – even for the 15th time – causes some new problems and begs for solutions to those problems, making the new detailed descriptions of the work interesting. Also, the “world’s best” results are again worthy of documentation.

The results for the re-measured standard baselines are not always satisfying, as long-term changes in the lengths of the baseline sections may be many times larger than the uncertainty of the measurement. Knowledge about the possible instability of a baseline is not available beforehand, and the possible changes are still too small to detect with any other measurement instrument than laborious interference measurements. In addition to the Nummela Standard Baseline, the repeated measurements at the Gödöllő Standard Baseline in Hungary have yielded quite similar results that show good stability. Kääriäinen et al. (1988) reported the first measurements in Hungary in 1987. The remeasurements performed in 1999 are presented in detail in Jokela et al. (2001) and summarized in Chapter 6 of this thesis. They are included not only for showing the excellent capability of interference measurements under favourable conditions, but also for showing a successful concurrent extension to double length using high-precision EDM instruments.

Konttinen (1988) reported on an earlier experiment that is comparable to the one done at the Gödöllő Standard Baseline, which the FGI did in 1984 at the Nummela Standard Baseline in connection with the interference measurements. As an essential technical solution, the forced-centring plates of the EDM equipment were installed on special mountings so that they could be adjusted on the same rails as the mirrors of the Väisälä interference comparator on the observation pillars. Using the same transferring and projection measurement methods for both, the relative positions of the mirrors and the EDM equipment could be determined with an extremely small degree of uncertainty, making the comparison reliable. A Kern ME3000 EDM instrument was used to multiply the distances, 2 x 216 m and 2 x 432 m, and a standard uncertainty of 0.1 mm/km was obtained after the projection measurements. The differences between the two multiplication methods – Väisälä and EDM – were insignificant. Konttinen (1988) recommended the baseline multiplication using a high-precision EDM instrument, as the use of the Väisälä method seldom produces lengths longer than 0.5 km without major difficulties.

In the years 1985–1998, the FGI made five interference measurements at three standard baselines in China, all of which were unfortunately only used for a short period of time. The Chang Yang Standard Baseline, which had been successfully measured three times, had to give way to the expanding Chinese capital of Beijing; Kääriäinen et al. (1986), Konttinen et al. (1991) and Jokela (1996) reported the measurements. Earthquakes have caused damages to the Taoyuan Standard Baseline in Taiwan; Poutanen (1995) reported the interference measurements. Some scale transfer measurements from the Nummela Standard Baseline to Taiwan using high-precision EDM instruments were performed in 1997. The fate was also bad for the Chengdu Standard Baseline in Sichuan, which was destroyed in the great Sichuan earthquake in May 2008. Nevertheless, the Chengdu Standard Baseline is discussed in Chapter 5 of this thesis because of its special design and the noteworthy

experiences with the measurements. The project has been discussed in detail by Jokela et al. (2000).

The HUT Väisälä Baseline was established in the 1960s in the basement of the main building of the Helsinki University of Technology (HUT). Since 2011, the site has been a part of Aalto University. This baseline was already originally specially equipped for the measurements done with the Väisälä interference comparator, and the 11-pillar baseline design allowed for different multiplications of up to 72 m or 75 m. Before the latest measurements in 1998, it had been measured only once with the Väisälä interference comparator. Unfortunately, the documentation on how the measurement was done is inadequate, thus making it impossible to properly compare the earlier measurement with the newer measurements. Instead, to maintain its short-range calibration facilities, HUT performed measurements with a laser interferometer. The Department of Surveying actively used the baseline in calibrations for tens of years until 2011, when the new School of Engineering at Aalto University had to abandon it for operational reasons without giving any weight to scientific considerations. The baseline was an excellent place for indoor examinations of various surveying instruments, including the tests done with the Väisälä interference comparator. The author's experiences at the HUT Väisälä Baseline are presented in detail in a study by Jokela and Poutanen (1998, 47–61) and summarized in Chapter 7 of this thesis.

1.3.3 Scale transfers

An inclusive review of the activities related to geodetic length measurements in the bustling age of trilateration was presented in an IAG Symposium in Helsinki in 1978; Parm (1980) compiled the proceedings. The Väisälä interference comparator, invar wires and developing EDM instruments were widely used to determine the scale for triangulation. Also, several other conferences on EDM instruments were arranged in the 1960s and 1970s; Whitten and Schmidt (1960) documented one of the first such conferences. – Later, Rüeger (1996) wrote a renowned textbook about EDM instruments.

Though internationally recommended, measurements of new geodetic baselines with the Väisälä interference comparator gradually came to be regarded as arduous. Together with the retreat of invar wire measurements and the progress made with EDM instruments, alternative methods for traceable lengths in field conditions came under consideration in the 1980s. At the FGI, Konttinen's (1988) works were some of the first realizations of this change.

At the turn of the decade from the late 1980s to the early 1990s, it became necessary for both the FGI and the Department of Surveying at HUT to purchase new high-precision EDM instruments. The FGI decided to fix the old Kern Mekometer ME3000 and to purchase Wild T2000 + DI2000 tacheometer equipment, whereas HUT decided to purchase a new Kern Mekometer model ME5000. The use of the instruments at the FGI focused primarily on miniature triangulation networks. HUT kindly made their new equipment available also to

postgraduate students for scientific work. Actually, the author of this thesis and some colleagues at the FGI have been the most frequent users of the Mekometer equipment. Likewise, some of the FGI's quality instruments have been made mutually available in good cooperation with HUT (or present-day Aalto University). Using an existing standard baseline and high-precision EDM instruments, the author began measuring traceable scale transfers from the Nummela Standard Baseline to other geodetic baselines and test fields in 1997. An introduction of the method and a brief summary of the results during the first 12 years are presented in a study by Jokela et al. (2009 a). The work has successfully continued until present. At HUT and Aalto University, Professor Teuvo Parm first, and Professor Martin Vermeer later, have greatly advanced the work.

The Institute of Geodesy at Vilnius Gediminas Technical University (VGTU) established a 6-pillar, 1 320-m calibration baseline in Kyviškės, Lithuania, in 1996. In 2000, the baseline was expanded to a 7-pillar triangle-shaped test field. Since 1997, the FGI and the VGTU have repeatedly measured the baseline with high-precision EDM instruments using scale transfer from the Nummela Standard Baseline. The purpose has been to establish and maintain the calibration facilities for surveying instruments in Lithuania so that they meet the national and international requirements. The repeated measurements have proved that the baseline and test field are stable. The measurements and results from 1997–2007 are scrutinized in this thesis; summaries are also presented in studies by Būga et al. (2008, 2014).

Since the location is also nearly optimal for geodetic satellite positioning, the FGI used the Kyviškės Calibration Baseline as a test field to compare the scale of GPS (Global Positioning System) measurements with the scale of the EDM instruments in 2008 (Koivula et al. 2012a). Again, a scale transfer with high-precision EDM instruments was part of the measurement. This comparison is a complementary part of the studies on local geodynamical phenomena in the monitoring network around the Finnish Olkiluoto nuclear power plants and a disposal site of spent nuclear fuel.

The Vääna Calibration Baseline of *Maa-amet*, the Estonian Land Board, is another example of a recent scale transfer from Nummela to another favourable measurement site. The FGI first measured the reconditioned 1 728-m baseline in 2000. For the remeasurement done in 2008, the baseline was shortened to its flattest part, but then it was also equipped with several new observation pillars, enabling more comprehensive instrument analyses. Now, the distances between the 13 observation pillars range from 5 m to 1 344 m. The location of the baseline is much like that in Nummela, probably with even fewer disturbances. Some results of the measurements at this new and very promising measurement site, briefly introduced in a study by Jokela et al. (2009a), are included in this thesis.

In 2008–2011, the FGI participated in the joint research project "Absolute Long-distance Measurement in Air" within the European Metrology Research

Programme (EMRP 2014). This project, which included nine European metrology institutes, sought to develop and validate new techniques for long-distance measurements in air, beyond the current state-of-the-art techniques being used. As an essential part of the project, the Nummela Standard Baseline was utilized as a reference and test site, and the results of the interference measurements from 2007 were used as true distance values in the comparisons. Experts from four metrology institutes worked at the baseline in autumn 2010 with new prototypes of ADM instruments (based on laser interferometry using synthetic wavelengths) and weather data acquisition systems (spectroscopy). In addition, to improve another European site for the testing and validation, a scale transfer measurement from Nummela to the geodetic baseline of the *Bundesamt für Eich- und Vermessungswesen* (BEV) in Innsbruck, Austria, was performed in autumn 2008. A documentation of this measurement is presented in the study by Jokela et al. (2010). A new EMRP joint research project "Metrology for long distance surveying" is continuing the work in 2013–2016.

The latest international scale transfer measurements include calibrations of geodetic baselines for the PTB in Braunschweig, Germany, in 2011 and for *Universidad Politécnica de Valencia* (UPV) in Valencia, Spain, in 2012.

1.3.4 International and national comparisons

After the early comparisons of invar wires and quartz gauges, international comparisons for length in geodesy have been few. Recently, the increased interest in quality management and growing awareness of the benefits offered by metrological co-operation have generated some activity in this area. The international comparisons also provide an advantage for testing of the new ADM instruments. In recent years, the FGI has participated in two international comparisons of EDM instruments: in Japan in 2003 and in the Republic of Korea in 2006. Some results of the unpublished comparisons are included in this thesis.

An interesting comparison was recently organized at the new geodetic baseline of the University of the Federal Armed Forces Munich (UniBW) in Germany (Heunecke 2012, Neumann 2012). To determine the nominal distances optimally, seven German, Swiss and Austrian institutes measured the 8-pillar 1 100-m baseline with different instruments and procedures. In addition to four Kern ME5000 instruments and several Leica total stations, the instruments included – as a novelty – three Leica laser trackers (models AT901 and AT401) and even GNSS equipment. Use of reflectors built in precise spherical frames improved accuracy of centrings. The "absolute trackers" – not to be confused with the abovesaid long distance ADM instrument prototypes – are actually coordinate measuring machines (CMM) for industrial applications. Their operational range is up to 80 m or 160 m only, but accuracy of measured distances is one order of magnitude better than with classical EDM instruments. An expanded relative measurement uncertainty of 2×10^{-7} was obtained in the comparison. Expanded uncertainties for baseline section lengths from 19 m to

1 100 m were from 0.04 mm to 0.22 mm. The UniBW baseline is one venue of an international comparison within the EMRP in 2014.

1.3.5 Length metrology for local geodynamical research

Geodynamics is a science that examines the motions of the Earth, both in a global and a local scope. The idea of using high-precision EDM to monitor networks for local geodynamical phenomena – or man-made structures – is not new, and analyses based on repeated trilateration have been performed for as long as suitable EDM instruments have been available. Konttinen (1981, 1985) has reported on continental plate motion studies that the FGI conducted in the Gissar fault deformation zone between the Alai (Eurasian plate) and Pamir (Indian plate) mountains in Tajikistan. The studies were a cooperative effort between the FGI and the Academy of Sciences of the Soviet Union. A Kern ME3000 EDM instrument was one of the instruments that was used. In addition to the calibrations done at the Nummela Standard Baseline, frequency calibration had to be used to determine the largely temperature-dependent scale correction of the EDM instrument. After making repeated measurements, the indications of plate movements, congruent with geological interpretations, were soon clear.

Compared with the aged Kern ME3000, several high-precision tacheometer models were just as accurate and their ease of operation was superior already in the late 1980s. Takalo et al. (2004) present an example of how the FGI used angle and length measurements with tacheometers – along with several other geodetic techniques – to research postglacial fault lines in the crust of the Earth in north-western Finland. The length measurements are traceable to the Nummela Standard Baseline. The time span, from 1987 to 2002, is too short to reveal the suspected deformations, but the monitoring networks created a reliable basis for further studies in the geodynamically interesting test area. The FGI has also used tacheometer measurements in a miniature network to complement the precise levelling analysis of seasonal changes in bedrock elevations at the Metsähovi levelling test field (Lehmuskoski et al. 2006).

Very Long Baseline Interferometry (VLBI), Satellite Laser Ranging (SLR) and Global Navigation Satellite System (GNSS) measurements are methods used for space geodesy and satellite geodesy as well as in global geodetic observation networks. To combine the measurements with different methods at the same locations, tie measurements between the reference points of different instruments and systems are essential. The FGI determines the ties – coordinate differences – at its fundamental station, Metsähovi, using GPS, tacheometry and precise levelling. Jokela et al. (2009b) gave an intermediate report of the ongoing measurements, which serve as a present-day application of dimensional metrology for large structures. Lately, the FGI has largely expanded this work, especially in terms of centring the VLBI telescope (Kallio and Poutanen 2012, 2013).

At the monitoring network around the Olkiluoto nuclear power plants and the disposal site for spent nuclear fuel, the FGI repeatedly used both GPS measurements and high-precision EDM measurements in the years 2002–2012. An upgrade (in 2013) of the monitoring network consists of a set of permanent GPS stations. In addition, the FGI has initiated a programme for repeated precise levellings (Saaranen et al. 2014) and gravity measurements. The purpose is to determine possible deformations of the Earth's crust. As a part of this research project, the GPS-based scale of the local network can be compared with the traceable length of a geodetic baseline. In this thesis, the Olkiluoto network is referred to as a recent example of how to use the scale transfer from the Nummela Standard Baseline to improve the traceability of lengths and scale in local geodynamical measurements (Jokela et al. 2012a). Posiva Oy, an expert organization responsible for the safe final disposal of spent nuclear fuel, is funding this ongoing work.

1.3.6 Remarks on the compilation of the thesis

The author of this thesis has worked with geodetic baseline measurements for more than twenty years, both with the Väisälä interference comparator and with high-precision EDM instruments. Scientific material has been gathered deliberately, since the possibilities to establish a Väisälä baseline and perform measurements at it are few. Additionally, metrology is not always rewarding: one measurement may go on for a couple of months and then it produces only one quantity as a result. If the result is about the same as before, you have succeeded; if not, you have something to explain. Neither case helps a researcher obtain further funding. The Nummela Standard Baseline has been in our service for a long time, and also there the resources are limited and environmental conditions are often challenging. Fortunately, adequate resources could be allocated for the latest measurements, resulting again in remarkable results.

The three other Väisälä baselines included in this thesis represent the available capabilities when using different baseline designs or measurement procedures. The scale transfer measurements and other high-precision EDM experiments included in this thesis represent state-of-the-art techniques for establishing and maintaining geodetic baselines. In addition to meeting the current needs for calibration services, some of the present operational geodetic baselines act as testing sites for new measurement methods and instruments. The examples of applications in geodynamics presented in this thesis are limited to a few cases, which the FGI is advancing.

The numerous scale transfer measurements are shortly introduced in Section 9, which is an essential part of this thesis. Unfortunately the more comprehensive articles could not be published here, due to the unexpected change in formal requirements for theses in Aalto University in 2013; the prepared article dissertation had to be changed to a monograph.

All of the measurement projects reported on here resulted from fruitful co-operation between the FGI and other institutes around the world, working with

metrology, geodesy, surveying or geospatial education. The author has conducted or participated in all of the standard baseline or scale transfer projects reported on here since 1996. This has created a large network of international contacts. Continuing the work of the late great geodesists, Väisälä, Kukkamäki and Honkasalo, and working with some of the best present-day experts in length measurements and metrology, has been encouraging and rewarding when preparing this thesis.

2 Instruments, facilities and methods

This chapter briefly lists the instruments, facilities and methods used for a traceable transfer of the scale from the measurement unit to the applications of geodetic metrology (Fig. 2.1). The specifics of select cases are included to highlight some of the challenges and insights encountered while working on the measurement projects.

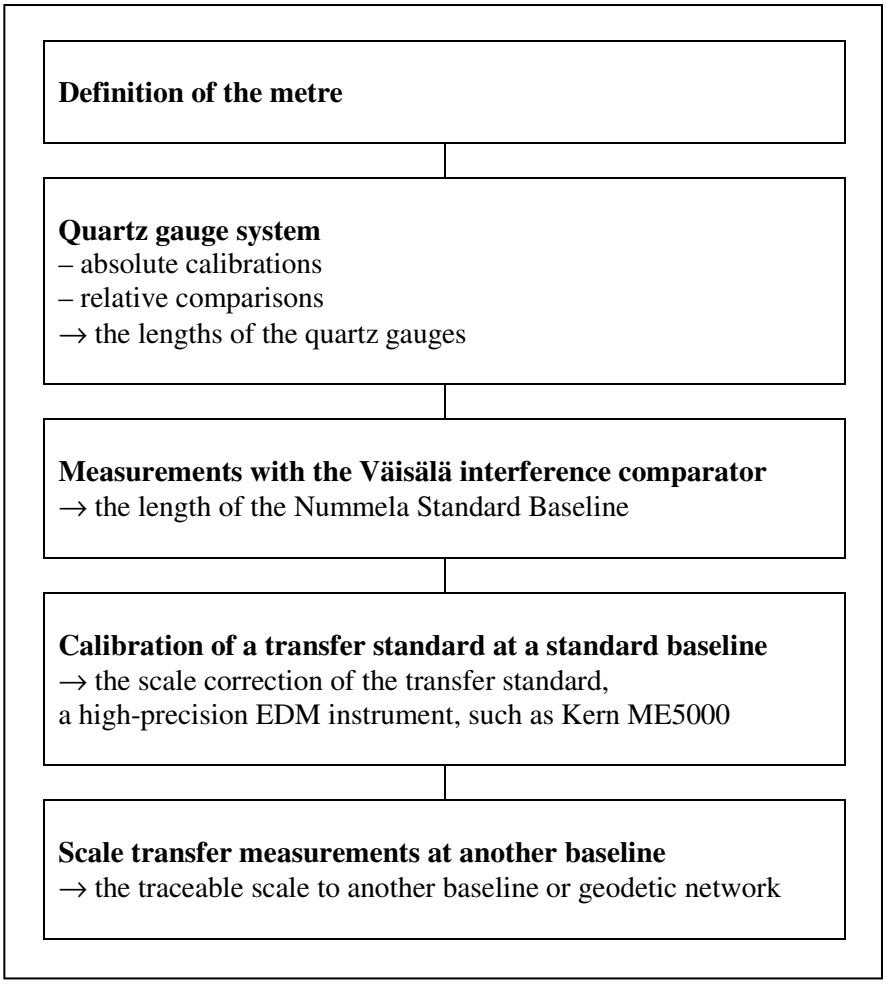

Figure 2.1 *Overview of traceability chain of geodetic length measurements.*

The procedure for traceability in geodetic length measurements presented in this work is based on the well-known, but nowadays seldom used, method of making interference measurements with a Väisälä comparator, in which a quartz gauge determines the scale of the measurement and transmits the traceability chain. The scale is traceably transferred further using the best available EDM equipment. For decades, the FGI has been the only institute in the world maintaining and developing this method. In addition to the technical competence needed for the measurements, careful selection of the transfer site – a baseline or a test field – reasonable planning of its geometric design and durable permanent structures are essential for obtaining a successful result. All stages of the scale transfer include a detailed calculation of uncertainty of measurement, and the combined estimation of uncertainty in the traceability chain is presented as part of the final result; the result is determined using internationally recommended methods. Thus, the scale transfer method of the FGI both utilizes the best geodetic measurement skills and meets the metrological requirements set for calibration laboratories.

2.1 Traceability chain of geodetic length measurements

According to the current definition of the metre, one agreed upon in the 17th General Conference on Weights and Measures (CGPM) in 1983, "*the metre is the length of the path travelled by light in vacuum during a time interval of 1/299 792 458 of a second*". Iodine-stabilized lasers are used as primary wavelength standards in the realization of this definition and in fundamental length measurements with laser interferometers. In the near future, new frequency comb techniques may be used as well in the realization of this definition.

Absolute calibrations with gauge-block interferometers for quartz gauges introduce an absolute and traceable scale to the quartz gauge system, in which the resulting lengths of the quartz gauges are stated. Lassila et al. (2003) documented the latest absolute calibrations using a combined white-light and laser gauge block interferometer. The main principle for operation is the same as that described by Engelhard (1959), and the gauge block interferometer is described in more detail by Ikonen and Riski (1993). Fig. 2.2 shows the presently used configuration of the setup for quartz gauges at MIKES.

In the latest absolute calibrations the experimental standard deviation of the mean from repeated observations was 12 nm. Some sources of uncertainty were length dependent (25 nm in all) and mostly related to uncertainty of pressure and temperature measurements. Together with some sources of uncertainty which were independent of length (19 nm in all), a total standard uncertainty of 35 nm (or expanded uncertainty of 71 nm) was obtained. In the uncertainty computations for this thesis this value (and an equal previous value determined at the PTB) are used as, according to GUM, "data provided in calibration certificates".

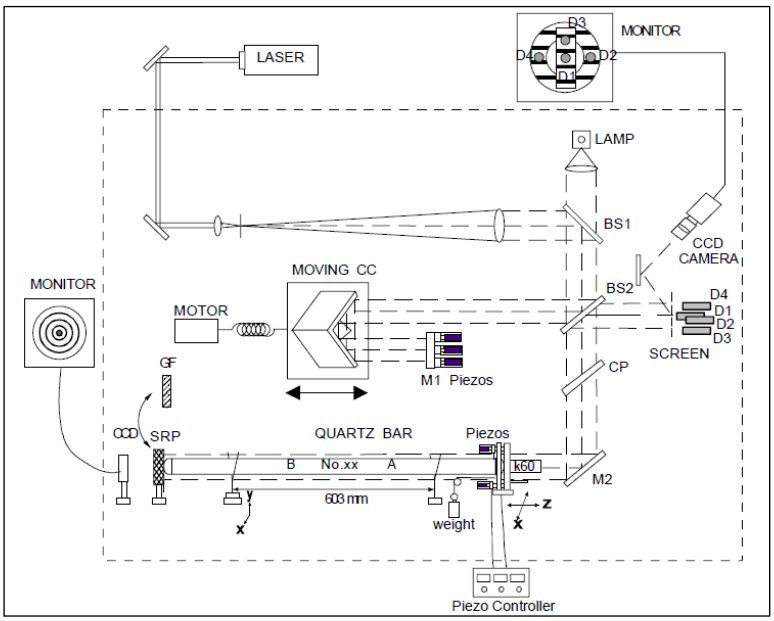

Figure 2.2 *Setup for calibration of quartz gauges at MIKES, according to Lassila et al. (2003). In the gauge block interferometer, a quartz gauge (quartz bar) is placed between a normal steel reference platen (SRP) and a good quality steel gauge block (k60). BS are beam splitters, CC is corner cube retroreflector, CP is compensation plate, M are mirrors and D are photo detectors.*

Rather laborious absolute calibrations are supplemented with more frequent comparison measurements in the maintenance of the quartz gauge system. Repeated measurements are necessary since the lengths of quartz gauges change slightly over time.

In comparison measurements at the Tuorla Observatory (Chapter 3, Fig. 3.2), adjustments of the comparator equipment are not a significant source of uncertainty of measurement. The observers can monitor their adjustments in two computer displays, and correct positions for end planes or quartz gauges are easy to find precisely enough when observing the changing interference fringes during adjustments. Light sources, optics, photographing system, image processing software and computation methods seldom need adjustments and due to the relative nature of the comparing measurement method used there are no significant sources of uncertainty. A major concern that remains is to monitor the thermometers in the comparator room and let the temperature become stable before every image recording. Smaller than 10 nm standard uncertainties in quartz gauge lengths are obtained.

The Nummela Standard Baseline is one of the few geodetic baselines in the world maintained with regular measurements using the Väisälä interference

comparator. These measurements transfer the traceable scale from the length of the quartz gauge to the baseline sections, which range from 24 m to 864 m, with the latter number obviously being close to the maximum range of operation of the comparator under field conditions. The actual length of the quartz gauge during the measurements is determined using the auxiliary temperature and air pressure observations and multiplied using the comparator. The temporary locations of the mirrors in the comparator are recorded relative to the transferring bars on the observation pillars; the distances between them can then be obtained. The lengths between the transferring bars are projected onto the lengths between more stable underground benchmarks. The equipment installed on the observation pillars is different for interference measurements and for the calibration of EDM instruments, and reverse projection measurements from underground benchmarks to the observation pillars are needed later for calibrations.

According to metrological terminology (BIPM 2008a), the quartz gauge system and the Nummela Standard Baseline can be regarded as secondary measurement standards. High-precision EDM instruments are used as transfer standards or working standards when transferring the traceable scale further to other geodetic baselines or applications. These instruments are calibrated at the standard baseline, where the scale correction and the additive constant of the instrument are determined by comparing the observed values with the "true" values from the interference measurements. (It is more common to calibrate the modulation frequency for an EDM instrument, but the method discussed in this publication provides a completely different and independent traceability chain.) Calibrations are usually performed both before and after the measurements at the baseline or geodetic network; the scale is then transferred to this baseline or network. The observed values always need velocity corrections due to weather conditions and often also geometric corrections due to height differences or horizontal non-parallelism. Most of the recent scale transfers have been made using Kern Mekometer ME5000 EDM instruments. There is a problem, however, in that these instruments are ageing, manufacturer support no longer exists and few other suitable instruments are available.

Jokela et al. (2009a, 2010) document some recent scale transfer measurements that utilize the new results from the latest interference measurements. Typical achievable combined standard uncertainties are 4×10^{-8} for the lengths of the quartz gauges, 1×10^{-7} for the standard baselines and from 2×10^{-7} to 5×10^{-7} for the lengths after scale transfer with an EDM instrument. These values are valid for an adequate number of observations and proper processing.

2.2 Maintenance of the quartz gauge system

The standard baseline measurements done with the Väisälä interference comparator are connected to the SI system and the definition of the metre using the quartz gauges, which are compared with the principal normal of the quartz

gauge system at the Tuorla Observatory. Comparisons are performed – at minimum – before and after the standard baseline measurements. The author and Mr Pasi Häkli became acquainted with the quartz gauge system and performed most of the comparisons during four comparison periods between 2005 and 2007, and again in 2013–2014. The expert in the system and in the comparisons, Dr Aimo Niemi, then retiring, guided the team at the beginning in 2005. He also did the comparisons, the results of which the author used for the standard baseline measurements until 1999. Based on the experience, Mr Häkli and the author prepared a large illustrated manual on how to perform a comparison. At present (in 2014), Dr Kaj Wiik of the Tuorla Observatory is also participating in the development work.

The results of the new comparisons of the quartz gauges are inserted into the long time series, which includes abundant data from previous comparisons during the last tens of years, and the fix points, which are derived based on the results for several absolute calibrations of a few quartz gauges. Both an interpolation using the time series and the single results from the latest comparisons (before and after) are considered when calculating the final length of the quartz gauge. The difference between these two results should not be significant, and they usually can be equally weighted, thus paying attention both to those from the past and those from the present. A detailed description of how the scale was determined for the standard baseline measurements in 2005 and 2007 is presented in Chapter 3.

2.3 Geodetic baselines

Geodetic baselines are used for calibration of geodetic length measurement instruments, most typically EDM instruments. The purpose of calibration is quality control, a regular check that the instrument meets its accuracy specifications. Determined instrument errors and corrections for them improve measurement results. Most calibration results presented in this thesis are related to calibrations of transfer standards at standard baselines and used for scale transfer measurements to other geodetic baselines and test fields.

The optimal length of a baseline to be established matches with the operating range of a typical EDM instrument to be calibrated. The baseline should consist of observation pillars in line at such locations that it is possible to measure a set of evenly spread distances along the entire baseline length. A typical number of observation pillars is from five to eight, but also larger numbers are common. Another requirement for the design is to take into account the typical unit length of the instruments to be calibrated. Then a favourable design may permit the detection of short-periodic errors – when present – in addition to additive constant and scale error.

Rüeger (1996) presents some geometric baseline designs. Equations for Heerbrugg-and Aarau-type designs include four parameters as input: unit length, shortest distance, total length and number of baseline stations. The first design includes fractions of the unit length, whereas the second one only includes exact

multiples of the unit length and calibrations using it require use of a separate cyclic error test line. The output of the baseline design procedure includes coefficients of optimal section lengths for baselines consisting of five to eight stations. Calibration measurements are performed in all combinations of distances (10 to 28 distances for five to eight stations). Hobart-type design only uses one end point and at least one auxiliary point a fraction of a unit length apart as observation stations, and the other (five to eleven) stations are spaced at equal intervals over the total baseline range. Rüeger (1996) also lists properties of a baseline with ideal physical design.

Because of the multiplications needed for interference measurements using the Väisälä interference comparator, Nummela and other standard baselines do not have optimal features of calibration baseline design. The situation can be improved with additional observation pillars, as at the Chengdu and HUT baselines (Chapters 5 and 7). The Nummela Standard Baseline is equipped with facilities for determining short-periodic errors, too, but this service is seldom used, since in the high-precision instruments used for scale transfer these errors do not exist (as in Kern Mekometer ME5000) or they are insignificant.

Foundations of all baselines, at which the FGI has measured with the Väisälä interference comparator, consist of a line of concrete observation pillars, with or without a line of underground markers alongside. Most of the baselines have been proved stable by repeated measurements, but some places have not been stable. Obvious reasons for problems are unstable ground, thermal behaviour of the structures, and low-quality constructions. Unfortunately the problems often are difficult to foresee and discernible only during the interference observations. Layered tubular pillar structures are common and recommended at modern calibration baselines; the outer layer creates an insulating shaft around the pillar block. This structure would be workable also at Väisälä baselines. The centring equipment and other precision mechanics on observation pillars could utilize some modern implementations of industrial metrology, instead of or in addition to traditional surveying applications.

2.4 Standard baselines

This thesis includes four different measurement projects performed using the Väisälä interference comparator. Two of the baselines have recently been destroyed, but the experiences are still worth reporting.

The FGI's Nummela Standard Baseline is a national measurement standard for length measurements in geodesy and the basis for many national and international scale transfer measurements. This baseline is special due to its 80-year history, sub-millimetre stability and less than 10^{-7} relative uncertainty. With a length of 864 123 mm, it is the longest Väisälä baseline in the world. The design of the baseline is a multiplication of 24 metres, originating from the era when measurements were done with 24-m invar wires. Starting from the quartz metre length of 1 m, a complete measurement to 864 m includes the multipliers $2 \times 2 \times 3 \times 3 \times 4 \times 6 \times 1$ m. Jokela and Häkli (2010, 10–13) report on the large

construction and refurbishing works done on the baseline buildings, pillars and other structures in 2004–2007.

The time series of measurements done with the Väisälä interference comparator includes 15 measurements during a 60-year period, from 1947 to 2007. The FGI carefully maintains the baseline and has active international co-operation with surveying and metrology expert organizations that want to use the baseline. This has resulted in the fact that the Nummela Standard Baseline is continuously acknowledged as a world-class measurement standard and the FGI as a top-level laboratory for length standards in geodesy. The latest remeasurement of the Nummela Standard Baseline was performed in autumn 2013; completing the computations waits for the results of new absolute calibrations and comparisons of quartz gauges.

The Gödöllő Standard Baseline of the Institute of Geodesy, Cartography and Remote Sensing (*Földmérési és Távérzékelési Intézet*, FÖMI) in Hungary has a similar design as the Nummela Standard Baseline: $2 \times 3 \times 3 \times 4 \times 6 \times 1$ m = 432 m. However, the structure of the pillars is different, since the underground markers are placed under the observation pillars. Experts from the FGI measured the baseline with the Väisälä interference comparator up to 432 metres twice, in 1987 and in 1999. During both measurement periods, the Hungarian experts simultaneously multiplied the length up to 864 metres using high-precision EDM. A time series of annually repeated, high-precision EDMs exists, too. A remeasurement with the Väisälä interference comparator will also be possible in the future.

The Chengdu Standard Baseline (1990–2008) of the Sichuan Bureau of Surveying and Mapping (SBSM) in China was special due to its ingenious design and massive structures. The measurements done at Chengdu included a Väisälä baseline in the middle and integrated extensions in two directions using high-precision EDM. In 1998, experts from the FGI performed a baseline extension with high-precision EDM up to 1 488 metres; they started from 378 metres, which they measured with the Väisälä interference comparator placed in between the two distances. The central part includes the calculation $2 \times 2 \times 4 \times 4 \times 6 \times 1$ m = 384 m, subtracted by the first 6 m, which was omitted in the final results. Due to the high observation pillars, the observers could set the measurement beam travelling a couple of metres above the ground level. In more favourable conditions, interference measurements up to 768 m would have been possible. The pillar structure even allowed for simultaneous GPS observations, but this was not done during the project. The forced-centring method for the EDM equipment was distinctive but serviceable. An adverse factor was the thermal behaviour of the baseline structures. This caused serious instability among the pillars, which, unfortunately, only the interference measurements revealed. Being located just several dozen kilometres from the epicentre, the baseline was reportedly destroyed in the great Sichuan earthquake on 12 May 2008.

The HUT Väisälä Baseline (1964–2011), which was in the basement of the main building of the Helsinki University of Technology in Otaniemi, Espoo, Finland, was a measurement standard for length measurements indoors. Together with other measurement facilities there, it was an excellent site for many kinds of geodetic and photogrammetric instrument research and calibrations. In February 1998, the FGI calibrated the 75-m geodetic baseline with the Väisälä interference comparator, using the observation pillars at 5 m and 25 m as intermediate points. During this measurement, it was interesting to research the metrological capability of the instrument indoors and to develop a user interface for the scale transfer between different instruments on an observation pillar. Unfortunately, the requirements for cost-effectiveness faced by the reorganized Aalto University recently forced it to abandon the internationally remarkable measurement standard.

Auxiliary measurements are an essential part of standard baseline measurements. Projection corrections and transfer readings are needed to determine the mutual positions of the reference points of the baseline and of the measurement equipment. The projection measurements are based on optical measurements with precise theodolites. A few distances consisting of a few metres are measured with sub-millimetre uncertainty using precise tapes. The transfer measurements include mechanical distance measurements of a few centimetres with a few micrometres of uncertainty using specially designed equipment. The methods used in these auxiliary measurements are very different in the four presented cases.

Measurements for air temperature, pressure and humidity are other essential measurements, which the observers have to perform simultaneously with the distance measurements. For example, for an 864-m standard baseline this includes an observation scheme using 31 thermometers. The temperature observations produce the data for the difference of temperatures and, thus, difference in refractive index between the two parts of the baseline; no absolute values are needed. Kukkamäki's computation formulas have always been used for computation of relative refraction correction. Processing of weather data for EDM is different, since absolute values are needed.

2.5 Calibrations at standard baselines

Since working at the Nummela Standard Baseline, the author has performed most of the scale transfer measurements during the years 1997–2014 using a single EDM instrument, the Kern Mekometer ME5000 no. 357094 (with prism reflector no. 374414). This instrument is the property of what is currently (in 2014) the Department of Real Estate, Planning and Geoinformatics at the Aalto University School of Engineering. A few other identical instruments, as well as a few precise Wild distance meters and Leica tacheometers, have been used in some projects included in this thesis. The Kern Mekometer ME5000 has been the only EDM instrument that is capable of making observations with a less than

10^{-6} relative uncertainty. Meier and Loser (1986) presented this instrument when it was new.

The Kern Mekometer ME5000 follows the basic principle of EDM: The measurement beam, which an EDM instrument sends, travels to a reflecting prism at the other end of the distance and back. Since the characteristics of the beam (frequency and wavelength) are known, the distance can be computed. The travel time depends upon the refractive index of the air. Along the path of the measurement beam, an integral number of wavelengths plus a fractional part of a wavelength need to be determined.

The integral number is found by measuring using several predefined frequencies. The fractional part can be eliminated in the instrument, as in Kern Mekometer ME3000, by changing the path until a zero phase difference is obtained, or, as in Kern Mekometer ME5000, by changing the frequency until the phase difference is zero. These methods do not generate cyclic errors, contrary to a common phase resolution method, which determines the fractional part by measuring the phase angle between the sent and received beams (Bell 1992).

The carrier beam of Kern Mekometer ME5000 is a class II 1 mW He-Ne laser of 632.8 nm wavelength. The modulation frequency is from 460 MHz to 500 MHz with 15 MHz bandwidth, and the effective wavelength (half-wavelength, unit length) is about 0.3 m. The operating range is from 20 m to 8 000 m. Outside this range an additional software in an external guiding computer is needed. According to the technical specifications (Kern 1986), the standard deviation of a measurement, with sufficiently accurate determination and correction for meteorological influences, is 0.2 mm + 0.2 mm/km.

For atmospheric corrections Kern (1986) lists three well-known formulas (Owens 1967 simplified, Edlen 1966 and IUGG 1960 / Barrel & Sears 1939) and recommends choosing one of them. For the distance observations processed for this thesis the new IAG formula has been used after it was published (IAG 2000, Ciddor 1996). The 0.1 mm-level or smaller differences in computed distances when using different formulas do not give an adequate reason for reprocessing of the old observations.

Bell (1992a) compiled one of the first reports about measurements using the Kern Mekometer ME5000. In it, Curtis (1992) reported on an achievable accuracy of ±0.5 mm/km as part of the English Channel Tunnel project. The instrument allowed for observations even in poor conditions, though with the level of accuracy downgraded to ±3 mm/km. In repeated calibrations on a multi-pillar baseline, the internal accuracy of the instrument was better than that stated by the manufacturer – a fact acknowledged during FGI's calibrations as well.

The FGI is the only institute that utilizes high-precision EDM instruments sequentially or even simultaneously with the Väisälä interference comparator for scale transfer. The high-precision EDM instrument is a transfer standard; it is calibrated at the standard baseline, which is the national standard. The distances measured with the EDM instrument are compared with the known distances of

the baseline sections, and the scale correction and the additive constant are determined for the EDM instrument. Several calibrations are performed at the beginning and at the end of a scale transfer project. Every calibration includes observations of all available distances from both ends, which at the Nummela Standard Baseline means two times 15 distances between the six pillars. The EDM instruments are fixed onto the observation pillars using a more or less standard-type forced-centring method, with applications of a 5/8-inch, standard-size fixing screw being the most typical fixing method.

Air temperature, pressure and humidity are recorded during the EDM observations to determine the weather-dependent velocity correction. Usually, psychrometers and aneroids are used at the end points of the distance to be measured. Handy electronic weather instruments seldom are suitable for precise measurements. However, the use of modern weather stations is increasing. Comparisons between the aging traditional weather instruments and a modern automatic weather station system have been ongoing at the FGI since 2012; the instruments may need to be replaced in the future. If the exact scale is not needed, as in some repeated deformation surveys, there are also different manners of approach for refraction, such as the local scale parameter method proposed by Brunner and Rüeger (1992).

If possible, the same set of weather instruments is used for all the calibrations and for the scale transfer measurements between the calibrations. This decreases the influence of possible small instrument-dependent errors in the weather observations, and thus it decreases the uncertainty due to weather observations; of course, calibration programmes at the FGI also cover the weather instruments. Cloudy, slightly windy weather with small temperature differences would keep the variation in results small, but in practice observations have to be made according to a schedule, independent of the weather.

In a multiplication or extension of a standard baseline, like in Gödöllő and Chengdu, sections of the baseline that the observers have just measured with the Väisälä interference comparator are fixed for further computation. These sections and the unknown sections are then measured with the EDM instrument, and the fixed sections determine the scale of the EDM instrument and the baseline.

2.6 Calibration baselines and test fields

The material for this thesis includes experiences and results from nine calibration baselines and test fields. In addition to five calibrations from the calibration baselines, two projects represent attempts at piloting international comparisons and two other projects serve the purposes of local geodynamical research. All of these calibrations are examples of successful scale transfer measurements, with the results benefiting surveyors, geodesists and metrologists. The customers have funded most of the projects, though pricing has always been moderate in the name of scientific cooperation.

There are few other recent reports on the measurements done at calibration baselines. Matsui and Kimura (2008) compared a Kern Mekometer ME5000 and GNSS at distances ranging from 200 m to 760 m and obtained uncertainties of 0.3 mm and less, but with much larger levels of instability at the surveying monuments. Lechner et al. (2008) used terrestrial metrological methods at a 12-pillar, 1 450-m baseline and desired a standard uncertainty of 2 mm/km. İnal et al. (2008) scaled a 7-pillar, 1 450-m calibration baseline for a low-precision EDM using GPS.

For the FGI, calibrations of calibration baselines are typical objects of scale transfer. Measurements at the transfer site are very similar to the measurements done for the calibrations at the standard baselines. Again, one "double-in-all-combinations" measurement includes observations of all available distances from both ends. A few such measurements are performed if the number of observation points is not too large (less than ten). A procedure with less repetition or fewer instrument stations is sufficient if the number of observation points is large. Observation points are typically, and even optimally, pillars with permanently installed fixing systems for measurement instruments.

The VGTU Kyviškės Calibration Baseline, extended to a triangle-shaped network, is located in a quite optimal open grassland airfield environment, which is also suitable for geodetic satellite positioning. The forced-centring method is simple: a standard-size screw through the fixing hole of the pillar top plate.

In both 1997 and 2007, the calibration projects at Kyviškės included four single double-in-all-combinations calibrations, whereas they included three such calibrations in 2001 and 2014 and two in 2008. The number of related annual calibrations of the transfer standard at the Nummela Standard Baseline was four in 1997, two in 2001, eight in 2008 and six in 2014. In 2007, the number of calibrations was 12, but then only the first 432-m section of the Nummela Standard Baseline was in use because of the delayed interference measurements since 1996 (due to the incomplete interference measurements in 2005). In 2007, the FGI's Wild DI2002 was used as another transfer standard, with one calibration of the baseline at Kyviškės and four calibrations of the transfer standard at Nummela.

The calibration projects at Kyviškės have yielded a large data set for analyzing the stability, repeatability, reproducibility and influence of weather conditions. In particular, the temperature conditions have varied quite a bit, allowing for some analysis of the impact of weather dependence on the measurements.

The *Maa-amet* Vääna Calibration Baseline is a newly reconditioned measurement standard in a quite optimal forested environment, though it is not suited for satellite positioning. The standard-size, forced-centring threads are now permanently installed on the plates on the observation pillars. Together with favourable measurement conditions, this fixing method is expected to keep the uncertainty of measurement particularly small. Because of the large number of observation pillars, the calibration project in 2008 included only one single

double-in-all-combinations calibration, even after distances shorter than 20 m had been excluded. The calibration of the transfer standard was the same occasion as for the measurements in Kyviškės in 2008.

Within the EMRP, the FGI calibrated the 7-pillar 1 080-m BEV Geodetic Baseline in Innsbruck, Austria, in 2008. The calibration was successful, though the location of the baseline on a land strip between a busy motorway and a cool river at the foot of a high mountain caused environmental disturbances. The project included four single double-in-all-combinations calibrations of the baseline in Innsbruck. The calibration of the transfer standard in Nummela was the same occasion as for the measurements in Lithuania and Estonia in 2008.

The FGI calibrated the 8-pillar, 600-m PTB Geodetic Baseline in Braunschweig, Germany, in 2011. The scale transfer included three single calibrations of the baseline in Braunschweig and five calibrations of the transfer standard at Nummela. The speciality of the baseline, refurbished in 2010–2011, is its automated network of 60 temperature sensors at 10 metre intervals along the baseline. There are also six humidity sensors and two pressure gauges along the baseline. The main purpose is to improve facilities for testing new ADM instruments, in addition to calibrating traditional instruments. Also, weather instrument research is now possible when comparing the readings from the traditional weather instruments and the new weather observing and recording system.

The new ADM instruments are expected to shorten the traceability chain. The first "absolute trackers" are already available: According to the manufacturer, Leica AT402 is the first laser tracker certified for outdoor use. The instruments developed within the EMRP utilize laser interferometry using synthetic wavelengths or femtosecond frequency comb technology. Comparisons between the different methods, planned for years 2014–2015, will be interesting.

Most recently, a scale transfer was performed in May–June 2012 at UPV's School of Engineering in Geodesy, Cartography and Surveying in Valencia, Spain. The object of calibration was a 6-pillar, Heerbrugg-type geodetic baseline with pillars at distances of approximately 28.4 m, 94.4 m, 198.0 m, 282.8 m and 330.0 m from the first pillar and a seventh pillar for angle measurements approximately 43.4 m away from the baseline, which created a triangle-shaped test field. One special feature is that the esthetical pillars are made of steel. The calibration was done in a large grassy and wooded court on the campus area, a "Mediterranean forest". In addition to terrestrial surveying techniques, GNSS metrology is one field of application at this baseline, though only a part of it is serviceable for such an application.

2.7 Piloting international comparisons

In July 2003, the National Metrology Institute of Japan, which is part of the National Institute of Advanced Industrial Science and Technology (NMIJ/AIST), organized an unofficial bilateral comparison of EDM instruments

with the FGI at the NMIJ's indoor baseline in Tsukuba, Japan. One of the NMIJ's instruments and two of the FGI's instruments were tested in a 310-m optical tunnel.

A 96-m rail with a carriage for moving reflectors, and laser interferometers, which were installed side by side at the end point, were used to determine the scale corrections, and an adjacent 7-point baseline was used to determine the additive constants. The pair of interferometer reflectors and the EDM reflector conversely between them were moved along the rail. Three observation stands at 99 m, 153 m and 206 m made EDM observations possible from the other end, ranging from 6 m to 204 m. The reflector set was moved and the EDM observations were performed at 1.0714 m intervals. A system of 53 platinum resistance thermometers recorded the temperature, and the pressure, humidity and CO_2-content were also measured in stable tunnel conditions. Unlike with other scale transfer measurements, in Japan the FGI used tacheometers, a Wild T2002+DI2002 and a Leica TC2003; it calibrated the transfer standards at the Nummela Standard Baseline five and eight times, respectively.

The Korea Research Institute of Standards and Science (KRISS) organized an interesting international comparison of EDM instruments in autumn 2006. KRISS, the NMIJ, the Industrial Technology Research Institute (ITRI) of Taiwan and the FGI all participated in the comparison for a pilot study on the calibration of EDM instruments at KRISS in Daejeon, Republic of Korea. The comparison was carried out as part of the Asia-Pacific Metrology Programme (APMP); the FGI was invited because of the previous bilateral comparison that it had done with the NMIJ. All of the participants used their best available EDM instruments: the Kern Mekometer ME5000 (FGI and ITRI), the Leica TC2003 (KRISS and NMIJ) and even a prototype of a laser comb distance meter (NMIJ). Minoshima and Matsumoto (2000) provided an initial description of how frequency comb technology is used for distance measurements in Japan, and Matsumoto et al. (2012) presented a recent update with 10^{-8}-level accuracies at a 403 m baseline.

The four participating institutes first measured the KRISS's 7-pillar, 280-m geodetic baseline eight times each with the Kern and Leica instruments. The participants made the observations and computations according to the previous version of the present international standard, ISO 17123-4:2012 (ISO 2012 a). After that, the NMIJ completed the comparison with measurements performed using the new laser comb instrument and according to a simplified observation schedule. The comparisons of the instruments used by the different institutes made it possible to compare different realizations of traceability. The results have not been published, and analysis of baseline stability continues, though an almost final version of the results is now available.

In autumn 2010, the Nummela Standard Baseline served in a joint research project of the EMRP called "Absolute Long-distance Measurement in Air". This project, which involved a number of European metrology institutes, was partly funded by the European Commission's Seventh Framework Programme, ERA-

NET Plus (EMRP 2014). Experts from *Conservatoire national des arts et métiers* (CNAM), the NMI of France, and from the PTB, the NMI of Germany, visited Nummela to test their new ADM instrument prototypes based on synthetic wavelength interferometry. The results of the latest (2007) interference measurements made using the Väisälä interference comparator were used to compare the distance measurements. The FGI-GG provided up-to-date distances between observation pillars by performing projection measurements before and after the visits. Also, some auxiliary stands at the pillars and connections for data transmission were constructed. To improve the determination of the refractive index of air, MIKES of Finland simultaneously tested some new instrumentation using spectroscopic methods. The work is continuing in the years 2013–2016 as a part of the new EMRP joint research project "Metrology for long distance surveying" (EMRP-SIB60 2014).

2.8 Control networks for local geodynamical research and their scale determination

Two ongoing research projects (at Olkiluoto and Metsähovi, already referred to in Section 1.3.4) are briefly introduced in this thesis as examples of metrological applications in local control networks for geodynamical research in Finland. At Olkiluoto, the control network surrounds the nuclear power plants and a safe disposal site for spent nuclear fuel, and the purpose is to examine possible crustal deformations. At Metsähovi, the control network establishes local ties between various observation instruments for global geodesy at the FGI's fundamental observation station.

The FGI has measured approximately ten observation pillars at Olkiluoto with GPS semi-annually since 1996. In the years 2002–2012, the FGI measured one pillar interval simultaneously with EDM instruments, making comparisons between the traceable scale of EDM and the scale of GPS possible at the 511-m baseline. The scale variation in GPS measurements and the small but significant systematic scale difference between them and the EDM motivated the investigations.

The purpose of the ongoing local tie measurements at the FGI's Metsähovi research station is to determine geodetic coordinate differences between the various reference points of the observation instruments, such as GNSS (including GPS and GLONASS) antennas, the VLBI telescope and SLR equipment. The results have been discussed by Jokela et al. (2009b) and include the measurements for stability control until 2006. Since then, the control network has been greatly improved. In 2007, the FGI constructed a loop of seven observation pillars around the VLBI telescope and the satellite laser. Since 2008, the FGI has repeatedly measured and analysed the improved control network with combined GPS and high precision tacheometry observations. The control network has been expanded inside the VLBI telescope's radome and some research on the tie measurements has been performed simultaneously with international geo-VLBI observation sessions (Kallio and Poutanen 2012, 2013).

There is also international interest in this: in the years 2013–2016, dimensional metrology of local ties at fundamental geodetic stations and their utilization in global geodesy is one research subject being addressed by the EMRP joint research project "Metrology for long distance surveying" (EMRP-SIB60 2014).

For the correctness and traceability of the scale, the FGI calibrates the tacheometers used in the control and tie measurements (at least) annually at the Nummela Standard Baseline. In the complicated tie measurement this is not a major source of uncertainty; the geometry between the reference points, often virtual and invisible, causes more difficult problems to solve. Efforts to obtain the desired millimetre accuracy (up to real-time) in the varying telescope positions still continue and the tie measurements to the new satellite laser (under construction) and the planned new VLBI telescope will no doubt bring new challenges.

2.9 Estimation of uncertainty of measurement

Estimating the uncertainty of measurement is an essential part of reporting the results of the measurement. For estimating the total uncertainty in the traceability chain, all sources of uncertainty must be identified and their influences must be estimated. Several components contribute to the uncertainty of measurement: measurement standards, measurement instruments, measurement methods, measurement conditions and measurement personnel. All of these influences must be estimated for every stage of the scale transfer procedure. For length measurements in geodesy, there is a large amount of variation in the components; they range from the nanometre-level variations in interferometry under laboratory conditions to millimetre-level variations in EDM observations under field conditions. By combining the components and presenting the results using the recommended methods, as documented in GUM, it is possible to obtain the estimate of total uncertainty, a measure of usability of the result.

In this thesis, the experimental standard deviation of the mean is often used in the estimation of uncertainty of a random variable component, expressing "Type A" standard uncertainty, according to GUM. A sufficient number of independent observations under same conditions of measurement are needed to determine this. "Type B" standard uncertainty components are estimated by other means, such as previous experience with or general knowledge of the method, or using manufacturer's specifications or calibration certificates. The final measurement results included in this thesis are now presented with expanded uncertainties with the coverage factor $k = 2$, although standard uncertainties may have been used in the original reporting. Also standard uncertainties are often used, but only as components of uncertainty or with intermediate results. The sign "±" is used or not used, depending on the context.

3 Quartz gauges as length standards

This chapter lists the quartz gauge systems, which have been used to determine the scale in the standard baseline measurements done with the Väisälä interference comparator. The comparison method for the quartz gauges is presented, and the length of quartz gauge no. VIII is computed using the present BTM00 system.

3.1 Review of quartz gauge systems at Tuorla Observatory

The scale of the Väisälä interference comparator is traceable to the definition of the metre, an SI unit, through a quartz gauge system, in which the lengths of tens of quartz gauges (also known as quartz metres or quartz bars) are determined through repeated comparisons and absolute calibrations. The lengths do not remain unchanged; instead, a fairly regular, slow lengthening process has been observed with most quartz gauges. Several systems have been used since 1933. In practice, introducing a new system means that the best possible new measurement results are used to compute the lengths: new or upgraded systems are needed after every absolute calibration. The review presented here is mostly based on the manuscripts by Dr Aimo Niemi, noted in 2001 and 2005.

After Yrjö Väisälä had first presented the interferometrical method for length measurements in his dissertation in 1923 (Väisälä 1923), he manufactured the first quartz gauges in 1927. At that time, he was a professor of physics at the University of Turku. The most commonly used quartz gauges are 1-m-long, 23 mm thick hollow quartz tubes sealed with 10-mm to 15-mm-thick cylindrical ends, which are spherical with different radii of curvature; for special purposes, other dimensions and materials and flat-end gauges are also available.

In 1933, when 18 quartz gauges were available, T.J. Kukkamäki published their lengths and temperature and atmospheric pressure coefficients in his doctoral thesis (Kukkamäki 1933). His thesis also included a comparison of the Finnish platinum-iridium prototype no. 5. In addition, Kukkamäki's system (TKK) was compared with the German prototype of metre no. 18. The standard uncertainty of the first absolute measurement was 300 nm, that is, 3×10^{-7}; in relative comparisons, it was of the order of 1×10^{-8}.

During the next years, researchers, including some of Väisälä's students at the University of Turku, made more comparisons and initial applications for the geodetic baseline measurements. The purpose was to calibrate invar wires and tapes; also, an alternative quartz gauge system (LKL) was introduced in 1937 by M. Laaksokivi and S. Lekkala. In 1947, T.J. Kukkamäki and T. Honkasalo measured the 864-m-long Nummela Standard Baseline of the Finnish Geodetic Institute. It had already been used to transfer the scale for the triangulation and mapping of Finland since its establishment in 1933. Since 1947, the Nummela Standard Baseline has served not only Finnish geodesists; it also has served as a world-class length standard of geodetic metrology.

The quartz gauges are stored and compared in "Sauna", a cave room inside the granite hill of Laukkavuori at the Tuorla Manor. This is the place where the

University of Turku's Tuorla Observatory was founded in 1952. Nowadays, the Tuorla Observatory, a division of the Department of Physics and Astronomy, together with the Space Research Laboratory, form the Väisälä Institute for Space Physics and Astronomy (VISPA) at the University of Turku. The name "Sauna" stands for the possibility to control temperature – the comparator is called "Saunapiano", which is distinct from a set of string systems found in the older "piano" comparators (Fig. 3.1).

The present principal normal of the quartz gauge system, quartz gauge no. 29, was made in 1953. Older comparisons have been tied to later systems using common quartz gauges at comparisons at different times. Even the definition of the metre has changed twice during the comparisons, in 1960 and in 1983. New absolute calibrations for some Finnish quartz gauges (nos. VIII and IX) at the BIPM in 1953 resulted in a new quartz gauge system (T, Terrien). These were the first absolute calibrations tied to the wavelength of light. Later absolute calibrations of the quartz gauges (nos. 42 and 53, used in Germany) were made at the PTB in Braunschweig, Germany, in 1964 (quartz gauge system E, Engelhard) and again at the BIPM in 1965. The incompatibility of the results both internationally and with the Tuorla system (K, Kukkamäki) prompted Väisälä and L. Oterma to improve the absolute calibration facilities at Tuorla (Väisälä and Oterma 1967). The results (for gauge nos. 30 and 32) obtained in 1966 improved the reliability of the lengths of the Tuorla system. Later on, absolute calibrations were performed at the PTB in 1970 (gauge nos. 42 and 53), 1978 (gauge nos. 30, 49 and 51), 1993 (gauge nos. 49 and 51) and 1995 (gauge nos. 30, 49 and 51; PTB 1996), and, finally, at MIKES in Helsinki, Finland, in 2000 (gauge nos. VIII, 49, 50 and 51; MIKES 2000). The method used at MIKES is described in a study by Lassila et al. (2003). Comparisons with the principal normal (gauge no. 29) have been performed before and after every absolute measurement. The absolute calibrations done at the PTB and MIKES and the comparisons done at Tuorla determine the present quartz gauge system, BTM00 (Braunschweig–Tuorla–MIKES 2000), which replaced the previous BT systems.

3.2 Comparisons at Tuorla Observatory

In the comparator box, two plane-convex lenses are adjusted parallel to one another at a distance of 1 001 mm (Fig. 3.2). The 1 mm shorter quartz gauges are adjusted horizontally on the supports between the plane surfaces. Outside the box, two Cd (cadmium) spectral lamps are used as light sources in the focal points of the lenses, and two CCD cameras are used for recording the images from the interference fringes. Part of the light is reflected from the end plane and part of it is reflected from the gauge end, producing interference fringes. The auxiliary parts include prisms, filters, screens and diaphragms to direct the light beam and thermometers for monitoring the temperature.

Before making the comparison, the temperatures of the comparator room and quartz gauges must be steady; the air-conditioning must be turned on at least

one day beforehand. After every adjustment of the gauges, which requires the presence of personnel in the room, cooling of the temperatures typically continues for 10–20 minutes.

Figure 3.1 *Some of the most frequently used quartz gauges at Tuorla (left), and tuning a middle quartz gauge in the comparator "Saunapiano". The side quartz gauges no. 63 and no. 64 are used to control the parallelism of the end planes.*

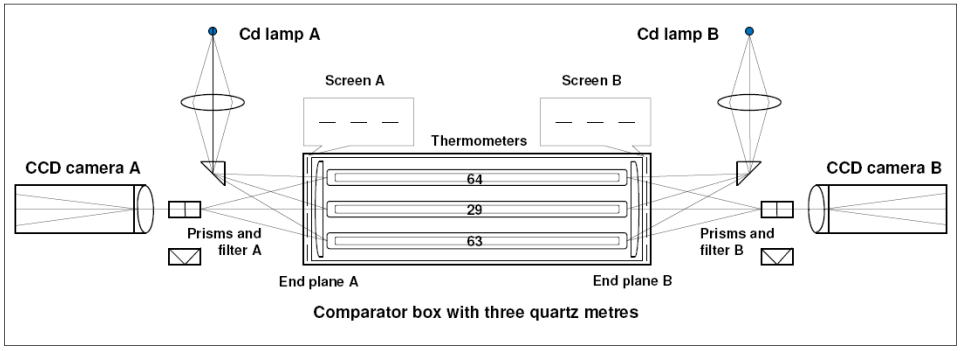

Figure 3.2 *Sketch of the comparator for relative comparisons of quartz gauges (not drawn to scale).*

The parallelism of the end planes is checked with quartz gauge no. 60, which has flat and parallel ends, and placed in the middle between the side

quartz gauges nos. 63 and 64. After making some careful adjustments, only 1–2 interference fringes are visible at both ends of gauge no. 60, and the fringes turn along with the quartz gauge when it is turned and adjusted from an "up" to a "down" position. Adjustment of the end planes is seldom needed. This check is performed before and after every comparison. Also, the positions of the side quartz gauges are checked and adjusted, if needed. The end planes and quartz gauges have aiming lines and markers to help in finding the correct positions. The comparator box has a set of adjusting screws (Fig. 3.3), and the positions can be viewed on the computer monitor (Fig. 3.4). During the comparison, the side quartz meters control the change between the end planes; the closing error, caused by uncertainty in the measurement and deformation, is typically ±40 nm. The quartz gauge to be measured or compared is adjusted in the middle of the side gauges and measured in the "up" and "down" positions.

In every comparison, the principal normal, quartz gauge no. 29, is measured first and last and the other quartz gauges are measured in between. Distances of less than 1 mm between the ends of the quartz gauges and end planes are measured at both ends (A and B) and at the two gauge positions (up and down). It takes a few minutes to measure one quartz gauge in a single position, and the temperature should be stable within a few millikelvins. During the measurement, the lid of the comparator box is closed and the personnel leave the room. The movement of the motorized cameras and the process of taking pictures are controlled with the computer in the outer room (Fig. 3.5). Ten pictures are usually taken in the following order: A2, A1, A2, A3, A2, B2, B1, B2, B3 and B2. In this sequence, A and B stand for the comparator ends, 1 and 3 are the side quartz gauges nos. 63 and 64, and 2 is the actual quartz gauge to be measured. More pictures may be necessary for problematic cases, such as the A-end of quartz gauge no. VIII, which has a short (1 m) radius of curvature. The processing of different pictures (A2, B2) should give the same result, with an experimental standard deviation of the mean of about 5 nm. Kukkamäki (1933, p. 15–47) describes in detail how to compute the distances between the ends of the quartz gauges and end planes. Later modifications to the instrumentation and computation include changes in the light sources and camera systems and the use of computers. Nonetheless, the main principle has remained the same. When analyzing the pictures, the fraction part and the integer number of halves of the wavelength between the quartz gauge and the end plane are determined using four different wavelengths.

The distance between the end planes is determined based on the approximate lengths of the side quartz gauges nos. 63 and 64 and the length of quartz gauge no. 29, with temperature (and pressure) corrections made to them, and from the measured gaps between the quartz gauges and the end planes. Using the average value of the lengths at the two side gauges removes the influence of possible non-parallelism of the end planes in the middle. The length of another quartz gauge is determined by replacing quartz gauge no. 29 in the middle of the comparator with the other quartz gauge and subtracting the

measured gaps at the end planes from the now known distance between the end planes.

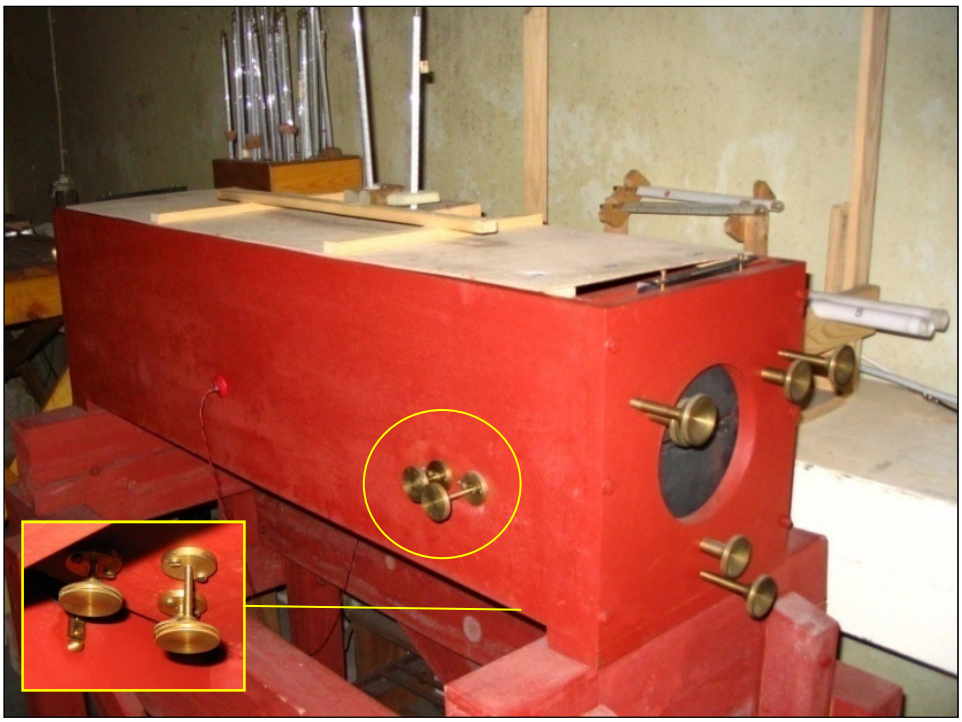

Figure 3.3 *Most of the adjustments are made at the B-end of the comparator box.*

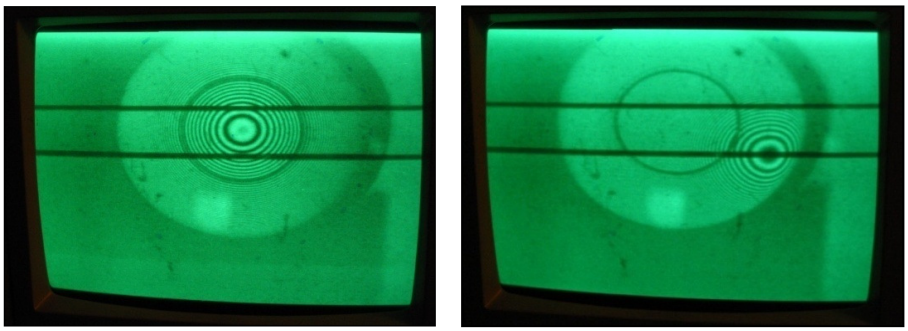

Figure 3.4 *After turning quartz gauge no. VIII around on its axis (from the "up" to "down" position, or vice versa), both vertical and horizontal adjustments are needed to return the B-end to its proper position for taking pictures for the measurements.*

Figure 3.5 *A picture of the B-end of quartz gauge no. VIII in the up position. The cameras, computers and monitors will be replaced with modern ones by 2014.*

3.3 Determining the length of quartz gauge no. VIII in BTM00

With the present constellation of observation pillars, the only quartz gauge that can be used in the Väisälä interference comparator at the Nummela Standard Baseline is the exceptionally long quartz gauge no. VIII. For example, a 100 µm shorter quartz gauge would produce an 86.4 mm shorter baseline, demanding modified observation pillars. Quartz gauge no. XI has also been used until 1977, but not later, since the shape of it is slightly imperfect and inconvenient to use.

The length of quartz gauge no. VIII was determined in comparisons made at the Tuorla Observatory before and after the measurements at Nummela both in 2005 and in 2007. In these comparisons, the principal normal, quartz gauge no. 29, was measured every day first and last, and no. VIII and a couple of other quartz gauges (no. 49 and no. 51) were measured in between. The principal normal, quartz gauge no. 29, is used to determine the distance between the end planes in the quartz gauge comparator.

The observed absolute length, L_{abs}, of quartz gauge no. VIII is obtained from the measured length, L_{meas}, by making a temperature correction to the normal conditions and correcting the nominal length of the principal normal to the absolute value:

$$L_{abs,VIII,epoch} = L_{meas,VIII,epoch} - a(t-20) - b(t-20)^2 - c(t-20)^3 + L_{corr,29,epoch} - L_{29}, \qquad \text{(Eq. 3.1)}$$

where t is the temperature (°C), and the coefficients determined at the Tuorla Observatory (in the quartz gauge system BTM00) are a = 0.4003, b = 0.00141 and c = 0.0000605, all in units µm/°C. L_{29} is the nominal length –100.550 µm

(+1 m). The temperature correction makes the absolute length of quartz gauge no. VIII comparable with the principal normal. The corrected length, $L_{corr,29,epoch}$, takes into account the lengthening of the principal normal after the reference epoch, to which the nominal length, based on previous absolute measurements and relative comparisons, is related:

$$L_{corr,29,epoch} = p + q_1[(epoch–1971)/(epoch–1956)] \text{ , if } epoch \geq 1971, \quad \text{(Eq. 3.2)}$$

or

$$L_{corr,29,epoch} = p + q_2(epoch–1971) \text{ , if } epoch < 1971, \quad \text{(Eq. 3.3)}$$

where $p = –100.5314$ µm (+1 m), $q_1 = 0.2818$ µm and $q_2 = 0.02017$ µm are constants determined in a polynomial fit of absolute calibrations and comparisons for BTM00. The years 1971 and 1956 are the reference epochs for the system. For epoch 2000, $L_{corr,29,2000} = –100.3457$ µm (+1 m).

The results from recent comparisons done at the Tuorla Observatory are presented in Table 3.1. The comparisons were performed by Aimo Niemi (spring 2005), Joel Ahola (autumn 2007), Pasi Häkli (spring and autumn 2005 and spring 2007) and Jorma Jokela (all comparisons).

When utilizing the abundant absolute calibration (Fig. 3.6) and comparison data (Fig. 3.7) in the long time series, the calculated lengths can also be obtained fairly independently of the current measurement:

$$L_{calc,VIII,epoch} = L_{calc,VIII,2000} + dL(epoch–2000) + L_{calc,29,epoch} – L_{calc,29,2000} . \quad \text{(Eq. 3.4)}$$

$L_{calc,VIII,2000} = +151.3160$ µm (+1 m) is the length of quartz gauge no. VIII at epoch 2000 in BTM00 and $dL = +0.0027$ µm a^{-1} is its annual change of length relative to the principal normal. The values, $L_{calc,29,epoch}$, are listed in Table 3.1; $L_{calc,29,2000} = –100.3457$ µm (+1 m). The results are presented in Table 3.2.

When choosing the final length of quartz gauge no. VIII for the computations of measurements with the Väisälä interference comparator, either the calculated or the just-measured values can be used. Generally, it is reasonable to pay attention to both of them. The latest absolute calibration at epoch 2000.2 gave the result 1.000 151 371 m with 72 nm combined expanded uncertainty and with the coverage factor $k = 2$ (MIKES 2000). Also, three of the other quartz gauges (nos. 49, 50, and 51) were then calibrated, which all contribute to the BTM00 system.

From the average values of the spring and autumn measurements done in 2005 (Table 3.1), the value +151.3014 µm (+1 m) is obtained for the mean epoch of interference measurements at Nummela, 2005.8. Respectively, the value +151.3696 µm (+1 m) is obtained for the mean epoch of the next interference measurements done at Nummela, 2007.8. These are the results based on the measurements done at Tuorla. The calculated values (Table 3.2) from the time series are +151.3429 µm (+1 m) for epoch 2005.8 and +151.3516 µm (+1 m) for epoch 2007.8. The conclusion is that the average values of the observed and calculated values should be used for processing the

interference measurements at Nummela: the length of quartz gauge no. VIII in standard conditions (t = 20 °C, p = 760 mmHg) was 1.000 151 322 m at epoch 2005.8 and 1.000 151 361 m at epoch 2007.8. The length of gauge no. VIII during each interference measurement at the Nummela Standard Baseline can be computed based on these values by correcting the standard length to the actual length during the observations using temperature and atmospheric pressure corrections (see Section 4.4.1).

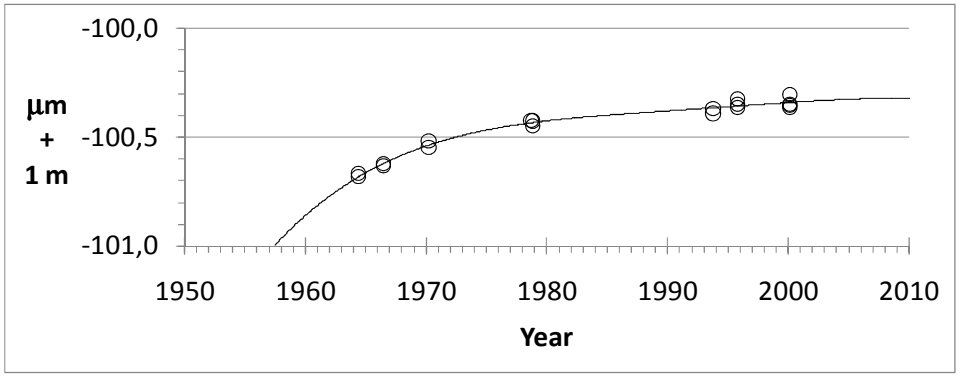

Figure 3.6 *Length of the principal normal, quartz gauge no. 29, determined from absolute calibrations at PTB, Tuorla and MIKES.*

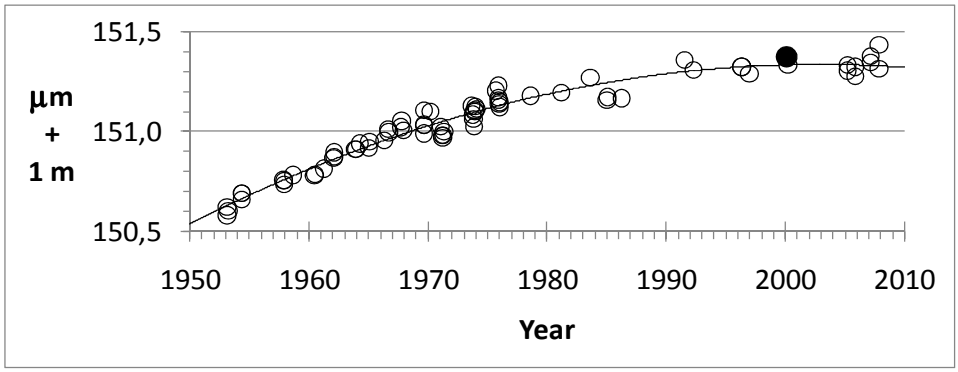

Figure 3.7 *The length of quartz gauge no. VIII, determined from comparisons at Tuorla. The black spot at 2000 signifies the absolute calibration of this particular gauge at MIKES.*

Table 3.1 *The observed length L_{meas} of quartz gauge no. VIII is reduced to absolute value L_{abs} with the temperature correction and when using the calculated length $L_{calc,29}$ of principal normal, quartz gauge no. 29. The lengths L are in µm (+ 1 m), and the temperatures t in °C.*

Epoch	$L_{meas,\ VIII}$	***t***	$L_{calc,29}$	$L_{abs,\ VIII}$
2005.282	+149.8143	16.790	–100.3354	+151.3014
2005.299	+149.9403	17.035	–100.3353	+151.3310
average 2005.290				+151.3162
2005.937	+150.2658	18.005	–100.3342	+151.2750
2005.937	+150.3520	18.110	–100.3342	+151.3197
average 2005.937				+151.2974
2007.236	+150.4775	18.290	–100.3321	+151.3761
2007.236	+150.4999	18.430	–100.3321	+151.3430
average 2007.236				+151.3596
2007.926	+150.4034	18.270	–100.3310	+151.3110
2007.926	+150.5587	18.355	–100.3310	+151.4326
average 2007.926				+151.3718

Table 3.2 *The calculated length L_{calc} of quartz gauge no. VIII, based on the time series from 1953 to 2007.*

Epoch	$L_{calc,VIII}$
2005.290	+151.3406
2005.937	+151.3435
2007.236	+151.3491
2007.926	+151.3521

4 Latest interference measurements at the Nummela Standard Baseline in 2005 and 2007

As a continuation of the impressive time series since 1947, the performance and results of the latest interference measurements made at the Nummela Standard Baseline in 2005 and 2007 are presented in detail here. The section provides a summary of the rare measurement method and is a detailed supplement to the previously published or internal instruction manuals. Two consecutive measurements within a short time span were necessary, since only half of the baseline could be measured in 2005 due to unfavourable weather conditions. The new results again confirm the excellent stability and unique accuracy, 9×10^{-8}, of the baseline. The baseline is the basis for the calibration, testing and validation of electronic distance measurement (EDM) instruments for precise surveying and mapping and for scale transfer measurements to other geodetic baselines, test fields and local geodynamical networks. The measurements are metrologically traceable to the definition of the metre through a quartz gauge system, as presented in Chapter 3.

The numerous stages in preparing a standard baseline for interference observations are described in Section 4.1, and the observation procedure is presented in Section 4.2. Corrections to the observations are provided in Section 4.3, including a detailed description of the principle and the results of the projection measurements.

Before utilizing the results from the interference observations, which were performed with temporarily installed adjustable equipment, they must be connected to something more permanent. At most standard baselines, underground sheltered benchmarks next to the observation pillars serve this purpose. The distances between the mirror surfaces in the comparator must be transferred to the distances between the permanently fixed transferring bars on the observation pillars and, ultimately, to the baseline lengths between the underground benchmarks. The connection between the two arrays of observation points, from aboveground to underground, is realized in the projection measurements. These theodolite-based, high-precision measurements are repeated during the entire two-three month interference observation period. For calibrating the EDM instruments, reverse projection measurements from underground to aboveground are needed; then, the observation pillars are equipped with forced-centring plates for surveying instruments instead of equipment from the Väisälä interference comparator.

The structure of Section 4.4 is adapted to make the reader abundantly familiar with the computation of interference observations: the numerous but essential computation tables for the interference observations are provided sequentially. At first is explained, how the actual values for the quartz gauge lengths, which were used to produce the scale of the latest interference measurements, were computed. After making compensator and refraction corrections, the lengths between the mirrors' surfaces are obtained. After another set of corrections, these lengths are reduced to the lengths between the

underground markers. The final results consist of values attributed to the measurands (here, the lengths of the baseline sections) determined in the measurements and of the uncertainty parameters associated with them.

The estimation of uncertainty is described in Section 4.5; by combining all of the sources of the uncertainty in the traceability chain the estimation of the uncertainty of measurement is presented as standard and expanded uncertainties.

A comparison with previous results since 1947 is presented in a short concluding section, Section 4.6. The expanded uncertainties of the new results range from 0.04 mm to 0.15 mm for the lengths of the baseline sections between 24 m and 864 m. The result for the length of the entire baseline, 864 122.86 mm ±0.15 mm, differs by +0.11 mm from the previous result obtained in 1996 and by +0.08 mm from the first result obtained in 1947. The largest difference between the results in 2005 and 2007 is –0.08 mm. The state-of-the-art Nummela Standard Baseline remains a world-class measurement standard of geodetic length metrology.

4.1 Preparing a standard baseline for interference measurements

For the interference measurements, observers must construct the comparator separately for every baseline. The preparations and installations for this process are described here, followed by the observation and computation procedures. The abundant illustrations clarify the many stages of the process.

How to install the Väisälä interference comparator at an existing baseline is described in detail, the Nummela Standard Baseline as an example. For a demonstration under indoor laboratory conditions, the installation for a "baseline" that is a few metres long is possible in one day. Under field conditions, the work is more challenging and preparations for an array of pillars, up to nearly a distance of 1 km, usually take at least two weeks. After this, the centre points of the mirrors should be on the same line in space and approximately at correct distances to enable the discovery of interference fringes. Also, the components for making the observations (light source, telescope, and so forth) must be adjusted, and the quartz gauge must be tuned to determine the scale. After this, the most interesting part of the measurement procedure awaits.

How to build a baseline for measurements with the Väisälä interference comparator is not discussed in detail in this publication. The basic requirement is evident: observation pillars or other foundations must be located in such places that the parts of the comparator can be installed along a single line in space at the level of 1 mm. This sets strict constraints on baseline design, and only multiples of the lengths of the quartz gauges are allowed as suitable locations for observation pillars or mirrors. The baseline designs recommended for EDM calibration are, therefore, not practicable. The constructions on observation pillars must also have sufficient margins and adjusting mechanisms for the installation of the required instruments.

Finding interference fringes for short lengths is rather effortless after careful installations and adjustments have been made. For long lengths, the procedure is often extremely laborious and impeded by unfavourable weather conditions. Advice for conducting observations, learnt from experience, is given in Section 4.1.5. Once found, the fringes should be found the next time using roughly the same adjustments. To eliminate questionable observations and ensure a reliable result, two observers participate in observing the interference fringes. This is essential, especially if the number of observations remains small.

4.1.1 Principle of the Väisälä interference comparator

There are a few publications, for example by Kukkamäki (1969) and Jokela and Poutanen (1998), which describe in detail how to install the Väisälä interference comparator on the observation pillars and how to use it. The principle is briefly repeated here, and more details are presented in the next pages.

The design of the Nummela Standard Baseline was originally adapted for the calibration of 24-m-long invar wires. The entire length, 36 x 24 m = 864 m, was equipped with wooden stands at every 24 m between the underground markers at 0 m, 432 m and 864 m. These underground markers are brass bolts cast in concrete pillars and covered with small concrete blocks and wooden boxes in the ground. In the design for taking measurements with the Väisälä interference comparator, a longer length is always a multiple of a shorter length. This was realized up to 864 m using several multiplications: 2 x 2 x 3 x 3 x 4 x 6 x 1 m = 864 m. The observation pillars were cast at the intermediate and end points at 864 m, 432 m, 216 m, 72 m, 24 m, 6 m, 1 m and 0 m. This line was placed approximately 2 m away from the line between the underground markers. The heights of the observation pillars are between 0.7 m and 1.4 m from the ground, and the depths are 0.8 m, except for the especially wide pillar 0–1, which is only 0.3 m deep (Honkasalo 1950). The underground markers extend to a depth of 2 m, with the surface area being about 1 m^2.

In the comparator (Fig. 4.1), the white light from a point-like source is arranged parallel with the collimator lens and divided into two beams. One part of the light travels between the front mirror and the middle mirror, while the other part travels to and from the back mirror. The distance between the front and back mirrors is an integer multiple n of the distance between the front and middle mirrors. The light beam travels n times between the first two mirrors, and once to and from the back mirror. The mirrors are adjusted in such a way that the two beams, travelling different paths but equal distances, meet at the focal plane of the observing telescope. The light source and the telescope include fine-mechanical and optical components to control the light beams, whereas the structures of the other parts of the comparator are quite simple. The reflections are directed to the telescope by the numerous adjustment screws for mirrors. The final adjustment of the incoming beams with adequate accuracy is made with the screen and the compensator glasses in front of the telescope.

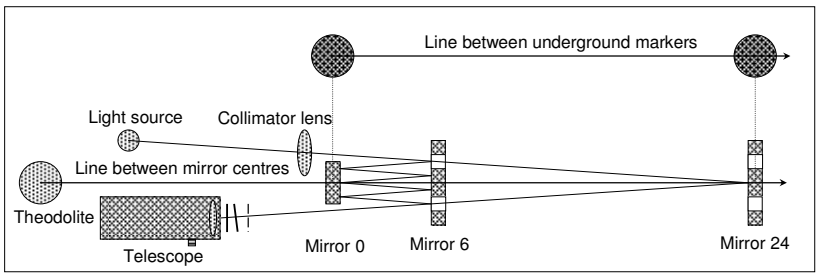

Figure 4.1 *The principle of the Väisälä interference comparator and the geometry of the 0–6–24-interference (not drawn to scale, reprint from Jokela and Poutanen 1998).*

The observations include: (1) recording the mirror positions relative to the permanently fixed transferring bars on the observation pillars; (2) the rotation angles of the compensator glasses, leading to compensator corrections; (3) measuring the inter-mirror distance of the shortest interference with the quartz gauge, which is somewhat more complicated; and, (4) making temperature observations, which accompany every interference observation. The transfer readings in item (1) are taken last, after all of the observations for the shorter interferences have been made and before the mirrors are removed for longer interferences. For further utilization, the positions of the transferring bars (and mirrors) relative to the underground markers are determined in the projection measurements, which are repeated several times during the interference measurement period.

To avoid observer-dependent systematic or random errors, two observers always perform the observations. About 1 μm repeatability is obtained in taking transfer readings; their reproducibility is maintained by taking daily calibration readings at an auxiliary pillar. Number of compensator readings and temperature observations is always large enough to ensure conformity. Uncertainty of compensator corrections is typically a few μm and seldom larger than 10 μm. This uncertainty is included in the uncertainty component of interference observations. In favourable conditions variation in the nightly temperatures usually remains smaller than 0.5 °C and uncertainties at a few 0.01 °C-level. Also this uncertainty, covering reading uncertainty, thermometer uncertainty and local temperature gradients, is included in the uncertainty component of interference observations. In addition to statistics, the computing programs for corrections produce illustrating graphs, which help controlling of observations. Both of the observers also perform all the works with the quartz gauge.

4.1.2 Preparing the observation pillars for interference measurements

The observation pillars are usually equipped with forced-centring plates for calibration measurements. They are fixed onto heavy iron plates, which are then fixed onto the observation pillars. The plates cannot be used with the Väisälä interference comparator. When removing them, it is advisable to record their old

exact locations on the iron stands emerging from the observation pillars. This helps when installing the plates again after the interference measurements, since the space on the supports for making adjustments is very limited and all the plates should, again, be on approximately the same line in space. Broken threads or nuts for fixing screws in the pillars are replaced, where needed, and rusty parts are polished and painted. Visibility between the pillars is cleared by removing disturbing vegetation.

4.1.3 Precise levellings – start of the measurements

Measurements are begun with precise levellings (Fig. 4.2). Height differences are needed to install the components of the Väisälä interference comparator on the same line in space and to reduce the resulting slope lengths to a preferred reference height level.

At the old baselines, the height differences are known from previous measurements and possible small changes are insignificant when determining the height reductions. Levelling is still recommended, since it is a precise measurement method that easily reveals possible instability. Tenths of a millimetre differences are acceptable, since all of the benchmarks have flat tops rather than rounded tops; flat tops are not optimal for levelling. A Zeiss DiNi12 digital level and two bar code rods were used for the precise levellings in 2005 and 2007. The digital levelling instrument and rods are regularly calibrated at the FGI's system calibration comparator.

The height differences between underground markers are determined first, both to and fro. After this, one point is levelled on every observation pillar relative to the corresponding underground marker; a point on pillar 0 may also serve levellings for pillars 1 and 6 and the telescope pillar. The levelled points are later used to adjust and mount all parts of the comparator at the correct heights. The heights of end points 0 and 864 are fixed, and everything else is fitted along the same sloping line. The curvature of the Earth must not be forgotten; for example, at 432 m the straight line must be 14.6 mm lower than what levellings along an equipotential surface would suggest (Fig. 4.3).

Another detail is that at the 0-end of the baseline, all instruments must be slightly inclined according to the slope of the baseline (about 0.309 gon). Height references on the observation pillars are used in the levellings for mirror rails, supports and centres. A short (1.2 m) wooden rod, measurement tape or a ruler were used as a rod, and the Wild N3 level was used in addition to digital levelling. When adjusting the heights, pieces of aluminium plate are often needed between the iron supports and the mirror rail stands to raise the height of the instruments, or else some screws must be shortened or exchanged for longer ones. At a new baseline, this can be eliminated by careful planning and construction of the observation pillars.

The results of the precise levellings and the resulting corrections are presented in Section 4.3.4.

Figure 4.2 *Arrangements for precise levellings with a Zeiss DiNi12 digital level and two bar code rods. The height differences between the underground markers are levelled first, both to and fro. The height differences between the underground markers and the reference points on the observation pillars are levelled next. Common levelling accessories and auxiliary pillars are used as intermediate points. Rulers or homemade bar code rods may be needed to determine the heights of the observation instruments.*

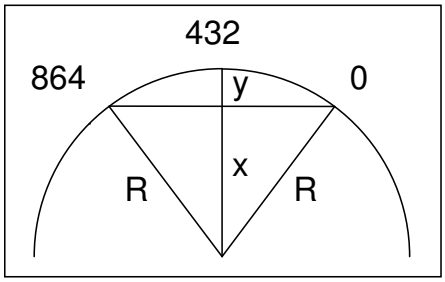

Figure 4.3 *Curvature of the Earth: R = 6 370 km. At 432 m, the line in space between mirror centres 0 and 864 must be 14.6 mm lower than the levelled height. For shorter lengths, the correction is 10.9 mm at 216 m, 4.4 mm at 72 m, 1.5 mm at 24 m, and 0.4 mm at 6 m.*

4.1.4 Aligning the mirrors

The most accurate theodolite available should be used to align the mirror centres along the same line in space. In this instance, a Kern DKM3 was used, which was placed on the theodolite pillar along the continuation of the baseline, approximately 20 metres behind the 0 pillar (Fig. 4.4). The final position of the theodolite and the centre of mirror 864 determine the line upon which the other mirror centres are adjusted. When the final position is chosen, one should make sure that there is enough room left to adjust the mirrors on every pillar. The position of the theodolite is marked on the theodolite pillar. At this point, the theodolite is kept under cover during the entire measurement period. It can later be used to find the correct positions of the mirrors if some of them become badly directed so that a reflection is completely lost.

Figure 4.4 *Kern DKM3 theodolite with an autocollimation lamp on the theodolite pillar.*

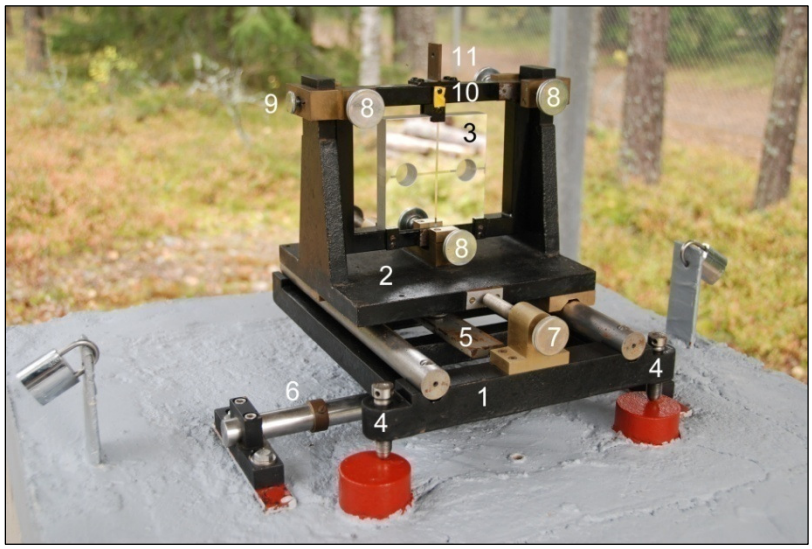

Figure 4.5 *Mirror equipment: (1) mirror rail, (2) mirror stand and (3) mirror in its frame, above a transferring bar and on three iron supports on an observation pillar. First, the rail is levelled and adjusted to the correct height (4, three screws). After the correct position of the mirror rail is found, it is permanently fixed to the observation pillar (5, one screw). The transferring bar (6) is equipped with a collar ring, which directs the probing point of the transferring device to the centre of the mirror (see also Fig. 4.7). The mirror stand can be moved along the rail in the direction of the baseline (7, two screws) and the mirror in its frame can be tilted in its stand (8, six screws). The mirror frame can also be moved or straightened in a direction perpendicular to the baseline (9, two screws). The targets (10, as a distant mirror, or 11, as a mirror to be projected) serve in the projection measurements.*

Using the theodolite, the observers first adjust the mirror rails along the line (Fig. 4.5). The aim is directed towards the front and back screws of the mirror rails (or to clearly visible targets placed on top of them), and the positions of the rails are corrected as necessary. In spite of using a precise instrument, it is important always to read the angles at the two theodolite face positions. The mirror rails are also levelled horizontally (along and across the baseline) and adjusted and fixed at the correct height. When the mirror rails are in the correct positions (usually after a few days' effort), it should be quite easy to install the mirror centres along the same line, again by making observations with the theodolite in a constant direction in relation to the mirror centres. At the distant mirrors, visibility can be improved by illuminating the mirrors from behind with a torch.

It is more difficult to turn the mirrors in the correct positions exactly perpendicular to the line of sight so that a reflection from the telescope returns back to the telescope. In order to first approximately find the reflection, a hand-held torch is useful, especially for the longest lengths. The torch can be used to

direct the mirror perpendicular to the baseline by first adjusting the mirror with the torch reflection close to the mirror and then by repeating the procedure while moving farther away from the mirror (and thus approaching the theodolite). The final adjustments are done with the theodolite. A small battery-operated lamp is permanently fixed in front of the theodolite objective to help with the final tuning. The light reflecting from the centre of mirror 864 is first directed to the crosshairs of the telescope, and then reflections of other mirror centres are directed to the same point. The mirror centres must be adjusted both vertically and horizontally along the same line within about a 1-mm degree of accuracy before the mirrors can by successfully directed.

4.1.5 Setting the mirrors at correct positions in the baseline direction

Before searching for the interference fringes, the mirrors must also be at correct positions in the baseline direction, again preferably within 1 mm. This can be measured and adjusted using a precise tacheometer and a prism reflector, which is placed above a mirror (freehand, since it may be difficult to fix) and similarly above every mirror to be measured. The tacheometer is set up behind the telescope along the continuation of the baseline. To prevent disturbing extra reflections, the reflecting mirror surfaces of the comparator must be covered during the EDM observations. The multiplied length of the quartz gauge determines the correct positions; later, the already found shorter interferences can give the scale for the measurement. The distant mirror is always moved to a proper distance by using the front and back screws of the mirror rail. One rotation of the screws moves the mirror stand 1 mm. Since the distances between the reflecting surfaces are determined, the thickness of the front mirror must also be taken into account.

At the old Väisälä baselines with known lengths, the previous results can be very useful for finding the interference fringes again. Of course, this has no influence on the new results. The method is presented here (Fig. 4.6) and was successfully applied when searching for the 864 m interference in 2007 and in 2013. The previous results were from the lengths of the baseline sections, 432 m and 864 m, between the underground markers in the interference measurements taken in 1996.

When a shorter interference, 432 m, had been found, mirrors 0, 216 and 432 were at definite positions; also, the quartz gauge was already being used to determine the exact scale. When using the new projection corrections, P, at pillars 0 and 432, the difference between transfer readings, L, at the interference positions and the projection positions, and the approximate thicknesses, D, of the mirrors, 20 mm, it was possible to compute the distance, M_1, between mirror surfaces 0 and 432 by assuming the known length between underground markers 0 and 432, which was unchanged from 1996, X_1 = 432 095.36 mm, such that:

$$M_1 = X_1 - P_{432} - \tfrac{1}{2}D - L^P{}_{432} + L^I{}_{432} - P_0 - \tfrac{1}{2}D - L^P{}_0 + L^I{}_0. \qquad \text{(Eq. 4.1)}$$

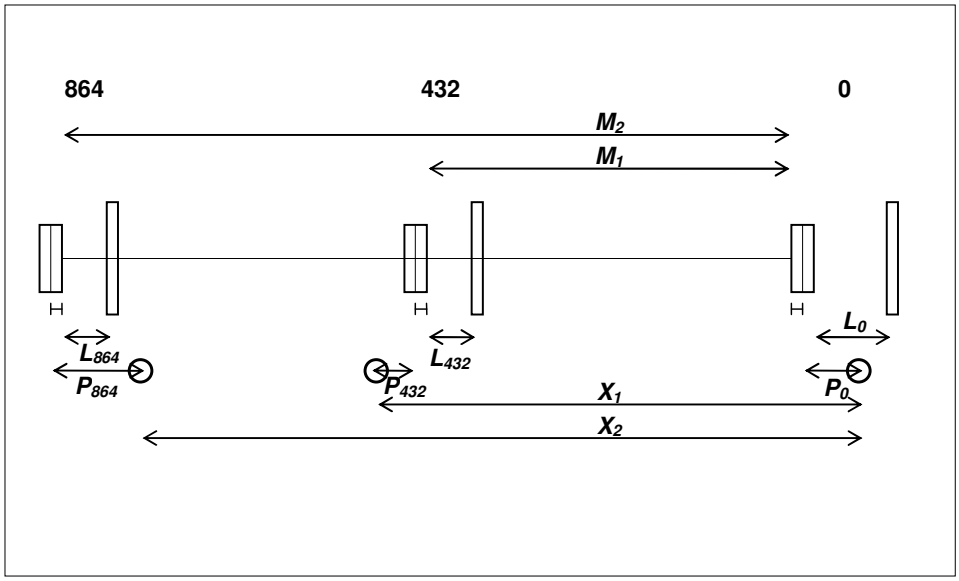

Figure 4.6 *Using previous results X for setting mirrors at approximately the correct positions in the baseline direction. X are lengths of baseline sections between underground markers from previous measurements. M are distances between mirror surfaces in the interference position. P are projection corrections between underground markers and mirror centres. L are transfer readings between transferring bars and mirror surfaces.*

Here, the projection corrections $P_{432} = 16.97$ mm and $P_0 = 0.83$ mm, and the transfer readings $L^P_{432} = 14.21$ mm and $L^P_0 = 11.40$ mm, are from the projection measurements, whereas the transfer readings $L^I_{432} = 14.86$ mm and $L^I_0 = 11.43$ mm are related to the interference position. Based on these values, the distance $M_1 = 432\,058.24$ mm can be obtained.

The distance between mirror surfaces 0 and 864 in the interference position is a multiple of this shorter distance: $M_2 = 2M_1 = 864\,116.48$ mm. Using $X_2 = 864\,122.75$ mm from 1996, as well as $P_{864} = 24.07$ mm, $P_0 = 0.83$ mm, $L^P_{864} = 21.87$ mm and $L^P_0 = 11.40$ mm from the projection measurements, an estimate for the transfer reading, L^I_{864}, in the interference position can be obtained:

$$L^I_{864} = M_2 - X_2 - P_{864} + \tfrac{1}{2}D + L^P_{864} + P_0 + \tfrac{1}{2}D + L^P_0 - L^I_0 . \qquad \text{(Eq. 4.2)}$$

The plus and minus signs in the formulas are not always applicable, but they must be deduced on a case-by-case basis. This computation resulted in $L^I_{864} = 12.33$ mm. This is exactly the position at which the 864 m interference was found and measured for the first time on 26 October 2007.

Particularly when searching for the 864 m interference, even with a search interval of a few millimetres (which is normally scanned by moving the mirror at 0.5 mm intervals), it may be laborious to find the interference fringes. Some

older instructions recommend using a spectroscope, which can be set in the telescope instead of the normal ocular and which disperses white light into colours. Using this, the interference fringes should be easier to find, since seeing them is less dependent on the angles of the compensator glasses in front of the telescope. However, this was not very useful; when the atmospheric conditions are good enough for observations, the fringes can be found without this device.

4.1.6 Installing the transferring bars onto the observation pillars

A special transferring device is used to determine the distances between the permanently fixed transferring bars and the adjustable temporal positions of the mirrors (Fig. 4.7). The reading accuracy of the instrument is 1 μm and the repeatability of the measurements is about the same. Only one of the two identical (though reverse) micrometre scales (red or black) is in use during a measurement project.

When mounting the transferring bars onto the observation pillars, the range of the micrometer of the transferring device determines the correct distances of the transferring bars relative to the mirror surfaces in the baseline direction. All mirrors must be approximately in their final positions, including perpendicular to the baseline, before the transferring bars can be mounted onto the observation pillars. The transferring bars are adjusted parallel to the mirror surfaces by taking transfer readings at both edges of the mirrors (or as close to the edges as possible). If the micrometer readings are not the same, the transferring bar needs to be adjusted. Based on the differences between the transfer readings and the probing points for them, and based on the length of the transferring bar, a correction for straightening can be computed. Usually it is necessary to repeat this procedure a few times before the final positions are found. This stage is extremely essential, since the positions of the transferring bars cannot be changed afterwards. It is equally important to check that there is enough room in the mirror rail screws and in the transferring device scale to adjust the mirrors. The same rule applies even if more than one quartz gauge is used. The transferring bars are also adjusted so that they are level.

Though all of the centres of the mirrors must be in line in space, they are not always at the same height from the pillar structures, including the transferring bar. The transfer readings should also be taken as close to the mirror centres as possible in the vertical direction. This can be optimized by changing the length of the transferring device legs, which rest against the transferring bar. It is more important, though, that the observation pillars have been successfully designed and constructed. The height differences of the probing points relative to the mirror centres were from 0 mm to +8 mm in 2005 and from –2 mm to +2 mm in 2007, with the exception of +17 mm at pillar 24 in 2005. This difference is significant at sloping baselines such as Nummela, but the eccentricity is the same when transferring for projections or transferring for interference observations, and thus eliminated. Before taking the measurements

in 2007, the bottom plate of transferring bar 24 was made 8 mm thinner, enabling a smaller vertical deviation from the mirror centre.

In the horizontal direction perpendicular to the baseline, the probing points are fixed to the centres of the mirrors by fixing a collar ring at the correct place around every transferring bar.

4.1.7 Installations on the telescope pillar

The lamp and the telescope are levelled (and slightly inclined according to the slope of the baseline) and adjusted on the telescope pillar. The rail for the lamp is fixed with a screw, whereas the telescope can be moved quite freely. A point-like source of white light is used. Point-like light is obtained when a filament of a small common light bulb (also used in cars as a back light!) is set at the horizontal position perpendicular to the baseline, and when a narrow (a few tenths of a mm) slit is placed in front of the lamp (top right in Fig. 4.8). The brightness of the light is adjustable. Like mirrors, the lamp is resting on rails with adjustment screws so that it can be moved in all necessary directions. Next to one screw that is perpendicular to the baseline, there is a scale for recording the position of the lamp. This is important, since the measurement geometry and the position of the lamp are different for every interference.

Before making the observations, the telescope must be focused to infinity. Otherwise, the reflections cannot be directed to one spot. The reflections are gathered in the telescope by moving and turning it. The compensator glasses and the screen are placed in front of the telescope to control the arriving light beams (Fig. 4.8). With the screen, either the upper or lower reflection from the middle mirror is observed together with the reflection from the back mirror, which arrives in the middle. During the observations, if possible the upper and lower reflections are observed in turns.

The final adjustment of the mirrors is controlled by the telescope. For doing this, the ocular can be removed and the screen can be turned away. Orders from the observer behind the telescope to the person adjusting the mirrors are transmitted with radio telephones. When the correct reflections are found and they arrive in the telescope, observers continue to adjust the mirrors using the ocular and the screen. (More details are presented in Section 4.2.1.) The purpose is to get the reflections to arrive at one spot in the telescope. This is not possible, however, when the temperature conditions change because the travel paths of the light beams change continuously and the front and back beams cannot be directed to one spot.

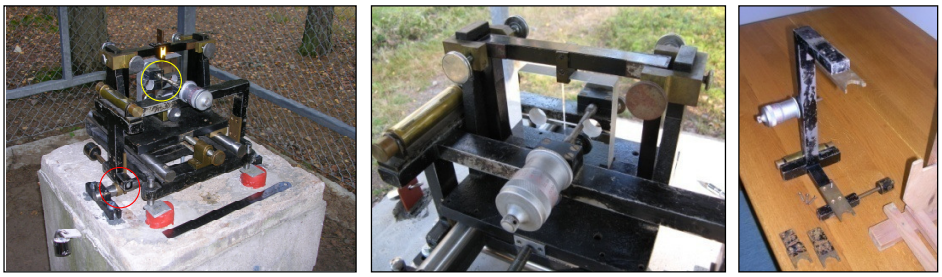

Figure 4.7 *Transferring device on the transferring bar for one of the mirrors (left). With the adjustable collar ring (lower circle) around the bar, the probing point (upper circle) can be adjusted in the centre of the mirror. When adjusting the transferring bar parallel to the mirror surface, transfer readings cannot always be taken from the edges of the mirror (centre). The legs of the transferring device are changeable (right).*

Figure 4.8 *Searching for interference fringes by adjusting the screen and turning the compensator glasses in front of the telescope. A detail of the lamp at the top right.*

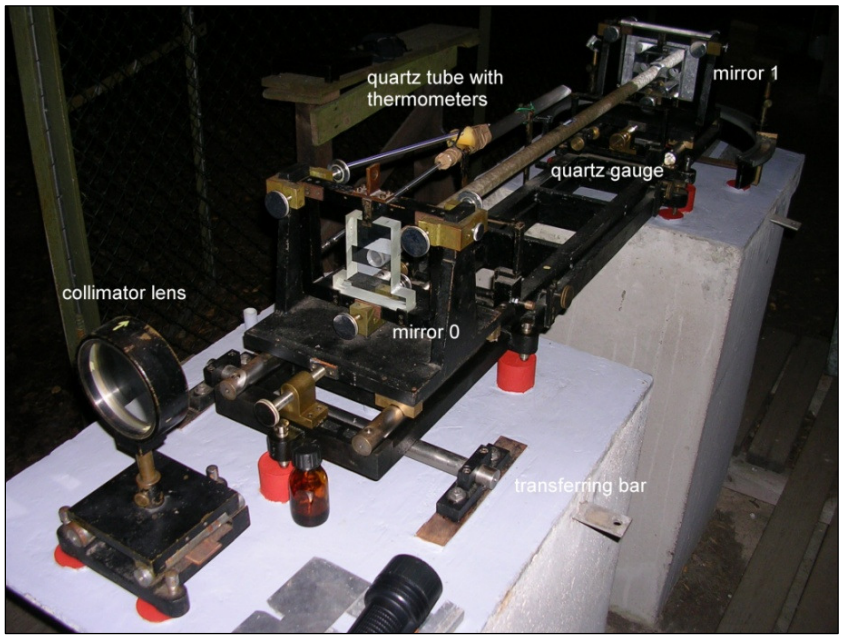

Figure 4.9 *Instruments on observation pillars 0 and 1.*

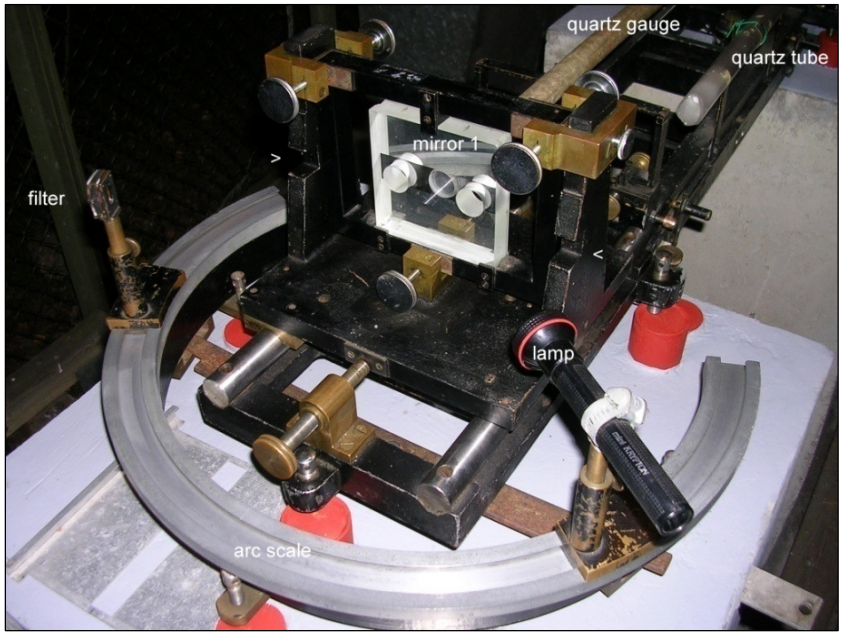

Figure 4.10 *Instruments at mirror 1. Indentations in the mirror stand determine the correct position of the back surface of mirror 1 and the zero angle of the arc scale.*

4.1.8 Installations on pillars 0 and 1

The collimator lens is placed on pillar 0, close to mirror 0, to cover the left half of the mirror frame with the light passing through the lens (Fig. 4.9). (Using the right half of the mirror, the reflections from the middle and back mirrors return to the telescope.) The edge of the lens must be exactly on the centre line of the comparator. The distance between the lens and the light source is the focal length of the lens: 2.97 m. In the installation (if using the present equipment), it is more useful to know the distance between the edge of the stand for the light source and the edge of the stand for the collimator: 2.91 m. Also, the correct height must be computed and carefully levelled and adjusted (again, with a small inclination of approximately 0.309 gon).

The support for the quartz gauge rests on pillars 0 and 1 between the mirror rails. The positions of the mirrors are exactly determined by the length of the quartz gauge. The position of the quartz gauge support must be adjusted horizontally and vertically so that the ends of the quartz gauge are close to the centres of mirrors 0 and 1. The final adjustment is made exactly in the centres of the mirrors during the measurements. The quartz gauge is not completely symmetrical, and adjustments are always needed between the two measurement positions ("up" and "down") of the quartz gauge.

It is necessary to clean the quartz gauge ends and the mirror surfaces with ethanol before installing the quartz gauge in the support, leaning on mirror 0 and just a few micrometres from mirror 1 (which is adjusted last). To prevent compression, mirror 1 must not come into contact with the quartz gauge. The correct contact between the quartz gauge and the surface of mirror 0 appears as a black spot at the contact point when illuminating the contact point obliquely with diffuse light through the glass of mirror 0 and viewing the reflection of it symmetrically. A colourful spot indicates bad contact between moist or dirty surfaces, whereas a large black spot indicates compression (to be avoided!).

The arc instrument with a lamp and a filter, which can be slid along the arc-shaped rail, is placed behind mirror 1 (Fig. 4.10), where it is levelled and fixed. This is used for measuring the gap between the quartz gauge and mirror 1. The gap is adjusted to between 1 μm and 3 μm, which is equivalent to 3 to 10 Newton's rings that can be observed with the arc instrument.

A piece of quartz tube and two fixed thermometers that are in contact with it are also placed in the support; this is used to simulate the temperature of the quartz gauge (both inside and outside). Other arrangements for temperature observations are described in Section 4.3.2.

4.2 Interference observations

4.2.1 Observation procedure

A complete series of interference observations includes 16 observed interferences (shown in Table 4.1). At least seven hours of cloudy autumn night with very small temperature differences are needed for this, even if everything

proceeds favourably. Observing the last interference, 0–432–864, or even shorter intervals, is often unachievable, as the weather changes too much. To avoid this, work breaks are not allowed during favourable conditions; but the observation time has to be minimized.

Table 4.1 *Interference observation procedure.*

1st observer					**2nd observer**			
↓	864–432–0						↑	0–432–864
↓	432–216–0						↑	0–216–432
↓	216–72–0						↑	0–72–216
↓	72–24–0			→			↑	0–24–72
↓	24–6–0	↑	0–6–24		↓	24–6–0	↑	0–6–24
↓	6–1–0	↑	0–1–6		↓	6–1–0	↑	0–1–6
	quartz gauge		quartz gauge			quartz gauge		quartz gauge
	position A	→	position B			position B	→	position A

The first observer observes the first eight interferences, while the second observer observes the last eight interferences. Before the observations can be started, the interferences must be found by adjusting the mirrors to favourable positions. For every mirror, six screws are available for directing the mirror to obtain reflections from the lamp to the telescope. While observing the first half of the procedure, the first observer is behind the telescope and instructs the second observer to adjust the mirrors to their proper positions. When an 864-m interference is found (or 432 m, if 864 m is not obtainable), measurements are started immediately.

First, at the telescope end the lamp must be moved to a position at which the light travels (through the collimator lens and past mirror 0) through the hole (on the lamp side) of the middle mirror and to the centre point of the back mirror. A non-reflecting plate with two holes should be placed behind the middle mirror to prevent disturbing extra reflections.

By carefully turning the adjustment screws in the back mirror, the light beam is reflected back through the second hole of the middle mirror. Now the first observer must observe the situation at the middle mirror. After adjusting the reflecting beam to travel through the hole, it should be caught in the telescope. All this requires careful preparation, measurement and adjustments at a degree of accuracy of less than a millimetre.

A non-reflecting plate, which covers the upper and lower part of the mirror, is also available for mirror 0. With this plate, the light travelling between the front and the middle mirrors (vertically at the top and bottom levels) can be blocked, thus making it easier to find the light beam coming from the back mirror, which is travelling vertically in the middle level because of the holes in the middle mirror. Alternatively, the front surface of the middle mirror can be temporarily covered. Sometimes turning the screen to obscure a part of the light

departing from the light source helps the observer to better interpret the constellation of reflections.

After finding the reflection from the back mirror in the telescope, the observer adjusts the middle mirror to direct its reflection to the telescope, too. The middle mirror is adjusted with very small movements to make the reflection arrive at exactly the same spot as the reflection from the back mirror. It is essential, but not always easy, that the correct reflection is selected. For the longest distances, both single and double reflections are often visible in the telescope at the same time. For the shortest distance (0–1–6-interference), the correct sixth reflection can be ensured, for example by moving a pencil slowly across the upper reflecting part of mirror 1 and counting the number of dark points visible in the telescope. The number of these points should be six.

It is necessary to adjust mirror 0 (in turns with the middle mirror), especially when searching for interference fringes for the first times and for long distances. This often helps direct both the upper and the lower reflection from the middle mirror to the telescope. In later adjustments, after mirror 0 had been previously adjusted for a longer distance or interference, the adjusting of mirror 0 should not be done by default, but only in cases when reflections from the middle mirror are weak or totally lost and cannot be found by adjusting the middle mirror.

The observer first views the light beams arriving in the telescope without the ocular. By adjusting the mirrors, the three reflections (top, middle and bottom) in the telescope can be adjusted one after the other such that the round reflection from the back mirror is in the centre and the more or less rectangular reflections from the middle mirror are above and below it. After that, the observer views the reflections with the ocular and adjusts the mirrors to get the light beams to converge in one spot. By turning the compensator glasses, interference fringes can be found in this spot if the distances between the mirrors are correct. It may still take several hours to find the interference fringes for the first time; even if the reflections seem to be correct, further adjustment of the mirrors may still be needed or the weather conditions may not be good enough. When the preparations and adjustments are very carefully made using both the upper and lower reflections from the middle mirror, it is more likely that the observation series will be successfully concluded than when using approximate, though observable, positions. This is difficult to obtain in unfavourable weather conditions, since the reflections may continue not to overlap properly and they may completely disappear after more adjustments have been made.

To find the interference fringes, the observer makes the final adjustments with the two compensator glasses in front of the telescope, where one of the beams (from the back mirror or from the middle mirror, depending on which compensator glass is turned) can be delayed. To obtain good accuracy, the compensator angles must not be too large, preferably less than 30°; in contrast, angles close to 0° are difficult to observe, especially at long distances, since the interference fringes may rapidly drift from one glass to the other during

changing weather conditions. To adjust the distances between the mirrors, all of the mirrors can be moved on their rails in the direction of the baseline with two adjustment screws; one full rotation of a screw means one millimetre movement along the baseline.

Observing the second half of the procedure can usually be done more quickly, since it is no longer permissible to make adjustments to the mirrors. At that point, only the lamp can be moved (both vertically and horizontally) when trying to compensate for the weather changes. This does not help in unfavourable weather conditions, as the reflecting light beams disappear and the measurement remains unfinished. The observations, as far as they are obtained, are still usable.

Finding the interference fringes for the first time and adjusting the mirrors to their proper positions (to also allow for adequate adjusting possibilities for changing conditions later) takes several nights. They can be found in almost any type of weather at up to a 72-m interference. On some particular night, the observers must also make preliminary adjustments using the quartz gauge to obtain an approximate (but almost final) scale and, thus, the near final mirror positions. Later, finding all of the previously found interference fringes again before measuring them takes one to two hours because the approximate mirror positions, with respect to the transferring bars, are known. The observers search for shorter interferences first, beginning usually from a 24-m interference. After finding this, middle mirror 6 can be removed and the search for the next 72-m interference can be started. It is always necessary to make minor adjustments to the mirrors before conducting the observations. Similarly, the observers must search for all of the interferences up to a distance of 864 metres, after which they begin to immediately take measurements. After observing a 864–432–0 interference, mirrors at 216 m, 72 m, 24 m, 6 m and 1 m are put up and adjusted on their pillars one by one, and the corresponding interferences are observed. The correct position of the lamp is recorded in the notebook to help find the same interferences later in the night.

Observations of the interference positions consist of taking readings of the compensator angles. One set consists of four readings: (1) with the reflection from the back mirror and the upper reflection from the middle mirror in compensator position 1; (2) with the reflection from the back mirror and the lower reflection from the middle mirror in compensator position 1; (3) with the reflection from the back mirror and the lower reflection from the middle mirror in compensator position 2; and, (4) with the reflection from the back mirror and the upper reflection from the middle mirror in compensator position 2. The upper and lower reflections from the middle mirror are chosen with the screen in front of the telescope. Compensator positions 1 and 2 are angles symmetrical to the zero angle, at which the both compensator glasses are perpendicular to the baseline.

To observe the interference fringes, the compensator glasses must be turned very slowly. Either of the compensator glasses can be turned, depending on

which particular light beam needs to be delayed; the other compensator glass must remain at the zero position. For each of the 16 interferences, as many sets should be observed as possible, depending on how the thermometer readers move ahead. For the shortest interference, one set is enough, whereas for the longest interference under favourable conditions there is usually time for more than ten sets. For the shortest interference, an observation set also includes reading of Newton's rings with the arc scale and temperatures of the quartz tube. Examples from the observation records are presented in Figs. 4.11 and 4.12.

The shortest interference that includes the quartz gauge must be observed in two quartz gauge positions relative to its longitudinal axis. Quartz gauge no. VIII is slightly deformed, and some adjusting of the quartz gauge on the support is needed for this rotation. Measuring the distance between mirrors 0 and 1 (from observations such as those in Fig. 4.12) has been described in more detail by, for example, Jordan et al. (1958) and Jokela and Poutanen (1998, p. 16–18); the description is revised in the next paragraphs.

When the quartz gauge is placed on its support between mirrors 0 and 1, it comes into optical and physical contact with mirror 0. The observers can check this when they see interference rings through the glass of mirror 0 at the contact point. A medium-size black spot in the centre of the rings means perfect contact; coloured rings or no rings at all are signs of damp or dusty surfaces, which should be cleaned with pure spirit and a lens paper. The ends of the quartz gauge are of varying spherical shape. The radius of curvature at the 0-end is 1 m, whereas at the 1-end it is 5 m. The larger radius leads to larger Newton's rings, thus enabling more precise determination of ring behaviour.

At mirror 1 the observers must leave a gap of 1 µm to 3 µm between the quartz gauge and the mirror. Physical contact at both ends would easily cause compression which could damage the gauge. When adjusting the gauge on its support, a large-size black spot at mirror 0 is a warning for such a situation. In examining the interference rings behind mirror 1 one can measure the width of the gap. To see the Newton's rings, the gap must not be wider than several micrometres.

For measurement of the gap a semicircularly shaped rail is used on which the observer places a lamp (L) and a monochromatic filter (F, Fig. 4.13). Moving the lamp and the filter equally in opposite directions along the arc rail and looking through the filter, the observer can see interference rings (Fig. 4.14). The scale on the rail is according to 100 cosα, in which the angle α (or actually 100 cosα) of every medium-black ring is taken at the arc scale; usually 5 to 10 rings can be observed (Fig. 4.15). Rings near 0° are not observable, but are interpolated in the calculations. At 90° the observer takes the ring he sees using a six-step scale (0/6 = medium black, 1/6 = small black, 2/6 = large white, 3/6 = medium white, 4/6 = small white, 5/6 = large black). The width w of the gap is

$$w = (n+\varepsilon)\lambda/2. \qquad \text{(Eq. 4.3)}$$

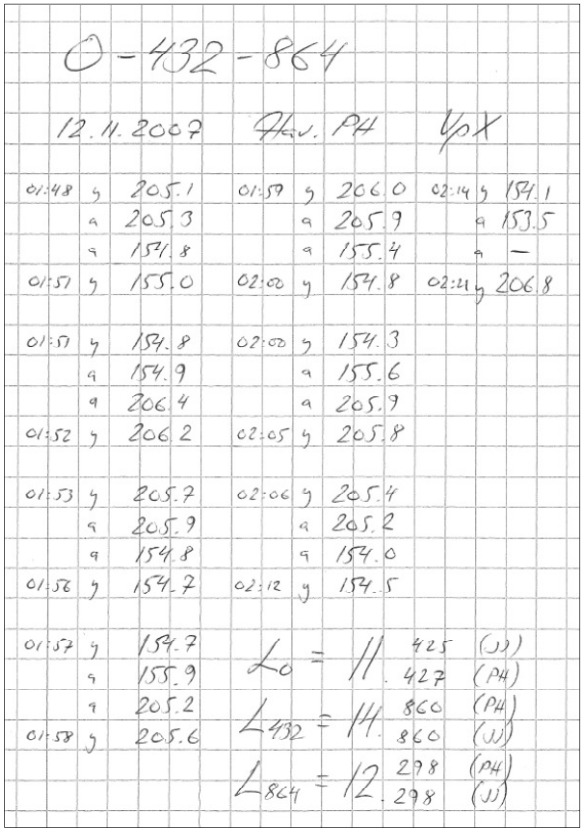

Figure 4.11 *An authentic example of the recording of interference observations, with the latest 0–432–864-interference observed on 12 November 2007, at 2 a.m. The observations include eight sets of compensator angles (in degrees and in screen positions y, "up", and a, "down") during the course of 33 minutes (the start and end times of every set are shown). The observations end with three transfer readings, L (in millimetres), which determine the distances between mirror centres and transferring bars. The notation "Vp X" indicates that the observers had not forgotten to place a heavy iron plate on mirror rail 1, compensating for the mass of the removed mirror stand 1 and keeping the loading on the pillar constant. The slowing pace of observations and one missing observation in the last set indicate weakened measurement conditions.*

where n is the integer part (number of medium blacks between 0° and 90°) and ε is the fraction of six at 90°.

The transmittance of the filter behind mirror 1 was confirmed in a measurement done by Mr Juha Suomalainen at the FGI on 31 January 2006: the value $\lambda/2$ = 315.5 nm was used to compute the gap between the quartz gauge and mirror 1 (Tables 4.13 and 4.19). In autumn 2013 a new small electric torch was constructed as a light source.

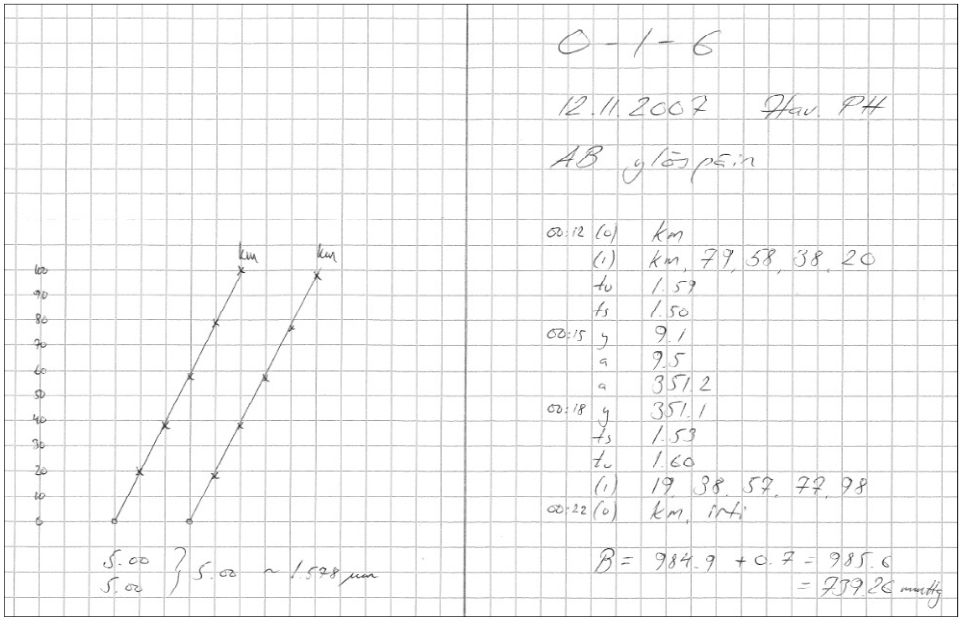

Figure 4.12 *An example of recording the 0–1–6-interference in the same measurement series as in Fig. 4.11, but two hours earlier. The observations include checking the contact of the gauge and 0 mirror at the 0 end of the quartz gauge at the beginning and at the end (0), two determinations of the gap between the quartz gauge and mirror 1 (1), four temperature readings at the quartz tube (outer surface, t_u, and inner surface, t_s), and one set of compensator angles (in screen positions y and a). Also, the air pressure (B) is recorded. All of this took 10 minutes. At the 1 end of the quartz gauge, the observations consist of the angles at which the lamp-filter-arc system creates "middle black" Newton's rings (1/6 of half a wavelength scale for the Newton rings, and 100 cos α arc scale for the angles α). Here, the determination of the gap is based on five observed Newton rings (as illustrated on the left), equal to 5 x λ/2 = 1.578 µm. The notation "AB ylöspäin" indicates the "up" position of the quartz gauge.*

After the first observer has finished, the second observer observes the same eight interferences in the opposite order. It is no longer permissible to make any adjustments to the mirrors (except for mirror 1). For the last interferences, it is often necessary to change the height of the light source. This may help the observer find the reflecting lights. It is still often possible to make observations, though the lights do not necessarily arrive exactly in one spot anymore. To record the interference positions of the mirrors, transfer readings between the transferring bars and mirror surfaces are taken before the mirrors are removed from the pillars one by one.

In spite of the rather detailed descriptions and instructions provided here, it is recommended that new observers become acquainted with log books on previous measurements.

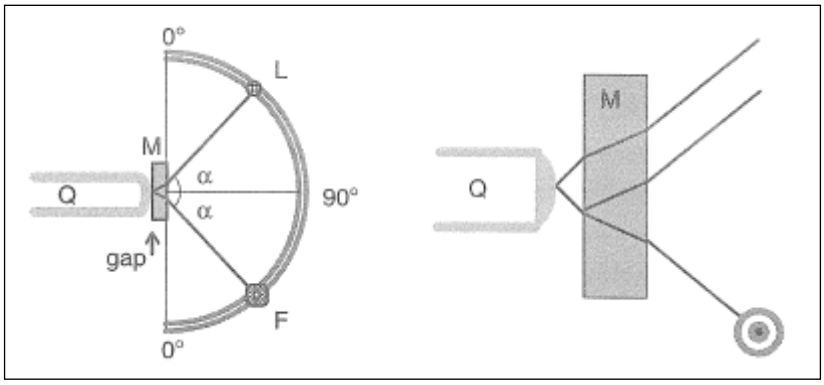

Figure 4.13 *Measuring the gap between the quartz gauge (Q) and mirror 1 (M).*

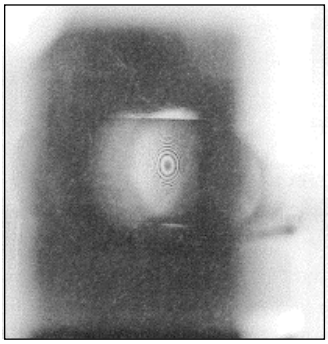

Figure 4.14 *Newton's rings, with a large black spot in the centre.*

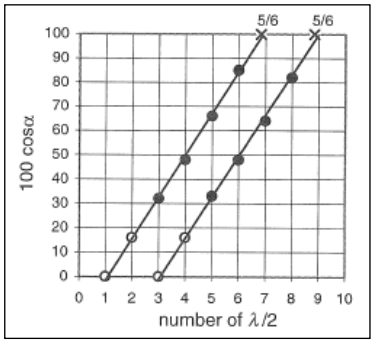

Figure 4.15 *An example of a gap measurement. Four black spots in both observation sets were observed as medium blacks, white spots (at 100 cos α ≈ 16) were interpolated as medium blacks. The centre ring was estimated as a large black, which is equivalent to 5/6 × λ/2. Both of these two observations resulted in a value of (5 + 5/6) × λ/2 = 1.97 μm.*

4.2.2 About the weather conditions

In general, desperate attempts to adjust the mirrors and direct the light beams in clear weather should be avoided. Rather than advance the measurement, they often cause more trouble for the subsequent days. Also, humidity may prevent the observations. Drying off the instruments is not always advisable; problems with moistness and wetness disappear on their own when the weather becomes dryer.

The measurements in both 2005 and 2007 were made under exceptional weather conditions. The 864-m interference was not found during the entire autumn of 2005. It was not even attempted much because of more or less clear nights; the autumn was the warmest in several decades. The first half of the baseline could be measured seven times under mostly poor conditions. The weather for autumn 2007 was for the most part better, though far from optimal. The 864-m interference was measured eight times, which was unprecedented, including five complete series, whereas, for example, the eight interference measurements during the years 1947–1975 included only one or two measurements up to 864 m. The interference observations made between 1947 and 2013 were performed during the autumn months between 27 September and 23 November, except in 1955, when they were done on 20 May.

Temperature data for refraction correction was obtained by reading the 29 precise thermometers along the baseline. Two more thermometers are fixed at the quartz tube next to the quartz gauge, as described earlier. Thermometers at 0, 1 and 4 metres are hanging from the roof of the Väisälä comparator shelter, and wooden poles were set up to hang the rest. Metal tubes in the ground at the correct positions are used as stands for the wooden thermometer poles. The heights of the thermometers are fitted equal to the height of the light beam with hanging threads, and clothing pegs tied to the poles prevent them from swaying in the wind. To prevent heat radiation from above and from below, the lower ends of the thermometers are placed between two aluminium plates. Horizontally, the thermometer line runs just outside the mirror line, parallel to it (Fig. 4.16). For safety reasons, the poles and the thermometers are erected again before every measurement night and gathered up in the storeroom before morning.

Two thermometer readers read the thermometers to and fro; thus, every thermometer is read four times for each interference, which takes from a few minutes (6-m interference) to half an hour (864 m). Small torches are used to provide light in the dark autumn night. The thermometers must be read without breathing on them or otherwise heating them. Since slant readings are not allowed, observer's stands are needed to read the highest hanging thermometers. Processing and analysis of the temperature observations is presented in Section 4.3.2.

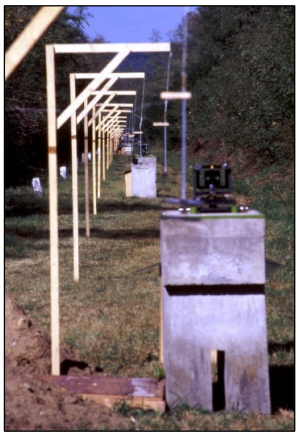

Figure 4.16 *Line of thermometers along a standard baseline, next to the line of mirrors on observation pillars (photo from Gödöllő, Hungary, in 1999).*

4.2.3 Personnel

Interference observations in 2005 were performed by Messrs Jorma Jokela (JJ) and Pasi Häkli (PH). In 2007, the team was complemented by Mr Joel Ahola (JA). The observers are shown in Tables 4.13 and 4.19. In autumn 2013, in addition to Jokela and Häkli, Professor Markku Poutanen and Mr Timo Saari performed the newest interference measurements, four times up to 864 m and four more times up to 432 m. The final results are not yet available.

Mr Paavo Rouhiainen performed the levellings along the baseline, both on 6 September 2005, on 13 September 2007 and on 22 August 2013. Mr Martin Rub, a visiting researcher from Switzerland, was assisting all of autumn 2007. He also made some of the computations and weighting investigations for this publication. Mr Veli-Matti Salminen contributed to the work by solving many practical hardware problems in the, then, Laboratory of Geoinformation and Positioning Technology of the Department of Surveying of Helsinki University of Technology (HUT). Mr Filip Dvořáček, a visiting researcher from Czech Republic, was assisting all of autumn 2013.

Several other people assisted with the projection measurements, temperature observations and other tasks. In addition to a few permanent people from the FGI, these people were mostly students from the Department of Surveying at HUT and from the Department of Astronomy at Helsinki University. In 2005, these people were, in order of appearance: Jani Uusitalo, Markku Poutanen, Janne Kovanen, Kaisa Laatikainen, Maaria Tervo, Mikko Moisander, Matti Christersson, Katri Koistinen, Jyrki Puupponen, Henrikki Nordman and Joel Ahola. In 2007, they included: Jaakko Järvinen, Elisa Hautamäki, Olli Wilkman, Arttu Raja-Halli, Terhi Ahola, Sebastian Porceddu, Emilia Järvelä, Sonja Nyberg, Essi Korpela, Juulia Laine, Ville Vuokko, Lauri Kajan, Petteri Salmi and Jaakko Kuokkanen.

The abundant photo material used in this chapter was provided by, in addition to the author, Messrs Pasi Häkli, Joel Ahola and Martin Rub.

4.3 Determination of corrections

4.3.1 Compensator corrections

It is infeasible to adjust the mirrors accurately enough to find the interference fringes in the telescope, particularly under field conditions. The solution is to delay one of the reflecting light beams by rotatable compensator plates in front of the telescope (Fig. 4.8). This fits the phase differences in the two beams equal for all colours, and interference fringes can be seen and the corresponding rotation angle measured. The compensator plates are achromatic and consist of two components. The thicknesses δ and the refractive indices n are

δ_{cr} = 10.015 mm, n_{cr}^{red} = 1.51485, n_{cr}^{blue} = 1.52288

for the crown glass component, and

δ_{fl} = 5.005 mm, n_{fl}^{red} = 1.60911, n_{fl}^{blue} = 1.62562

for the flint glass component; the wavelengths are $\lambda_{red} = 656.3$ nm and $\lambda_{blue} = 486.1$ nm (Fraunhofer lines 'C' and 'F').

The relation between the rotation angle α of the compensators and the corresponding change in distance of the optical light path can be computed with the formula (Väisälä 1956)

$$ds = [(\lambda_{blue}\psi_{cr}^{red} - \lambda_{red}\psi_{cr}^{blue})\delta_{cr} - (\lambda_{blue}\psi_{fl}^{red} - \lambda_{red}\psi_{fl}^{blue})\delta_{fl}] / (\lambda_{blue} - \lambda_{red}), \quad \text{(Eq. 4.4)}$$

where

$$\Psi_{cr}^{red} = \sqrt{(n_{cr}^{red})^2 - \sin^2\alpha} - n_{cr}^{red} + 1 - \cos\alpha, \quad \text{(Eq. 4.5)}$$

$$\Psi_{cr}^{blue} = \sqrt{(n_{cr}^{blue})^2 - \sin^2\alpha} - n_{cr}^{blue} + 1 - \cos\alpha, \quad \text{(Eq. 4.6)}$$

$$\Psi_{fl}^{red} = \sqrt{\left(n_{fl}^{red}\right)^2 - \sin^2\alpha} - n_{fl}^{red} + 1 - \cos\alpha, \quad \text{(Eq. 4.7)}$$

$$\Psi_{fl}^{blue} = \sqrt{\left(n_{fl}^{blue}\right)^2 - \sin^2\alpha} - n_{fl}^{blue} + 1 - \cos\alpha, \quad \text{(Eq. 4.8)}$$

the compensator correction (equivalent mirror shift) is $ds / 2$. A summary of corrections is provided in Table 4.2.

Compensator angles of less than 30° (meaning compensator corrections of less than 0.1 mm) require that the mirrors be adjusted to correct positions within 0.1 mm. When searching for the interferences, much larger angles (at least up to 60°, which means a 0.5 mm correction) can be utilized; but before making the actual observations, such angles should be reduced by moving the back mirror a few tenths of a millimetre closer to or further away (or less, if the middle mirror is moved).

Table 4.2 *Compensator corrections.*

°	µm	°	µm	°	µm	°	µm
0	0.00	20	47.61	40	206.32	60	527.96
1	0.12	21	52.64	41	217.93	61	549.79
2	0.46	22	57.94	42	229.95	62	572.25
3	1.04	23	63.52	43	242.38	63	595.36
4	1.86	24	69.38	44	255.24	64	619.13
5	2.90	25	75.53	45	268.54	65	643.57
6	4.18	26	81.97	46	282.29	66	668.69
7	5.70	27	88.71	47	296.49	67	694.51
8	7.45	28	95.75	48	311.16	68	721.04
9	9.44	29	103.11	49	326.31	69	748.28
10	11.67	30	110.77	50	341.96	70	776.25
11	14.14	31	118.76	51	358.10	71	804.95
12	16.85	32	127.08	52	374.76	72	834.40
13	19.81	33	135.74	53	391.94	73	864.60
14	23.01	34	144.73	54	409.67	74	895.56
15	26.47	35	154.08	55	427.94	75	927.29
16	30.18	36	163.78	56	446.77	76	959.79
17	34.15	37	173.85	57	466.18	77	993.07
18	38.37	38	184.29	58	486.17	78	1027.14
19	42.86	39	195.11	59	506.76	79	1061.99

4.3.2 Refraction correction

The thermometers used to determine the refraction correction are of a classical mercury-in-glass type. Their locations and the corrections made based on the calibrations are listed in Table 4.3. An example of how to derive the coefficients for the formulas for the refraction correction is presented later on in Table 5.5. Table 4.4 shows the coefficients for Nummela and also the thermometers that should be read for each interference; for example, 4 thermometers are read for the 6-m interference and 19 thermometers for the 864-m interference.

The equation for refraction correction is as follows (Kukkamäki 1969, p. 16–18):

$$r_{\Delta t} = \frac{dn_L}{dt} \Delta t \, s, \qquad \text{(Eq. 4.9)}$$

where the temperature derivative of the refractive index of air is

$$\frac{dn_L}{dt} = \frac{(0.399063p - 0.055e)\alpha}{(1+\alpha t)^2 \cdot 10^6}. \qquad \text{(Eq. 4.10)}$$

The coefficient α is equal to 0.003661, t is the temperature in °C, p is the pressure in mmHg and e is the estimated partial pressure of water vapour. The actual value of n_L is not needed, and s is the length to be measured. The

coefficients c_v for the five formulas of temperature difference, Δt, are listed in Table 4.4:

$$\Delta t = \Sigma(c_v t_v). \qquad \text{(Eq. 4.11)}$$

The average temperatures in Fig. 4.17 do not show any differences along the baseline (with one exception). Fig. 4.18 shows changes in temperature during successful interference measurements; they remained within two degrees during all of the nights. It is only necessary to take into account the small differences between the weather conditions along the two paths of the light beams (from the back and middle mirrors) in the refraction correction.

In several previous measurements before 1996 the final result has been computed using individual weights for the single results of every observation night. The weights have been determined according to maximum temperature differences along the baseline during the measurement. This practice has later been ignored, since the justification for weighting may be questioned and its influence is fairly negligible. For the abundant observation data in 2007, this weighting method was tested again. The weighting would cause a lengthening of 6 µm to 14 µm in the lengths 24 m to 432 m, and a lengthening of 31 µm in 864 m. Since no clear dependence between the maximum temperature differences and the difficulties in observation work was found, the single results used for the overall final result have been kept equally weighted (except the not ended one-way measurements with half-weight).

Table 4.3 *Corrections to the thermometers based on certificates of calibration.*

Thermometer at (m)	Thermometer no.	Correction (°C) at 0°C	5°C	10°C	Thermometer at (m)	Thermometer no.	Correction (°C) at 0°C	5°C	10°C
t_i	11138 [1)]	–0.06	–0.02	–0.05	192	7352	+0.03	+0.02	+0.02
t_i	850 [2)]	–0.01	+0.01	–0.01	216	7348 [3)]	+0.06	+0.02	–0.02
t_o	857	–0.04	0.00	–0.01	216	11133 [4)]	–0.05	–0.01	+0.01
0	7932	–0.03	–0.07	–0.03	264	47	–0.05	–0.02	+0.02
1	7931	–0.02	–0.03	–0.01	312	7351	+0.02	0.00	–0.01
4	7937	0.00	–0.02	+0.01	360	44	–0.03	–0.04	–0.05
10	7936	+0.01	0.00	+0.02	408	7929	–0.01	–0.02	0.00
17	7349	–0.04	–0.04	–0.03	456	7939	–0.01	–0.03	–0.01
24	45	–0.04	–0.04	–0.05	504	3864	–0.06	–0.02	–0.08
36	4484	+0.04	+0.02	+0.03	552	7350	+0.05	+0.02	–0.01
48	7935	–0.02	–0.03	–0.01	600	48	–0.05	–0.04	–0.02
60	4480	0.00	–0.02	+0.02	648	76	–0.15	–0.08	0.00
72	4483	0.00	0.00	–0.01	696	7933	0.00	–0.01	0.00
96	11135	–0.07	–0.06	0.00	744	46	–0.04	–0.02	–0.01
120	3867	0.00	–0.02	+0.02	792	850 [1)]	–0.01	+0.01	–0.01
144	7938	–0.01	–0.02	0.00	792	3857 [2)]	0.00	+0.04	+0.10
168	3868	0.00	–0.02	0.00	840	4479	0.00	0.00	–0.03

[1)] in 2005, [2)] in 2007, [3)] until 16 October 2007, when broken, [4)] since 25 October 2007

Table 4.4 *Coefficients for computation of temperature differences.*

v	0–1–6	0–6–24	0–24–72	0–72–216	0–216–432	0–432–864
0	–0.417	–0.062	–0.014			
1	–0.167	–0.250	–0.056			
4	+0.528	–0.340	–0.125	–0.077	–0.019	–0.010
10	+0.056	+0.215	–0.180	–0.080	–0.020	–0.010
17		+0.292	–0.194			
24		+0.146	–0.014	–0.120	–0.072	–0.036
36			+0.167	–0.111		
48			+0.167	–0.111		
40			+0.167	–0.111		
72			+0.083		–0.111	
96				+0.111		
120				+0.111	–0.111	–0.056
144				+0.111		
168				+0.111	–0.111	–0.056
192				+0.111		
216				+0.056		–0.056
264					+0.111	–0.056
312					+0.111	–0.056
360					+0.111	–0.056
408					+0.097	–0.042
456					+0.014	+0.042
504						+0.056
552						+0.056
600						+0.056
648						+0.056
696						+0.056
744						+0.056
792						+0.049
840						+0.063

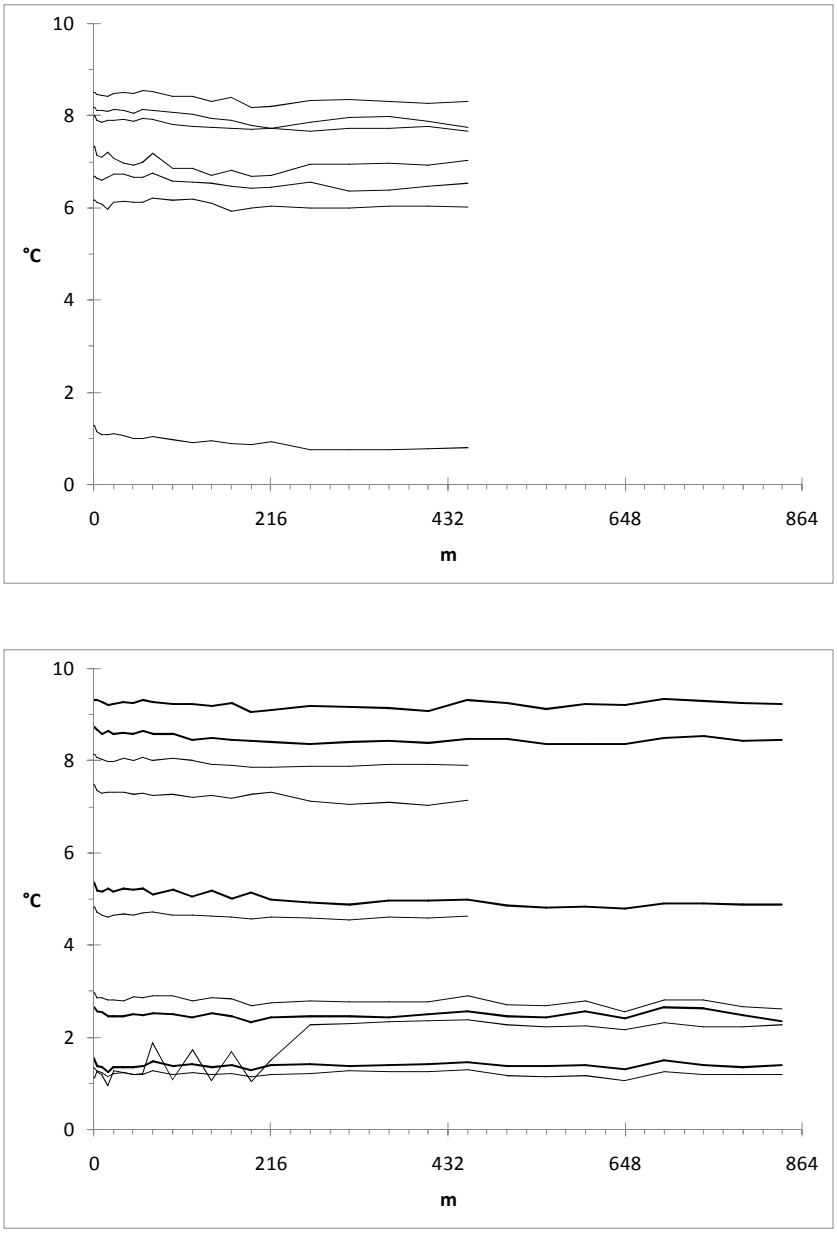

Figure 4.17 *The temperature profiles for the seven interference measurements made in 2005 (above) and the eleven measurements in 2007 (below) show mostly stable temperatures. The thick lines show the five complete two-way measurements made in 2007. One of the thin lines is exceptional. It shows a night when return was possible just to 216 m, and the late-night temperatures close to 0°C for the thermometers at 72, 120, 168 and 264 metres and beyond are missing due to an unfinished measurement.*

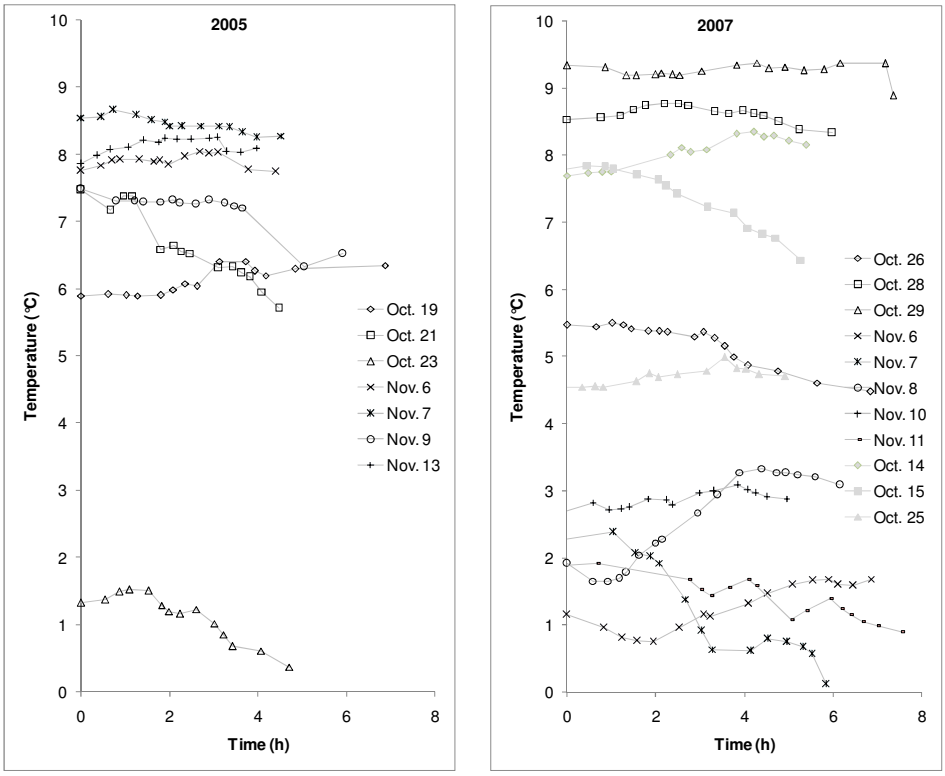

Figure 4.18 *The change of temperature during the nights with successful interference measurements up to 432 m in 2005 and up to 864 m on 26 Oct. – 11 Nov. and up to 432 m on 14 Oct. – 25 Oct. in 2007. The changes for 2005 were not considerably larger than those for 2007, but missing cloud cover continually impeded the observations. In 2007, the graph for 7 Nov. gives an example of "the worst successful night" with extreme temperature conditions for interference measurements (the same exceptional line as in Fig. 4.17). Observations during the first six hours proceeded as usual, regardless of the drop in temperature, because interferences at short distances were quite easy to find. After six hours, a more than two degree drop in temperatures prevented the observers from finding the longer and more difficult 432 m and 864 m interferences. Also, thickening fog and humidity started to impede measurements at the end of this observation night.*

4.3.3 Corrections due to mirrors

The previously determined thicknesses of the mirrors used at Nummela are listed in Table 4.5; the array was identical in 2005 and 2007. Though light reflects from the front surface of a mirror, the centre of the mirror body is used in the projection measurements; the different thicknesses necessitate making corrections. For every distance 0–v, the mirror body correction $(D_v–D_0) / 2$ is computed, where D_v and D_0 are the thicknesses.

Between mirrors 0 and 1, the scale-determining quartz gauge is placed between the glass surfaces, whereas light travels between the shorter aluminium-covered surfaces above and below it. A correction of –11 nm/m ±40 nm/m has been used since the latest resurfacing of the mirrors in 1998. This value is related to the thicknesses of the aluminium layers on mirrors 0 and 1. It is much smaller than those which were used in previous measurements, but the degree of uncertainty of the determination has increased. Later determinations of correction have yielded slightly larger values, but with still larger degrees of uncertainty; the procedure is difficult and the mirror surfaces are not perfectly flat.

Table 4.5 *Mirrors.*

Pillar	Mirror no.	Thickness at 20°C (mm)	Interference	Mirror body correction (mm)
0	40	19.985		
1	36	20.001		
6	38	19.932		
24	35	19.843	0 – 6 – 24	–0.071
72	53	19.981	0 – 24 – 72	–0.002
216	39	19.966	0 – 72 – 216	–0.010
432	41	19.959	0 – 216 – 432	–0.013
864	37	19.983	0 – 432 – 864	–0.001

4.3.4 Geometric corrections

The height reference at the Nummela Standard Baseline is the top surface of underground marker 0. Table 4.6 shows that the height difference to the other end of the baseline is approximately 4 m. The corrections, ds_{vert}, for reducing the final results, s (slope distances), to the reference height level (Table 4.7) are computed using a well-known formula:

$$ds_{vert} = \sqrt{\left(s^2 - \left(h_v - h_0\right)^2\right) / \left(\left(1 + \frac{h_0}{R}\right)\left(1 + \frac{h_v}{R}\right)\right)} - s, \qquad \text{(Eq. 4.12)}$$

where h_0 and h_v are the heights of the centres of mirrors 0 and v above underground marker 0, and R is the radius of the Earth. Here, R = 6 370 km.

Table 4.6 *Height differences (mm) between the top surfaces of the underground markers and the height references on the observation pillars. The height reference is one of the three iron supports sticking out of the concrete pillar at the front on pillar 0 and at the back on the other pillars (the point is not necessarily the same every year, e.g. pillar 24 was reconstructed in 2007; and at pillar 0 the centre of the support was measured in 1996 and the edge of the support in 2005 and 2007).*

	Underground marker			Observation pillar		
	1996	**2005**	**2007**	**1996**	**2005**	**2007**
0	**0.0**	**0.0**	**0.0**	+1 515.3	+1 516.9	+1 516.9
24	–101.6	–101.7	–101.8	+1 406.2	+1 406.2	+1 406.9
72	–377.9	–377.8	–377.8	+1 166.2	+1 166.6	+1 166.4
216	–1 118.2	–1 118.1	–1 118.1	+467.0	+466.9	+467.2
432	–2 244.0	–2 243.7	–2 243.8	–565.6	–565.1	–565.1
864	–3 959.2	–3 959.4	–3 959.4	–2 606.0	–2 607.9	–2 607.6

Table 4.7 *Heights (mm) of the mirror centres above underground marker 0 and vertical reductions (mm) made to the slope distances in order to correct the slope distances to the reference height level of underground marker 0.*

	Length	**Mirror centre 2005**		**Mirror centre 2007**	
	(mm)	**Height**	**Reduction**	**Height**	**Reduction**
0		+1 691		+1 692	
24	24 033	+1 575	–0.286	+1 577	–0.281
72	72 015	+1 344	–0.853	+1 346	–0.848
216	216 053	+652	–2.538	+653	–2.538
432	432 095	–378	–4.998	–378	–5.003
864	864 123	–2 418	–9.720	–2 418	–9.725

Table 4.8 *Horizontal distances between the underground markers and the mirror centres, with non-parallelism corrections. The differences between the horizontal distances in 2005 and 2007 reveal larger than 1 mm deviations from the straight line between the mirror centres. These deviations are insignificant for the result and small enough not to block the light beams.*

	2005		**2007**	
	Distance (mm)	**Correction (mm)**	**Distance (mm)**	**Correction (mm)**
0	2 021		2 022	
24	2 020	+0.000	2 019	+0.000
72	2 023	+0.000	2 020	+0.000
216	2 001	+0.001	2 001	+0.001
432	1 992	+0.001	1 989	+0.001
864	2 093	+0.003	2 097	+0.003

The air pressure slightly increases from 0 m to 864 m due to the height difference. This causes a small difference in the progress of the light beams between mirrors 0 and 1 and for longer baseline sections. The necessary correction, ds_p, is computed using the following formula (Kääriäinen et al. 1992):

$$ds_p = -1.734 \times 10^{-8}\, dh\, s, \qquad \text{(Eq. 4.13)}$$

in which dh is the height difference between mirror 0 and the other mirror and s is the distance to be measured. All quantities in the formula are in metres. The correction ds_p is negative when pillar 0 is higher than the other pillars.

In addition to vertical geometrical reductions, small horizontal geometrical reductions (non-parallelism corrections) are necessary since the straight line between the mirror centres on the observation pillars is not exactly parallel with the chain between the underground markers, with both being projected onto a horizontal plane (Table 4.8).

4.3.5 Projection corrections

With projection measurements, the temporary locations of the mirrors on the observation pillars are projected onto the line between the underground benchmarks. The principle is shown in Fig. 4.19, while the practical arrangements are shown in Figs. 4.20–4.22 and an illustration of the underground markers is provided in Fig. 4.23.

The temporary mirror locations associated with the interference observations and with the projection measurements (at so-called projection positions) are recorded relative to the permanently fixed transferring bars with a 1 µm reading accuracy using the transferring device (Fig. 4.7). This instrument is checked daily on a transferring bar, which is permanently fixed to a sturdy angle iron and installed on the unoccupied old pillar close to the 24-m pillar. Variations in these checks will remain within a few µm if the temperature of the instrument is balanced to match the outdoor temperature. To obtain the projection corrections from the transferring bars to the underground markers, theodolite-based, high-precision measurements are needed before and after, and usually also during, the long-lasting interference measurement period.

Wild T2002 Theomat (no. 346317) and Leica TC2003 (no. 439351) theodolites were used to measure the angles between the mirrors and the underground markers. The reading accuracy was 0.1 mgon. The theodolites are usually aimed at two distant mirrors (D_1 and D_2 in Fig. 4.19), preferably as far away as possible, without at the same time causing difficulties in visibility. During the dark autumn days, visibility can be improved by showing light with a torch either from behind the mirror to the see-through centre cross of the mirror or from in front of the mirror to the luminous tag above the mirror. The computation gives two slightly different projection values (one for each distant mirror), of which the weighted average value is then used. The weights are directly proportional to the distances to the distant mirrors. The mirror to be

projected (*M* in Fig. 4.19) is visualized using a mirror index, an auxiliary target that is strung alternately in front of (*M*–, for the 1st and 4th angle observation set) and behind (*M*+, the 2nd and 3rd set) the mirror. Observations are made using the small target hole of the mirror index (Fig. 4.20). For the computation, the average value gives the location of the centre point independent of the thickness of the mirror. There are several target holes in the plumbing rod, *L*, which is adjusted above the underground marker, *U*; the smallest of these target holes is observed. The instrument is observed in two positions (with the long level turned along the baseline direction, either to the "road side, L_{tp}", or to the "forest side, L_{mp}", with a 180° rotation between them), and in two theodolite face positions (I, II) for every four observation sets. As a concluding example, the observation procedure for the first angle observation set is as follows: (I) D_1, D_2, *M*–, L_{tp}, L_{mp}, (II) L_{mp}, L_{tp}, *M*–, D_2, D_1, where I and II refer to the two theodolite face positions. In the second and third sets, *M*– is replaced by *M*+, and again in the 4th set *M*– is observed.

The distances were measured with Metri and Richter steel tapes (no. VJ6675 and no. VJ6837). The reading accuracy was 0.1 mm; due to the different tape corrections, the difference between the two tapes was much larger before applying the corrections from the calibrations. Distances are measured from the reference point of the theodolite to the sharp top point of the plumbing rod and to the index line on the top surface of the mirror frame (Fig. 4.20). Distance observations are made first, since they are more exposed to disturbances (e.g. that the instruments do not stay levelled) than the angle observations. All of the instruments must stay levelled during the observations (especially theodolite; the plumbing rod is always re-levelled when turned to another position). Also, with distance observations there are two positions for the plumbing rod (the long level turned perpendicular to the baseline direction, either the "0 side, L_0", or the "864 side, L_{864}", with a 180° rotation between them). An example of an observation procedure for distances is as follows: (I) $T–L_0$, $T–L_{864}$, (II) $T–L_{864}$, $T–L_0$, $T–M$, (I) $T–M$, where *T* is the theodolite and I and II refer to the two tapes. The observed distances need some geometrical reductions (for sloping, based on vertical angle observations, and for eccentricity, depending on the location of the reference point in the theodolite), tape corrections (based on calibrations) and corrections due to thermal expansion (based on temperature observations).

For a preliminary computation of the projections, approximate distances can be used for the long triangle sides, $M–D_i$, from the mirror that is to be projected to the distant mirrors. For the final computation, the long triangle sides are obtained from the distances between the transferring bars and the transfer readings. The thicknesses of the mirrors (Table 4.5) must also be taken into account: for the mirror to be projected, the centre of the mirror is measured and approximately 1 cm must be added to the transfer reading. When aiming at a distant mirror from behind, the distance is 2 cm shorter than to the front surface used for the transfer reading.

The results are presented in Tables 4.9 and 4.10, in which the measure of uncertainty is expressed as an experimental standard deviation of the mean, according to GUM (BIPM 2008b). In addition to angle and distance measurements, recording the associated transfer readings is an essential part of projection measurements and computation. The observed angle *M–T–L* (Fig. 4.19) is very small and its geometry varies. Therefore, to be sure about the correct signs of the (small) projection corrections, manual checking of the projections is recommended in addition to making calculations with computer programmes.

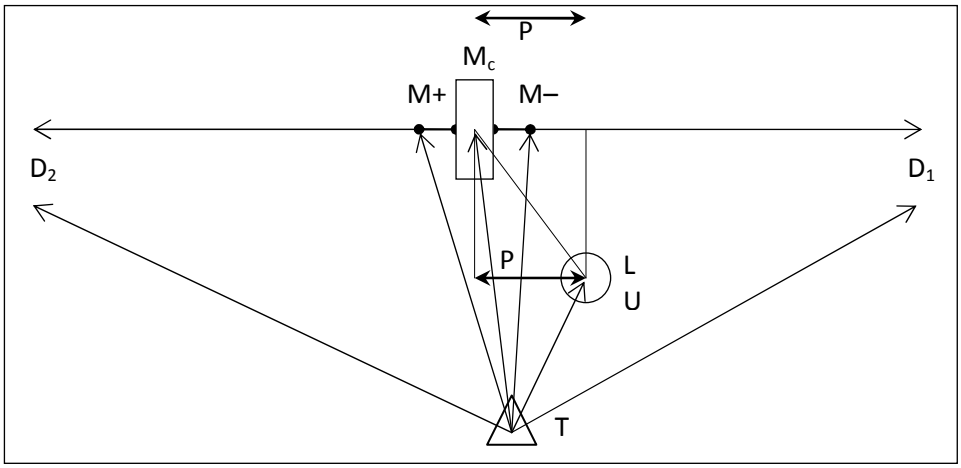

Figure 4.19 *Geometry of the projection measurements. Theodolite (T) on a tripod is used to measure the angles between the mirror centre (M_c), the plumbing rod (L) above the underground marker (U) and the distant mirrors (D_1, D_2). The mirror centre is visualized with a special target, fixed by turns symmetrically on both sides of the mirror (M–, M+). Mechanical plumbing is used to visualize the underground marker. To keep vertical angles small, the theodolite telescope and the top of the plumbing rod should be at about the same height as the mirror centre. To minimize uncertainty caused by the measurement geometry, the theodolite should be placed horizontally on approximately the same line as the plumbing rod and the mirror centre; for visibility, the plumbing rod may even be turned aside when making observations to the mirror. Four sets of horizontal angles are observed in two telescope face positions. Distances T–U and T–M are obtained using tape measurements, and the long distances from M to D_1 and D_2 can be first estimated and computed afterwards. The figure is not drawn to scale: typically T–U is 2 m, T–M is 4 m and the angles between them are close to zero. Projections P, which are a couple of centimetres at maximum, are computed with formulas from plane geometry.*

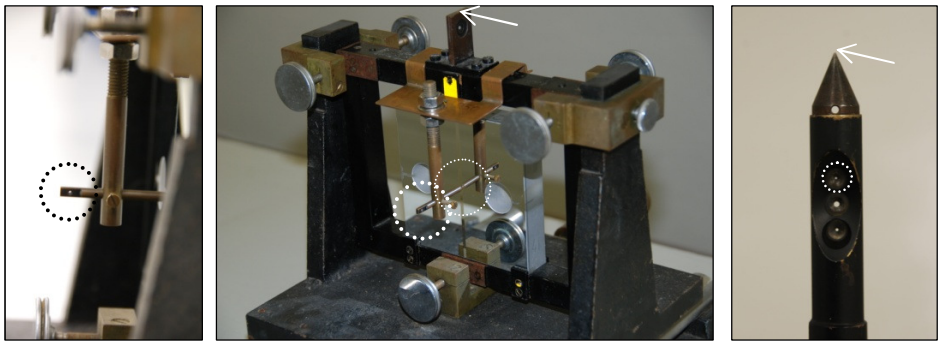

Figure 4.20 *Target points in angle observations for projection measurements. The centre point of the body of a mirror is accessed with the mirror index (left and centre), which is adjusted perpendicular to the mirror surface at the centre of it. The reflecting image helps with the adjustment. Both sides of the mirrors need to be measured. The smallest of the four pinholes is observed at the top of the plumbing rod (right). The points to be used for tape measurements are marked with arrows. Symmetry between the observation series must be ensured: it is important that the target holes in the mirror index and in the plumbing rod are always adjusted perpendicular to the aiming direction from the theodolite and that they appear exactly circular in the telescope.*

Figure 4.21 *Arrangements for projection measurements. The theodolite and the (top of the) adjustable plumbing rod are set up at about the same height as the mirror centre and perpendicular to the baseline (left). Marking the location of the theodolite with a wooden stick in the ground helps with finding the best location for later measurements. Four persons are needed for a properly performed tape measurement: two people holding the tape at a constant strain and two people reading it (right).*

Figure 4.22 *A plumbing rod with two levels is adjusted above an underground marker using a special tripod with a stage slide system (left). A set of adaptor bars can be used to adjust the height of the plumbing rod (right).*

Figure 4.23 *The baseline lengths in the final results are the distances between the centres of the holes in the benchmark bolts of the underground markers, reduced to a reference height level.*

After making the interference measurements, the mirror equipment is removed from the observation pillars and replaced with forced-centring plates for calibration measurements in order to transfer the scale further using EDM instruments. The Kern-type plates are fixed onto heavy iron plates, which are levelled and adjusted and installed permanently (until the next interference measurements), standing on the same supports as the ones onto which the mirror rails were installed. Adapter plates with a 5/8 inch thread are available to fix most EDM instruments onto the Kern-type plates. Reverse projections from the underground markers to the forced-centring plates are needed to utilize the baseline lengths in the calibrations.

Table 4.9 *Projections, P, transfer readings, L, and projection corrections to distance 0–v: $P_v + L_v - P_0 - L_0$ (mm, with experimental standard deviations, $s(\bar{q})$, of the mean) in 2005.*

Date 2005	P_0	L_0	$P_0 + L_0$	P_{24}	L_{24}	$P_{24} + L_{24}$
3 Oct.	–0.8618	10.8875	10.0257			
4 Oct.				+9.2256	10.2875	+19.5131
10 Oct.				+9.2228	10.2775	+19.5003
28 Oct.	–1.0980	10.8865	9.7885			
10 Nov.	–0.9471	10.8930	9.9459			
15 Nov.				+9.0351	10.4850	+19.5201
17 Nov.	–1.0222	10.9005	9.8783			
18 Nov.	–0.9878	10.8985	9.9107			
24 Nov.	–0.9250	10.8990	9.9740			
			9.9205			+19.5112
			±0.0336			±0.0058
Proj.corr.						+9.5907
$s(\bar{q})$						±0.0341

Date 2005	P_{72}	L_{72}	$P_{72} + L_{72}$	P_{216}	L_{216}	$P_{216} + L_{216}$
5 Oct.	–15.4898	21.1920	+5.7022			
7 Oct.				+3.7278	7.2770	+11.0048
2 Nov.				+2.0409	8.9320	+10.9729
11 Nov.	–16.0121	21.7695	+5.7574			
29 Nov.				+1.9834	8.9575	+10.9409
			+5.7298			+10.9729
			±0.0276			±0.0184
Proj.corr.			–4.1907			+1.0524
$s(\bar{q})$			±0.0435			±0.0383

Date 2005	P_{432}	L_{432}	$P_{432} + L_{432}$
8 Oct.	17.1960	15.0210	+32.2170
1 Nov.	14.0457	18.2075	+32.2532
23 Nov.	14.0137	18.2075	+32.2212
			+32.2305
			0.0114
Proj.corr.			+22.3100
$s(\bar{q})$			±0.0355

Table 4.10 *Projections, P, transfer readings, L, and projection corrections to distance 0–v: $P_v + L_v - P_0 - L_0$ (mm, with experimental standard deviations, $s(\bar{q})$, of the mean) in 2007.*

Date 2007	P_0	L_0	$P_0 + L_0$	P_{24}	L_{24}	$P_{24} + L_{24}$
1 Oct.	–0.8268	11.4005	+10.5737			
8 Oct.				+9.0829	14.4570	+23.5399
18 Oct.	–0.9016	11.4280	+10.5264			
23 Oct.				+9.1535	14.3335	+23.4870
2 Nov.	–0.9146	11.4280	+10.5134			
6 Nov.				+9.2001	14.3325	+23.5326
12 Nov.	–0.9089	11.4270	+10.5181			
16 Nov.				+9.2751	14.3545	+23.6296
			+10.5329			+23.5473
			±0.0139			±0.0298
Proj.corr.						+13.0144
$s(\bar{q})$						±0.0329

Date 2007	P_{72}	L_{72}	$P_{72} + L_{72}$	P_{216}	L_{216}	$P_{216} + L_{216}$
3 Oct.				+4.2409	10.1090	+14.3499
4 Oct.	–17.8179	24.2205	+6.4026			
22 Oct.				+3.2269	11.1105	+14.3374
24 Oct.	–15.5792	22.0280	+6.4488			
15 Nov.				+3.3059	11.0680	+14.3739
21 Nov.	–15.6214	22.0410	+6.4196			
			+6.4237			+14.3537
			±0.0135			±0.0107
Proj.corr.			–4.1092			+3.8208
$s(\bar{q})$			±0.0193			±0.0175

Date 2007	P_{432}	L_{432}	$P_{432} + L_{432}$	P_{864}	L_{864}	$P_{864} + L_{864}$
2 Oct.	+16.9705	14.2125	+31.1830			
9 Oct.				–24.0662	21.8700	–2.1962
19 Oct.	+16.3168	14.8620	+31.1788			
25 Oct.				–14.5467	12.3020	–2.2447
1 Nov.				–14.4953	12.3025	–2.1928
5 Nov.	+16.3117	14.8595	+31.1712			
13 Nov.				–14.5166	12.3015	–2.2151
14 Nov.	+16.2874	14.8610	+31.1484			
			+31.1704			–2.2122
			±0.0077			±0.0119
Proj.corr.			+20.6375			–12.7451
$s(\bar{q})$			±0.0159			±0.0183

4.4 Computation of baseline lengths

The distances between the transferring bars are the final lengths between the observation pillars based on the interference observations and transfer readings, as listed in Tables 4.13–4.25. They cannot be used in further works as such. With a set of corrections, they can be projected onto and reduced to the distances between the underground markers, and hence, become accessible. The final lengths from the interference measurements are presented in Table 4.26 for autumn 2005 and in Table 4.27 for autumn 2007.

The projection corrections are the largest corrections, ranging now from 1 mm to 22 mm. Large values can only be avoided through careful planning and the construction of baseline structures. Much larger values than those obtained at Nummela would remarkably increase the uncertainty of the measurement. Even with favourable geometry, the determination of projection corrections is the main source of uncertainty of measurement. This also explains why the combined uncertainty can be smaller for longer lengths than for shorter lengths; the success and uncertainty of the projection measurements do not depend on the length. The uncertainty of the projection measurements for underground marker 0 was reduced between 2005 and 2007, possibly due to the new drainage system built in 2007. This influences all distances and uncertainties, as all projection corrections are computed relative to underground marker 0.

The vertical corrections to the level of underground marker 0, which range from 0 mm to 10 mm, are necessary because of the 4 m height difference between the ends of the baseline and because of the curvature of the Earth. The height differences between the underground markers are also not equal with the height differences between the mirrors, which have to be on the same sloping line in space.

Even the air-pressure difference correction is related to the height differences. This correction, as well as the corrections due to the different dimensions of the mirrors, is small. The line between the mirrors is also exactly straight horizontally, whereas the line between the underground markers is not, giving cause for a very small non-parallelism correction.

4.4.1 Computation of the actual length of the quartz gauge

A piece of quartz tube simulates the thermal behaviour of the quartz gauge in the Väisälä interference comparator. The piece is placed in the same stand as the quartz gauge and equipped with two mercury thermometers (Fig. 4.24) that measure the temperature of the inner (t_i) and the outer (t_o) surface of the tube. The thermometers are read twice for every 6–1–0 or 0–1–6 interference. The average values of the temperature readings, t_i and t_o, with corrections dt interpolated from the calibration certificates, are presented in Tables 4.11 and 4.12; t is the corrected average temperature of t_i and t_o and p is the corrected atmospheric pressure from a Thommen aneroid barometer. The barometer was compared with the FGI Fuess mercury barometer before and after performing the interference measurements. The quartz gauge lengths, l, for the interference

measurements done in 2005 (Table 4.11) were computed using the following formula (see Section 3.3):

$$l_{VIII} = 151.322 + 0.4003(t-20) + 0.00141(t-20)^2 + 0.0000605(t-20)^3 - 0.00347(p-760). \quad \text{(Eq. 4.14)}$$

Likewise, the interference measurements done in 2007 (Table 4.12) were computed using the formula

$$l_{VIII} = 151.361 + 0.4003(t-20) + 0.00141(t-20)^2 + 0.0000605(t-20)^3 - 0.00347(p-760). \quad \text{(Eq. 4.15)}$$

Here, l is in µm, and needs to be added to 1 m, while t is the temperature in °C and p is the pressure in mmHg.

Table 4.11 *Computation of the length of quartz gauge no. VIII for the seven interference measurements in autumn 2005. The temperatures are in °C, the air pressures in mmHg and the lengths in µm (+ 1 m).*

Date and time	t_i	$d\,t_i$	t_i+dt_i	t_o	$d\,t_o$	t_o+dt_o	t	p	*Length*
19 Oct. 21:27	6.105	–0.027	6.078	6.020	–0.002	6.018	6.05	754.3	145.867
21:44	6.185	–0.027	6.158	6.150	–0.002	6.148	6.15	754.3	145.909
22:45	6.475	–0.029	6.446	6.590	–0.003	6.587	6.52	754.0	146.054
23:21	6.650	–0.030	6.620	6.610	–0.003	6.607	6.61	753.9	146.092
21 Oct. 21:31	6.870	–0.031	6.839	6.700	–0.003	6.697	6.77	741.2	146.197
21:48	6.775	–0.031	6.744	6.750	–0.004	6.747	6.75	741.3	146.188
22:47	6.705	–0.030	6.675	6.600	–0.003	6.597	6.64	741.7	146.143
23:06	6.595	–0.030	6.565	6.520	–0.003	6.517	6.54	741.7	146.106
23 Oct. 21:47	1.905	–0.045	1.860	1.765	–0.026	1.739	1.80	741.7	144.202
22:05	1.610	–0.047	1.563	1.485	–0.028	1.457	1.51	741.9	144.083
22:50	1.660	–0.047	1.613	1.590	–0.027	1.563	1.59	742.1	144.114
23:16	1.495	–0.048	1.447	1.295	–0.030	1.265	1.36	742.2	144.019
6 Nov. 21:27	8.110	–0.039	8.071	8.110	–0.006	8.104	8.09	751.9	146.679
21:46	8.130	–0.039	8.091	8.105	–0.006	8.099	8.10	751.9	146.682
22:28	8.115	–0.039	8.076	8.185	–0.006	8.179	8.13	752.3	146.694
22:50	8.260	–0.040	8.220	8.280	–0.007	8.273	8.25	752.2	146.741
7 Nov. 21:49	8.615	–0.042	8.573	8.625	–0.007	8.618	8.60	754.3	146.870
22:05	8.605	–0.042	8.563	8.595	–0.007	8.588	8.58	754.3	146.863
22:55	8.520	–0.041	8.479	8.560	–0.007	8.553	8.52	754.5	146.838
23:19	8.535	–0.041	8.494	8.570	–0.007	8.563	8.53	754.6	146.843
9 Nov. 21:00	7.480	–0.035	7.445	7.395	–0.005	7.390	7.42	758.7	146.393
21:18	7.470	–0.035	7.435	7.440	–0.005	7.435	7.44	758.7	146.399
22:06	7.400	–0.034	7.366	7.440	–0.005	7.435	7.40	758.5	146.387
22:25	7.400	–0.034	7.366	7.400	–0.005	7.395	7.38	758.4	146.379
13 Nov. 19:00	8.220	–0.039	8.181	8.275	–0.007	8.268	8.22	748.3	146.746
19:21	8.290	–0.040	8.250	8.305	–0.007	8.298	8.27	748.1	146.766
20:03	8.300	–0.040	8.260	8.325	–0.007	8.318	8.29	748.2	146.771
20:28	8.320	–0.040	8.280	8.315	–0.007	8.308	8.29	748.2	146.773

Table 4.12 *Computation of the length of quartz gauge no. VIII for the 11 interference measurements in autumn 2007. The temperatures are in °C, the air pressures in mmHg and the lengths in μm (+ 1 m).*

Date and time	t_i	$d\,t_i$	t_i+dt_i	t_o	$d\,t_o$	t_o+dt_o	t	p	*Length*
14 Oct. 23:32	8.100	–0.002	8.098	8.115	–0.006	8.109	8.10	749.9	146.732
23:49	8.210	–0.003	8.207	8.210	–0.006	8.204	8.21	749.7	146.772
15 Oct. 01:03	8.420	–0.004	8.416	8.485	–0.007	8.478	8.45	749.3	146.868
01:27	8.425	–0.004	8.421	8.490	–0.007	8.483	8.45	749.3	146.870
15 Oct. 21:30	7.880	–0.002	7.878	7.865	–0.006	7.859	7.87	749.0	146.643
21:58	7.835	–0.001	7.834	7.825	–0.006	7.819	7.83	748.8	146.627
23:05	7.420	0.000	7.420	7.470	–0.005	7.465	7.44	749.0	146.475
23:40	7.400	0.000	7.400	7.430	–0.005	7.425	7.41	749.0	146.463
26 Oct. 00:11	4.730	0.009	4.739	4.790	–0.002	4.788	4.76	765.1	145.358
00:28	4.840	0.009	4.849	4.910	–0.001	4.909	4.88	765.1	145.404
01:46	5.020	0.010	5.030	5.105	0.000	5.105	5.07	765.2	145.478
02:10	5.145	0.009	5.154	5.215	0.000	5.215	5.18	765.1	145.525
26 Oct. 22:58	5.515	0.008	5.523	5.510	–0.001	5.509	5.52	764.6	145.659
23:12	5.520	0.008	5.528	5.520	–0.001	5.519	5.52	764.4	145.663
27 Oct. 00:12	5.495	0.008	5.503	5.485	–0.001	5.484	5.49	764.4	145.651
00:28	5.430	0.008	5.438	5.425	–0.001	5.424	5.43	764.4	145.626
28 Oct. 23:19	8.855	–0.005	8.850	8.835	–0.008	8.827	8.84	754.7	147.003
23:38	8.830	–0.005	8.825	8.810	–0.008	8.802	8.81	754.6	146.994
29 Oct. 00:46	8.660	–0.005	8.655	8.710	–0.007	8.703	8.68	754.2	146.942
01:05	8.715	–0.005	8.710	8.735	–0.007	8.728	8.72	754.1	146.958
29 Oct. 19:43	9.350	–0.007	9.343	9.305	–0.009	9.296	9.32	750.3	147.206
19:57	9.305	–0.007	9.298	9.290	–0.009	9.281	9.29	750.2	147.195
21:24	9.410	–0.008	9.402	9.435	–0.009	9.426	9.41	749.8	147.245
21:52	9.440	–0.008	9.432	9.450	–0.009	9.441	9.44	749.8	147.254
6 Nov. 20:53	1.005	–0.006	0.999	1.030	–0.032	0.998	1.00	743.3	143.907
21:25	1.205	–0.005	1.200	1.255	–0.030	1.225	1.21	743.1	143.995
22:53	1.540	–0.004	1.536	1.565	–0.027	1.538	1.54	742.5	144.131
23:27	1.680	–0.003	1.677	1.715	–0.026	1.689	1.68	742.3	144.191
7 Nov. 21:21	1.510	–0.004	1.506	1.505	–0.028	1.477	1.49	737.3	144.130
21:42	1.155	–0.005	1.150	1.095	–0.031	1.064	1.11	737.3	143.972
23:12	0.910	–0.006	0.904	0.945	–0.032	0.913	0.91	738.0	143.888
23:38	0.895	–0.006	0.889	0.920	–0.033	0.887	0.89	738.1	143.879
8 Nov. 19:08	2.115	–0.002	2.113	2.165	–0.023	2.142	2.13	739.1	144.384
19:29	2.290	–0.001	2.289	2.335	–0.021	2.314	2.30	739.0	144.455
20:54	3.020	0.002	3.022	3.080	–0.015	3.065	3.04	738.5	144.758
21:54	3.440	0.004	3.444	3.430	–0.013	3.417	3.43	738.2	144.916
10 Nov. 18:51	2.940	0.002	2.942	2.970	–0.016	2.954	2.95	731.9	144.742
19:15	2.985	0.002	2.987	2.990	–0.016	2.974	2.98	731.9	144.756
20:20	3.035	0.002	3.037	3.090	–0.015	3.075	3.06	732.3	144.785
20:52	3.050	0.002	3.052	3.120	–0.015	3.105	3.08	732.4	144.794
11 Nov. 21:55	1.720	–0.003	1.717	1.785	–0.026	1.759	1.74	738.4	144.227
22:20	1.840	–0.003	1.837	1.910	–0.025	1.885	1.86	738.6	144.277
23:40	1.430	–0.004	1.426	1.500	–0.028	1.472	1.45	739.1	144.107
12 Nov. 00:12	1.515	–0.004	1.511	1.595	–0.027	1.568	1.54	739.3	144.143

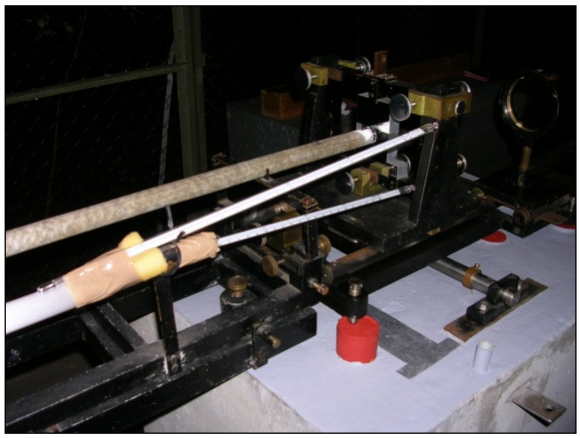

Figure 4.24 *Measuring the temperature of the quartz gauge in the Väisälä comparator.*

Before the year 2005, the quartz gauge was stored all autumn between measurements in the old unheated storehouse, where the temperature differed little from the outdoor measurement conditions. During the measurements done in 2005 and 2007, it was mostly stored in the new heated building, and it was taken outdoors a few hours before the first observations of the 6–1–0 interference. During the first cold observation nights in November 2007, it was found that this may not be adequate since cooling down of the temperature of the quartz gauge may still continue afterwards. This was seen in the large variation when reading the scale of the arc-shaped rail behind mirror 1. However, the variation remained, when the quartz gauge was kept in outdoor temperature all autumn in the newest measurements in 2013. This variation is difficult to distinguish from other thermal variations, but if ignored, it may increase the variation and uncertainty in lengths. Also in the future, keeping the quartz gauge in its stand between mirrors 0 and 1 during the entire several-week observation period should be considered.

4.4.2 Results from interference observations done in 2005

The computation of the seven interference series from autumn 2005 is listed in Tables 4.13–4.17. Again, the measure of uncertainty is expressed as an experimental standard deviation of the mean based on GUM (BIPM 2008b). The computation proceeds from the shortest length to the longest length, though this is not the order of observations, which start and end with the longest length. The accurate but non-permanent distances between the mirrors are obtained from the interference series. For the observation results to be more permanent, the mirror positions are saved along with the simultaneous transfer readings (the distances between the mirror surface and the transferring bar) to obtain the distances between the transferring bars attached to the pillars. They are listed in Table 4.18. They comprise the result obtained between the observation pillars, which is projected onto the distances between the underground markers.

Table 4.13 *Computation of interference 0–1–6. The distance [0–1] is the sum of the lengths of the quartz gauge (from Table 4.11) and the gap between the quartz gauge and mirror 1. The distance [0–6] is six times the distance [0–1], corrected with compensator and refraction corrections.*

Date and time 2005	Obs.	Gap (µm)	[0–1] (µm + 1 m)	Comp. corr. (µm)	Refr. corr. (µm)	[0–6] (µm + 6 m)
19 Oct. 21:27	JJ	3.208	149.075	–108.633	–0.397	785.419
21:44	JJ	2.314	148.222	–103.481	–0.490	785.362
22:45	PH	2.419	148.472	–104.803	–0.238	785.794
23:21	PH	2.471	148.563	–103.105	–0.510	787.766
						786.085
						±0.568
21 Oct. 21:31	JJ	1.157	147.354	28.480	–0.154	912.450
21:48	JJ	2.130	148.318	21.461	–0.228	911.139
22:47	PH	1.840	147.984	24.196	–0.417	911.681
23:06	PH	1.130	147.236	28.202	–0.308	911.311
						911.645
						±0.291
23 Oct. 21:47	JJ	1.578	145.780	17.712	–0.252	892.139
22:05	JJ	1.394	145.476	19.273	–0.377	891.755
22:50	PH	1.709	145.823	17.422	–0.563	891.798
23:16	PH	1.630	145.649	17.567	–0.318	891.142
						891.709
						±0.207
6 Nov. 21:27	JJ	1.893	148.572	13.182	–0.347	904.268
21:46	JJ	3.628	150.310	3.610	–0.500	904.973
22:28	PH	2.314	149.007	11.087	–0.310	904.820
22:50	PH	0.763	147.503	20.823	–0.543	905.300
						904.840
						±0.215
7 Nov. 21:49	JJ	1.025	147.896	36.227	–0.422	923.179
22:05	JJ	2.577	149.439	26.292	–0.461	922.466
22:55	PH	2.182	149.021	26.921	–0.228	920.817
23:19	PH	1.656	148.499	31.540	–0.262	922.274
						922.184
						±0.496
9 Nov. 21:00	JJ	2.918	149.311	3.513	–0.451	898.928
21:18	JJ	1.341	147.740	14.267	–0.252	900.457
22:06	PH	1.183	147.570	14.925	–0.188	900.155
22:25	PH	2.209	148.587	7.543	–0.226	898.842
						899.595
						±0.415
13 Nov. 19:00	JJ	2.366	149.112	17.567	–0.184	912.055
19:21	JJ	1.972	148.738	20.902	–0.190	913.138
20:03	PH	2.840	149.611	14.792	–0.144	912.313
20:28	PH	1.919	148.693	20.902	–0.092	912.965
						912.618
						±0.258

Table 4.14 *Computation of interference 0–6–24. The distance [0–24] is four times the distance [0–6] (from Table 4.13), corrected with compensator and refraction corrections.*

Date and time 2005	*4 × [0–6] (μm + 24 m)*	*Comp. corr. (μm)*	*Refr. corr. (μm)*	*[0–24] (μm + 24 m)*
19 Oct. 20:58	3 141.676	–5.616	–0.553	3 135.507
22:03	3 141.448	–8.179	–0.784	3 132.485
22:19	3 143.175	–7.708	–0.619	3 134.848
23:38	3 151.062	–9.865	–5.008	3 136.189
				3 134.757
				±0.805
21 Oct. 20:55	3 649.799	–3.042	–0.250	3 646.507
22:00	3 644.554	5.402	–1.313	3 648.643
22:13	3 646.724	5.684	–0.551	3 651.857
23:23	3 645.244	10.897	–1.214	3 654.927
				3 650.484
				±1.845
23 Oct. 21:24	3 568.557	45.164	–1.767	3 611.954
22:17	3 567.018	47.289	–1.440	3 612.867
22:32	3 567.192	48.597	–1.282	3 614.507
23:31	3 564.570	51.740	–3.312	3 612.998
				3 613.082
				±0.529
6 Nov. 21:04	3 617.074	52.811	–0.260	3 669.625
21:57	3 619.890	54.638	–0.981	3 673.547
22:10	3 619.280	53.373	–0.220	3 672.433
23:05	3 621.199	53.460	–1.012	3 673.647
				3 672.313
				±0.937
7 Nov. 21:30	3 692.717	–12.302	–0.791	3 679.624
22:16	3 689.865	–10.954	–0.488	3 678.423
22:32	3 683.268	–10.784	–0.545	3 671.939
23:36	3 689.096	–8.298	–1.123	3 679.675
				3 677.416
				±1.848
9 Nov. 20:40	3 595.710	37.372	–0.487	3 632.595
21:29	3 601.827	39.001	–1.263	3 639.565
21:51	3 600.620	39.285	–1.016	3 638.889
22:43	3 595.366	42.208	–0.556	3 637.018
				3 637.017
				±1.569
13 Nov. 18:42	3 648.220	–12.342	–0.028	3 635.850
19:31	3 652.552	–11.390	–0.196	3 640.966
19:48	3 649.253	–10.634	0.385	3 639.004
20:42	3 651.861	–10.218	–0.876	3 640.767
				3 639.147
				±1.184

Table 4.15 *Computation of interference 0–24–72. The distance [0–72] is three times the distance [0–24] (from Table 4.14), corrected with compensator and refraction corrections.*

Date and time 2005	*3 × [0–24] (μm + 72 m)*	*Comp. corr. (μm)*	*Refr. corr. (μm)*	*[0–72] (μm + 72 m)*
19 Oct. 20:43	9 404.272	–18.139	3.521	9 389.654
23:52	9 404.272	–25.937	5.714	9 384.049
				9 386.852
				±2.803
21 Oct. 20:42	10 951.451	–22.108	0.783	10 930.126
23:33	10 951.451	–9.008	0.113	10 942.556
				10 936.341
				±6.215
23 Oct. 21:10	10 839.245	51.001	–0.976	10 889.270
23:44	10 839.245	58.176	–3.245	10 894.176
				10 891.723
				±2.453
6 Nov. 20:53	11 016.939	–100.237	0.645	10 917.347
23:17	11 016.939	–103.246	2.314	10 916.007
				10 916.677
				±0.670
7 Nov. 20:59	11 032.247	–103.952	3.349	10 931.644
23:54	11 032.247	–99.619	1.661	10 934.289
				10 932.966
				±1.322
9 Nov. 20:27	10 911.051	19.693	1.625	10 932.369
22:54	10 911.051	26.159	2.885	10 940.095
				10 936.232
				±3.863
13 Nov. 18:18	10 917.440	9.438	4.877	10 931.755
20:55	10 917.440	9.650	2.630	10 929.720
				10 930.738
				±1.018

For interferences 0–72 and longer, the average value of the observations made at the shorter distance is used every night as a final value to be multiplied (the second column in Tables 4.15–4.17 and 4.21–4.24). For interference 0–24, it is still reasonable to distinguish between the four observations every night, since the 1st and 4th observations are related to the "up" position of the quartz gauge position, whereas the 2nd and 3rd observations are related to the "down" position of the quartz gauge. Another reason for making these distinctions is that the observer changes between the 2nd and 3rd observations. Using the average values from interference 0–24 would also produce equal lengths, but the estimate of uncertainty would be needlessly increased.

Table 4.16 *Computation of interference 0–72–216. The distance [0–216] is three times the distance [0–72] (from Table 4.15), corrected with compensator and refraction corrections.*

Date and time 2005	*3 × [0–72] (μm + 216 m)*	*Comp. corr. (μm)*	*Refr. corr. (μm)*	*[0–216] (μm + 216 m)*
19 Oct. 20:19	28 160.555	134.967	–3.283	28 292.239
20 Oct. 00:33	28 160.555	184.287	–25.521	28 319.321
				28 305.780
				±13.541
21 Oct. 20:24	32 809.022	74.143	–20.409	32 862.756
23:50	32 809.022	85.064	–15.419	32 878.667
				32 870.711
				±7.956
23 Oct. 20:51	32 675.168	11.472	–16.759	32 669.881
24 Oct. 00:22	32 675.168	19.680	–13.820	32 681.028
				32 675.455
				±5.574
6 Nov. 20:38	32 750.031	27.771	–15.246	32 762.556
23:58	32 750.031	24.196	–8.179	32 766.048
				32 764.302
				±1.746
7 Nov. 20:42	32 798.899	21.668	–23.985	32 796.582
8 Nov. 00:13	32 798.899	27.771	–23.909	32 802.761
				32 799.672
				±3.090
9 Nov. 20:03	32 808.696	9.951	–2.181	32 816.466
10 Nov. 00:18	32 808.696	13.423	–0.648	32 821.471
				32 818.968
				±2.502
13 Nov. 18:00	32 792.213	27.141	–23.945	32 795.409
21:14	32 792.213	24.339	–18.222	32 798.330
				32 796.870
				±1.460

Table 4.17 *Computation of interference 0–216–432. The distance [0–432] is two times the distance [0–216] (from Table 4.16), corrected with compensator and refraction corrections.*

Date and time 2005	*2 × [0–216] (μm + 432 m)*	*Comp. corr. (μm)*	*Refr. corr. (μm)*	*[0–432] (μm + 432 m)*
19 Oct. 19:42	56 611.560	31.559	–7.210	56 635.909
20 Oct. 02:34	56 611.560	82.363	–65.855	56 628.068
				56 631.989
				±3.921
21 Oct. 19:45	65 741.423	–73.553	–29.540	65 638.330
22 Oct. 00:13	65 741.423	–48.990	–47.654	65 644.779
				65 641.554
				±3.224
23 Oct. 20:18	65 350.910	–12.847	–31.125	65 306.938
24 Oct. 01:00	65 350.910	–18.726	–24.985	65 307.199
				65 307.068
				±0.130
6 Nov. 20:11	65 528.604	–99.369	–16.339	65 412.896
7 Nov. 00:35	65 528.604	–108.536	–10.554	65 409.514
				65 411.205
				±1.691
7 Nov. 20:15	65 599.343	–125.153	–38.761	65 435.429
8 Nov. 00:46	65 599.343	–124.092	–33.683	65 441.568
				65 438.499
				±3.070
9 Nov. 19:15	65 637.936	–136.041	–18.617	65 483.278
10 Nov. 01:10	65 637.936	–134.564	–12.801	65 490.571
				65 486.925
				±3.646
13 Nov. 17:38	65 593.740	–127.216	–28.990	65 437.534
21:36	65 593.740	–115.214	–20.625	65 457.901
				65 447.717
				±10.184

Table 4.18 *Distances B between the transferring bars (mm) in 2005, using equal weights. For interference observations I (from Tables 4.13–4.17), the difference between the transfer readings, L, and the thickness of mirror 0, D_0 = 19.985 mm, are added: $B_v = I_v - L_v + L_0 + D_0$. $s(\bar{q})$ is the experimental standard deviation of the mean, $\bar{q}$.*

2005	I_6	L_6	L_0	B_6	I_{24}	L_{24}	L_0	B_{24}
19–20 X	0.7861	20.1850	10.8990	11.485	3.1348	10.0440	10.8990	23.975
21–22 X	0.9116	20.2845	10.8980	11.510	3.6505	10.5385	10.8980	23.995
23–24 X	0.8917	20.3070	10.9040	11.474	3.6131	10.5410	10.9040	23.961
6–7 XI	0.9048	20.2400	10.8930	11.543	3.6723	10.5360	10.8930	24.014
7–8 XI	0.9222	20.2500	10.8935	11.551	3.6774	10.5345	10.8935	24.021
9–10 XI	0.8996	20.2420	10.8960	11.539	3.6370	10.5005	10.8960	24.018
13 XI	0.9126	20.2485	10.8920	11.541	3.6391	10.4970	10.8920	24.019
$\bar{q}$				11.520				24.000
$s(\bar{q})$				±0.012				±0.009
2005	I_{72}	L_{72}	L_0	B_{72}	I_{216}	L_{216}	L_0	B_{216}
19–20 X	9.3869	20.2630	10.8990	20.008	28.3058	4.5205	10.8990	54.669
21–22 X	10.9363	21.7900	10.8980	20.029	32.8707	9.0665	10.8980	54.687
23–24 X	10.8917	21.7870	10.9040	19.994	32.6755	8.9225	10.9040	54.642
6–7 XI	10.9167	21.7570	10.8930	20.038	32.7643	8.9325	10.8930	54.710
7–8 XI	10.9330	21.7610	10.8935	20.050	32.7997	8.9460	10.8935	54.732
9–10 XI	10.9362	21.7620	10.8960	20.055	32.8190	8.9460	10.8960	54.754
13 XI	10.9307	21.7610	10.8920	20.047	32.7969	8.9430	10.8920	54.731
$\bar{q}$				20.032				54.704
$s(\bar{q})$				±0.009				±0.015
2005	I_{432}	L_{432}	L_0	B_{432}				
19–20 X	56.6320	9.4625	10.8990	78.053				
21–22 X	65.6416	18.4735	10.8980	78.051				
23–24 X	65.3071	18.2130	10.9040	77.983				
6–7 XI	65.4112	18.2070	10.8930	78.082				
7–8 XI	65.4385	18.2035	10.8935	78.113				
9–10 XI	65.4869	18.2015	10.8960	78.166				
13 XI	65.4477	18.2085	10.8920	78.116				
$\bar{q}$				78.081				
$s(\bar{q})$				±0.022				

4.4.3 Results from interference observations done in 2007

The computation of the eleven interference series and the distances between the transferring bars in autumn 2007 are listed in Tables 4.19–4.25.

Table 4.19 *Computation of interference 0–1–6. The distance [0–1] is the sum of the lengths of the quartz gauge (from Table 4.12) and the gap between the quartz gauge and mirror 1. The distance [0–6] is six times the distance [0–1], corrected with compensator and refraction corrections.*

Date and time 2007	Obs.	Gap (µm)	[0–1] (µm + 1 m)	Comp. corr. (µm)	Refr. corr. (µm)	[0–6] (µm + 6 m)
14 Oct. 23:32	JJ	2.787	149.518	–29.798	–0.398	866.914
23:49	JJ	1.761	148.534	–23.182	–0.230	867.790
15 Oct. 01:03	PH	2.287	149.156	–24.367	–0.298	870.269
01:27	PH	1.998	148.869	–23.940	–0.212	869.059
						868.508
						±0.734
15 Oct. 21:30	JJ	2.314	148.956	17.639	–0.703	910.673
21:58	JJ	2.787	149.413	15.260	–0.558	911.182
23:05	JA	2.077	148.552	20.665	–0.591	911.386
23:40	JA	1.709	148.172	20.902	–0.394	909.541
						910.696
						±0.413
26 Oct. 00:11	JJ	1.946	147.303	–0.511	–0.225	883.083
00:28	JJ	2.866	148.269	–5.296	–0.456	883.864
01:46	PH	2.761	148.239	–4.009	–0.662	884.764
02:10	PH	1.656	147.182	2.403	–0.412	885.082
						884.198
						±0.452
26 Oct. 22:58	JJ	2.287	147.947	2.483	–0.295	889.867
23:12	JJ	1.840	147.503	3.139	–0.466	887.691
27 Oct. 00:12	PH	1.315	146.966	7.263	–0.376	888.681
00:28	PH	0.947	146.572	10.747	–0.267	889.915
						889.038
						±0.532
28 Oct. 23:19	JJ	2.051	149.054	–2.429	–0.243	891.649
23:38	JJ	1.578	148.571	0.536	–0.126	891.836
29 Oct. 00:46	PH	1.656	148.599	2.350	–0.309	893.632
01:05	PH	0.920	147.879	5.375	–0.296	892.351
						892.367
						±0.447
29 Oct. 19:43	JJ	0.657	147.863	18.521	–0.324	905.378
19:57	JJ	1.761	148.956	12.687	–0.246	906.179
21:24	JA	1.604	148.849	13.497	–0.217	906.373
21:52	JA	0.999	148.253	16.779	–0.114	906.184
						906.028
						±0.221

Table 4.19 *continued.*

Date and time 2007	*Obs.*	*Gap (µm)*	*[0–1] (µm + 1 m)*	*Comp. corr. (µm)*	*Refr. corr. (µm)*	*[0–6] (µm + 6 m)*
6 Nov. 20:53	JJ	1.972	145.879	–36.651	–0.168	838.453
21:25	JJ	2.761	146.756	–40.024	–0.134	840.378
22:53	PH	2.524	146.655	–38.809	–0.128	840.991
23:27	PH	3.865	148.056	–45.561	–0.250	842.526
						840.587
						±0.843
7 Nov. 21:21	JJ	1.288	145.419	–31.835	–0.193	840.483
21:42	JJ	1.578	145.549	–32.529	–0.929	839.838
23:12	PH	2.182	146.070	–38.590	–0.364	837.466
23:38	PH	1.446	145.325	–33.535	–0.371	838.044
						838.958
						±0.717
8 Nov. 19:08	JJ	3.339	147.723	–41.827	–0.225	844.287
19:29	JJ	1.394	145.849	–31.051	–0.192	843.851
20:54	PH	2.498	147.256	–36.544	–0.195	846.797
21:54	PH	1.315	146.231	–27.102	–0.136	850.146
						846.270
						±1.446
10 Nov. 18:51	JJ	1.630	146.373	–20.902	–0.531	856.802
19:15	JJ	1.919	146.675	–21.220	–0.477	858.352
20:20	PH	1.078	145.863	–15.531	–0.249	859.397
20:52	PH	1.735	146.529	–20.196	–0.190	858.788
						858.335
						±0.554
11 Nov. 21:55	JJ	2.603	146.830	–15.804	–1.005	864.173
22:20	JJ	3.023	147.301	–18.670	–1.199	863.934
23:40	PH	2.314	146.420	–13.815	–1.185	863.521
12 Nov. 00:12	PH	1.578	145.720	–9.597	–0.254	864.472
						864.025
						±0.201

Table 4.20 *Computation of interference 0–6–24. The distance [0–24] is four times the distance [0–6] (from Table 4.19), corrected with compensator and refraction corrections.*

Date and time 2007	*4 × [0–6] (μm + 24 m)*	*Comp. corr. (μm)*	*Refr. corr. (μm)*	*[0–24] (μm + 24 m)*
14 Oct. 22:14	3 467.656	41.401	–0.745	3 508.312
15 Oct. 00:01	3 471.158	30.117	–1.171	3 500.104
00:23	3 481.075	30.149	0.287	3 511.511
01:40	3 476.237	21.194	–0.737	3 496.694
				3 504.155
				±3.458
15 Oct. 20:57	3 642.693	–125.955	–0.874	3 515.864
22:10	3 644.728	–125.288	–1.860	3 517.580
22:25	3 645.545	–123.507	–1.821	3 520.217
16 Oct. 00:00	3 638.163	–120.916	–0.866	3 516.381
				3 517.511
				±0.971
25 Oct. 23:26	3 532.333	–50.428	–1.307	3 480.598
26 Oct. 00:40	3 535.458	–51.996	–1.875	3 481.587
01:06	3 539.054	–52.295	–2.349	3 484.410
02:26	3 540.327	–56.319	–2.338	3 481.670
				3 482.066
				±0.818
26 Oct. 22:34	3 559.468	–66.851	–0.520	3 492.097
23:24	3 550.762	–66.410	–1.220	3 483.132
27 Oct. 00:00	3 554.724	–66.900	–0.528	3 487.296
00:41	3 559.659	–66.166	–0.934	3 492.559
				3 488.771
				±2.224
28 Oct. 22:53	3 566.597	–55.952	–0.420	3 510.225
23:52	3 567.345	–59.031	–0.720	3 507.594
29 Oct. 00:27	3 574.529	–60.831	–0.775	3 512.923
01:20	3 569.403	–59.904	–1.192	3 508.307
				3 509.762
				±1.191
29 Oct. 19:18	3 621.512	–97.016	–0.866	3 523.630
20:07	3 624.715	–97.500	–0.541	3 526.674
20:37	3 625.492	–98.046	–1.090	3 526.356
22:08	3 624.735	–100.496	–1.445	3 522.794
				3 524.863
				±0.971
6 Nov. 20:17	3 353.813	79.032	–1.037	3 431.808
21:35	3 361.512	80.873	–1.395	3 440.990
22:27	3 363.965	78.549	–1.121	3 441.393
7 Nov. 00:16	3 370.104	74.480	–1.226	3 443.358
				3 439.387
				±2.579

Table 4.20 *continued.*

Date and time 2007	*4 × [0–6] (μm + 24 m)*	*Comp. corr. (μm)*	*Refr. corr. (μm)*	*[0–24] (μm + 24 m)*
7 Nov. 20:45	3 361.933	105.626	–2.691	3 464.868
21:57	3 359.354	108.247	–2.992	3 464.609
22:49	3 349.864	115.730	–5.076	3 460.518
23:59	3 352.178	117.140	–1.570	3 467.748
				3 464.436
				±1.487
8 Nov. 18:50	3 377.146	90.556	–0.657	3 467.045
19:39	3 375.403	87.108	–0.740	3 461.771
20:26	3 387.187	83.125	–0.596	3 469.716
22:14	3 400.582	71.089	–0.669	3 471.002
				3 467.384
				±2.044
10 Nov. 18:25	3 427.209	35.884	–1.655	3 461.438
19:24	3 433.406	33.866	–1.699	3 465.573
20:01	3 437.589	32.930	–0.361	3 470.158
21:06	3 435.152	29.703	–0.615	3 464.240
				3 465.352
				±1.819
11 Nov. 21:30	3 456.693	23.686	–0.631	3 479.748
22:31	3 455.737	23.517	–2.101	3 477.153
23:19	3 454.084	25.408	–1.814	3 477.678
12 Nov. 00:27	3 457.887	25.583	–3.267	3 480.203
				3 478.695
				±0.752

Table 4.21 *Computation of interference 0–24–72. The distance [0–72] is three times the distance [0–24] (from Table 4.20), corrected with compensator and refraction corrections.*

Date and time 2007	*3 × [0–24] (μm + 72 m)*	*Comp. corr. (μm)*	*Refr. corr. (μm)*	*[0–72] (μm + 72 m)*
14 Oct. 22:01	10 512.466	34.004	2.559	10 549.029
15 Oct. 01:54	10 512.466	27.856	1.636	10 541.958
				10 545.494
				±3.535
15 Oct. 20:46	10 552.532	–24.496	–3.043	10 524.993
16 Oct. 00:20	10 552.532	–17.518	2.076	10 537.090
				10 531.042
				±6.049
25 Oct. 23:15	10 446.198	82.363	1.979	10 530.540
26 Oct. 02:39	10 446.198	80.329	–0.032	10 526.495
				10 528.518
				±2.022
26 Oct. 22:24	10 466.314	64.161	2.283	10 532.758
27 Oct. 00:53	10 466.314	63.301	3.163	10 532.778
				10 532.768
				±0.010
28 Oct. 22:37	10 529.286	31.461	1.852	10 562.599
29 Oct. 01:34	10 529.286	26.168	1.637	10 557.091
				10 559.845
				±2.754
29 Oct. 19:08	10 574.590	–2.285	0.476	10 572.781
22:29	10 574.590	–0.363	0.391	10 574.618
				10 573.700
				±0.918
6 Nov. 19:56	10 318.161	146.574	0.953	10 465.688
7 Nov. 00:20	10 318.161	146.286	1.262	10 465.709
				10 465.699
				±0.011
7 Nov. 20:33	10 393.307	91.769	2.910	10 487.986
8 Nov. 00:11	10 393.307	103.858	1.576	10 498.741
				10 493.363
				±5.377
8 Nov. 18:40	10 402.151	100.403	0.363	10 502.917
20:26	10 402.151	87.549	1.870	10 491.570
				10 497.243
				±5.674
10 Nov. 18:15	10 396.057	108.904	0.485	10 505.446
21:17	10 396.057	107.235	2.118	10 505.410
				10 505.428
				±0.018
11 Nov. 21:17	10 436.086	49.404	1.297	10 486.787
12 Nov. 00:39	10 436.086	50.124	1.506	10 487.716
				10 487.252
				±0.464

Table 4.22 *Computation of interference 0–72–216. The distance [0–216] is three times the distance [0–72] (from Table 4.21), corrected with compensator and refraction corrections.*

Date and time 2007	*3 × [0–72] (μm + 216 m)*	*Comp. corr. (μm)*	*Refr. corr. (μm)*	*[0–216] (μm + 216 m)*
14 Oct. 21:42	31 636.481	41.656	–6.444	31 671.693
15 Oct. 02:14	31 636.481	41.118	–13.321	31 664.278
				31 667.986
				±3.708
15 Oct. 20:22	31 593.126	–10.668	–10.863	31 571.595
16 Oct. 00:38	31 593.126	–18.521	–1.727	31 572.878
				31 572.236
				±0.642
25 Oct. 22:58	31 585.553	–60.668	0.288	31 525.173
26 Oct. 02:57	31 585.553	–55.413	–11.951	31 518.189
				31 521.681
				±3.492
26 Oct. 22:09	31 598.303	–33.993	0.176	31 564.486
27 Oct. 01:12	31 598.303	–42.591	2.119	31 557.831
				31 561.158
				±3.328
28 Oct. 22:19	31 679.536	–80.139	–7.991	31 591.406
29 Oct. 01:55	31 679.536	–76.251	–15.283	31 588.002
				31 589.704
				±1.702
29 Oct. 18:55	31 721.100	–88.501	–11.644	31 620.955
22:55	31 721.100	–77.427	–20.537	31 623.136
				31 622.045
				±1.091
6 Nov. 19:36	31 397.097	51.959	–4.027	31 445.029
7 Nov. 00:48	31 397.097	60.096	–4.949	31 452.244
				31 448.636
				±3.608
7 Nov. 20:13	31 480.090	–17.639	–6.055	31 456.396
8 Nov. 00:31	31 480.090	–15.036	–6.301	31 458.753
				31 457.574
				±1.178
8 Nov. 18:26	31 491.729	–9.004	2.017	31 484.742
22:43	31 491.729	–12.589	–8.277	31 470.863
				31 477.803
				±6.940
10 Nov. 17:58	31 516.283	–21.929	–1.485	31 492.869
21:31	31 516.283	–22.541	–0.233	31 493.509
				31 493.189
				±0.320
11 Nov. 21:00	31 461.755	22.884	–6.556	31 478.083
12 Nov. 00:55	31 461.755	18.225	–6.810	31 473.170
				31 475.626
				±2.457

Table 4.23 *Computation of interference 0–216–432. The distance [0–432] is two times the distance [0–216] (from Table 4.22), corrected with compensator and refraction corrections.*

Date and time 2007	*2 × [0–216] (µm + 432 m)*	*Comp. corr. (µm)*	*Refr. corr. (µm)*	*[0–432] (µm + 432 m)*
14 Oct. 21:14	63 335.972	50.439	–9.026	63 377.385
15 Oct. 02:37	63 335.972	59.306	–13.611	63 381.667
				63 379.526
				±2.141
15 Oct. 19:55	63 144.473	33.576	–22.031	63 156.018
16 Oct. 01:12	63 144.473	11.445	2.287	63 158.205
				63 157.111
				±1.093
25 Oct. 22:37	63 043.362	65.368	–3.408	63 105.322
26 Oct. 03:32	63 043.362	80.982	–25.539	63 098.805
				63 102.063
				±3.258
26 Oct. 21:08	63 122.316	30.453	–10.232	63 142.537
27 Oct. 01:53	63 122.316	28.001	–5.287	63 145.030
				63 143.784
				±1.247
28 Oct. 21:54	63 179.408	32.194	–11.983	63 199.619
29 Oct. 02:21	63 179.408	33.855	–17.271	63 195.992
				63 197.806
				±1.814
29 Oct. 18:26	63 244.091	–6.435	–23.623	63 214.033
23:44	63 244.091	9.878	–31.253	63 222.716
				63 218.374
				±4.341
6 Nov. 19:11	62 897.273	85.276	–5.711	62 976.838
7 Nov. 01:12	62 897.273	96.956	–5.817	62 988.412
				62 982.625
				±5.787
7 Nov. 19:43	62 915.149	119.071	–6.357	63 027.863
8 Nov. 18:05	62 955.606	126.660	–1.612	63 080.654
23:05	62 955.606	125.604	–0.020	63 081.190
				63 080.922
				±0.268
10 Nov. 17:36	62 986.378	99.734	–8.221	63 077.891
21:58	62 986.378	91.566	–10.014	63 067.930
				63 072.911
				±4.981
11 Nov. 18:57	62 951.252	95.410	–5.823	63 040.839
12 Nov. 01:16	62 951.252	95.552	–11.511	63 035.293
				63 038.066
				±2.773

Table 4.24 *Computation of interference 0–432–864. The distance [0–864] is two times the distance [0–432] (from Table 4.23), corrected with compensator and refraction corrections.*

Date and time 2007	*2 × [0–432] (μm + 864 m)*	*Comp. corr. (μm)*	*Refr. corr. (μm)*	*[0–864] (μm + 864 m)*
26 Oct. 21:08	126 287.567	80.207	31.731	126 399.505
27 Oct. 03:58	126 287.567	132.984	–8.374	126 412.177
				126 405.841
				±6.336
28 Oct. 21:08	126 395.612	45.204	14.560	126 455.376
29 Oct. 03:07	126 395.612	42.141	–4.815	126 432.938
				126 444.157
				±11.219
29 Oct. 17:35	126 436.749	22.354	33.982	126 493.085
30 Oct. 00:56	126 436.749	–4.758	46.327	126 478.318
				126 485.701
				±7.384
6 Nov. 18:21	125 965.249	73.473	8.144	126 046.866
7 Nov. 18:40	126 055.726	107.849	–13.775	126 149.800
8 Nov. 17:30	126 161.844	80.442	1.661	126 243.947
23:40	126 161.844	74.214	3.841	126 239.899
				126 241.923
				±2.024
10 Nov. 17:01	126 145.822	68.132	11.131	126 225.085
11 Nov. 18:16	126 076.133	98.077	–10.719	126 163.491
12 Nov. 01:48	126 076.133	78.992	–2.386	126 152.739
				126 158.115
				±5.376

Table 4.25 *Distances B between the transferring bars (mm) in 2007, using equal weights. For interference observations I (from Tables 4.19–4.24), the difference between the transfer readings, L, and the thickness of mirror 0, D_0 = 19.985 mm, are added: $B_v = I_v - L_v + L_0 + D_0$. $s(\bar{q})$ is the experimental standard deviation of the mean, $\bar{q}$.*

2007	I_6	L_6	L_0	B_6	I_{24}	L_{24}	L_0	B_{24}
14–15 X	0.8685	20.0390	11.4225	12.237	3.5042	14.3145	11.4225	20.597
15–16 X	0.9107	20.0640	11.4285	12.260	3.5175	14.3305	11.4285	20.601
25–26 X	0.8842	20.0680	11.4265	12.228	3.4821	14.3385	11.4265	20.555
26–27 X	0.8890	20.0645	11.4270	12.237	3.4888	14.3390	11.4270	20.562
28–29 X	0.8924	20.0300	11.4210	12.268	3.5098	14.3270	11.4210	20.589
29–30 X	0.9060	20.0395	11.4220	12.274	3.5249	14.3395	11.4220	20.592
6–7 XI	0.8406	20.0505	11.4275	12.203	3.4394	14.3360	11.4275	20.516
7 XI	0.8390	20.0405	11.4285	12.212	3.4644	14.3530	11.4285	20.525
8 XI	0.8463	20.0435	11.4245	12.212	3.4674	14.3505	11.4245	20.526
10 XI	0.8583	20.0480	11.4245	12.220	3.4654	14.3470	11.4245	20.528
11–12 XI	0.8640	20.0595	11.4260	12.216	3.4787	14.3640	11.4260	20.526
$\bar{q}$				12.233				20.556
$s(\bar{q})$				±0.007				±0.010
2007	I_{72}	L_{72}	L_0	B_{72}	I_{216}	L_{216}	L_0	B_{216}
14–15 X	10.5455	21.9840	11.4225	19.969	31.6680	11.0995	11.4225	51.976
15–16 X	10.5310	21.9990	11.4285	19.946	31.5722	11.1005	11.4285	51.885
25–26 X	10.5285	22.0355	11.4265	19.905	31.5217	11.0875	11.4265	51.846
26–27 X	10.5328	22.0285	11.4270	19.916	31.5612	11.1025	11.4270	51.871
28–29 X	10.5598	22.0275	11.4210	19.938	31.5897	11.0885	11.4210	51.907
29–30 X	10.5737	22.0380	11.4220	19.943	31.6220	11.1105	11.4220	51.919
6–7 XI	10.4657	22.0115	11.4275	19.867	31.4486	11.0810	11.4275	51.780
7 XI	10.4934	22.0305	11.4285	19.876	31.4576	11.0650	11.4285	51.806
8 XI	10.4972	22.0245	11.4245	19.882	31.4778	11.0600	11.4245	51.827
10 XI	10.5054	22.0325	11.4245	19.882	31.4932	11.0700	11.4245	51.833
11–12 XI	10.4873	22.0175	11.4260	19.881	31.4756	11.0715	11.4260	51.815
$\bar{q}$				19.910				51.860
$s(\bar{q})$				±0.010				±0.017
2007	I_{432}	L_{432}	L_0	B_{432}	I_{864}	L_{864}	L_0	B_{864}
14–15 X	63.3795	14.8625	11.4225	79.925	–	–	–	–
15–16 X	63.1571	14.8595	11.4285	79.711	–	–	–	–
25–26 X	63.1021	14.8625	11.4265	79.651	–	–	–	–
26–27 X	63.1438	14.8595	11.4270	79.696	126.4058	12.3285	11.4270	145.489
28–29 X	63.1978	14.8585	11.4210	79.745	126.4442	12.2985	11.4210	145.552
29–30 X	63.2184	14.8615	11.4220	79.764	126.4857	12.3020	11.4220	145.591
6–7 XI	62.9826	14.8625	11.4275	79.533	126.0469	12.3020	11.4275	*145.157
7 XI	63.0279	14.8635	11.4285	*79.578	126.1498	12.3050	11.4285	*145.258
8 XI	63.0809	14.8600	11.4245	79.630	126.2419	12.3025	11.4245	145.349
10 XI	63.0729	14.8630	11.4245	79.619	126.2251	12.3020	11.4245	*145.333
11–12 XI	63.0381	14.8600	11.4260	79.589	126.1581	12.2980	11.4260	145.271
$\bar{q}$				79.681				145.404
$s(\bar{q})$				±0.034				±0.053

* with ½-weight

4.4.4 Final lengths

The distances between the transferring bars are corrected to the final lengths between the underground markers, as shown in Tables 4.26 and 4.27.

Table 4.26 *Computation of baseline length in 2005.*

	0–24 24 m + (mm)	**0–72 72 m + (mm)**	**0–216 216 m + (mm)**	**0–432 432 m + (mm)**
Distance between transferring bars (Table 4.18)	24.000	20.032	54.704	78.081
Projection correction (Table 4.9)	+9.591	–4.191	+1.052	+22.310
Correction to the level of underground marker 0 (Table 4.7)	–0.286	–0.853	–2.538	–4.998
Mirror coating correction (Section 4.3.3)	–0.000	–0.001	–0.002	–0.005
Mirror body correction (Section 4.3.3)	–0.071	–0.002	–0.010	–0.013
Air-pressure difference correction (Section 4.3.4)	–0.000	–0.000	–0.004	–0.016
Non-parallelism correction (Table 4.8)	+0.000	+0.000	+0.001	+0.001
Final length	33.234	14.985	53.203	95.360

Table 4.27 *Computation of baseline length in 2007.*

	0–24 24 m + (mm)	**0–72 72 m + (mm)**	**0–216 216 m + (mm)**	**0–432 432 m + (mm)**	**0–864 864 m + (mm)**
Distance between transferring bars (Table 4.25)	20.556	19.910	51.860	79.681	145.404
Projection correction (Table 4.10)	+13.014	–4.109	+3.821	+20.638	–12.745
Correction to the level of underground marker 0 (Table 4.7)	–0.281	–0.848	–2.538	–5.003	–9.725
Mirror coating correction (Section 4.3.3)	–0.000	–0.001	–0.002	–0.005	–0.010
Mirror body correction (Section 4.3.3)	–0.071	–0.002	–0.010	–0.013	–0.001
Air-pressure difference correction (Section 4.3.4)	–0.000	–0.000	–0.004	–0.016	–0.062
Non-parallelism correction (Table 4.8)	+0.000	+0.000	+0.001	+0.001	+0.003
Final length	33.218	14.950	53.128	95.283	122.864

4.5 Estimation of uncertainty of measurement

4.5.1 Combined uncertainty of the lengths between the underground markers

Since the principle of the Väisälä interference measurement method is essentially simple and straightforward, the list of components involved in the uncertainty of measurement remains rather short. In practice, the performance is extremely laborious because measurements under unfavourable conditions are not possible at all. This self-protective mechanism is the main reason why the results and uncertainties are for the most part not affected by the measurement conditions (if a measurement succeeds). An evaluation of the combined uncertainty of the measurement for the lengths between the underground markers is presented in Tables 4.28 and 4.29.

The evaluation of standard uncertainty due to interference observations, transfer readings and projection measurements is based on statistical analysis, and experimental standard deviations of the means are used (Type A, according to GUM; BIPM 2008b). Figs. 4.25 and 4.26 present an overview of included components. Evaluation of the other components (Type B) is based on calibration results for the absolute length of the quartz gauge and on previous knowledge about the thicknesses of the mirror coatings as well as on experience with the thermal behaviour of the quartz gauge.

For the absolute length of the quartz gauge, an estimated standard uncertainty of 35 nm is reasonable based on the latest absolute calibrations and frequent comparisons. The estimate of uncertainty due to the temperature of the quartz gauge, 20 nm/m, is equivalent to the determination of the temperature with a 0.05° standard uncertainty, which seems realistic. Tables 4.11 and 4.12 show that (with a few exceptions) the observed temperature, t, changes during one half-set with the quartz gauge placed in two positions, 0.1° or less. The estimate of uncertainty is valid only if the quartz gauge is properly stored and handled before and during the measurement.

Some dependence on temperature can be found both in the distances between the mirrors and between the transferring bars, especially for the shortest distances measured in both 2005 and 2007. The mechanism causing this is not clear. Most of this variation seems not to multiply. The variation is of the order of approximately 0.01 mm/°C. The variation is at the same tens of micrometres level as what is often present in the projection measurements at 0. It is not possible to perform interference measurements in warm temperatures in order to examine the variation more thoroughly, but most calibrations utilizing the baseline can also be performed in circumstances close to those that prevail during the interference measurements.

The different thicknesses of the mirror coatings at mirrors 0 and 1 are difficult to determine since the mirror surfaces are not perfectly flat. Therefore, the estimated standard uncertainty must be kept quite large. There is no reason to change the values that were determined for the measurements done in Chengdu, China, in 1998 (see Section 5.4.2). The estimated standard uncertainty was first

20 nm/m, but for the measurements done in Gödöllő, Hungary, in 1999 (Chapter 6) and later in Nummela it was doubled to 40 nm/m. There have been no noteworthy changes (e.g. due to scuffing) to the mirrors and their coatings since 1998. The estimated standard uncertainty was increased just to be on the safe side, since the much smaller uncertainty that was previously achieved when determining the thicknesses of the mirror coatings has not been achieved in the latest determinations. Improving the method for determining the thickness of the mirror coatings is one of the first challenges in decreasing the combined measurement uncertainty.

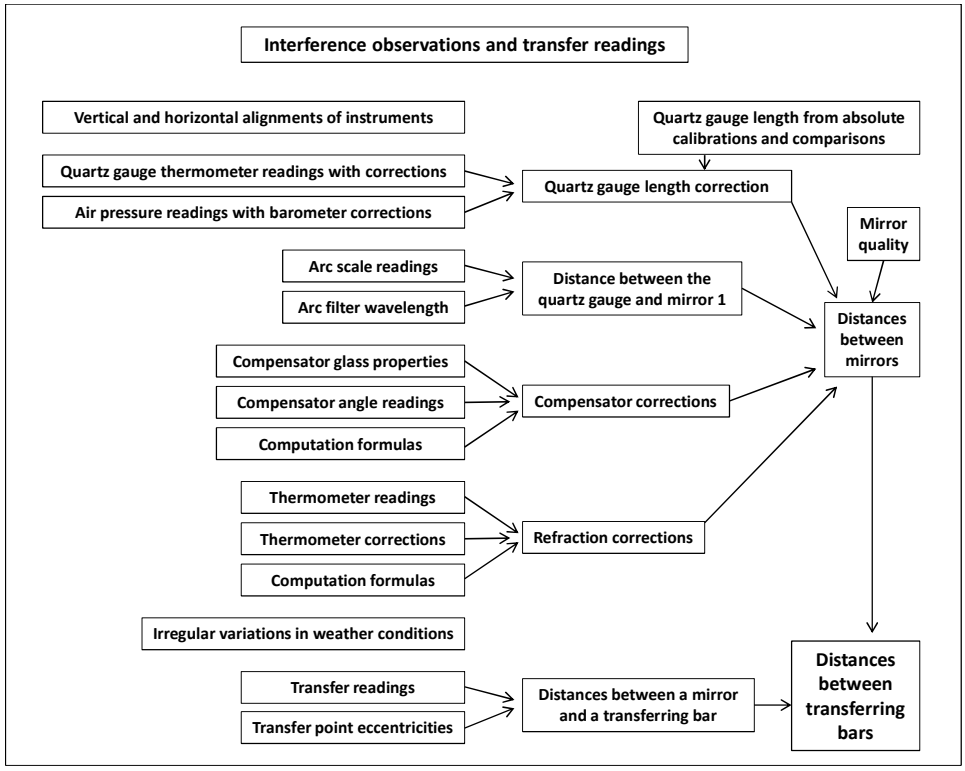

Figure 4.25 *Components to be taken into account when estimating uncertainty of single interference observations and transfer readings (cf. Tables 4.28 and 4.29). Careful work in vertical and horizontal alignments is a prerequisite for successful measurements, but in a comparator in operation, alignments have little significance for the uncertainty of measurement. In the presence of irregular variations in weather conditions it is difficult to measure, but due to the relative measurement method, also they have little significance for the uncertainty of measurement, if the measurement is possible at all.*

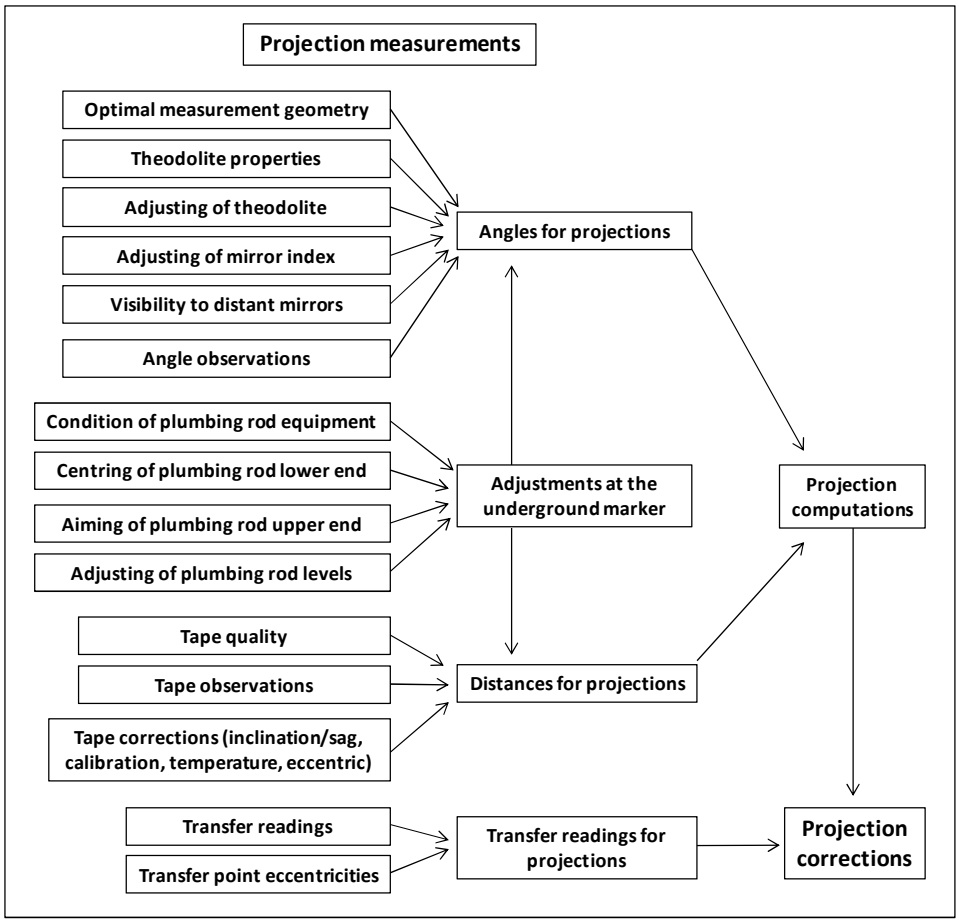

Figure 4.26 *Components to be taken into account when estimating uncertainty of projection measurements (cf. Tables 4.28 and 4.29).*

The uncertainty due to precise levellings is related to the geometrical reductions and evaluated based on the levelling results. This includes both levelling along the baseline and the levelling of instruments on the observation pillars. Smaller than 1 mm uncertainties in the levelled heights are fairly easy to obtain with calibrated instruments, which keeps the uncertainty of the geometrical reductions at a micrometre level.

The combined standard uncertainty in Tables 4.28 and 4.29 has been computed according to GUM (BIPM 2008b) based on the standard uncertainties of listed components. The combined expanded uncertainty is the combined standard uncertainty multiplied by the coverage factor, $k = 2$.

Table 4.28 *Evaluation of the combined uncertainty of measurement in 2005 (μm).*

	0–24	**0–72**	**0–216**	**0–432**
Uncertainty u_B due to interference observations and transfer readings	9	9	15	22
Uncertainty u_P due to projection measurements	34	43	38	35
Uncertainty due to the absolute length of the quartz gauge	1	3	8	15
Uncertainty due to the temperature of the quartz gauge	0	1	4	9
Uncertainty due to the thicknesses of the mirror coatings	1	3	9	17
Uncertainty due to the levellings	0	1	2	2
Combined standard uncertainty u_c	35	44	43	48
Combined expanded uncertainty $U=2u_c$	**70**	**88**	**86**	**96**

Table 4.29 *Evaluation of the combined uncertainty of measurement in 2007 (μm).*

	0–24	**0–72**	**0–216**	**0–432**	**0–864**
Uncertainty u_B due to interference observations and transfer readings	10	10	17	34	53
Uncertainty u_P due to projection measurements	33	19	18	16	18
Uncertainty due to the absolute length of the quartz gauge	1	3	8	15	30
Uncertainty due to the temperature of the quartz gauge	0	1	4	9	17
Uncertainty due to the thicknesses of the mirror coatings	1	3	9	17	34
Uncertainty due to the levellings	0	1	2	2	4
Combined standard uncertainty u_c	34	22	28	45	74
Combined expanded uncertainty $U=2u_c$	**69**	**45**	**55**	**89**	**149**

4.5.2 Some supplementary analysis of uncertainty of measurement

When estimating the uncertainty of interference measurements, it has been customary to compute two uncertainty estimates. In addition to the one previously presented for the distances between the transferring bars, u_B, another one for the distances between the mirror surfaces, u_M, can be computed and compared to it. The former should theoretically be larger than the latter, since it includes possible movements of the observation pillars during the several weeks or months of measurements. It also includes the (very small) degree of

uncertainty of the transfer readings. Only the former is used in the final computation of combined uncertainty, whereas the latter is computed just for scrutiny. The computation method applied here is identical and thus comparable with the computations in the several previous publications on interference measurements.

In Tables 4.30 and 4.31, uncertainties, u_I, for every interference observation stage ($I = 72$, 216, 432 or 864) are derived from experimental standard deviations of the means, $s(\bar{q}_{I,i})$ (from Tables 4.13–4.17 and 4.19–4.24), and the number of observation nights, n_s, using the following formula:

$$u_I = \sqrt{\sum s^2\left(\bar{q}_{I,i}\right)/n_s}. \qquad \text{(Eq. 4.16)}$$

Half nights in 2007 resulted in half (one-way) measurements, and n_{obs} is the number of observations made in one night. The accumulated uncertainties, u_I^{acc}, are obtained from the uncertainties, u_I, by using the formulas for the standard deviations of products and sums. In 2005, they were as follows:

$$\text{0–72:}\quad \sqrt{(3\times1.34)^2+(3.18)^2}\ \mu\text{m} = 5\ \mu\text{m},$$
$$\text{0–216:}\quad \sqrt{(9\times1.34)^2+(3\times3.18)^2+(6.53)^2}\ \mu\text{m} = 17\ \mu\text{m},$$
$$\text{0–432:}\quad \sqrt{(18\times1.34)^2+(6\times3.18)^2+(2\times6.53)^2+(4.71)^2}\ \mu\text{m} = 34\ \mu\text{m},$$

and in 2007:

$$\text{0–72:}\quad \sqrt{(3\times1.85)^2+(3.34)^2}\ \mu\text{m} = 6\ \mu\text{m},$$
$$\text{0–216:}\quad \sqrt{(9\times1.85)^2+(3\times3.34)^2+(3.17)^2}\ \mu\text{m} = 20\ \mu\text{m},$$
$$\text{0–432:}\quad \sqrt{(18\times1.85)^2+(6\times3.34)^2+(2\times3.17)^2+(3.26)^2}\ \mu\text{m} = 40\ \mu\text{m},$$
$$\text{0–864:}\quad \sqrt{(36\times1.85)^2+(12\times3.34)^2+(4\times3.17)^2+(2\times3.26)^2+(7.12)^2}\ \mu\text{m} = 79\ \mu\text{m}.$$

With these accumulated uncertainties, the value, u_{24}, for 0–24, 1.34 µm in 2005 and 1.85 µm in 2007, is treated differently from the other values since it includes a set of components of uncertainty that do not accumulate in the longer distances. These components are mostly related to working with the quartz gauge.

From the accumulated uncertainties, u_I^{acc}, in one observation series, the uncertainties, u_M, for the distances between the mirror surfaces after the entire measurement are estimated by dividing u_I^{acc} by $\sqrt{n_s}$ (Tables 4.30 and 4.31). The uncertainties, u_B, for the distances between the transferring bars are computed in Tables 4.18 and 4.25 and used in the evaluation of combined uncertainty in Tables 4.28 and 4.29. As expected, for all distances the u_M are smaller than the u_B.

Table 4.30 *Comparison of the standard uncertainties of the distances between the mirror surfaces (u_M) or between the transferring bars (u_B) in 2005.*

	0–24	0–72	0–216	0–432
n_s	7	7	7	7
n_{obs}	4	2	2	2
u_I (μm)	1	3	7	5
u_I^{acc} (μm)	1	5	17	34
u_M (μm)	0	2	6	13
u_B (μm)	9	9	15	22

Table 4.31 *Comparison of the standard uncertainties of the distances between the mirror surfaces (u_M) or between the transferring bars (u_B) in 2007.*

	0–24	0–72	0–216	0–432	0–864
n_s	11	11	11	10 + ½	5 + 3×½
n_{obs}	4	2	2	2 (1)	2 (1)
u_I (μm)	2	3	3	3	7
u_I^{acc} (μm)	2	6	20	40	79
u_M (μm)	1	2	6	12	31
u_B (μm)	10	10	17	34	53

4.6. Intermediate summary and conclusions

The computation of baseline lengths (Tables 4.26 and 4.27) and the uncertainty associated with them (Tables 4.28 and 4.29) are summarized in Table 4.32. Previous results have been reported with standard uncertainties, and the same manner of representation is used in Table 4.32, which is an update of the previous versions published by Kääriäinen et al. (1992, p. 48) and Jokela and Poutanen (1998, p. 39). The results are illustrated in Fig. 4.27, now with expanded uncertainties. The new results again show excellent reproducibility and repeatability, confirming the excellent stability of the baseline. The results are the basis for the latest scale transfer measurements discussed in Chapter 9.

The short lengths, 24 m, 72 m and 216 m, in the measurements done during the years 1947−1975 have not been published since there were no underground markers for them yet. Originally, there were only three underground markers: at 0 m, 432 m and 864 m. The longest length could not be observed in 1983 and 2005. The significant changes at 72 m and 216 m between 1977 and 1991 were probably caused by the settling down of the new underground markers after they had been put in place or by the extensive construction work taking place in the neighbourhood (excavation of sand, and new school buildings and sports facilities placed in the large sandpit, the edge of which is, at its closest, 60 m from the baseline). The time series for 24 m and 432 m are impressive; they are also quite consistent for 864 m. When comparing the time series at 432 m and 864 m, a clear correlation is visible, which makes it possible to infer that part of the variation is related to the scale; this becomes apparent especially for the longest distances. Most probably this variation originates when working with the

most problematic multiplication from 1 m to 6 m. Also, sub-millimetre level movements of the underground markers are possible, though hardly discernible. The reconditioning work done at the baseline in 2004 and 2007 seems to have been successful and did not disturb it, since all of the changes from 1996 to 2005 and 2007 were less than 0.2 mm.

Table 4.32 *The baseline lengths at the Nummela Standard Baseline from the 15 interference measurements during the years 1947–2007. These are the lengths between the underground markers, reduced to the height level of underground marker 0. The number following the symbol ± is the numerical value of the combined standard uncertainty.*

Epoch	**0 – 24** mm + 24 m	**0 – 72** mm + 72 m	**0 – 216** mm + 216 m	**0 – 432** mm + 432 m	**0 – 864** mm + 864 m
1947.7	—	—	—	95.46 ±0.04	122.78 ±0.07
1952.8	—	—	—	95.39 ±0.05	122.47 ±0.08
1955.4	—	—	—	95.31 ±0.05	122.41 ±0.09
1958.8	—	—	—	95.19 ±0.04	122.25 ±0.08
1961.8	—	—	—	95.21 ±0.04	122.33 ±0.08
1966.8	—	—	—	95.16 ±0.04	122.31 ±0.06
1968.8	—	—	—	95.18 ±0.04	122.37 ±0.07
1975.9	—	—	—	94.94 ±0.04	122.33 ±0.07
1977.8	33.28 ±0.02	15.78 ±0.02	54.31 ±0.02	95.10 ±0.05	122.70 ±0.08
1983.8	33.50 ±0.02	15.16 ±0.02	53.66 ±0.04	95.03 ±0.06	—
1984.8	33.29 ±0.03	15.01 ±0.03	53.58 ±0.05	94.93 ±0.06	122.40 ±0.09
1991.8	33.36 ±0.04	14.88 ±0.04	53.24 ±0.06	95.02 ±0.05	122.32 ±0.08
1996.9	33.41 ±0.03	14.87 ±0.04	53.21 ±0.04	95.23 ±0.04	122.75 ±0.07
2005.8	33.23 ±0.04	14.98 ±0.04	53.20 ±0.04	95.36 ±0.05	—
2007.8	33.22 ±0.03	14.95 ±0.02	53.13 ±0.03	95.28 ±0.04	122.86 ±0.07

Preliminary results of the interference measurements in autumn 2013 are (within the uncertainty of measurement) equal with the results of 2005 and 2007. Depending on the present and future activities at the baseline, re-measurements with interference measurements, supported with new absolute calibrations and comparisons of the quartz gauges, are necessary every few years. New innovations in absolute long-distance measurements are being developed all the time, and the new results from interference measurements made at the Nummela Standard Baseline can be used for validating or comparing new methods or instruments. So far, the Nummela Standard Baseline still remains the most accurate measurement standard for length measurements under field conditions.

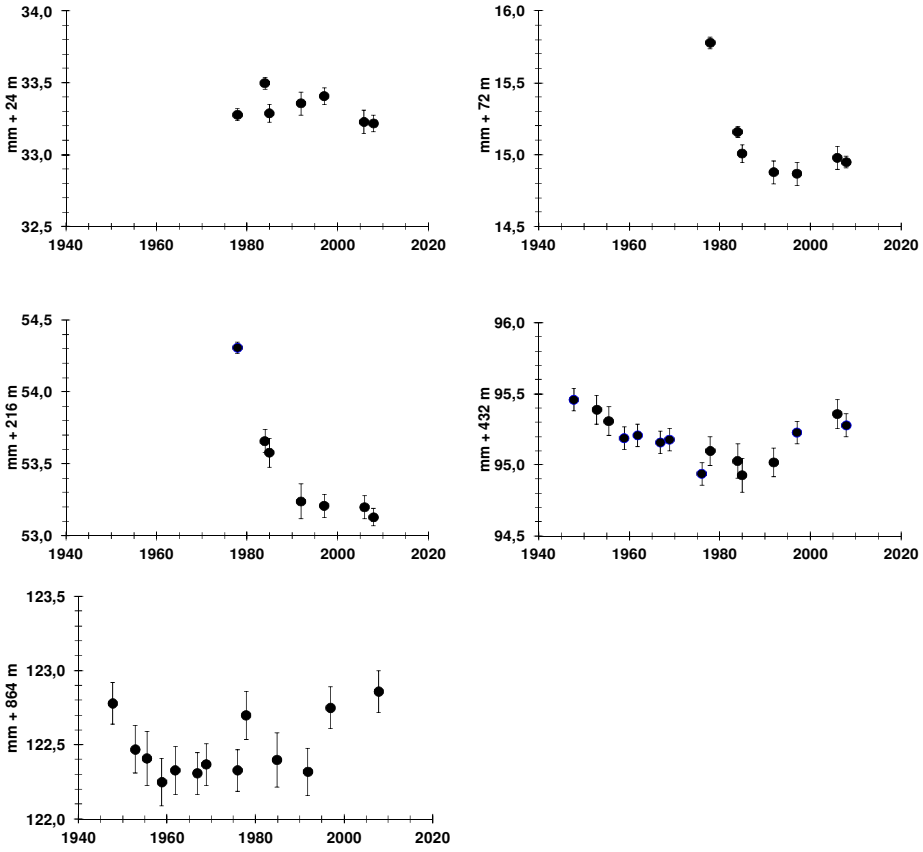

Figure 4.27 *The results from the 15 interference measurements at the Nummela Standard Baseline during the years 1947–2007. The error bars indicate expanded uncertainties.*

5 Chengdu Standard Baseline

5.1 History of the project

The Chengdu Standard Baseline measurement was carried out in cooperation between the FGI and the Sichuan Bureau of Surveying and Mapping (SBSM), based on an agreement between the National Bureau of Surveying and Mapping (NBSM) in the People's Republic of China and the FGI. The purpose was to improve the accuracy of the 1 488-m-long geodetic calibration baseline by measuring it with high-precision instruments: the Väisälä interference comparator and the Kern Mekometer ME5000.

In 1987, the SBSM began to study eight possible baseline sites and finally selected one site based on favourable geological, meteorological and environmental conditions. Planning and construction of the baseline was initiated in 1989 and completed in late 1990. In November 1991, January 1993 and October 1993, the baseline was measured with the Kern Mekometer ME5000 (nos. 357021 and 357039) and with invar wires. In 1995, measurements with invar wires were performed again, with an accuracy of up to 1 ppm.

In March 1997, Professor Juhani Kakkuri, Director General of the FGI at that time, inspected the baseline accompanied by Professor Chen Jun Yong, academician of the Chinese Academy of Sciences and special advisor to the SBSM. During the inspection, they discovered that the design, construction and stability of the baseline were compatible with the demands of interference measurements.

In July 1997, Jorma Jokela and Markku Poutanen from the FGI visited the baseline, continuing the investigations and preparations. The work was continued the following year, when the Väisälä interference comparator and a Kern Mekometer ME5000 were transported to Chengdu. Interference observations and high-precision electronic distance measurements were performed at the Chengdu Standard Baseline between 23 September and 9 November 1998.

The Chengdu Standard Baseline was destroyed in the great Sichuan earthquake on 12 May 2008.

5.2 Location of the baseline

The Chengdu Standard Baseline was located in the village of Xin Hua, in He Zhuo town, Pi Xian County, northwest of Chengdu, the capital of Sichuan Province. The distance from the urban area was 22 km. The baseline consisted of 12 observation pillars for calibration and several additional pillars for the interference measurements. Every part of the baseline was easily accessible from the adjoining road. The visibility was unobstructed in the open field area; the smooth terrain was covered with crops or other short vegetation most of the year. The line was slightly sloping: the north end of the baseline was 4 m higher than the south end. No disturbing thermal or vibrating sources or magnetic or

electric fields, such as high-voltage power lines, substations, large transformers or radio stations, were located in the neighbourhood. The daily mean temperature in the area varies between 0ºC and 35ºC, while typical air pressure is between 94.0 kPa and 96.5 kPa and relative humidity between 60% and 85%. There is hardly any frost period; daily temperature differences are usually small, since most days are more or less cloudy. Before selecting the most suitable baseline location, Chinese experts also performed thorough geological investigations and groundwater analyses.

5.3 Baseline design

The baseline must be suitable for comparison and calibration of the EDM instruments and invar wires. To obtain accurate and reliable results, the baseline should consist of short and long sections in appropriate proportions. The unit lengths of the most common instruments needing to be calibrated must be taken into account during the design phase. The influence of changing air temperature, pressure and humidity on the measurements must also be examined. Due to the many uses of the Chengdu Standard Baseline, its design and construction differ from those of conventional baselines.

Multiples of 24 m or 6 m were used in the section design along the 768-m southern part of the baseline. They serve the invar wire measurements and are feasible in the Väisälä interference comparator. For the best possible accuracy, up to 10^{-7}, this part of the baseline was equipped for light-interference measurements. Multiples of 5 m were used along the 720-m northern part of the baseline. The common 0-pillar is in the centre part of the 1 488-m-long baseline.

The Chengdu Standard Baseline thus differs greatly from all other Väisälä baselines. From the stand point of interference measurements, it originally consisted of two sets of multiplications, seen from the common zero (between pillars 4 and 5) of the baseline:

$$2 \times 2 \times 4 \times 8 \times 6 \text{ m} = 768 \text{ m},$$
$$(1½ \times)\ 2 \times 2 \times 2 \times 3 \times 4 \times 5 \text{ m} = 720 \text{ m}.$$

From the standpoint of the EDM, a large number of distances from 11 m to 1 488 m can be utilized in measurements in all combinations (Table 5.1). During the EDM observations, all of the distances were measured twice before and twice after the interference measurements.

The plan was to measure the 768-m part with interference measurements and to use high-precision EDM for the extension. For the Väisälä comparator, new pillars were needed between the old pillars 2 and 3 and 3 and 4 (at 96 m and 24 m, as seen from the common zero of the baseline; Fig. 5.14). New pillars at 0 m and 1 m and the telescope pillar were built between the old pillars 4 and 5. The multiplications are now:

$$2 \times 2 \times 2 \times 2 \times 2 \times 4 \times 6 \times 1 \text{ m} = 768 \text{ m},$$
$$(1½ \times)\ 2 \times 2 \times 2 \times 3 \times 4 \times 5 \times 1 \text{ m} = 720 \text{ m}.$$

The new pillars were built during the years 1997–1998, and their upper plates were finished just before the interference observations. To avoid using too many and too complex multiplications,

$$2 \times 2 \times 4 \times 4 \times 6 \times 1 \text{ m} = 384 \text{ m}$$

was finally measured in the interference observations. The last multiplication up to 768 m could not be measured due to unstable weather conditions.

Underground reference markers at baselines are usually stable, but they make complementary projections onto observation pillars necessary. These projections increase the degree of uncertainty in the measurement and traceability chain. Unlike the situation at most Väisälä baselines, there were no underground markers at the Chengdu Standard Baseline, and no projection measurements were needed. The only reference markers were the permanently installed, cone-shaped markers on the tops of the observation pillars, which also enabled the forced-centring for the EDM. These markers could be linked to the Väisälä interference comparator references (transferring bars) by transferring the measurements.

The pillars were roofed with concrete and steel shelters. A longer and heavier shelter was located at the centre of the baseline, extending 50 m from the telescope pillar (Figs. 5.2–5.3, 5.7 and 5.15). All of the surrounding buildings and other structures were isolated from the old observation pillars. The stability of the pillars was controlled, for example, by precise levelling.

Firm ground and flat topography enabled equal pillar foundations and observation heights; the slight sloping of the baseline caused few restrictions. With EDM and interference measurements, the influence of refraction must be taken into consideration. Observation pillars are usually low, which makes them easy to use, although the observations are exposed to disturbing refraction near the ground. High pillars may be advantageous if refraction varies as a function of height.

Fig. 5.1 (though with no scale) is an example of a temperature gradient at different height intervals, showing that 2 m is a better observation height than 1 m. In contrast, with high pillars observers need stands that must be isolated from the pillars. Furthermore, pillars that are too high cause problems with invar wire measurements. However, since the impact of propagation media was an important subject of study at the Chengdu Standard Baseline, there were good reasons for the high (up to 3 m) pillar heights. Their feasibilities and advantages of reduced atmospheric disturbances were tested. Thermal radiation from the varying soil cover is reduced at such heights, and the light travels in a more uniform isothermal layer than it does closer to the ground. The use of high pillars for interference measurements was also worth examining.

The foundations of the pillars must be steady. At the Chengdu Standard Baseline, the pillars were 0.5 m thick and the foundations reached depths of 10 m to 12 m, well below the frost and groundwater levels and deep in the

pebble layer. The soil load was far less than the calculated bearing capacity. As expected, the old pillars proved more stable than the new ones.

Table 5.1 *Distances (m) between the 12 observation pillars in all combinations.*

Pillar No.	0	1	2	3	4	5	6	7	8	9	10	11
0	–	384	576	720	762	773	788	828	888	1008	1248	1488
1		–	192	336	378	389	404	444	504	624	864	1104
2			–	144	186	197	212	252	312	432	672	912
3				–	42	53	68	108	168	288	528	768
4					–	11	26	66	126	246	486	726
5						–	15	55	115	235	475	715
6							–	40	100	220	460	700
7								–	60	180	420	660
8									–	120	360	600
9										–	240	480
10											–	240
11												–

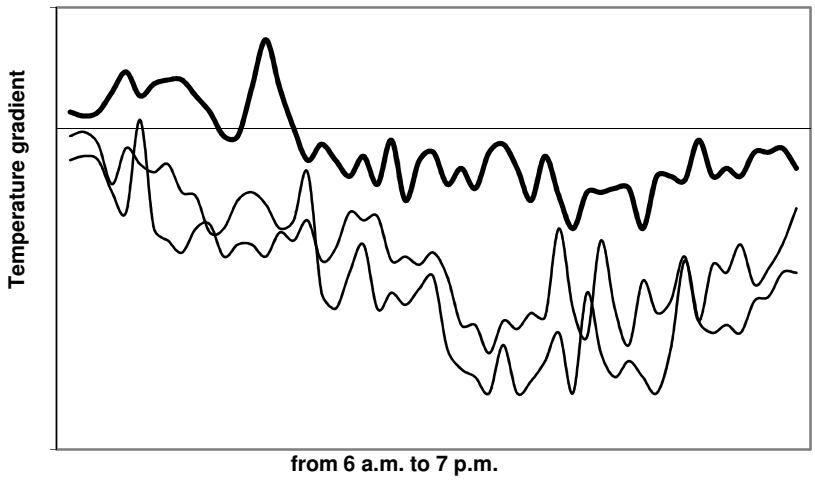

Figure 5.1 *An example of a direct survey of temperature gradient at heights from 0.5 m to 1.5 m, from 0.5 m to 2.5 m (thin lines) and from 1.5 m to 2.5 m (thick line). Picture: SBSM.*

Figure 5.2 *The central part of the Chengdu Standard Baseline in November 1998, showing the 50-m-long concrete shelter between pillars 3 and 5.*

Figure 5.3 *The central part of the Chengdu Standard Baseline in November 1998, showing the 0-end in the interference measurements.*

The load caused by wind pressure can at worst only result in small, short-lived elastic deformations. Uneven warming of the pillars may lead to more significant daily deformations and flexing. The problematic section of every pillar was the part above ground level, as this part is unevenly exposed to thermal expansion. This was clearly observable after sunny days. With EDMs,

such disturbances are detectable only as a large variation in results. With interference observations, the deformations cancelled out much of the advantage of decreasing the influence of refraction by high pillars.

In conclusion, high observation pillars are advantageous from the standpoint of refraction. If the stability of the pillars can be guaranteed, they can also be used in interference measurements. When single pillars are used instead of separate premium reference markers (underground), projection measurements can be replaced by more accurate and simple transferring measurements. A further problem is that even 0.1 mm-level pillar movements are detrimental to interference observations – and interference observations probably are the only method that can be used to find them.

5.4 Interference measurements

5.4.1 Scale of the measurement

For the interference measurements at the Chengdu Standard Baseline, the newest absolute calibrations for FGI quartz gauges nos. 30, 49 and 51 were performed at the PTB in Braunschweig, Germany, in 1995 (PTB 1996). During the years 1995–1999, several comparisons between the principal reference, quartz gauge no. 29 and other quartz gauges, nos. 30, 49, 51 and VIII, were performed by Dr Aimo Niemi at the University of Turku's Tuorla Observatory (Fig. 5.4). The lengths of the quartz gauges used at the Chengdu Standard Baseline at epoch 1998.8 were in the BT96 system:

no. 49 1 m + 32.37 µm ±0.06 µm,
no. 51 1 m + 18.41 µm ±0.06 µm.

The computation has been described by Jokela and Poutanen (1998, 14–15). The uncertainty estimates here are expanded values ($k = 2$). The lengths are valid at a temperature of 20°C. At temperature t (°C) and air pressure p (mmHg), they are as follows:

no. 49:

$$l_{49} = 1\ \text{m} + [\ 32.37 + 0.3938 \times (t - 20) + 0.00155 \times (t - 20)^2 - 0.00099 \times (p - 760.)\ ]\ \mu\text{m};$$

(Eq. 5.1)

no. 51:

$$l_{51} = 1\ \text{m} + [\ 18.41 + 0.3939 \times (t - 20) + 0.00172 \times (t - 20)^2 - 0.00099 \times (p - 760.)\ ]\ \mu\text{m}.$$

(Eq. 5.2)

The formulas are based on research performed at Tuorla. The lengths of the quartz gauges existing at that time at the Chengdu Standard Baseline are listed in Table 5.2.

The quartz gauge comes into optical and physical contact at mirror 0, but optical contact only at mirror 1. To obtain the distance between mirrors 0 and 1, the length of the quartz gauge and the width of the gap between it and mirror 1

are summed. In the gap measurement, filters with the wavelengths $\lambda = 675$ nm (17–18 Oct.) and $\lambda = 640$ nm (23 Oct. – 3 Nov.) were used.

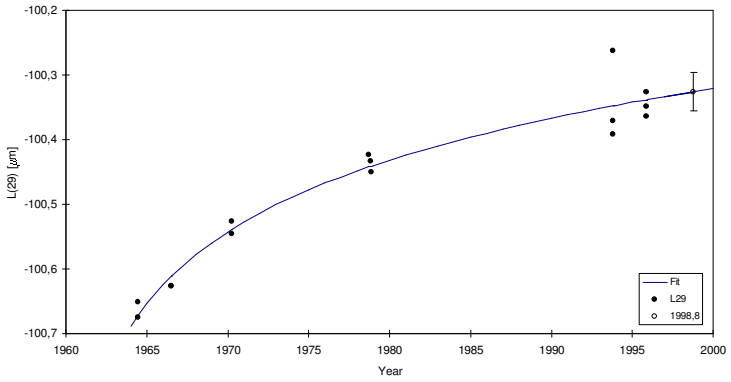

Figure 5.4 *Change in length of quartz gauge no. 29, based on absolute measurements of quartz gauges nos. 30, 32, 42, 49, 51 and 53 in Braunschweig and comparisons at Tuorla. Comparisons for computation of the Chengdu Standard Baseline were performed on 14 September 1998, and 1 March 1999.*

Table 5.2 *Lengths of quartz gauges under ambient temperature t (°C) and pressure p (mmHg).*

Quartz gauge no. 49					**Quartz gauge no. 51**				
Date and time		*t*	*p*	**µm + 1 m**	**Date and time**		*t*	*p*	**µm + 1 m**
1998-10-17	22:42	14.99	716.5	30.48	1998-10-30	20:45	15.95	716.7	16.89
	22:59	15.20	716.5	30.56		20:58	16.02	716.7	16.91
	23:38	14.97	716.3	30.47		21:28	15.85	717.2	16.85
	23:53	14.90	716.3	30.44		21:42	15.79	717.2	16.82
1998-10-18	21:55	14.85	718.2	30.43	1998-10-31	21:23	15.15	720.1	16.58
	22:08	14.71	718.2	30.37		21:35	15.25	720.1	16.62
	22:47	14.50	718.1	30.29		22:00	15.15	720.4	16.58
	23:03	14.48	718.1	30.28		22:10	15.06	720.4	16.55
1998-10-23	23:58	16.94	716.0	31.22	1998-11-03	21:03	15.98	717.5	16.90
1998-10-24	00:16	16.74	716.0	31.14		21:16	15.77	717.5	16.82
	00:47	16.57	715.8	31.08		21:46	15.25	718.0	16.62
	01:02	16.60	715.8	31.09		21:57	15.02	718.0	16.53
1998-10-27	00:03	16.08	716.5	30.89					
	00:15	15.98	716.5	30.86					
	00:46	15.84	716.3	30.80					
	01:00	15.71	716.3	30.75					
	22:03	14.15	715.6	30.16					
	22:15	14.10	715.6	30.14					
	22:46	14.12	715.7	30.15					
	23:00	14.14	715.7	30.16					
1998-10-28	20:15	15.73	714.5	30.76					
	20:27	15.68	714.5	30.74					
	20:54	15.74	715.1	30.76					
	21:08	15.76	715.1	30.77					

5.4.2 Mirrors and compensators

The mirrors are listed in Table 5.3. Since no projection measurements were necessary, no corrections for different mirror thicknesses were used. The quartz gauge was placed between the glass surfaces of mirrors 0 and 1. This distance is longer than the distance between the reflecting aluminium surfaces of the mirrors, which necessitates the small corrections in Table 5.4.

The mirrors were covered with a new aluminium layer and a protective silicon oxide layer during the summer of 1998. The influence of these layers on the propagation of light was estimated by measuring shifts in the interference bands with the same photographic and theodolite methods used for the two previous interference measurements (Fig. 5.5; Jokela and Poutanen 1998, 19–22).

The thickness, β, of the aluminium layer can be computed using the following equation:

$$\beta = cd / 2\cos\alpha, \qquad \text{(Eq. 5.3)}$$

where c is the observed change in direction of the central interference band (in radians), d is the distance of the two slits (here 1 mm) and α is the angle between the normal of the mirror and the direction of the theodolite. The value of α is close to 0, and one can approximate that $\cos\alpha = 1$.

Depending on the relative thicknesses of the Al and SiO layers, the optical distance Al/SiO → theodolite can be shorter or even longer than the optical distance glass → theodolite. In this case, the shift at the aluminium-glass border is opposite in mirrors 0 and 1. For mirror 0,

$$\beta_0 = -0.0025(\text{gon}) \cdot 0.0157 \cdot 1 \text{ mm}/2 = -20 \text{ nm},$$

and for mirror 1

$$\beta_1 = +0.0040(\text{gon}) \cdot 0.0157 \cdot 1 \text{ mm}/2 = +31 \text{ nm}.$$

The angles represent the means of the shifts at the upper and lower parts of the mirrors. The correction (Table 5.4) is as follows:

$$-(-20 \text{ nm} + 31 \text{ nm})/1 \text{ m} = -11 \text{ nm/m}.$$

The uncertainty estimate, 20 nm/m, makes the correction rather insignificant. Overall, the determination was difficult and not the most convincing due to the slight, but discernible, imperfectness of the mirror surfaces.

The formulas for the compensator corrections are identical to those used in the previous measurements (see Section 4.3.1).

Table 5.3 Mirrors.

Pillar (m)	Mirror no.	Thickness (mm)
0	40	19.985
1	36	20.001
6	38	19.932
24	35	19.843
96	53	19.981
192	39	19.966
384	41	19.959

Table 5.4 Corrections due to thicknesses of mirror coatings.

Distance	Correction (mm)
0–1	–0.000
0–6	–0.000
0–24	–0.000
0–96	–0.001
0–192	–0.002
0–384	–0.004

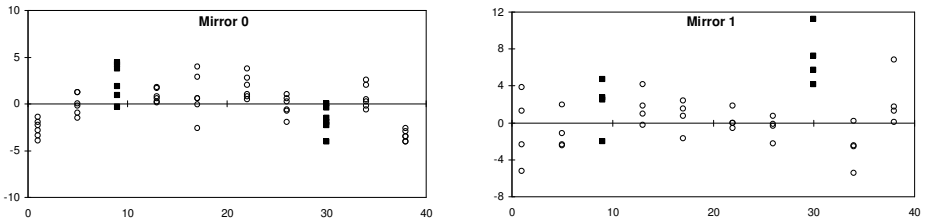

Figure 5.5 *Determining the optical thickness of the aluminium layer of mirrors 0 and 1 using the two-slit method. The abscissa is the distance (mm) from the bottom of the slit; the ordinate is the observed angle of the interference band (mgon), with the tilt and mean subtracted. Six sets were observed for mirror 0, four for mirror 1. Al-glass border observations are marked with filled symbols. On the left is the Al-coated lower part of the mirror, in the centre (between 10 and 30 mm) is glass only, and on the right is the upper Al-coated part of the mirror.*

5.4.3 Geometrical corrections

The height information is presented in Tables 5.15 and 5.20. The formula for the vertical geometric reduction at the reference height level (H = 0 at the foot of pillar 0 at 768 m) is the same for both the interference and Mekometer measurements, see Section 5.5.4 (Eq. 5.5). Using the heights, also the influence of the atmospheric pressure difference is obtained, as presented in Section 4.3.4 (Eq. 4.13). The corrections are listed in Table 5.16.

5.4.4 Refraction

For measurements with the Väisälä comparator, the absolute value of the refractive index for air is not needed; only the temperature differences in various parts of the baseline are significant. At the Chengdu Standard Baseline, the coefficients of formulas for the refraction correction are slightly different from those in other interference measurements because placing the thermometers at the 384-m baseline is somewhat different. The coefficients are computed by assuming that the temperature changes linearly between the two thermometers, and equal weight is given to both. The result is multiplied by the distance between the thermometers. Between the first two mirrors, the result is multiplied by the number of reflections and then subtracted from the coefficient for the entire distance. To obtain the coefficient per metre, the figure is divided by the total length. The sum of the coefficients for an interference will be zero. If a thermometer is not at the distance of the middle mirror, the coefficients for the previous and next thermometers are interpolated. An example of how to compute the coefficients is provided in Table 5.5.

All of the coefficients for computing the refraction correction are presented in Table 5.6 and the calibration data for the thermometers in Table 5.7. The figures t_o and t_i are thermometer locations at the quartz gauge. The temperature data are summarized in Fig. 5.6. The computation of the refraction correction is presented in Section 4.3.2. As usual, a greater than 1°C change in temperature during a measurement (several hours) appeared to make a complete measurement impossible, and even a 0.5°C change resulted in numerous difficulties.

At this baseline, the massive concrete structures around the pillars (above ground), especially the long building around the first 50 metres of pillars, caused additional problems. When the concrete was not at the same temperature as the air, wind caused not only turbulence, but also rapidly changing small-scale temperature gradients. After warm and sunny days, interferences were difficult to find, even at the shortest distances.

5.4.5 Interference observations

Interference observations with gap, refraction and compensator corrections are listed in Tables 5.8–5.12.

Often, interference observations are weighted according to the temperature differences. As in Nummela (Chapter 4), here this step is omitted because it is not possible to measure under poor conditions (with wide temperature variations), while in good or moderate conditions this type of weighting is of no significance. All observations have equal weights, except for the half measurement to 384 done on 26 October with a half-weight.

Table 5.5 *An example of computation of the refraction formula coefficients for 0–6–24 interference. Thermometers are located at 0, 1, 4, 10, 17 and 24 m. The number of reflections between 0 and 6 is n = 4. The length l of the entire distance is 24 m. There is no thermometer at the middle mirror 6, but by using the thermometers at 4 and 10 the coefficients for the interval 4–6 can be interpolated.*

Coefficients *i* for the individual intervals between 0 and 24

	0	1	4	10	17	24	× distance
	1/2	1/2					× (1–0)
		1/2	1/2				× (4–1)
			1/2	1/2			× (10–4)
				1/2	1/2		× (17–10)
					1/2	1/2	× (24–17)
Sum	1/2	4/2	9/2	13/2	14/2	7/2	24

Coefficients *j* for the individual intervals between 0 and 6

	0	1	4	10	× distance
	1/2	1/2			× (1–0)
		1/2	1/2		× (4–1)
			5/6	1/6	× (6–4)
Sum	1/2	4/2	19/6	2/6	6

Coefficients for the thermometers in the 0–6–24 interference

Thermometer	$i - n \times j$	/ *l*	Coefficient
0	$1/2 - 4 \times 1/2$	/ 24	–0.062
1	$4/2 - 4 \times 4/2$	/ 24	–0.250
4	$9/2 - 4 \times 19/6$	/ 24	–0.340
10	$13/2 - 4 \times 2/6$	/ 24	+0.215
17	14/2	/ 24	+0.292
24	7/2	/ 24	+0.146

Table 5.6 *Weights for computing the refraction correction.*

ν	0–1–6	0–6–24	0–24–96	0–96–192	0–192–384
0	–0.417	–0.062	–0.016	–0.026	–0.031
1	–0.167	–0.250	–0.062		
4	+0.528	–0.340	–0.141		
10	+0.056	+0.215	–0.203	–0.062	
17		+0.292	–0.219		
24		+0.146	–0.047	–0.099	–0.062
36			+0.125		
48			+0.125	–0.125	–0.094
60			+0.125		
72			+0.188	–0.125	
96			+0.125	(0.000)	–0.125
120				+0.125	
144				+0.125	–0.125
168				+0.125	
192				+0.062	(0.000)
240					+0.125
288					+0.125
336					+0.125
384					+0.062

Table 5.7 *Corrections to the thermometers.*

Thermometer		**Correction (°C) at**			**Thermometer**		**Correction (°C) at**		
at (m)	**no.**	**+10°C**	**+15°C**	**+20°C**	**at (m)**	**no.**	**+10°C**	**+15°C**	**+20°C**
0	7936	+0.02	+0.02	0.00	120	47	+0.02	–0.02	–0.05
1	3868	0.00	0.00	+0.02	144	7939	–0.01	0.00	–0.02
4	7937	+0.01	+0.01	+0.01	168	48	–0.02	–0.06	–0.10
10	4484	+0.03	+0.04	+0.06	192	7938	0.00	+0.01	0.00
17	4480	+0.02	+0.06	+0.04	240	46	–0.01	–0.02	–0.03
24	3864	–0.08	–0.04	–0.02	288	3867	+0.02	0.00	+0.02
36	7932	–0.03	0.00	–0.01	336	7935	–0.01	0.00	–0.02
48	7929	0.00	0.00	–0.03	384	7933	0.00	+0.01	–0.01
60	4483	–0.01	–0.02	–0.04					
72	44	–0.05	–0.06	–0.06	t_o	7349	–0.03	–0.06	–0.08
96	45	–0.05	–0.04	–0.04	t_i	7350	–0.01	0.00	+0.01

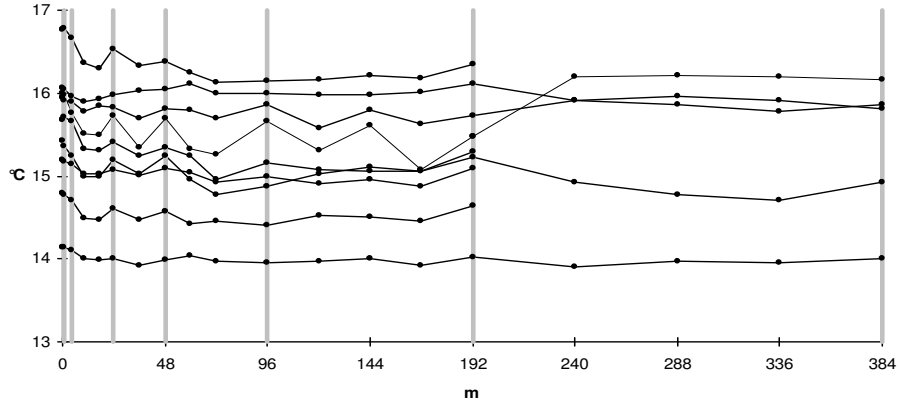

Figure 5.6 *Mean temperatures during the nine interference measurements at the Chengdu Standard Baseline on 17 October – 3 November 1998. Pillars (and thermometers) 0–48 are located between concrete walls, where the night temperature was higher than outside the building; 0–4, 24 and 48 are under a roof, but 10, 17 and 36 are not. Locations 96, 192 and 384 are also roofed. On 26–27 October, interference 0–192–384 could be observed only once (thin line) due to the tremendous temperature gradient. The figure also shows the ideal weather conditions that occurred on 27–28 October (the lowest profile).*

Figure 5.7 *The southern part of the Chengdu Standard Baseline, with a new pillar at 96 m in front.*

Table 5.8 *Computation of interference 0–1–6. The distance [0–1] is the sum of the lengths of the quartz gauge (from Table 5.2) and the gap between the quartz gauge and mirror 1. The distance [0–6] is six times the distance [0–1], corrected with compensator and refraction corrections.*

Date and time 1998	Obs.	Q. g. no.	Gap (μm)	[0–1] μm + 1 m	Comp. corr. (μm)	Refr. corr. (μm)	[0–6] μm + 6 m
17 Oct. 22:42	JJ	49	1.74	32.22	+81.72	–0.47	274.57
22:59	JJ	49	1.52	32.08	+83.21	–0.68	275.01
23:38	MP	49	2.08	32.55	+81.64	–0.12	276.82
23:53	MP	49	1.10	31.54	+89.92	–0.12	279.04
							276.36
							±1.02
18 Oct. 21:55	MP	49	2.08	32.51	+65.10	–0.30	259.86
22:08	MP	49	2.02	32.39	+69.45	–0.40	263.39
22:47	JJ	49	1.35	31.64	+72.57	–0.42	261.99
23:03	JJ	49	2.56	32.84	+66.63	–1.01	262.66
							261.98
							±0.76
23 Oct. 23:58	MP	49	2.05	33.27	+45.08	–0.33	244.37
24 Oct. 00:16	MP	49	1.44	32.58	+48.66	–0.77	243.37
00:47	JJ	49	1.04	32.12	+48.23	–0.36	240.59
01:02	JJ	49	2.61	33.70	+38.86	–0.66	240.40
							242.18
							±1.00
27 Oct. 00:03	JJ	49	1.36	32.25	–0.61	–0.64	192.25
00:15	JJ	49	2.85	33.71	–10.78	–1.06	190.42
00:46	MP	49	2.72	33.52	–14.10	–0.79	186.23
01:00	MP	49	2.40	33.15	–13.15	–0.55	185.20
							188.52
							±1.68
27 Oct. 22:03	JJ	49	1.04	31.20	+10.80	–0.30	197.70
22:15	JJ	49	2.00	32.14	+4.67	–0.16	197.35
22:46	MP	49	1.55	31.70	+6.26	–0.07	196.39
23:00	MP	49	2.45	32.61	+1.40	–0.15	196.91
							197.09
							±0.28
28 Oct. 20:15	JJ	49	2.11	32.87	–7.95	–0.16	189.11
20:27	JJ	49	3.12	33.86	–13.43	–0.24	189.49
20:54	MP	49	2.16	32.92	–8.64	–0.27	188.61
21:08	MP	49	2.77	33.54	–11.76	–0.26	189.22
							189.11
							±0.18

Table 5.8 *continued.*

Date and time 1998	Obs.	Q. g. no.	Gap (μm)	[0–1] μm + 1 m	Comp. corr. (μm)	Refr. corr. (μm)	[0–6] μm + 6 m
30 Oct. 20:45	JJ	51	2.69	19.58	–31.44	–0.28	85.76
20:58	JJ	51	3.25	20.16	–35.75	–0.54	84.67
21:28	MP	51	2.72	19.57	–34.04	–0.51	82.87
21:42	MP	51	2.88	19.70	–35.34	–0.64	82.22
							83.88
							±0.81
31 Oct. 21:23	JJ	51	2.56	19.14	–68.11	–1.00	45.73
21:35	JJ	51	2.11	18.73	–65.68	–0.90	45.80
22:00	MP	51	2.83	19.41	–68.55	–0.56	47.35
22:10	MP	51	3.12	19.67	–70.51	–0.57	46.94
							46.46
							±0.41
3 Nov. 21:03	JJ	51	3.09	19.99	–48.84	–0.07	71.03
21:16	JJ	51	1.39	18.21	–36.92	–0.17	72.17
21:46	MP	51	2.53	19.15	–41.49	–0.77	72.64
21:57	MP	51	3.55	20.08	–47.43	–0.96	72.09
							71.98
							±0.34

Table 5.9 *Computation of interference 0–6–24. The distance [0–24] is four times the distance [0–6] (from Table 5.8), corrected with compensator and refraction corrections.*

Date and time 1998	4 × [0–6] μm + 24 m	Comp. corr. (μm)	Refr. corr. (μm)	[0–24] μm + 24 m
17 Oct. 22:04	1 098.28	–108.15	–2.32	987.81
23:13	1 100.04	–122.94	–2.41	974.69
23:19	1 107.28	–121.84	–2.51	982.93
18 Oct. 00:03	1 116.16	–122.73	–1.70	991.73
				984.29
				±3.67
18 Oct. 21:33	1 039.44	–42.44	–3.60	993.40
22:20	1 053.56	–52.42	–4.00	997.14
22:34	1 047.96	–58.98	–3.25	985.73
23:16	1 050.64	–51.58	–6.14	992.92
				992.30
				±2.38
23 Oct. 23:34	977.48	–90.96	–4.01	882.51
24 Oct. 00:27	973.48	–79.90	–5.34	888.24
00:32	962.36	–79.41	–4.74	878.21
01:13	961.60	–67.64	–6.67	887.29
				884.06
				±2.32

Table 5.9 *continued.*

Date and time 1998	4 × [0–6] μm + 24 m	Comp. corr. (μm)	Refr. corr. (μm)	[0–24] μm + 24 m
26 Oct. 23:43	769.00	+40.02	–3.74	805.28
27 Oct. 00:26	761.68	+63.42	–5.49	819.61
00:33	744.92	+64.91	–3.12	806.71
01:11	740.80	+80.98	–6.43	815.35
				811.74
				±3.44
27 Oct. 21:44	790.80	+70.94	–1.25	860.49
22:27	789.40	+67.24	–2.03	854.61
22:33	785.56	+69.93	–1.81	853.68
23:21	787.64	+69.08	–1.61	855.11
				855.97
				±1.53
28 Oct. 20:00	756.44	+49.34	–1.79	803.99
20:37	757.96	+48.23	–1.41	804.78
20:44	754.44	+48.80	–0.86	802.38
21:20	756.88	+47.41	+0.61	804.90
				804.01
				±0.58
30 Oct. 20:29	343.04	+81.80	–1.73	423.11
21:10	338.68	+95.66	–1.69	432.65
21:17	331.48	+96.74	–1.01	427.21
21:52	328.88	+106.80	–1.56	434.12
				429.27
				±2.54
31 Oct. 20:54	182.92	+23.06	–1.59	204.39
21:45	183.20	+23.86	–5.34	201.72
21:50	189.40	+22.40	–5.69	206.11
22:21	187.76	+24.50	–3.79	208.47
				205.17
				±1.42
3 Nov. 20:50	284.12	–103.04	–1.28	179.80
21:25	288.68	–101.48	–3.03	184.17
21:34	290.56	–100.74	–4.83	184.99
22:08	288.36	–110.54	–7.30	170.52
				179.87
				±3.32

Table 5.10 *Computation of interference 0–24–96. The distance [0–96] is four times the distance [0–24] (from Table 5.9), corrected with compensator and refraction corrections.*

Date and time 1998	**4 × [0–24] µm + 96 m**	**Comp. corr. (µm)**	**Refr. corr. (µm)**	**[0–96] µm + 96 m**
17 Oct. 21:47	3 937.16	–89.20	–7.40	3 840.56
18 Oct. 00:15	3 937.16	–136.18	–3.15	3 797.83
				3 819.20
				±21.36
18 Oct. 21:18	3 969.19	–89.26	–13.63	3 866.30
23:29	3 969.19	–135.14	–7.08	3 826.97
				3 846.64
				±19.66
23 Oct. 23:19	3 536.25	+56.03	–17.74	3 574.54
24 Oct. 01:30	3 536.25	–8.62	–13.84	3 513.79
				3 544.16
				±30.38
26 Oct. 23:29	3 246.95	+34.51	–13.29	3 268.17
27 Oct. 01:23	3 246.95	–0.06	–7.36	3 239.53
				3 253.85
				±14.32
27 Oct. 21:30	3 423.89	–39.25	–1.56	3 383.08
23:21	3 423.89	–36.44	–2.43	3 385.02
				3 384.05
				±0.97
28 Oct. 19:45	3 216.05	+72.91	–4.40	3 284.56
21:28	3 216.05	+65.33	–1.34	3 280.04
				3 282.30
				±2.26
30 Oct. 20:05	1 717.09	–18.62	–4.02	1 694.45
22:02	1 717.09	–26.40	–0.23	1 690.46
				1 692.46
				±2.00
31 Oct. 20:41	820.69	+126.98	–13.32	934.35
22:30	820.69	+62.97	–14.64	869.02
				901.68
				±32.66
3 Nov. 20:37	719.48	–44.35	–5.50	669.63
22:18	719.48	–110.54	–18.20	590.74
				630.18
				±39.44

Table 5.11 *Computation of interference 0–96–192. The distance [0–192] is two times the distance [0–96] (from Table 5.10), corrected with compensator and refraction corrections.*

Date and time 1998	**2 × [0–96] µm + 192 m**	**Comp. corr. (µm)**	**Refr. corr. (µm)**	**[0–192] µm + 192 m**
17 Oct. 21:15	7 638.39	–1.28	–17.76	7 619.35
18 Oct. 00:44	7 638.39	–24.88	–4.25	7 609.26
				7 614.30
				±5.04
18 Oct. 20:54	7 693.27	–46.04	–11.60	7 635.63
23:57	7 693.27	–56.50	–2.97	7 633.80
				7 634.72
				±0.92
23 Oct. 23:57	7 088.33	–11.01	–8.72	7 068.60
24 Oct. 01:47	7 088.33	–13.43	–11.57	7 063.33
				7 065.96
				±2.64
26 Oct. 23:05	6 507.70	–100.98	–2.03	6 404.69
27 Oct. 01:43	6 507.70	–80.98	–30.25	6 396.47
				6 400.58
				±4.11
27 Oct. 21:07	6 768.10	–52.77	–2.86	6 712.47
23:37	6 768.10	–72.93	–1.37	6 693.80
				6 703.14
				±9.34
28 Oct. 19:28	6 564.60	+116.20	–5.74	6 675.06
21:43	6 564.60	+105.60	–1.40	6 668.80
				6 671.93
				±3.13
30 Oct. 19:45	3 384.91	+138.94	–0.58	3 523.27
22:16	3 384.91	+149.13	+1.34	3 535.38
				3 529.32
				±6.06
31 Oct. 20:18	1 803.37	+64.43	+7.91	1 875.71
22:48	1 803.37	+54.02	+0.03	1 857.42
				1 866.56
				±9.14
3 Nov. 20:22	1 260.37	–0.68	+0.06	1 259.75
22:37	1 260.37	–31.42	–12.11	1 216.84
				1 238.30
				±21.46

Table 5.12 *Computation of interference 0–192–384. The distance [0–384] is two times the distance [0–192] (from Table 5.11), corrected with compensator and refraction corrections. In the first measurement, only the first half could be observed.*

Date and time 1998	2 × [0–192] μm + 384 m	Comp. corr. (μm)	Refr. corr. (μm)	[0–384] μm + 384 m
26 Oct. 22:30	12 801.16	+91.36	–26.48	12 866.04
27 Oct. 20:33	13 406.27	–54.12	–2.89	13 349.26
28 Oct. 00:03	13 406.27	–41.24	–7.42	13 357.61
				13 353.44
				±4.18
28 Oct. 18:58	13 343.86	–55.19	–4.79	13 283.88
22:10	13 343.86	–41.03	–2.46	13 300.37
				13 292.12
				±8.24
30 Oct. 19:15	7 058.65	+88.44	+0.98	7 148.07
22:42	7 058.65	+99.02	–37.14	7 120.53
				7 134.30
				±13.77
3 Nov. 19:54	2 476.59	–121.28	–14.50	2 340.81
23:03	2 476.59	–93.96	–99.29	2 283.34
				2 312.08
				±28.74

5.4.6 Distances between transferring bars

Using the distances between the mirror surfaces, the data given in Tables 5.8–5.12 and the transfer readings after every interference measurement, the distances between the transferring bars were derived (Fig. 5.8 and Table 5.13). These distances were the most accurate length data at the baseline and were permanent as long as the transferring bars on the pillars were untouched.

5.4.7 Distances between central benchmarks

To provide lengths for calibration measurements, some kind of projections from the transferring bars to the central benchmarks were necessary. There are no underground markers or other more permanent benchmarks, and it was not possible to do projection measurements using traditional methods due to the high pillars and the constructions around them. The measurement was performed as a transfer measurement, similar to what was done at the HUT Väisälä Baseline earlier in 1998 (see Section 7.8). Before the transfer measurements could be performed, the mirror equipment on the pillars had to be removed.

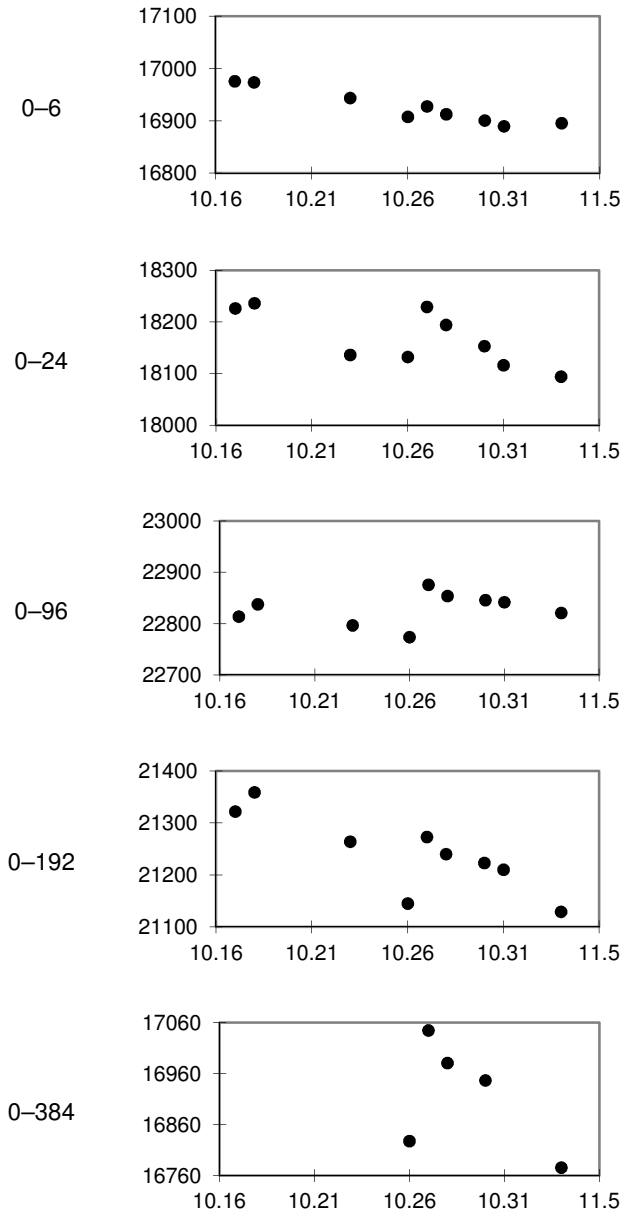

Figure 5.8 *Variation in distances between transferring bars; the μm part of the distance between bars on pillars 0 and ν is on the vertical axis, the date on the horizontal axis. At stable baselines, the variations remain smaller than 100 μm; here they are up to 270 μm (at 0–384, between 27 Oct. and 3 Nov.). Obviously, most of the instability is caused by the new pillars.*

A new accessory instrument was constructed to be fixed in the forced-centring device on the central benchmark. The probing point in it was at approximately the same location as the centre of the mirror, which made the transferring measurement possible: the same transferring instrument could be used for probing both the mirror and the accessory instrument (Fig. 5.9). It was not necessary to know the exact dimensions of the instrument because the measurements were performed identically at every pillar. Measurements in four symmetrical positions decreased uncertainty.

Table 5.13 *Distances B from the transferring bar at 0 to the transferring bars at other pillars (mm, metres for I and B not displayed). The difference in transfer readings L and the thickness of mirror 0, D_0 = 19.985 mm, are added to the interference observations I (from Tables 5.8–5.12): $B_v = I_v - L_v + L_0 + D_0$. A half-weight is used for the first measurement to 384. $s(\bar{q})$ is the experimental standard deviation of the mean $\bar{q}$.*

Date 1998	I_6	L_6	L_0	B_6	I_{24}	L_{24}	L_0	B_{24}
17–18 X	0.2764	8.9600	5.6745	16.976	0.9843	8.4175	5.6745	18.226
18 X	0.2620	8.9500	5.6765	16.974	0.9923	8.4180	5.6765	18.236
23–24 X	0.2422	8.9595	5.6765	16.944	0.8841	8.4095	5.6765	18.136
26–27 X	0.1885	8.9375	5.6720	16.908	0.8117	8.3370	5.6720	18.132
27–28 X	0.1971	8.9225	5.6685	16.928	0.8560	8.2805	5.6685	18.229
28 X	0.1891	8.9295	5.6680	16.913	0.8040	8.2635	5.6680	18.194
30 X	0.0839	8.8415	5.6740	16.901	0.4293	7.9355	5.6740	18.153
31 X	0.0465	8.8265	5.6850	16.890	0.2052	7.7590	5.6850	18.116
3 XI	0.0720	8.8465	5.6855	16.896	0.1799	7.7560	5.6855	18.094
$\bar{q}$				16.926				18.168
$s(\bar{q})$				±0.011				±0.018
Date 1998	I_{96}	L_{96}	L_0	B_{96}	I_{192}	L_{192}	L_0	B_{192}
17–18 X	3.8192	6.6650	5.6745	22.814	7.6143	11.9515	5.6745	21.322
18 X	3.8466	6.6700	5.6765	22.838	7.6347	11.9370	5.6765	21.359
23–24 X	3.5442	6.4085	5.6765	22.797	7.0660	11.4640	5.6765	21.264
26–27 X	3.2538	6.1365	5.6720	22.774	6.4006	10.9125	5.6720	21.145
27–28 X	3.3840	6.1610	5.6685	22.876	6.7031	11.0835	5.6685	21.273
28 X	3.2823	6.0810	5.6680	22.854	6.6719	11.0845	5.6680	21.240
30 X	1.6925	4.5050	5.6740	22.846	3.5293	7.9655	5.6740	21.223
31 X	0.9017	3.7295	5.6850	22.842	1.8666	6.3270	5.6850	21.210
3 XI	0.6302	3.4795	5.6855	22.821	1.2383	5.7800	5.6855	21.129
$\bar{q}$				22.829				21.241
$s(\bar{q})$				±0.010				±0.025
Date 1998	I_{384}	L_{384}	L_0	B_{384}				
26–27 X	12.8660	21.6950	5.6720	16.828				
27–28 X	13.3534	21.9620	5.6685	17.045				
28 X	13.2921	21.9645	5.6680	16.981				
30 X	7.1343	15.8460	5.6740	16.947				
3 XI	2.3121	11.2070	5.6855	16.776				
$\bar{q}$				16.925				
$s(\bar{q})$				±0.051				

The results of the transferring measurements are presented in Table 5.14. The forced-centring system was not completely compatible with the transferring measurements at the new pillars. The uncertainty was larger for pillars 24 and 96 than for pillars 6, 192 and 384, and the measurement at pillar 0 failed totally. (Solving the problem at pillar 0 would have required changing the pillar structure, which at that point was too late.) The final results for the interference measurements thus consist of lengths at the 378-m baseline between pillars 6 and 384.

By adding the transferring corrections, mirror-coating corrections, air-pressure difference corrections and vertical geometrical corrections (onto the height level $H = 0$) to the distances between the transferring bars, the final lengths from the interference observations at the Chengdu Standard Baseline in 1998 are obtained (Table 5.16).

Table 5.14 *Transferring measurements for the projections from distances between transferring bars to distances between central benchmarks.*

Pillar (m)	mm	
0		–
6	12.062	±0.006
24	13.967	±0.065
96	9.390	±0.025
192	10.031	±0.002
384	17.427	±0.014

Table 5.15 *Heights of mirror centres.*

Pillar (m)	m
0	4.279
6	4.264
24	4.220
96	4.044
192	3.811
384	3.349
768	2.442

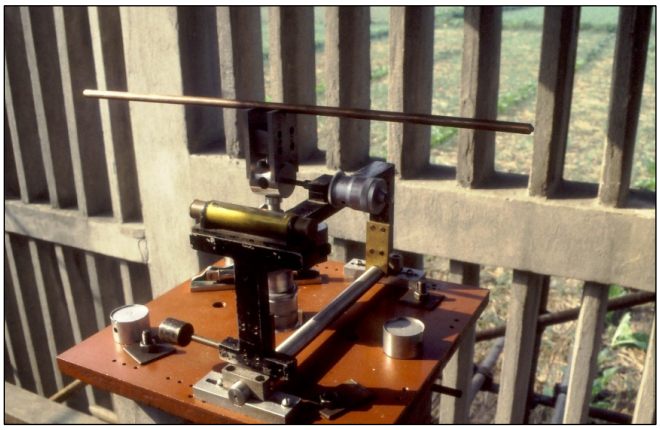

Figure 5.9 *A transferring measurement between the transferring bar and the central benchmark. The long tube on the top is for directing the instrument parallel (or perpendicular) to the baseline.*

Table 5.16 *Computation of baseline length.*

	6–24: 18 m + (mm)	**6–96: 90 m + (mm)**	**6–192: 186 m + (mm)**	**6–384: 378 m + (mm)**
Length between transferring bars	+1.242	+5.903	+4.315	–0.001
Projection correction	+1.905	–2.672	–2.031	+5.365
Correction to height level $H = 0$	–0.066	–0.328	–0.670	–1.333
Mirror-coating correction	–0.000	–0.001	–0.002	–0.004
Air-pressure difference correction	–0.000	–0.000	–0.002	–0.006
Final length	+3.081	+2.902	+1.610	+4.021

In Table 5.16, distances between the transferring bars are derived from Table 5.13 by subtracting the distance, B_6, from other distances, B_ν. Projection corrections are obtained from the transferring measurements after completing the interference measurements (Table 5.14). For every distance, $6 - \nu$, the correction is the difference between the transferring results, $L_\nu - L_6$.

When computing the vertical geometrical correction, it was necessary to correct for the curvature of the Earth. The levelling results refer to a curved equipotential surface, but in the interference observations a straighter line in space was measured. This line of sight (between mirror centres) was approximately 110 mm above the straight line between the central benchmarks at 0 and 768 m. The heights are listed in Table 5.15. Small deviations from such estimated heights cause no significant errors.

The computation for the mirror-coating correction and air-pressure difference correction is described on the previous pages.

5.4.8 Uncertainty of the measurement

Two accuracy estimates are presented in Table 5.17: uncertainties u_M for the distances between the mirror surfaces and u_B for the distances between the transferring bars (cf. Section 4.5.2). Factor n_s is the number of observation nights and factor n_{obs} the number of observations in one night. Uncertainties u_I for every interference observation stage are derived as square roots of the square sums of the experimental standard deviations of the means (in Tables 5.8–5.12) divided by n_s. Factors u_I^{acc} are accumulated uncertainties; for example, for one series of interferences, 0–384, the following result was obtained:

$$u^{acc}_{I(0-384)}=\sqrt{(2\times2\times4\times2.6)^2+(2\times2\times22.6)^2+(2\times9.0)^2+(16.6)^2}\ \mu\text{m}=102.5\ \mu\text{m}.$$

Dividing this by the square root of the number of observation nights, with a half night referring to a half measurement, u_M was derived. Table 5.13 gives the uncertainty u_B. Theoretically, and in Chengdu in practice, it should be equal to or larger than u_M, because it includes the pillar movements. When estimating the

total uncertainty budget (Table 5.18), u_B (Table 5.17) was used. The values are standard uncertainties ($k = 1$).

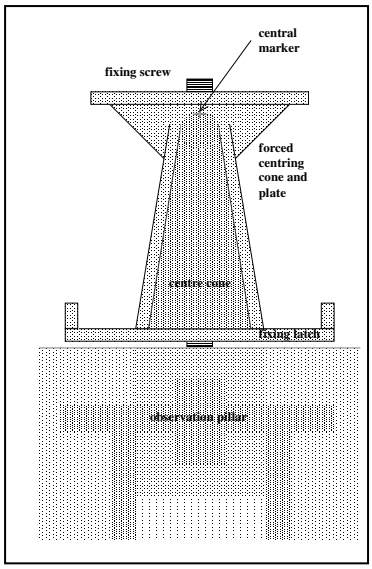

Figure 5.10 *Principle of ortho-truncated cone forced-centring.*

Figure 5.11 *The central marker of pillar no. 5 and the Wild T3 fixed on the forced-centring plate on the new theodolite pillar. The theodolite was used in alignment of the mirrors.*

Table 5.17 *Uncertainty of distances between mirror surfaces or transferring bars.*

	0–24	**0–96**	**0–192**	**0–384**
n_s	9	9	9	4½
n_{obs}	4	2	2	2 (1)
u_I (μm)	3	23	9	17
u_I^{acc} (μm)	3	25	51	102
u_M (μm)	1	8	17	48
u_B (μm)	18	10	25	51

Table 5.18 *Total uncertainty budget of interference measurements (μm).*

	6–24	**6–96**	**6–192**	**6–384**
Uncertainty in interference observations and transfer readings	18	10	25	51
Uncertainty in transfer measurements for projection	65	26	6	15
Uncertainty in determination of the absolute length of the quartz gauge	1	3	6	11
Uncertainty in thicknesses of mirror coatings	0	2	4	8
Uncertainty due to determination of temperature of the quartz gauge	0	2	4	7
Uncertainty due to determination of heights	0	1	2	4
Total standard uncertainty	67	28	27	55

5.4.9 Results from the interference measurements

The final results of the interference measurements are listed in Table 5.19. A complete list of slope distances between the central markers on the tops of the pillars is provided in Table 5.24.

Table 5.19 *Final results from the interference measurements. The length of the Chengdu Standard Baseline with its sections at height level H = 0 (i.e. at the foot of pillar 0 at 768 m) with expanded uncertainties.*

Interval		**Length (mm)**
6– 24		18 003.08 ±0.13
6– 96		90 002.90 ±0.06
6–192	(4–2)	186 001.61 ±0.05
6–384	(4–1)	378 004.02 ±0.11

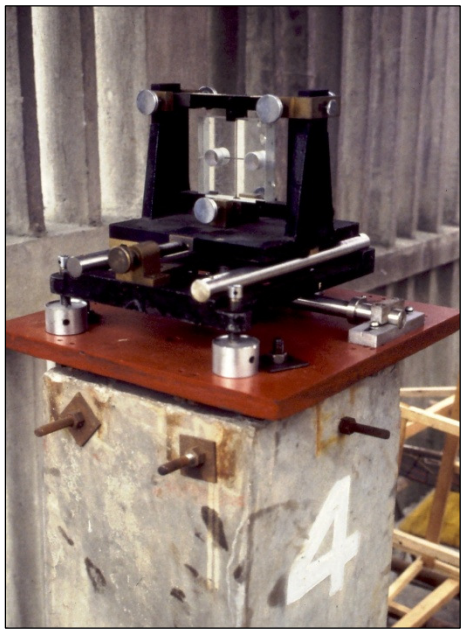

Figure 5.12 *Mirror equipment on pillar no. 4 (at 6 m in interference observations).*

Figure 5.13 *Kern Mekometer ME5000 on pillar no. 4.*

5.5 Kern Mekometer ME5000 measurements

The total length of the Chengdu Standard Baseline, 1 488 m, was far too long for the interference measurements. The section lengths between the 12 original observation pillars ranged from 11 to 384 m. The measurement of the baseline in its entirety was performed with high-precision EDMs using a Kern Mekometer ME5000 instrument (Fig. 5.13).

5.5.1 Measurement procedure

Measurement in all combinations at a 12-station baseline requires 2×66 single observations; one observation may include several single aimings. A complete measurement was performed once before and once after the interference measurements at the Chengdu Standard Baseline. The EDM observations required four days in September and four days in November, while the interference measurements required one month. As the number of unknowns is 12 (11 section lengths + 1 additive constant), sufficient redundancy of observations was obtained, even when the shortest distances (less than 20 m) could not be observed with the Mekometer.

In addition to the 12 original pillars, three new pillars were measured to aid in installing the Väisälä interference comparator instruments. The computation was performed separately, because in September only approximate centring was used at the new pillars and the forced-centring used at the new pillars in November was not as accurate as at the other pillars. The results with the new pillars are listed in Table 5.22, but not included in the final results.

5.5.2 Calibration of the Mekometer

The Kern Mekometer ME5000 no. 357094 and reflector no. 374414 were used, calibrated at the Nummela Standard Baseline in 1997. The instruments were then the property of HUT (Department of Surveying, Laboratory of Geodesy and Cartography). In the calibrations, no significant scale error was found (correction +0.03 mm/km ±0.10 mm/km), and consequently, no pre-set scale correction was applied. If the comparisons done at the Chengdu Standard Baseline would have indicated some change in the equipment, the appropriate corrections would have been considered. The additive constant could also be determined in Chengdu and compared with the values in 1997 (+0.11 mm ±0.02 mm, +0.14 mm ±0.10 mm).

5.5.3 Refraction

The dry temperature was measured using the FGI's Wilh. Lambrecht 761 psychrometer (no. 400077, thermometers 3467/73, 2727/86) at the Mekometer and a Chinese DHM2 psychrometer (no. 920416) at the reflector; the wet temperature for relative air humidity was measured at the Mekometer only. According to the calibration certificates for the FGI thermometer, uncertainty in the air temperature observations was less than 0.1°C. Air pressure was measured with the FGI's Thommen 3B4.01.1 aneroid (no. 164610). In the computation, the

input pressure values were corrected for the influence of altitude on atmospheric pressure. The aneroid was compared using the FGI's Fuess mercury barometer, the traceability of which results from comparisons done at the Finnish Meteorological Institute. Uncertainty in the pressure observations was less than 30 Pa. No significant difference between the Finnish and the Chinese weather instruments was found.

During the first measurements on 23–26 September, the weather was quite ideal: mostly cloudy, sometimes hazy. The temperature was between 18 °C and 23 °C, while the air pressure was between 95.0 kPa and 95.9 kPa and the relative air humidity between 65 % and 97 %. During the second measurement on 5–8 November, the weather was not that favourable: it included both sunny days with foggy mornings and cloudy days with some rain. The temperature was between 11 °C and 23 °C, while the air pressure was between 95.4 kPa and 96.0 kPa and the relative air humidity between 54 % and 98 %. The different weather conditions can be seen in the adjustment results.

The weather data are listed among distance observations in Appendices 1–4 in the study by Jokela et al. (2000, 39–46) and were used to compute the actual refractive index, n_{ACT}. Several formulas (Kern 1986; Rüeger 1996) were tested; formulas provided by Owens (1967) were used in the final computation. (The formulas recommended by IAG (2000), which were used in the later EDM works presented in this thesis, were not yet available at the time of original computation.) n_{ACT} index varied between 1.000258737 and 1.000272308. The reference refractive index for computing the first velocity correction was n_{REF} = 1.000284515. From the measured distance, s_m, the corrected distance, s_c ,was obtained:

$$s_c = \frac{n_{REF}}{n_{ACT}} s_m. \qquad \text{(Eq. 5.4)}$$

5.5.4 Geometrical corrections

The Mekometer and the reflector were placed above the central benchmarks on the observation pillars using Chinese forced-centring devices (Figs. 5.10–5.11 and 5.13). No horizontal projection corrections were needed, and the instrument heights (323 mm, about the same for every pillar) were included in the vertical geometrical correction when processing the measurements.

The levelled heights of the central benchmarks on the observation pillars are listed in Table 5.20. For the computation, all of the distances were reduced to the height level $H = 0$ in this local system using the following formula:

$$ds = \sqrt{\left(s^2 - \left(h_i - h_j\right)^2\right) / \left(\left(1 + \frac{h_i}{\mathrm{R}}\right)\left(1 + \frac{h_j}{\mathrm{R}}\right)\right)} - s, \qquad \text{(Eq. 5.5)}$$

where h_i and h_j are instrument heights, R = 6 370 km and ds is the correction to the measured distance s.

Table 5.20 *Pillar numbers in the calibration measurements (cf. Fig. 5.14), distances from the zero point of the interference measurements (i.e. pillar numbers in the Mekometer and interference measurements in 1998) and pillar heights in the local system. The listed heights are levelled heights for the top surfaces of the central benchmark bolts on the pillars. The instrument heights for the geometrical corrections of Mekometer observations were 0.323 m higher.*

Pillar no.	Distance (m)	Height (m)
0	768	2.3317
1	384	3.2541
2	192	3.7147
–	96	3.9402
3	48	4.0570
–	24	4.1193
4	6	4.1596
–	1	4.1666
–	0	4.1691
5	5	4.1865
6	20	4.2208
7	60	4.3193
8	120	4.4666
9	240	4.7544
10	480	5.3313
11	720	5.9055

5.5.5 Computation

Possible pillar movements during autumn could not be ignored, and the observations made in September and November were computed separately. All of the 12 + 3 pillars were in use throughout the four-day observation periods, and the dependence on time was not investigated in more detail; however, thermal expansion or other elastic deformation of pillars was discernible during the interference observations (Fig. 5.8).

After the first velocity correction and vertical geometrical correction, the measured distances were adjusted using least squares adjustments. Weights W of observations i were inversely proportional to the squares of the *a priori* standard errors,

$$W_i \propto 1 / (0.1 \text{ mm} + 0.1 \text{ ppm})^2;$$

smaller weights were used for the less accurate new pillars. Other weight models were also tested. The measured, corrected and adjusted distances and residuals are listed in Appendices 1–4 in Jokela et al. (2000, 39–46).

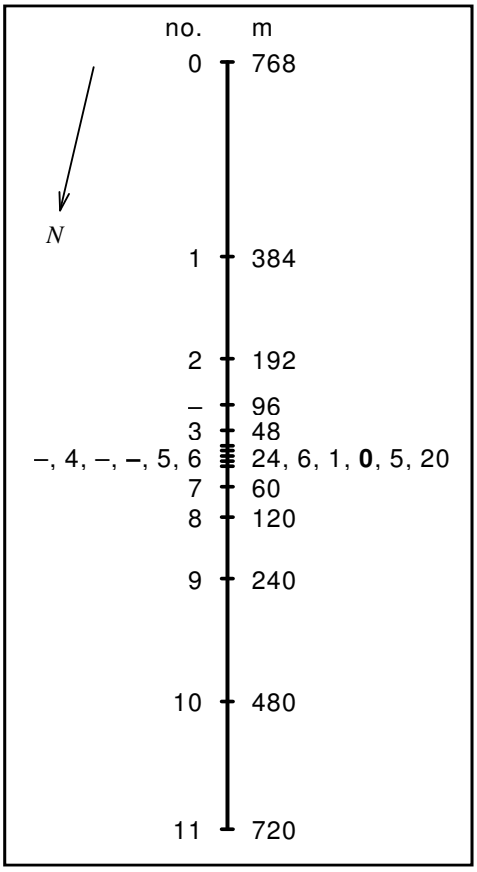

Figure 5.14 *Design of the Chengdu Standard Baseline.*

5.5.6 Results from the EDM

The final results of the Mekometer measurements at the Chengdu Standard Baseline in 1998 are presented in Table 5.21. The greatest change from September to November at pillar 5 results from the casting of a theodolite pillar for the interference measurements done in October. The new pillar had to be erected at a location where it leans against pillar 5 (Fig. 5.11). Pillar movements are also an obvious reason for the other 0.4-mm or larger differences; monitoring the elastic and other movements could have been continued with a repeated high-precision EDM. The additive constant differs from the values obtained in 1997, but all of the values are well within the normal accuracy limits of the instrument.

As much as 99% of the residuals are less than 0.5 mm. For the September measurements, 80% are less than 0.2 mm and 90% less than 0.3 mm; for November, 50% are less than 0.2 mm and 80% less than 0.3 mm.

Standard uncertainties of section lengths from the adjustments range from 0.04 mm to 0.08 mm. The uncertainty in the Mekometer measurements is between 0.1 mm and 0.2 mm, including the level of uncertainty in correcting the measured values (0.1 mm/km) and the level of uncertainty in the calibration (0.1 mm/km). The uncertainty in calibration (at Nummela) includes uncertainty in the projection measurements and possible pillar movements after the previous interference observations. The standard uncertainty of the Nummela Standard Baseline, estimated during the interference observation process in 1996, was 0.07 mm for the 864-m baseline. Using the calibration results from Nummela in 1997, and disregarding the interference measurements at Chengdu, the standard uncertainty in the traceability chain is from 0.1 mm to 0.2 mm (0.16 mm/km + uncertainty from the adjustment). When considering the pillar movements during the measurements, this does not appear to be overly pessimistic.

The interference measurements do not greatly improve the results. Doubling a stable Väisälä baseline under favourable conditions can yield more accurate results, such as 0.08 mm and 0.10 mm for two 2 × 432-m baselines (Konttinen 1988; Kääriäinen et al. 1988) using the Kern Mekometer ME3000. In Chengdu, the geometry was different, since only 25% of the baseline could be measured with both the Väisälä comparator and the EDM instrument. A more serious disadvantage is that the short-term stability was not favourable, which often means additional problems in the long run. Now the estimation of uncertainty only includes the measurement procedure and traceability chain until and including the measurement in 1998, and the owner of the baseline is responsible for the stability control and estimation of uncertainty for the later use of the baseline.

Figure 5.15 *The northern part of the Chengdu Standard Baseline, pillars no. 6, 7, 8, etc.*

Table 5.21 *Final results of Kern Mekometer ME5000 (no. 357094) measurements at the Chengdu Standard Baseline in 1998: section lengths and additive constant (ac). The results and the expanded uncertainties in the final column represent the combined adjustment of measurements in September and November.*

Interval		1998-09-23/24/25/26 Length (mm)	1998-11-05/06/07/08 Length (mm)	Diff. (mm)	1998 Length (mm)
768–384	0–1	384 005.13 ±0.12	384 005.20 ±0.18	+0.07	384 005.17 ±0.16
384–192	1–2	192 002.73 ±0.10	192 002.39 ±0.14	–0.34	192 002.56 ±0.12
192–48	2–3	144 001.16 ±0.08	144 001.65 ±0.14	+0.49	144 001.40 ±0.12
48–6	3–4	42 000.61 ±0.08	41 999.96 ±0.14	–0.65	42 000.29 ±0.12
6–5	4–5	11 005.10 ±0.10	11 004.76 ±0.16	–0.34	11 004.93 ±0.14
5–20	5–6	14 994.30 ±0.10	14 995.24 ±0.16	+0.94	14 994.77 ±0.14
20–60	6–7	40 001.87 ±0.08	40 001.34 ±0.14	–0.53	40 001.61 ±0.12
60–120	7–8	60 000.12 ±0.08	60 000.35 ±0.12	+0.23	60 000.24 ±0.12
120–240	8–9	119 998.50 ±0.08	119 998.27 ±0.14	–0.23	119 998.39 ±0.12
240–480	9–10	240 002.72 ±0.10	240 003.28 ±0.16	+0.56	240 003.00 ±0.12
480–720	10–11	240 005.22 ±0.10	240 005.06 ±0.16	–0.16	240 005.14 ±0.14
		ac: –0.01 ±0.06	ac: –0.08 ±0.08		ac: –0.04 ±0.08
768–720	0–11	1 488 017.46 ±0.32	1 488 017.50 ±0.50	+0.04	1 488 017.50 ±0.44

Table 5.22 *Final results of Kern Mekometer ME5000 (no. 357094) measurements at the Chengdu Standard Baseline in 1998: section lengths and additive constant (ac), with expanded uncertainties. The results of the measurements in September were used to adjust the mirrors of the Väisälä interference comparator in approximately the correct places and should not be used for any other purpose. The results of the measurements in November can be used when positions of the new pillars are required.*

Interval	1998-09-23/24/25/26 Length (mm)	1998-11-05/06/07/08 Length (mm)
768–384	384 005.13 ±0.10	384 005.21 ±0.16
384–192	192 002.73 ±0.08	192 002.39 ±0.34
192–96	95 999.16 ±0.38	95 998.62 ±0.34
96–48	48 002.00 ±0.38	48 003.04 ±0.34
48–24	23 998.04 ±0.40	23 997.01 ±0.36
24–6	18 002.57 ±0.40	18 002.95 ±0.36
6–0	5 999.88 ±0.42	5 999.82 ±0.36
0–5	5 005.22 ±0.42	5 004.95 ±0.36
5–20	14 994.30 ±0.10	14 995.25 ±0.14
20–60	40 001.88 ±0.08	40 001.34 ±0.12
60–120	60 000.12 ±0.08	60 000.35 ±0.12
120–240	119 998.50 ±0.08	119 998.28 ±0.12
240–480	240 002.71 ±0.10	240 003.29 ±0.14
480–720	240 005.22 ±0.10	240 005.05 ±0.16
	ac: –0.01 ±0.06	ac: –0.08 ±0.08

5.6 Comparison and combination of interference measurements and EDM

The time of the interference measurements is closer to the second than to the first Mekometer measurements, as is the case for the results, too. The results from the interference measurements differ from the first Mekometer measurements by –0.16 mm at distance 6–192 and by –0.32 mm at distance 192–384 (Fig. 5.16). The longest comparable distance is the sum of these, 6–384, with a difference of –0.48 mm. The corresponding differences from the second Mekometer measurements are 0.00 mm, +0.02 mm and +0.02 mm. The consistency in measurements is similar to that shown with the new pillars (Fig. 5.17), in which the large degree of uncertainty is caused by the inaccurate forced-centring device at the new pillars. When considering the possible pillar movements, there is no significant difference in the results between the interference measurements and the Mekometer measurements.

The final results (Table 5.23) are a weighted mean of the interference measurements (Table 5.19) and Mekometer measurements (Table 5.21). The results represent the entire measurement period from 23 September to 8 November 1998, including possible pillar movements. Most of the results come from the Mekometer measurements; the few distances measured with the Väisälä comparator confirm them. No cause for a scale correction for the Mekometer was found. The uncertainty estimates are expanded uncertainties in the traceability chain.

Possible pillar movements must be borne in mind when applying the results to the calibrations. These movements should be monitored with regularly repeated, high-precision EDMs. A sketch of the first monitoring results, including the results from the current project, is presented in Fig. 5.18 (a-c). Stabilization of a baseline may require more than a decade, and the first trends in the figures do not always give cause for concern. However, remeasurement of the Chengdu Standard Baseline with the Väisälä interference comparator appeared to be unnecessary, since EDM instruments would be better tools in such a case. When necessary, calibration of the most accurate control instruments could be performed, for example, at the Nummela Standard Baseline.

The computed lengths between all of the central markers are summarized in the final results presented in Table 5.24. These slope lengths can be used as such in most applications. If a different EDM instrument and reflector heights are used, new reductions with more precise heights may be necessary. The formula for the reductions is as follows:

$$s_{slope} = \sqrt{s_{h=0}^2 \left(1+\frac{h_i}{\mathrm{R}}\right)\left(1+\frac{h_j}{\mathrm{R}}\right) + \left(h_i - h_j\right)^2}, \qquad \text{(Eq. 5.6)}$$

where $s_{h=0}$ is a length taken from Table 5.23 (or a sum of several sections), h_i and h_j are the heights of the end points above $h = 0$, and R = 6 370 km.

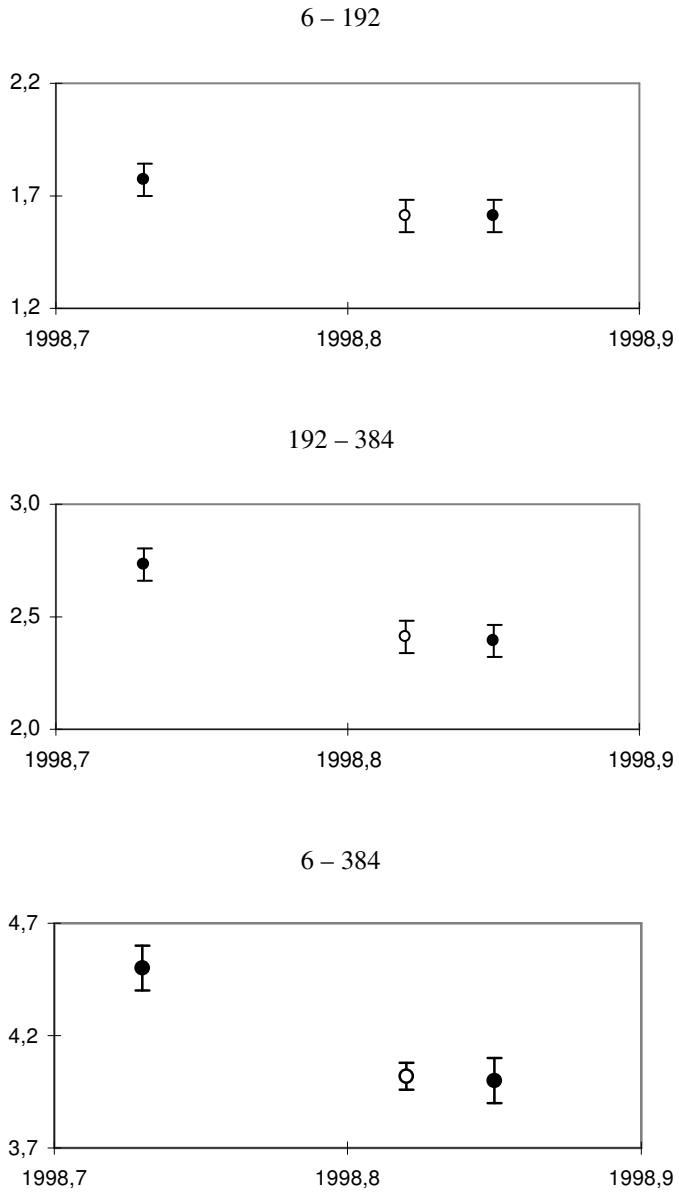

Figure 5.16 *Distances (mm part) between the old pillars based on the Kern ME5000 measurements performed in September and November (filled symbols) and the interference measurements performed in October (open symbol).*

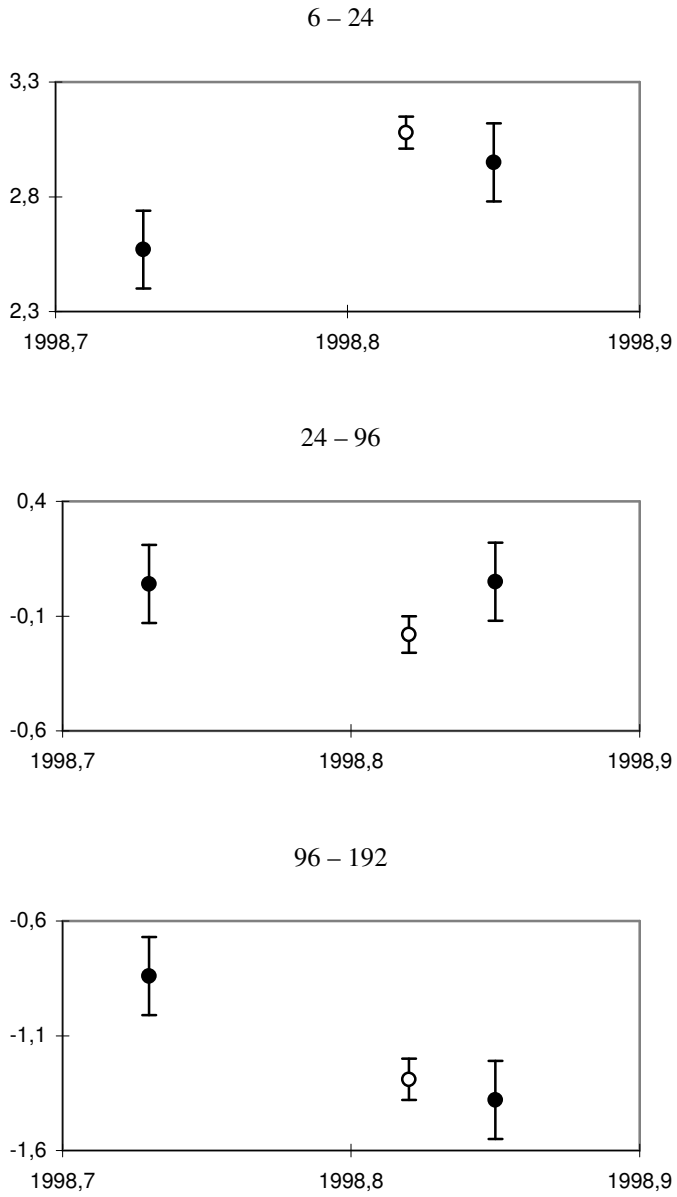

Figure 5.17 *Distances (mm part) between the new pillars based on the Kern ME5000 measurements performed in September and November (filled symbols) and the interference measurements performed in October (open symbol).*

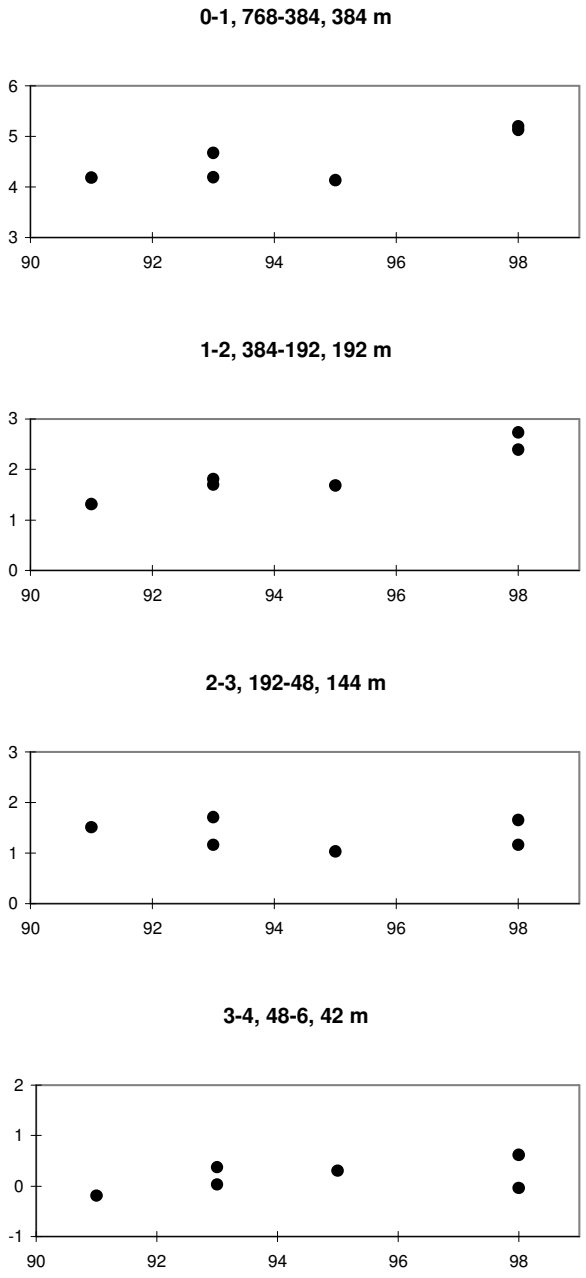

Figure 5.18a *Variation (mm) in lengths between reference markers at the Chengdu Standard Baseline based on the invar scale measurements (1993, 1995) and the Kern Mekometer ME5000 measurements (1991, 1993, 1998).*

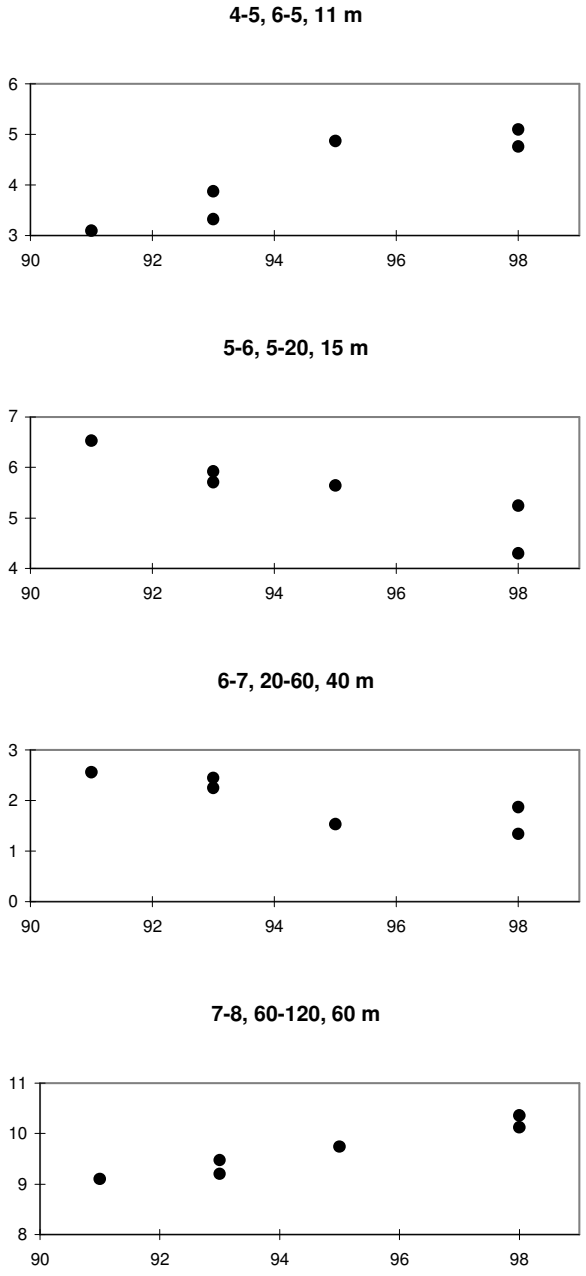

Figure 5.18b *Variation (mm) in lengths between reference markers at the Chengdu Standard Baseline based on the invar scale measurements (1993, 1995) and the Kern Mekometer ME5000 measurements (1991, 1993, 1998).*

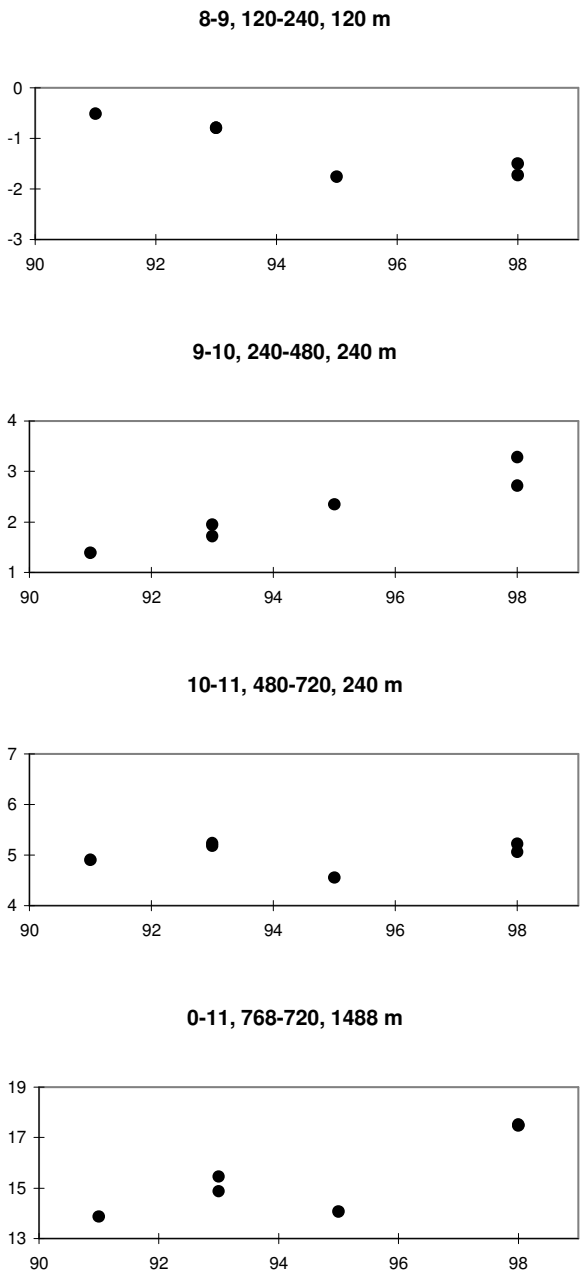

Figure 5.18c *Variation (mm) in lengths between reference markers at the Chengdu Standard Baseline based on the invar scale measurements (1993, 1995) and the Kern Mekometer ME5000 measurements (1991, 1993, 1998).*

Table 5.23 *Final results; the length of the Chengdu Standard Baseline with its sections at the height level H = 0 (i.e. at the foot of pillar 0 at 768 m), with expanded uncertainties.*

Interval		Length (mm)
768–384	0–1	384 005.17 ±0.16
384–192	1–2	192 002.50 ±0.14
192–48	2–3	144 001.35 ±0.06
48–6	3–4	42 000.27 ±0.06
6–5	4–5	11 004.93 ±0.14
5–20	5–6	14 994.77 ±0.14
20–60	6–7	40 001.61 ±0.12
60–120	7–8	60 000.24 ±0.12
120–240	8–9	119 998.39 ±0.12
240–480	9–10	240 003.00 ±0.12
480–720	10–11	240 005.14 ±0.14
768–720	0–11	1 488 017.37 ±0.42

Table 5.24 *Final results; the lengths of the Chengdu Standard Baseline sections at all combinations in autumn 1998. The values were computed using the results from Table 5.23 and the heights from Table 5.20; i and j are the pillar numbers, and H_i and H_j are the heights of the central markers i and j.*

i	*j*	Length *i–j* (mm), reduced onto the height level *H* = 0	H_i (mm)	H_j (mm)	Length *i–j* (mm), slope distance between central markers
0	1	384 005.17 ±0.16	2 332	3 254	384 006.45 ±0.16
0	2	576 007.67 ±0.22	2 332	3 715	576 009.60 ±0.22
0	3	720 009.02 ±0.22	2 332	4 057	720 011.45 ±0.22
0	4	762 009.29 ±0.22	2 332	4 160	762 011.87 ±0.22
0	5	773 014.22 ±0.26	2 332	4 186	773 016.84 ±0.26
0	6	788 008.99 ±0.30	2 332	4 221	788 011.66 ±0.30
0	7	828 010.60 ±0.32	2 332	4 319	828 013.42 ±0.32
0	8	888 010.84 ±0.34	2 332	4 467	888 013.88 ±0.34
0	9	1 008 009.23 ±0.36	2 332	4 754	1 008 012.70 ±0.36
0	10	1 248 012.23 ±0.38	2 332	5 331	1 248 016.59 ±0.38
0	11	1 488 017.37 ±0.42	2 332	5 906	1 488 022.62 ±0.42

Table 5.24 *continued.*

i	j	Length i–j (mm), reduced onto the height level $H = 0$	H_i (mm)	H_j (mm)	Length i–j (mm), slope distance between central markers
1	2	192 002.50 ±0.14	3 254	3 715	192 003.16 ±0.14
1	3	336 003.85 ±0.16	3 254	4 057	336 005.00 ±0.16
1	4	378 004.12 ±0.16	3 254	4 160	378 005.42 ±0.16
1	5	389 009.05 ±0.22	3 254	4 186	389 010.39 ±0.22
1	6	404 003.82 ±0.26	3 254	4 221	404 005.21 ±0.26
1	7	444 005.43 ±0.28	3 254	4 319	444 006.97 ±0.28
1	8	504 005.67 ±0.30	3 254	4 467	504 007.43 ±0.30
1	9	624 004.06 ±0.34	3 254	4 754	624 006.26 ±0.34
1	10	864 007.06 ±0.36	3 254	5 331	864 010.14 ±0.36
1	11	1 104 012.20 ±0.38	3 254	5 906	1 104 016.18 ±0.38
2	3	144 001.35 ±0.06	3 715	4 057	144 001.84 ±0.06
2	4	186 001.62 ±0.08	3 715	4 160	186 002.27 ±0.08
2	5	197 006.55 ±0.16	3 715	4.186	197 007.24 ±0.16
2	6	212 001.32 ±0.20	3 715	4 221	212 002.06 ±0.20
2	7	252 002.93 ±0.24	3 715	4 319	252 003.81 ±0.24
2	8	312 003.17 ±0.26	3 715	4 467	312 004.28 ±0.26
2	9	432 001.56 ±0.30	3 715	4 754	432 003.10 ±0.30
2	10	672 004.56 ±0.32	3 715	5 331	672 006.98 ±0.32
2	11	912 009.70 ±0.36	3 715	5 906	912 013.02 ±0.36
3	4	42 000.27 ±0.06	4 057	4 160	42 000.42 ±0.06
3	5	53 005.20 ±0.16	4 057	4 186	53 005.39 ±0.16
3	6	67 999.97 ±0.20	4 057	4 221	68 000.21 ±0.20
3	7	108 001.58 ±0.24	4 057	4 319	108 001.97 ±0.24
3	8	168 001.82 ±0.26	4 057	4 467	168 002.43 ±0.26
3	9	288 000.21 ±0.30	4 057	4 754	288 001.25 ±0.30
3	10	528 003.21 ±0.32	4 057	5 331	528 005.14 ±0.32
3	11	768 008.35 ±0.34	4 057	5 906	768 011.18 ±0.34

Table 5.24 *continued.*

i	***j***	**Length *i–j* (mm), reduced onto the height level $H = 0$**	H_i **(mm)**	H_j **(mm)**	**Length *i–j* (mm), slope distance between central markers**
4	5	11 004.93 ±0.14	4 160	4 186	11 004.97 ±0.14
4	6	25 999.70 ±0.20	4 160	4 221	25 999.79 ±0.20
4	7	66 001.31 ±0.24	4 160	4 319	66 001.55 ±0.24
4	8	126 001.55 ±0.26	4 160	4 467	126 002.01 ±0.26
4	9	245 999.94 ±0.28	4 160	4 754	246 000.83 ±0.28
4	10	486 002.94 ±0.32	4 160	5 331	486 004.71 ±0.32
4	11	726 008.08 ±0.34	4 160	5 906	726 010.75 ±0.34
5	6	14 994.77 ±0.14	4 186	4 221	14 994.82 ±0.14
5	7	54 996.38 ±0.18	4 186	4 319	54 996.58 ±0.18
5	8	114 996.62 ±0.22	4 186	4 467	114 997.04 ±0.22
5	9	234 995.01 ±0.26	4 186	4 754	234 995.86 ±0.26
5	10	474 998.01 ±0.28	4 186	5 331	474 999.74 ±0.28
5	11	715 003.15 ±0.32	4 186	5 906	715 005.78 ±0.32
6	7	40 001.61 ±0.12	4 221	4 319	40 001.76 ±0.12
6	8	100 001.85 ±0.16	4 221	4 467	100 002.22 ±0.16
6	9	220 000.24 ±0.20	4 221	4 754	220 001.04 ±0.20
6	10	460 003.24 ±0.24	4 221	5 331	460 004.93 ±0.24
6	11	700 008.38 ±0.28	4 221	5 906	700 010.96 ±0.28
7	8	60 000.24 ±0.12	4 319	4 467	60 000.46 ±0.12
7	9	179 998.63 ±0.16	4 319	4 754	179 999.28 ±0.16
7	10	420 001.63 ±0.20	4 319	5 331	420 003.17 ±0.20
7	11	660 006.77 ±0.26	4 319	5 906	660 009.21 ±0.26
8	9	119 998.39 ±0.12	4 467	4 754	119 998.82 ±0.12
8	10	360 001.39 ±0.16	4 467	5 331	360 002.71 ±0.16
8	11	600 006.53 ±0.22	4 467	5 906	600 008.74 ±0.22
9	10	240 003.00 ±0.12	4 754	5 331	240 003.88 ±0.12
9	11	480 008.14 ±0.18	4 754	5 906	480 009.92 ±0.18
10	11	240 005.14 ±0.14	5 331	5 906	240 006.04 ±0.14

6 Gödöllő Standard Baseline

6.1 History of the baseline

Based on a scientific-technical agreement between the Ministries of Agriculture in Finland and Hungary, the project for the Gödöllő Standard Baseline was established in 1985. The 864-m-long baseline was built in 1986 and measured in 1987 as a joint project between the FGI and FÖMI. The Väisälä light interference method and duplication with a Kern Mekometer ME3000 were used for the measurements (Kääriäinen et al. 1988). Since 1987, the FÖMI has controlled the lengths of the baseline sections with a high-precision electronic distance measurement (EDM) instrument, the Kern Mekometer ME5000, once or twice a year.

In Hungary, the law of measurements was enacted in 1991 and the act on surveying and mapping in 1995. In the 1990s, the status of the ISO quality systems was also emphasized. All of these actions require calibrations and certifications for the measuring instruments and increase demands for further improvement at the Gödöllő Standard Baseline.

Preparation and coordination of the remeasurement process in 1999 was assigned to the Satellite Geodetic Observatory of FÖMI. The Hungarian staff included research workers Dr Zsuzsanna Németh and Mr Gábor Virág. The interference measurements were performed by experts from the FGI, Dr Markku Poutanen and Mr Jorma Jokela, using the FGI's Väisälä light interference comparator. The interferometrically measured half of the baseline was doubled by Dr Károly Szaládi using a high-precision EDM instrument, the Kern Mekometer ME 5000, from the Hungarian Paks Atomic Power Station. This section summarizes the results and compares them with the previous measurements.

6.2 Scale and traceability of interference measurements

Quartz gauges no. 49 and 51 were used in the measurements done in Gödöllő. Results from the absolute calibrations done in the year 2000 and time series of comparisons were used to obtain the traceability to the definition of the metre.

6.2.1 Absolute calibrations of quartz gauges

The quartz gauges were calibrated at the Centre for Metrology and Accreditation (CMA, nowadays better known as MIKES), in Helsinki, Finland, using the interferometric equipment used for calibrating gauge blocks (MIKES 2000; Lassila 2003). The traceability of the He-Ne laser when using this equipment comes through calibrations done with an iodine-stabilized, He-Ne laser. The temperature, pressure and humidity meters are also traceable to national standards.

The quartz gauge was placed between a reference plate and a 60-mm gauge block, which were placed in mechanical contact with a force of 0.1 N. A glass plate was used for the adjustments and a steel plate for the measurements. The

length of the gauge block was determined before and after the measurements for the quartz gauge. The observed values were corrected for the length of the gauge block, temperature corrections were made for the quartz gauge and the gauge block, and air pressure and force corrections were made for the quartz gauge.

The uncertainty of the measurement was determined by estimating the uncertainty in repeatability, laser wavelength, temperatures, temperature coefficients, the refractive index of air, centring and adjusting the instruments, the gauge block length, the imperfection in optics, the imperfection in the flatness and parallelism of the surfaces, force correction, pressure correction and phase determination. The expanded uncertainty of the absolute calibrations was 72 nm.

The absolute calibrations were performed between January and March 2000; gauge no. 51 was calibrated on 2–22 February, and gauge no. 49 on 22 February – 7 March. The calibrations were performed at a temperature of 20 ºC and air pressures ranging from 98.5 kPa to 102.2 kPa; the results were reduced to 20 ºC and 101.325 kPa. Just as in the Väisälä comparator, the quartz gauges were measured in two different positions, "up" and "down", relative to their longitudinal axes. For some special quartz gauges, this difference may be significant, but not for gauges nos. 49 or 51.

The lengths of the quartz gauges were as follows at epoch 2000.16 (MIKES 2000):

no. 49: 1 000 032.346 μm ± 0.072 μm;
no. 51: 1 000 018.362 μm ± 0.072 μm.

The results fit well with previous absolute calibrations done at the PTB, in Braunschweig, Germany, in November 1995 (PTB 1996):

no. 49: 1 000 032.35 μm ± 0.06 μm;
no. 51: 1 000 018.38 μm ± 0.06 μm.

Annual changes in lengths are of the order of +5 nm; for these results obtained between the years 1995 and 2000, the changes cannot be distinguished.

6.2.2 Comparisons of quartz gauges

Between the absolute calibrations, the quartz gauge system is maintained by comparisons done at the University of Turku's Tuorla Observatory. Since 1953, the other quartz gauges have been compared using the principal normal, gauge no. 29. The method is based on optics, recording and measuring interference fringes, as presented in Chapter 3.

The absolute values can be directly traced to the definition of the metre. However, they represent only the calibration period and laboratory conditions, and the uncertainty is much larger than the repeatability of the comparisons. On the other hand, the recent history of the quartz gauges primarily concerns the present baseline measurement. The interpolation and extrapolation at the end of

the time series do not compensate well for the possible recent changes in the change of length of the quartz gauges.

The computed values using the continuum of absolute measurements and comparisons were as follows for the epoch of the latest absolute calibrations, 2000.16:

no. 49: 1 000 032.375 μm ± 0.004 μm;
no. 51: 1 000 018.415 μm ± 0.004 μm.

The uncertainties are small thanks to the long time series at the Tuorla Observatory. In addition to gauges nos. 49 and 51, quartz gauges nos. VIII and 50 and the results of their recent absolute calibrations were used in the latest comparisons. The means of the observed values were as follows when reduced to epoch 2000.16:

no. 49: 1 000 032.350 μm ± 0.035 μm;
no. 51: 1 000 018.382 μm ± 0.015 μm.

Two (for gauge no. 49) or three (for gauge no. 51) comparisons were made in March – September 1999 and two comparisons in December 1999 – March 2000. The values reported here are based on studies performed at the Tuorla Observatory by Dr Aimo Niemi.

6.2.3 Lengths of quartz gauges at Gödöllő

Since the recently observed values fit well with the old and new traceable absolute calibrations and with the long stable history of comparisons (Fig. 6.1), they were used in the final computation done for this project. The interference measurements done at the Gödöllő Standard Baseline were performed in October – November 1999. The lengths of the quartz gauges at the mean epoch 1999.8 were as follows:

no. 49: 1 000 032.35 μm ± 0.04 μm;
no. 51: 1 000 018.38 μm ± 0.04 μm.

The above lengths are valid at a temperature of 20 ºC. The lengths at temperature t (ºC) and pressure p (mmHg) are as follows:

no. 49:

$$l_{49} = 1\ \text{m} + [\ 32.35 + 0.3937 \times (t - 20) + 0.00155 \times (t - 20)^2 - 0.00099 \times (p - 760.)\ ]\ \mu\text{m};$$

(Eq. 6.1)

no. 51:

$$l_{51} = 1\ \text{m} + [\ 18.38 + 0.3938 \times (t - 20) + 0.00171 \times (t - 20)^2 - 0.00099 \times (p - 760.)\ ]\ \mu\text{m}.$$

(Eq. 6.2)

The formulas are based on studies conducted at the Tuorla Observatory by Dr Aimo Niemi.

In Gödöllő, the thermometer readings at the quartz gauge varied from 12.01 ºC to 5.75 ºC. Corrections varied from 0.00 ºC to –0.02 ºC, respectively, according to certificates of calibration.

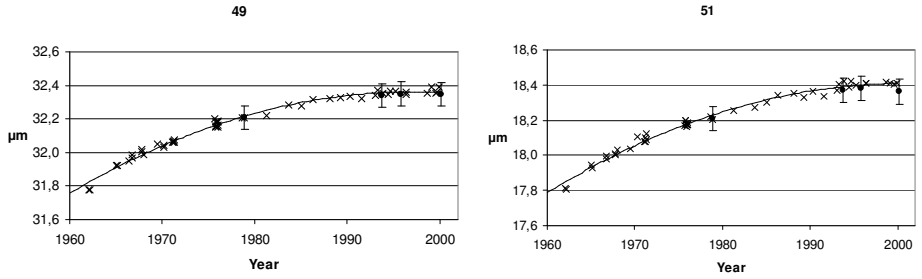

Figure 6.1 *Comparisons (×) and absolute calibrations (•) of quartz gauges nos. 49 and 51.*

Table 6.1 *Length of quartz gauge at ambient temperature t (℃) and pressure p (mmHg).*

Quartz gauge no. 49					Quartz gauge no. 51				
Date and time		***t***	***p***	**µm + 1 m**	**Date and time**		***t***	***p***	**µm + 1 m**
1999-10-09	22:44	10.56	747.7	14.83	1999-11-03	21:04	7.53	752.8	27.69
	23:06	10.81	747.7	14.92		21:16	7.39	752.8	27.64
	23:43	11.81	747.7	15.28		21:48	7.46	753.0	27.66
1999-10-10	00:04	11.94	747.7	15.33		21:58	7.50	753.0	27.68
1999-10-10	21:11	11.36	748.6	15.12	1999-11-06	00:28	8.44	747.3	28.02
	21:28	11.29	748.6	15.09		00:52	8.26	747.3	27.95
	22:17	11.63	748.3	15.22		01:20	8.26	746.8	27.95
	22:31	11.64	748.3	15.22		01:33	8.32	746.8	27.97
1999-10-23	00:29	8.12	747.0	13.95	1999-11-06	19:50	9.44	742.9	28.38
	00:46	8.31	747.0	14.02		20:01	9.30	742.9	28.33
	01:21	8.26	746.9	14.00		20:34	7.77	743.2	27.78
	01:39	8.18	746.9	13.98		20:55	7.16	743.2	27.57
1999-10-26	19:26	11.81	746.8	15.28					
	19:37	11.89	746.8	15.31					
	20:05	11.75	746.8	15.26					
	20:23	11.60	746.8	15.20					
1999-10-30	23:32	7.39	751.3	13.69					
	23:47	7.50	751.3	13.73					
1999-10-31	00:20	7.68	751.2	13.80					
	00:33	7.80	751.2	13.84					
1999-11-08	19:15	6.29	749.5	13.31					
	19:27	6.42	749.5	13.36					
	20:01	6.30	749.7	13.32					
	20:18	6.35	749.7	13.33					
1999-11-09	01:00	5.90	750.3	13.18					
	01:16	5.86	750.3	13.16					
	01:51	5.83	750.3	13.15					
	02:05	5.90	750.3	13.18					

The air pressure varied between 99.0 kPa and 100.4 kPa. The field barometer has been regularly compared with the Fuess mercury barometer at the FGI. In 1996–1999, deviation from the reference value varied between –0.27 kPa and –0.12 kPa. Here the correction is +0.16 kPa, which is based on the comparisons made on 1 September and 30 November 1999. The traceability of the mercury barometer results from comparisons done at the Finnish Meteorological Institute. Both Finnish and Hungarian weather instruments were used; the differences between them were insignificant. The computed actual lengths of quartz gauges at the Gödöllő Standard Baseline are listed in Table 6.1.

6.3 Interference measurements

6.3.1 Mirrors and compensators

In the computation done for the interference measurements, some corrections are needed depending on how the instruments are installed and adjusted. When using the Väisälä interference comparator, the quartz gauge is placed in optical and physical contact with mirror 0, but a 1 μm to 3 μm gap must be left between the quartz gauge and mirror 1. A red filter, $\lambda/2 = 320$ nm, was used for the optical measurement of the gap width. The measurement method is described in Section 4.2.1. The results are listed together with the interference observations in Table 6.6.

The thicknesses of the mirrors used in Gödöllő are listed in Table 6.2. Light reflects from the front surface of a mirror, but the centre of the mirror body is used in the projection measurements; the different thicknesses necessitate making corrections. For every length $0 - v$, the correction is $(D_v - D_0) / 2$, where D_v and D_0 are the thicknesses (Table 6.3).

Between mirrors 0 and 1, the scale-determining quartz gauge is placed between the glass surfaces, whereas light travels between the shorter aluminium-covered surfaces over and below. A correction of –11 nm/m ±40 nm/m has been used since the latest resurfacing of mirrors in 1998. Later determinations of the correction have yielded slightly larger values, but with a larger degree of uncertainty.

One of the reflecting beams is delayed in front of the telescope to facilitate finding the interference fringes. The delay in micrometres can be computed based on the rotation angle of the compensator glass; the formulas can be found in Section 4.3.1, and approximate values are listed in Table 4.2. Angles from 0º to 30º are preferable in interference observations, while larger angles should be decreased by moving a mirror by a comparable amount in the baseline direction.

There are many adjustable parts in the lamp and the telescope, and they essentially contribute to the success of the measurement but do not affect the results. The focal length of the collimator lens was 2.97 m.

Table 6.2 *Mirrors.*

Pillar ν	Mirror no.	Thickness (mm)
0	40	19.985
1	36	20.001
6	38	19.932
24	53	19.981
72	39	19.966
216	41	19.959
432	37	19.983

Table 6.3 *Corrections for thicknesses of mirror bodies.*

Distance	Correction (mm)
0–24	–0.002
0–216	–0.013
0–432	–0.001

Table 6.4 *Heights (mm) above/below underground marker 0.*

	Mirror centre	Forced centring plate	Users' marker
0	2 344	2 322	2 139
6	2 304	–	2 100
24	2 183	–	1 978
72	1 862	–	1 656
216	898	874	691
432	–548	–568	–753
864	–	–3 435	–3 625

6.3.2 Geometrical corrections

The final results are reduced to the level of underground marker 0. The heights used for the reductions are listed in Table 6.4. Not all heights are levelled, but the possible inaccuracy present is insignificant in the reductions. The correction to the reference height level (Table 6.19) is the sum of the inclination correction and height correction, which are combined in the formula presented in Section 4.3.4.

The degree of non-parallelism between the interference line and the line through the underground markers is small, and no horizontal reductions in the lengths are needed.

6.3.3 Refraction

Cloudy nights are needed for the interference measurements, and unfavourable weather conditions are often a problem. Nevertheless, waiting for 29 days is exceptional: in Gödöllő, the work proceeded rapidly up to the 216-m interference, which was found on 5 October, but the 432-m interference was not found until 3 November. The days were usually more or less cloudy, but at night the sky became clear. The nights from 15 October until 19 October were frosty. The weather changed in early November. Finally, two days and nights of pouring rain cheered the people up and provided ideal conditions for the last measurements.

Kukkamäki's (1969) equation for refraction correction is presented in Section 4.3.2. In Gödöllő, the coefficients, c_v, for the five formulas of temperature difference, Δt, are equal to those at Nummela (listed in Table 4.4; Eqs. 4.9–4.11). Thermometers and corrections to their readings are listed in Table 6.5; t_o and t_i are the thermometers at the quartz gauge.

If there are height differences at the baseline, the speed of light varies because of the different densities of the media. Using the heights in Table 6.4, and Eq. 4.13, it is possible to obtain the influence of the atmospheric pressure difference. In Gödöllő, the correction is negative, as pillar 0 is higher than the other pillars.

Table 6.5 *Corrections to the thermometers.*

Thermometer		Correction (°C) at			Thermometer		Correction (°C) at		
at (m)	**no.**	**+5°C**	**+10°C**	**+15°C**	**at (m)**	**no.**	**+5°C**	**+10°C**	**+15°C**
0	7933	–0.01	0.00	+0.01	144	7939	–0.03	–0.01	0.00
1	7936	0.00	+0.02	+0.02	168	7932	–0.07	–0.03	0.00
4	4480	–0.02	+0.02	+0.06	192	7938	–0.02	0.00	+0.01
10	4483	0.00	–0.01	–0.02	216	4484	+0.02	+0.03	+0.04
17	7935	–0.03	–0.01	0.00	264	47	–0.02	+0.02	–0.02
24	7348	+0.02	–0.02	0.00	312	46	–0.02	–0.01	–0.02
36	7349	–0.04	–0.03	–0.06	360	3867	–0.02	+0.02	0.00
48	7350	+0.02	–0.01	0.00	408	45	–0.04	–0.05	–0.04
60	7351	0.00	–0.01	–0.02	456	7937	–0.02	+0.01	+0.01
72	7352	+0.02	+0.02	+0.02					
96	48	–0.04	–0.02	–0.06	t_o	7929	–0.02	0.00	0.00
120	3864	–0.02	–0.08	–0.04	t_i	3868	–0.02	0.00	0.00

6.3.4 Interference observations

The interference measurements of the 432-m baseline consisted of five multiplications: 2 × 3 × 3 × 4 × 6 × 1 m = 432 m. Interference observations with the gap, refraction and compensator corrections are listed in Tables 6.6–6.10. The observations were performed by Jorma Jokela (JJ) and Markku Poutanen (MP). The lengths between the transferring bars, obtained from the interference observations, are presented in Table 6.11 and in Fig. 6.3.

Temperature observations were performed by Zsuzsanna Németh, Gábor Virág, Jenő Honfy, György Simeta and László Szücs. They, together with Béla László and Lajos László, also assisted in the projection measurements.

Table 6.6 *Computation of interference 0–1–6. The distance [0–1] is the sum of the lengths of the quartz gauge (from Table 6.1) and the gap between the quartz gauge and mirror 1. The distance [0–6] is six times the distance [0–1], corrected with compensator and refraction corrections.*

Date and time 1999	Obs.	Q. g. no.	Gap (μm)	[0–1] μm + 1 m	Comp. corr. (μm)	Refr. corr. (μm)	[0–6] μm + 6 m
9 Oct. 22:44	JJ	51	3.25	108.48	+91.40	–0.19	199.70
23:06	JJ	51	2.72	105.84	+94.32	–0.38	199.78
23:43	MP	51	4.24	117.12	+80.82	+0.09	198.03
10 Oct. 00:06	MP	51	2.96	109.74	+91.14	–0.11	200.77
							199.57
							±0.57
10 Oct. 21:11	JJ	51	1.71	100.98	+102.17	–0.09	203.06
21:28	JJ	51	1.89	101.88	+102.54	+0.01	204.43
22:17	MP	51	3.20	110.52	+93.96	+0.13	204.61
22:31	MP	51	2.29	105.06	+99.94	–0.04	204.96
							204.26
							±0.42
23 Oct. 00:29	JJ	51	1.97	95.52	+138.18	+0.22	233.92
00:46	JJ	51	1.95	95.82	+136.40	–0.02	232.20
01:21	MP	51	1.20	91.20	+142.22	+0.21	233.64
01:39	MP	51	1.33	91.86	+140.42	+0.27	232.54
							233.08
							±0.42
26 Oct. 19:26	JJ	51	2.29	105.42	+89.57	–0.58	194.42
19:37	JJ	51	0.99	97.80	+97.74	–0.56	194.99
20:05	MP	51	0.96	97.32	+98.29	–0.91	194.70
20:23	MP	51	2.03	103.38	+92.02	–0.72	194.67
							194.69
							±0.12

Table 6.6 *continued.*

Date and time 1999	Obs.	Q. g. no.	Gap (μm)	[0–1] μm + 1 m	Comp. corr. (μm)	Refr. corr. (μm)	[0–6] μm + 6 m
30 Oct. 23:32	JJ	51	2.37	96.36	+85.64	–0.09	181.91
23:47	JJ	51	2.37	96.60	+85.47	–0.23	181.84
31 Oct. 00:20	MP	51	2.08	95.28	+86.65	–0.03	181.90
00:33	MP	51	2.69	99.18	+81.31	–0.08	180.41
							181.52
							±0.37
3 Nov. 21:04	JJ	49	1.33	174.12	–24.54	–0.07	149.51
21:16	JJ	49	2.11	178.50	–26.83	–0.62	151.05
21:48	MP	49	2.61	181.62	–30.18	–0.23	151.21
21:58	MP	49	1.07	172.50	–20.35	–0.36	151.79
							150.89
							±0.49
6 Nov. 00:28	JJ	49	2.05	180.42	–48.60	–0.08	131.74
00:52	JJ	49	1.76	178.26	–45.80	–0.09	132.37
01:20	MP	49	2.43	182.28	–50.72	+0.04	131.59
01:33	MP	49	1.04	174.06	–41.49	+0.00	132.58
							132.07
							±0.24
6 Nov. 19:50	JJ	49	2.37	184.50	–54.99	+0.25	129.76
20:01	JJ	49	2.85	187.08	–59.31	+0.08	127.85
20:34	MP	49	2.77	183.30	–56.45	–0.54	126.31
20:55	MP	49	2.91	182.88	–55.39	–0.42	127.08
							127.75
							±0.74
8 Nov. 19:15	JJ	51	1.15	86.76	+49.59	–0.91	135.44
19:27	JJ	51	2.27	93.78	+42.06	–0.66	135.18
20:01	MP	51	1.84	90.96	+44.85	–0.25	135.56
20:18	MP	51	0.93	85.56	+49.59	–0.47	134.68
							135.21
							±0.20
9 Nov. 01:00	JJ	51	2.96	96.84	+45.20	–0.43	141.62
01:16	JJ	51	1.31	86.82	+54.99	–0.50	141.30
01:51	MP	51	2.96	96.66	+43.67	–0.50	139.83
02:05	MP	51	2.08	91.56	+48.72	–0.24	140.04
							140.70
							±0.45

Table 6.7 *Computation of interference 0–6–24. The distance [0–24] is four times the distance [0–6] (from Table 6.6), corrected with compensator and refraction corrections.*

Date and time 1999	4 × [0–6] µm + 24 m	Comp. corr. (µm)	Refr. corr. (µm)	[0–24] µm + 24 m
9 Oct. 22:18	798.78	+17.95	–3.87	812.86
23:17	799.12	+11.44	–3.36	807.20
23:31	792.10	+10.73	–3.06	799.78
10 Oct. 00:16	803.06	+3.69	–1.88	804.87
				806.18
				±2.71
10 Oct. 20:45	812.25	+59.91	–3.68	868.48
21:38	817.72	+61.77	–3.09	876.39
22:01	818.43	+57.09	–0.39	875.14
22:44	819.84	+56.72	–4.25	872.31
				873.08
				±1.75
22 Oct. 23:57	935.68	–109.99	–1.26	824.43
23 Oct. 00:57	928.79	–109.51	–1.68	817.60
01:10	934.55	–113.20	+0.39	821.74
01:49	930.18	–113.67	–0.10	816.41
				820.05
				±1.85
26 Oct. 19:00	777.66	+46.64	–1.60	822.71
19:45	779.94	+49.34	–2.82	826.46
19:54	778.79	+49.34	–3.07	825.06
20:34	778.69	+50.79	–4.13	825.35
				824.89
				±0.79
30 Oct. 23:15	727.63	+112.08	–2.56	837.16
23:57	727.37	+113.88	–2.23	839.02
31 Oct. 00:06	727.60	+114.66	–2.39	839.87
00:44	721.64	+117.21	–1.64	837.21
				838.31
				±0.68
3 Nov. 20:36	598.04	+13.94	–2.58	609.40
21:26	604.21	+13.06	–3.83	613.44
21:34	604.84	+12.87	–3.83	613.89
22:08	607.17	+14.99	–4.07	618.09
				613.70
				±1.78
6 Nov. 00:04	526.96	+28.02	+0.78	555.75
01:01	529.48	+31.67	–2.76	558.39
01:09	526.37	+31.21	–1.66	555.93
01:43	530.31	+29.99	–0.18	560.12
				557.55
				±1.05

Table 6.7 *continued.*

Date and time 1999	4 × [0–6] μm + 24 m	Comp. corr. (μm)	Refr. corr. (μm)	[0–24] μm + 24 m
6 Nov. 19:25	519.05	+43.36	–0.53	561.89
20:10	511.40	+47.41	–5.34	553.47
20:22	505.24	+46.88	–6.87	545.26
21:06	508.31	+55.65	–6.45	557.51
				554.53
				±3.54
8 Nov. 18:38	541.76	+17.25	–1.41	557.60
19:38	540.72	+19.91	–3.15	557.47
19:48	542.24	+21.33	–5.12	558.45
20:30	538.72	+22.96	–5.25	556.43
				557.49
				±0.41
8 Nov. 23:17	566.47	+6.37	–4.23	568.61
9 Nov. 01:27	565.22	+8.28	–2.96	570.54
01:39	559.34	+8.51	–2.39	565.46
02:17	560.15	+10.99	–3.08	568.06
				568.17
				±1.05

Figure 6.2 *Preparations for the doubling to 864 m.*

Table 6.8 *Computation of interference 0–24–72. The distance [0–72] is three times the distance [0–24] (from Table 6.9), corrected with compensator and refraction corrections.*

Date and time 1999	**3 × [0–24] µm + 72 m**	**Comp. corr. (µm)**	**Refr. corr. (µm)**	**[0–72] µm + 72 m**
9 Oct. 22:02	2 418.53	+110.34	–14.50	2 514.37
10 Oct. 00:28	2 418.53	+113.34	–21.45	2 510.42
				2 512.40
				±1.98
10 Oct. 20:28	2 619.24	–60.53	–16.24	2 542.47
22:58	2 619.24	–59.51	–23.29	2 536.43
				2 539.45
				±3.02
22 Oct. 23:15	2 460.14	+20.29	–12.43	2 468.00
23 Oct. 01:58	2 460.14	+14.92	–9.51	2 465.55
				2 466.77
				±1.22
26 Oct. 18:43	2 474.68	+6.71	–9.29	2 472.10
20:43	2 474.68	+4.37	–8.12	2 470.94
				2 471.52
				±0.58
30 Oct. 23:04	2 514.94	–36.02	–6.44	2 472.48
31 Oct. 00:57	2 514.94	–35.62	–4.37	2 474.95
				2 473.72
				±1.23
3 Nov. 20:28	1 841.11	–23.58	–10.98	1 806.54
22:20	1 841.11	–27.67	–8.03	1 805.41
				1 805.98
				±0.57
5 Nov. 23:53	1 672.64	+77.81	–8.60	1 741.85
6 Nov. 01:54	1 672.64	+72.48	–3.91	1 741.21
				1 741.53
				±0.32
6 Nov. 19:11	1 663.59	–7.68	–5.39	1 650.51
21:16	1 663.59	+15.85	–22.47	1 656.97
				1 653.74
				±3.23
8 Nov. 18:28	1 672.47	–32.46	–5.20	1 634.81
20:42	1 672.47	–30.40	–6.04	1 636.03
				1 635.42
				±0.61
8 Nov. 22:57	1 704.51	–51.74	–8.86	1 643.91
9 Nov. 02:27	1 704.51	–40.99	–15.78	1 647.74
				1 645.83
				±1.91

Table 6.9 *Computation of interference 0–72–216. The distance [0–216] is three times the distance [0–72] (from Table 6.8), corrected with compensator and refraction corrections. In the second measurement, only the first half could be observed.*

Date and time 1999	**3 × [0–72] µm + 216 m**	**Comp. corr. (µm)**	**Refr. corr. (µm)**	**[0–216] µm + 216 m**
9 Oct. 21:35	7 537.19	+263.26	–48.14	7 752.31
10 Oct. 01:02	7 537.19	+265.62	–71.06	7 731.75
				7 742.03
				±10.28
10 Oct. 20:03	7 618.35	+187.67	–51.16	7 754.86
				7 754.86
22 Oct. 22:46	7 400.32	+62.38	+1.02	7 463.72
23 Oct. 02:14	7 400.32	+75.84	+3.11	7 479.27
				7 471.49
				±7.78
26 Oct. 18:28	7 414.56	+40.19	–1.25	7 453.51
21:28	7 414.56	+27.77	+16.89	7 459.23
				7 456.37
				±2.86
30 Oct. 22:47	7 421.15	+26.76	–4.69	7 443.21
31Oct. 01:44	7 421.15	+45.68	–6.19	7 460.64
				7 451.92
				±8.71
3 Nov. 20:08	5 417.94	+12.41	–5.09	5 425.26
22:40	5 417.94	+19.35	+0.75	5 438.04
				5 431.65
				±6.39
5 Nov. 23:35	5 224.59	+137.42	+2.48	5 464.48
6 Nov. 02:20	5 224.59	+145.71	+5.46	5 375.76
				5 370.12
				±5.64
6 Nov. 18:46	4 961.22	+199.61	–19.63	5 141.21
22:02	4 961.22	+183.44	–5.61	5 139.05
				5 140.13
				±1.08
8 Nov. 18:09	4 906.26	+69.74	+2.43	4 978.43
21:11	4 906.26	+72.42	–1.80	4 976.87
				4 977.65
				±0.78
8 Nov. 22:41	4 937.48	+10.39	+6.21	4 954.08
9 Nov. 02:48	4 937.48	+69.89	–39.07	4 968.30
				4 961.19
				±7.11

Table 6.10 *Computation of interference 0–216–432. The distance [0–432] is two times the distance [0–216] (from Table 6.9), corrected with compensator and refraction corrections. In the third measurement, only the first half could be observed.*

Date and time 1999	2 × [0–216] µm + 432 m	Comp. corr. (µm)	Refr. corr. (µm)	[0–432] µm + 432 m
3 Nov. 18:33	10 863.30	+22.08	+45.43	10 930.81
23:18	10 863.30	+69.59	+0.91	10 933.79
				10 932.30
				±1.49
5 Nov. 23:06	10 740.24	+164.93	–83.27	10 821.89
6 Nov. 03:03	10 740.24	+149.44	–61.51	10 828.17
				10 825.03
				±3.14
6 Nov. 18:05	10 280.26	+76.73	+4.65	10 361.64
				10 361.64
8 Nov. 17:41	9 955.31	+31.77	+9.96	9 997.04
21:36	9 955.31	+33.23	+5.80	9 994.34
				9 995.69
				±1.35
8 Nov. 22:18	9 922.38	+37.38	+0.58	9 960.34
9 Nov. 03:26	9 922.38	+33.37	–1.31	9 954.43
				9 957.38
				±2.95

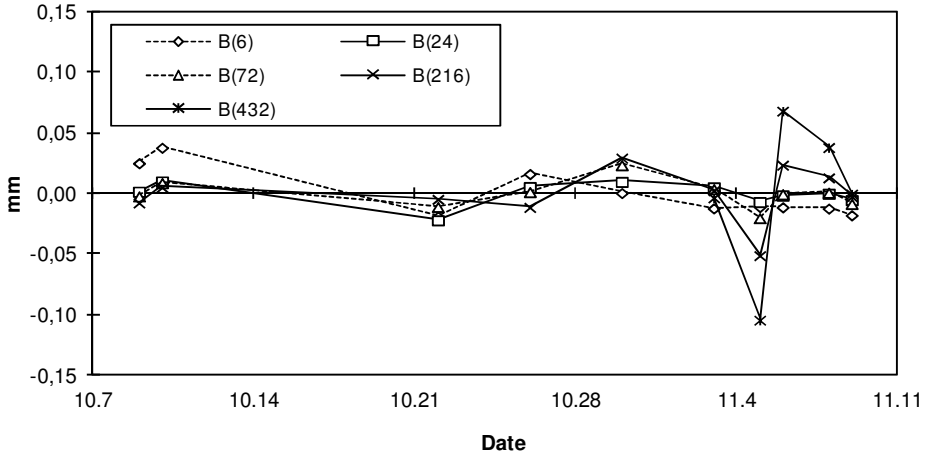

Figure 6.3 *Variation in lengths between transferring bars.*

Table 6.11 *Distances B from the transferring bar at 0 to the transferring bars at other pillars (mm, metres for I and B not displayed). The difference in transfer readings L and the thickness of mirror 0, D_0 = 19.985 mm, are added to the interference observations I (from Tables 6.6–6.10): $B_\nu = I_\nu - L_\nu + L_0 + D_0$. The weights are equal, except for B_{216} on 10 Oct and B_{432} on 6 Nov, which have half-weights because of incomplete observation series. $s(\bar{q})$ is the experimental standard deviation of the mean $\bar{q}$.*

Date 1999	I_6	L_6	L_0	B_6	I_{24}	L_{24}	L_0	B_{24}
9–10 X	0.200	15.611	15.650	20.224	0.806	8.916	15.650	27.525
10 X	0.204	15.601	15.648	20.236	0.873	8.973	15.648	27.534
22–23 X	0.233	15.683	15.645	20.180	0.820	8.948	15.645	27.502
26 X	0.195	15.620	15.655	20.215	0.825	8.936	15.655	27.529
30 –31 X	0.182	15.620	15.653	20.199	0.838	8.943	15.653	27.533
3 XI	0.151	15.590	15.641	20.186	0.614	8.711	15.641	27.529
5–6 XI	0.132	15.575	15.646	20.188	0.558	8.672	15.646	27.517
6 XI	0.128	15.566	15.641	20.187	0.555	8.658	15.641	27.522
8 XI	0.135	15.582	15.648	20.186	0.557	8.667	15.648	27.523
8–9 XI	0.141	15.592	15.647	20.181	0.568	8.682	15.647	27.518
$\bar{q}$				20.198				27.523
$s(\bar{q})$				±0.006				±0.003
Date 1999	I_{72}	L_{72}	L_0	B_{72}	I_{216}	L_{216}	L_0	B_{216}
9–10 X	2.512	4.884	15.650	33.263	7.742	14.499	15.650	28.878
10 X	2.539	4.899	15.648	33.274	7.755	14.497	15.648	28.891
22–23 X	2.467	4.842	15.645	33.254	7.471	14.220	15.645	28.881
26 X	2.472	4.845	15.655	33.267	7.456	14.222	15.655	28.874
30 –31 X	2.474	4.823	15.653	33.289	7.452	14.175	15.653	28.915
3 XI	1.806	4.163	15.641	33.269	5.432	12.169	15.641	28.888
5–6 XI	1.742	4.127	15.646	33.245	5.370	12.166	15.646	28.835
6 XI	1.654	4.015	15.641	33.265	5.140	11.857	15.641	28.909
8 XI	1.635	4.002	15.648	33.266	4.978	11.712	15.648	28.899
8–9 XI	1.646	4.021	15.647	33.257	4.961	11.710	15.647	28.883
$\bar{q}$				33.265				28.885
$s(\bar{q})$				±0.004				±0.007
Date 1999	I_{432}	L_{432}	L_0	B_{432}				
3 XI	10.932	5.033	15.641	41.525				
5–6 XI	10.825	5.032	15.646	41.424				
6 XI	10.362	4.391	15.641	41.596				
8 XI	9.996	4.062	15.648	41.566				
8–9 XI	9.957	4.062	15.647	41.528				
$\bar{q}$				41.528				
$s(\bar{q})$				±0.029				

6.3.5 Projection measurements

To compare and combine the interference measurements and EDMs, both the positions of the mirrors and those of the forced-centring plates had to be projected onto the line between the underground markers (Figs. 6.2 and 6.4–6.7). Since 22 October, both mirrors, the users' points and the forced-centring plates have been projected in the same theodolite and tape measurements, whereas previously only the first two had been projected.

For every projection, four sets of horizontal angles and two sets of vertical angles were observed at the mirror centre and the users' point, while at least two sets of horizontal and vertical angles were observed at the forced-centring plate.

Figure 6.4 *Tape measurements for projection at pillar 24.*

Figure 6.5 *The plumbing rod equipment on an underground marker.*

Figure 6.6 *Angle observations for projection at pillar 24.*

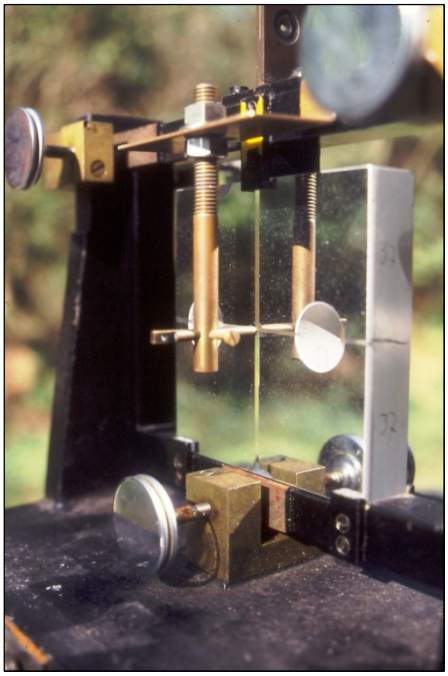

Figure 6.7 *The mirror index at a mirror (cf. Fig. 4.20).*

The old plumbing rod equipment was used on the underground markers, as the use of an optical precise plummet (which had been tested previously at the Nummela Standard Baseline) was not possible in the limited space between the underground markers and observation pillars. The traditional mirror index was used to visualize the centre of the mirror. A small target pellet was used on the users' markers, and a new target pinhole was carved in brass and fixed onto every forced-centring plate.

A Wild T2 (no. 92242) theodolite was used for the angle observations. The lengths were measured with Metri and Richter steel tapes (no. VJ6675 and VJ6837). The tape corrections were –0.3 mm and +0.5 mm, respectively, for the measured 2.3 m to 3.4 m slope lengths. Inclination, temperature, eccentricity and sag corrections were applied, too, based on the measurements of the vertical angle and the temperature observations as well as on the dimensions of the equipment.

The computation for projecting the interference measurements onto the line between the underground markers is presented in Table 6.12; the horizontal distance between a transferring bar (perpendicular to the baseline) and an underground marker (on the baseline) was determined. Both in interference observations and in projection measurements the actual objects of observation are the mirrors. During the interference observations, their positions are determined with regard to the transferring bar, whereas during the projection measurements the positions of the mirrors and transferring bars are determined with respect to the underground marker. The projection correction PC^i for a section, $0 - v$, of interference observations is obtained from the projections, P, and transferring readings, L, at 0 and v by

$$PC^i_{0-v} = L_v + P_v - L_0 - P_0. \qquad \text{(Eq. 6.3)}$$

The computation programme gives the projections seen from the mirror. A sum of two projections, from the underground marker to the mirror and from the mirror to the users' marker, give the projection from the underground marker to the users' marker (Table 6.13). The projection correction PC^u for a section, $0 - v$, of the users' markers is obtained from the projections at 0 and v by

$$PC^u_{0-v} = \Sigma P_v - \Sigma P_0. \qquad \text{(Eq. 6.4)}$$

The transferring readings in the projections for the EDM as well as the EDM observations were taken to the mirror surface in the same way as with the interference observations. The mirror was then removed and replaced with the forced-centring plate, which was placed on the mirror rails in the same way every time. After doing the projection measurements or EDM observations, the mirror again replaced the plate, and the transferring measurements were repeated. The same forced-centring plate was always used at the same pillar, so that any possible differences present in the plates would have no effect on the results. Plate no. 1 was used at 0 m, no. 2 at 432 m and no. 3 at 216 m and 864 m. The reinstallations were made with an accuracy of approximately 10 μm.

The projections, P, and the transferring readings, L, in the projection measurements and EDM observations are listed in Tables 6.14 and 6.15. The EDM observations (from station i to station j) are reduced to lengths between the underground markers (i and j) using the following correction (Table 6.16):

$$PC^{e}_{i-j} = -L_{\mathrm{EDM}\,j} + L_{\mathrm{proj}\,j} - P_j + L_{\mathrm{EDM}\,i} - L_{\mathrm{proj}\,i} + P_i \,. \qquad \text{(Eq. 6.5)}$$

The L values are always positive, and here the P values are positive if the forced-centring plate at a pillar is further away than the underground marker, as seen from the 0 end of the baseline. The mean values from the projection measurements and the actual values from the EDM observations were used.

Table 6.12 *Computation of projection corrections in interference measurements.*

v	**Date 1999**	**Projection (mm) from mirror to underground marker**	**Transfer (mm) from transferring bar to mirror**	**Sum (mm), from trans-ferring bar to underground marker**	**Projection correction 0 – v (mm)**
0	5 Oct.	–4.055	15.642	11.587	
0	22 Oct.	–3.928	15.638	11.709	
0	29 Oct.	–3.868	15.648	11.780	
0	10 Nov.	–3.968	15.646	11.678	
0				11.689	
				± 0.040	
24	7 Oct.	–7.324	9.082	1.758	
24	20 Oct.	–7.182	8.926	1.744	
24	7 Nov.	–7.038	8.672	1.634	
24				1.712	–9.977
				± 0.039	±0.056
216	6 Oct.	–10.166	16.632	6.466	
216	19 Oct.	–8.126	14.502	6.376	
216	27 Oct.	–7.927	14.222	6.295	
216	11 Nov.	–7.846	14.222	6.377	
216				6.379	–5.310
				± 0.035	±0.053
432	7 Oct.	–11.789	10.110	–1.679	
432	23 Oct.	–11.450	9.710	–1.740	
432	11 Nov.	–11.451	9.708	–1.742	
432				–1.720	–13.409
				± 0.021	±0.045

Table 6.13 *Computation of projection corrections for the users' markers.*

v	Date 1999	Projection (mm) from underground marker to mirror	Projection (mm) from mirror to users' marker	Sum (mm), from underground marker to users' marker	Projection correction 0 – v (mm)
0	5 Oct.	4.055	29.264	33.319	
0	22 Oct.	3.928	29.343	33.271	
0	29 Oct.	3.868	29.320	33.188	
0	10 Nov.	3.968	29.244	33.212	
0				33.248	
				±0.030	
24	7 Oct.	7.324	21.443	28.767	
24	20 Oct.	7.182	21.592	28.774	
24	7 Nov.	7.038	21.802	28.839	
24				28.793	–4.454
				±0.023	±0.037
216	6 Oct.	10.166	29.690	39.855	
216	19 Oct.	8.126	31.717	39.843	
216	27 Oct.	7.927	32.059	39.986	
216	11 Nov.	7.846	32.066	39.911	
216				39.899	+6.651
				±0.033	±0.044
432	7 Oct.	11.789	25.044	36.833	
432	23 Oct.	11.450	25.496	36.946	
432	11 Nov.	11.451	25.501	36.952	
432				36.910	+3.663
				±0.039	±0.049
864	25 Oct.	15.505	27.432	42.937	
864	5 Nov.	15.637	27.383	43.020	
864				42.979	+9.731
				±0.041	±0.051

Table 6.14 *Transferring readings (mm) in the EDM observations.*

Date 1999	0	216	432	864
28 Oct.	15.655	14.192	9.108	0.000
31 Oct.	15.647	14.182	9.075	0.000
4 Nov.	15.640	14.186	9.090	0.000

Table 6.15 *Projections and transferring readings (mm) in projection measurements for the EDM.*

	Date 1999	Projection	Transfer	Mean of projections	Mean of transfers
0	22 Oct.	–2.396	15.638		
0	29 Oct.	–2.463	15.648		
0	10 Nov.	–2.431	15.646		
0				–2.430	15.644
216	27 Oct.	–1.021	14.222		
216	11 Nov.	–0.976	14.222		
216				–0.998	14.222
432	23 Oct.	–6.091	9.710		
432	11 Nov.	–6.119	9.710		
432				–6.105	9.710
864	25 Oct.	–15.505	0.000		
864	5 Nov.	–15.636	0.000		
864				–15.571	0.000

Table 6.16 *Computation of projection corrections (mm) in EDM observations.*

Date	*i*	*j*	$L_{EDM\,j}$	$L_{proj\,j}$	P_j	*Sum j*	$L_{EDM\,i}$	$L_{proj\,i}$	P_i	*Sum i*	*Corr.*
28 Oct.	0	216	14.192	14.222	0.998	–0.968	15.655	15.644	–2.430	–2.419	–3.387
31 Oct.	0	216	14.182	14.222	0.998	–0.958	15.647	15.644	–2.430	–2.427	–3.385
4 Nov.	0	216	14.186	14.222	0.998	–0.962	15.640	15.644	–2.430	–2.434	–3.396
	0	**216**									–3.389
28 Oct.	0	432	9.108	9.710	6.105	–5.503	15.655	15.644	–2.430	–2.419	–7.922
31 Oct.	0	432	9.075	9.710	6.105	–5.470	15.647	15.644	–2.430	–2.427	–7.897
4 Nov.	0	432	9.090	9.710	6.105	–5.485	15.640	15.644	–2.430	–2.434	–7.919
	0	**432**									–7.913
28 Oct.	0	864	0.000	0.000	15.571	–15.571	15.655	15.644	–2.430	–2.419	–17.990
31 Oct.	0	864	0.000	0.000	15.571	–15.571	15.647	15.644	–2.430	–2.427	–17.998
4 Nov.	0	864	0.000	0.000	15.571	–15.571	15.640	15.644	–2.430	–2.434	–18.005
	0	**864**									–17.998
28 Oct.	216	432	9.108	9.710	6.105	–5.503	14.192	14.222	0.998	0.968	–4.535
31 Oct.	216	432	9.075	9.710	6.105	–5.470	14.182	14.222	0.998	0.958	–4.512
4 Nov.	216	432	9.090	9.710	6.105	–5.485	14.186	14.222	0.998	0.962	–4.523
	216	**432**									–4.523
28 Oct.	432	864	0.000	0.000	15.571	–15.571	9.108	9.710	6.105	5.503	–10.068
31 Oct.	432	864	0.000	0.000	15.571	–15.571	9.075	9.710	6.105	5.470	–10.101
4 Nov.	432	864	0.000	0.000	15.571	–15.571	9.090	9.710	6.105	5.485	–10.086
	432	**864**									–10.085

6.4 Kern Mekometer ME5000 measurements

In connection with the Väisälä measurement of the baseline, high-precision EDM observations were performed using a Kern Mekometer ME5000 (no. 357029) between 28 October and 4 November 1999. Since the instrument frequency was calibrated in December 1997 by Leica Geosystems AG in Heerbrugg, and later, in November 2000, by the MMSZ Accredited Calibration Laboratory of the Hungarian Academy of Science, EDM observations could be performed independently of interference observations. The frequency calibrations resulted in a scale factor of $m = 1.000\,000\,98$ in 1997 and $m = 1.000\,000\,99$ in 2000; the scale correction was applied when processing the Gödöllő measurements in 1999.

In the first measurements performed in 1987, only the duplication from 432 m to 864 m was measured with the EDM instrument. In 1999, the 216-m pillar was also measured, since interference measurements had not yet proceeded any further in October.

The EDMs (Table 6.17) were planned such that every distance could be measured back and forth with an independent set up and, as much as possible, under different temperature conditions. Every measurement was repeated at least 15 times, which means a total of approximately 700 single observations.

During the measurements, dry- and wet-bulb temperatures were measured with psychrometers at the EDM instrument, at the reflector prism and at the midpoint between them. The air pressure was measured with an aneroid barometer at the instrument. Table 6.18 presents the weather values.

Table 6.17 *Scheme of Kern ME 5000 measurements.*

28 October, 09:33–20:45 Sunshine, cloudless, calm		**31 October,** 09:18–16:56 Overcast, calm		**4 November,** 09:49–16:30 Cloudy, diffused sunshine, calm	
Instrument	**Reflector**	**Instrument**	**Reflector**	**Instrument**	**Reflector**
0	216	0	432	0	432
0	432	0	864	0	864
216	432	432	864	432	864
216	0	432	0	432	0
432	0	864	0	864	0
432	216	864	432	864	432
216	432	432	864	432	864
216	0	432	0	432	0
432	0	216	0	216	0
432	864	216	432	216	432
864	432	0	432	0	432
864	0	0	216	0	216
0	432	432	216	432	216
0	864	432	0	432	0
432	864	216	0		
432	0	216	432		

When calculating the results, those series with variations that were larger than 0.2 mm were divided into two, three or four sections. When computing the mean value, $\bar{q}$, of the distance, different weights (W) were used according to the number of measurements.

The results, summarized in Table 6.18, are the lengths between the forced-centring plates, which were temporarily placed on the same rails the on observation pillars as the mirrors were during the interference observations. The lengths include the velocity corrections and are reduced to the height level of the forced-centring plate on pillar 0, which is 2 322 mm above underground marker 0.

The mutual positions of the mirrors, forced-centring plates, users' markers and underground markers were determined during the projection measurements, as described in Section 6.7. Combined measurements are presented in Section 6.9.

The annual control for the years 1987–1999 is related to the lengths between the users' markers, which are presented in Fig. 6.8. It shows the lengths from the Kern Mekometer ME5000 on pillar 0 to the reflector prism on pillars 24, 216, 432 or 864. The horizontal axis shows the measured and reduced horizontal lengths, while the vertical axis shows the time of measurement.

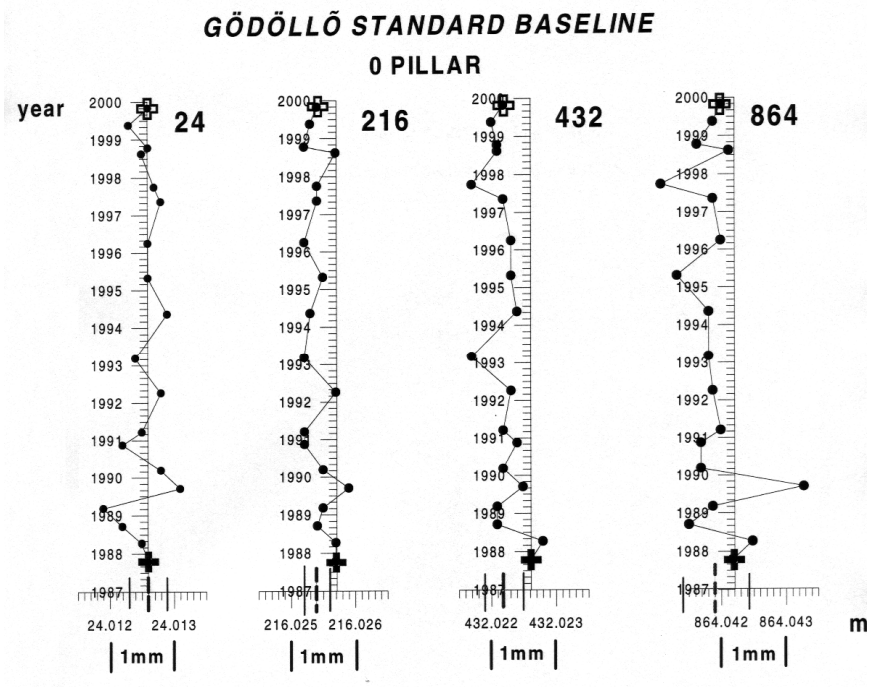

Fig. 6.8 *Control measurements with a Kern Mekometer ME5000 in 1987–1999. Variation in lengths from the users' marker on pillar 0 to the users' markers on the other pillars. Picture: FÖMI.*

Table 6.18 *Results of ME5000 measurements.*

Pillar interval	Date and time	Air temperature (°C) at EDM instrument	at middle point	at reflector	Air press. (kPa)	*W*	Length (m)
0-216	28 Oct. 09:33	10.4-10.6	10.4-10.8	10.6-10.7	100.39	1	216.0219
	28 Oct. 09:40	10.8-11.4	10.8-11.4	10.8-11.4	100.39	1	216.0219
	28 Oct. 09:46	11.7-12.0	11.7-11.9	11.6-12.0	100.39	1	216.0219
	28 Oct. 11:33	14.0-14.2	15.8-16.2	15.1-15.6	100.45	3	216.0220
	28 Oct. 13:45	16.5-17.0	16.6-17.1	17.8-18.3	100.39	3	216.0219
	31 Oct. 13:37	8.0-8.1	8.3-8.6	8.4-8.7	99.03	3	216.0219
	31 Oct. 14:55	9.0-9.7	9.5-9.9	9.7-9.8	99.93	3	216.0219
	31 Oct. 16:13	8.8-9.2	8.6-9.3	9.2-9.6	100.03	1	216.0219
	31 Oct. 16:21	7.4-8.0	7.6-8.0	8.2-8.8	100.03	1	216.0218
	31 Oct. 16:28	7.2-7.3	7.2-7.4	7.7-7.9	100.03	1	216.0219
	4 Nov. 14:18	11.0-12.4	13.2-13.4	14.0-14.2	100.42	3	216.0218
	4 Nov. 15:32	12.0-12.8	11.4-11.8	11.6-12.4	100.38	3	216.0218
						$\bar{q}$	**216.02188**
0-432	28 Oct. 10:15	12.2-12.6	13.1-13.1	13.2-13.2	100.39	2	432.0260
	28 Oct. 10:24	12.8-13.1	13.6-13.6	13.2-13.4	100.39	2	432.0261
	28 Oct. 12:06	15.3-16.0	15.8-16.2	16.2-16.4	100.51	3	432.0260
	28 Oct. 15:32	14.6-14.8	15.8-15.9	15.5-15.8	100.34	2	432.0258
	28 Oct. 15:42	14.4-15.0	15.4-15.8	15.4-15.8	100.34	2	432.0259
	28 Oct. 18:45	6.0-6.4	6.0-6.7	6.2-7.2	100.27	2	432.0261
	28 Oct. 18:57	5.8-6.2	5.1-5.6	6.1-6.4	100.27	2	432.0260
	28 Oct. 20:45	2.6-3.0	2.6-3.0	2.8-3.8	100.29	3	432.0260
	31 Oct. 09:18	7.5-7.8	7.5-7.9	7.7-8.1	99.90	3	432.0261
	31 Oct. 10:52	7.3-7.7	7.3-7.8	7.6-8.0	99.98	3	432.0261
	31 Oct. 13:02	8.1-8.2	8.1-8.2	8.4-8.6	99.98	3	432.0261
	31 Oct. 14:28	8.8-9.0	8.7-9.0	9.0-9.2	99.93	3	432.0261
	31 Oct. 15:51	9.6-9.8	9.6-10.0	9.8-10.1	100.01	3	432.0260
	4 Nov. 09:49	11.2-11.6	11.6-12.0	12.0-12.1	100.50	2	432.0261
	4 Nov. 10:00	11.2-11.9	12.0-12.4	12.0-12.2	100.50	2	432.0262
	4 Nov. 11:24	13.4-13.4	13.7-14.5	14.0-14.6	100.55	2	432.0262
	4 Nov. 11:34	13.6-13.7	13.5-14.0	14.0-14.4	100.55	2	432.0263
	4 Nov. 13:28	13.6-13.7	13.5-14.0	14.0-14.4	100.51	3	432.0261
	4 Nov. 15:06	12.6-13.0	12.4-13.1	12.4-13.2	100.38	2	432.0261
	4 Nov. 15:14	12.6-12.9	11.9-12.2	12.5-12.6	100.38	2	432.0261
	4 Nov. 16:16	7.6-8.2	8.4-9.3	9.7-10.2	100.41	1	432.0261
	4 Nov. 16:23	7.4-7.6	7.5-8.0	8.8-9.1	100.41	1	432.0260
	4 Nov. 16:30	6.7-6.9	8.7-8.7	7.0-7.0	100.41	1	432.0260
						$\bar{q}$	**432.02607**

Table 6.18 *continued.*

Pillar interval	Date and time	Air temperature (°C) at EDM instrument	at middle point	at reflector	Air press. (kPa)	*W*	Length (m)
0-864	28 Oct. 17:14	11.6-11.6	10.1-10.3	11.4-11.4	100.34	1	864.0498
	28 Oct. 17:20	11.6-11.8	9.2-9.7	10.6-11.2	100.34	1	864.0498
	28 Oct. 17:28	11.4-12.0	8.9-9.0	9.8-10.6	100.34	1	864.0498
	28 Oct. 17:38	10.9-11.6	7.9-8.6	9.2-9.6	100.34	1	864.0499
	28 Oct. 19:15	5.2-5.4	5.2-5.8	4.2-4.4	100.27	1	864.0497
	28 Oct. 19:24	4.6-4.8	5.1-5.4	4.0-4.0	100.27	1	864.0499
	28 Oct. 19:32	4.4-4.9	3.9-4.9	3.5-4.2	100.27	1	864.0500
	31 Oct. 09:45	7.4-7.8	7.5-7.8	7.6-8.0	99.90	3	864.0499
	31 Oct. 11:21	7.6-7.8	7.7-7.8	7.8-7.9	100.02	1	864.0499
	31 Oct. 11:30	7.6-7.8	8.0-8.1	8.0-8.2	100.02	1	864.0498
	31 Oct. 11:38	7.5-7.8	8.0-8.0	8.2-8.2	100.02	1	864.0500
	4 Nov. 10:16	12.0-12.2	12.2-12.3	12.3-12.5	100.50	1	864.0501
	4 Nov. 10:26	11.8-12.4	12.3-13.6	12.6-13.4	100.50	1	864.0503
	4 Nov. 10:35	12.6-12.8	13.7-13.7	13.2-13.4	100.50	1	864.0502
	4 Nov. 12:08	13.8-13.8	13.6-13.8	13.8-14.2	100.54	2	864.0501
	4 Nov. 12:20	13.5-13.6	14.0-14.0	14.2-9.3	100.54	2	864.0500
						$\overline{q}$	**864.04996**
216-432	28 Oct. 10:59	13.6-14.4	14.1-14.7	14.6-15.2	100.45	3	216.0040
	28 Oct. 12:34	15.9-16.4	16.9-17.6	16.6-17.0	100.49	3	216.0041
	28 Oct. 13:13	16.2-16.8	16.5-16.9	16.3-16.7	100.42	3	216.0040
	31 Oct. 14:02	8.0-8.4	8.4-8.9	8.7-8.9	99.90	3	216.0042
	31 Oct. 15:25	9.8-10.0	9.9-10.0	9.9-10.1	100.01	3	216.0041
	31 Oct. 16:45	6.2-6.4	6.2-6.6	6.2-6.9	100.02	2	216.0040
	31 Oct. 16:56	5.4-6.0	5.7-6.0	5.7-6.2	100.02	2	216.0040
	4 Nov. 14:44	12.4-12.9	12.5-13.0	13.2-13.8	100.42	3	216.0041
	4 Nov. 15:54	9.6-11.0	9.9-10.8	10.7-11.1	100.41	2	216.0041
	4 Nov. 16:04	8.6-9.6	9.0-9.8	9.6-9.9	100.41	2	216.0040
						$\overline{q}$	**216.00406**
432-864	28 Oct. 16:07	14.0-14.8	15.9-16.0	16.1-16.3	100.35	2	432.0235
	28 Oct. 16:18	13.7-14.4	15.5-15.6	16.0-16.2	100.35	2	432.0235
	28 Oct. 16:36	15.0-15.5	15.1-15.2	15.0-15.6	100.34	1	432.0238
	28 Oct. 16:51	14.9-15.2	14.0-14.4	12.7-13.8	100.34	1	432.0237
	28 Oct. 17:00	14.3-14.7	11.7-13.6	12.2-12.2	100.34	1	432.0236
	28 Oct. 17:04	13.4-14.3	12.1-12.1	11.8-11.8	100.34	1	432.0237
	28 Oct. 20:05	3.0-3.5	2.3-2.6	2.6-3.1	100.29	2	432.0236
	28 Oct. 20:18	3.0-3.0	2.2-2.6	2.0-2.7	100.29	2	432.0235
	31 Oct. 10:21	7.4-7.8	7.3-7.7	7.4-7.9	99.98	3	432.0237
	31 Oct. 11:57	7.8-8.0	8.0-8.2	8.0-8.5	100.01	3	432.0237
	31 Oct. 12:32	8.0-8.3	8.0-8.4	8.2-8.8	99.98	3	432.0237
	4 Nov. 11:02	13.2-14.0	13.9-14.4	13.6-14.4	100.55	3	432.0238
	4 Nov. 12:36	13.6-14.0	14.1-14.6	14.0-14.4	100.53	3	432.0238
	4 Nov. 13:00	14.0-14.3	14.5-14.8	13.9-14.6	100.50	3	432.0238
						$\overline{q}$	**432.02368**

6.5 Results and conclusion

The computation of the baseline section lengths derived from the interference measurements is presented in Table 6.19. All of the interference observations are tied to the permanently fixed transferring bars on the observation pillars. The lengths between the transferring bars are computed in Table 6.11, and more corrections for the reduction in the lengths between the underground markers are presented in Sections 6.3–6.7. The reference height level of the final lengths is the height level of underground marker 0.

Table 6.19 *Computation of baseline lengths from the interference measurements.*

	0–24: mm + 24 m	**0–216: mm + 216 m**	**0–432: mm + 432 m**
Length between transferring bars	+27.523	+28.885	+41.528
Projection correction	–9.977	–5.310	–13.409
Correction to the height level $H = 0$	–0.549	–4.895	–9.741
Mirror-body correction	–0.002	–0.013	–0.001
Mirror-coating correction	–0.000	–0.002	–0.005
Air-pressure difference correction	–0.000	–0.005	–0.022
Final length	+16.995	+18.660	+18.350

The uncertainty in the interference measurements is estimated in Table 6.21. The method is the same as in the other standard baseline measurements. Due to new absolute calibrations and comparisons, the value for the uncertainty originating from the absolute length of the quartz metre was decreased. In contrast, problems in determining the influence of mirror coatings increased the appropriate uncertainty value. The level of accuracy in the projection measurements was not the best possible because of the timeworn equipment, although the equipment was reconditioned before the last projections.

In addition to the experimental standard deviations of the mean of the lengths between the transferring bars (from Table 6.11), one again can estimate the uncertainty between the mirror surfaces, u_M (Table 6.20). Factors n_s and n_{obs} are the number of interference measurements and the number of observations in one measurement, respectively. Uncertainties, u_I, for every interference observation stage are derived as square roots of square sums of the experimental standard deviations of means (in Tables 6.6–6.10) divided by n_s.

Uncertainty u_I^{acc} is the accumulated uncertainty, for example,

$$u_{I(0-432)}^{acc} = \sqrt{(2\times3\times3\times u_{24})^2+(2\times3\times u_{72})^2+(2\times u_{216})^2+(u_{432})^2}\,. \qquad \text{(Eq. 6.6)}$$

When dividing this uncertainty by the square root of the number of interference measurements, u_M is obtained. Since u_B includes possible pillar movements

during the measurement season, it should be (and is) always equal to or larger than u_M. The u_B values are used in the total uncertainty budget in Table 6.21.

Table 6.20 *Uncertainty of distances between mirror surfaces or transferring bars.*

	0–24	**0–72**	**0–216**	**0–432**
n_s	10	10	9½	4½
n_{obs}	4	2	2 (1)	2 (1)
u_I (μm)	2	2	6	2
u_I^{acc} (μm)	2	6	18	37
u_M (μm)	1	2	6	12
u_B (μm)	3	4	7	29

Table 6.21 *Total uncertainty budget of interference measurements (μm).*

	0–24	**0–216**	**0–432**
Uncertainty in interference observations and transfer readings	3	7	29
Uncertainty in projection measurements	56	53	45
Uncertainty in determination of the absolute length of the quartz gauge	1	9	17
Uncertainty in thicknesses of mirror coatings	1	9	17
Uncertainty due to determination of temperature of the quartz gauge	0	4	9
Uncertainty due to determination of heights	2	2	3
Total standard uncertainty	56	55	59

Table 6.22 *Results (mm) of Kern Mekometer ME5000 measurements.*

Interval	**Length (unadjusted, from Table 6.18) between forced centring plates, on the height level of plate 0**	**Proj. corr.**	**Height corr.**	**Length (adjusted) between underground markers, on the height level of underground marker 0**
0–216	216 021.88	–3.39	–0.08	216 018.57
0–432	432 026.07	–7.91	–0.16	432 018.19
0–864	864 049.96	–18.00	–0.31	864 031.80
216–432	216 004.06	–4.52	–0.08	215 999.62
432–864	432 023.68	–10.08	–0.16	432 013.61

By adjusting the weighted mean lengths in Table 6.18, the results from the Mekometer measurements on the height level of forced-centring plate 0 are obtained (Table 6.22), as well as the constant correction: +0.16 mm. Here, the scale is not yet fitted with the interference measurements. After the projection (Tables 6.14–6.16) and height corrections, the lengths between the underground markers on the height level of underground marker 0 are obtained; now the Mekometer measurements are comparable with the interference measurements.

The comparable differences between the interference measurements and the Mekometer measurements are few (0–216, 0–432, 216–432). The differences are less than 0.2 mm, but compatible, and a scale correction can be justified. The frequency calibration and the comparison made with a Väisälä baseline yield a slightly different scale correction.

To determine a scale fully based on the interference measurements, a scale factor of +0.37 mm/km was applied for the EDM observations for the 864-m pillar. After correction, the length between underground markers 0 and 864 on the height level of underground marker 0 is 864 032.12 mm (and the length 432–864 is 432 013.77 mm). The combined final results are presented in Table 6.23.

The positions of the forced-centring plates were determined in the same projection and transfer measurements as the positions of the mirrors, underground markers and users' markers. The uncertainty in the traceability chain up to 432 m can be estimated as being equal with the uncertainty in the interference measurements. In the doubling to 864 m, the influence of refraction, for example, is more significant. The standard uncertainty of the 864-m interval was estimated to be ±0.1 mm in the entire traceability chain.

The lengths between the users' markers (Table 6.24) are obtained using projection (Table 6.13) and height corrections. The uncertainties are not any larger than for the underground markers, but the stability of the observation pillars is not that good, and for more reliable results the projection measurements should be repeated, e.g. once per year. Here, standard uncertainty values of ±0.1 mm have been used with the final results (Table 6.25).

The Gödöllő Standard Baseline is the only standard baseline in Hungary. The results from the measurements done in 1987 and 1999 (Table 6.26), as well as the control measurements presented in Fig. 6.8, suggest a good stabilization of the pillars. This clearly strengthens the position of the baseline as the main length standard for geodesy in Hungary.

FÖMI is acting as an accredited calibration laboratory, and the Gödöllő Standard Baseline is the measurement standard in the calibration of EDM instruments. The users' markers on the observation pillars are used in the calibrations: ten different lengths can be measured between the five markers. The measured lengths are compared with the lengths determined when using the Väisälä method. After least-squares adjustments, instrument corrections (scale correction, additive constant) are obtained, as well as an estimate of the accuracy of the instrument.

Table 6.23 *Final results. Lengths of baseline sections between underground markers at the height level of underground marker 0, with expanded uncertainties.*

Interval	Length (mm)
0–24	24 017.00 ±0.11
0–216	216 018.66 ±0.11
0–432	432 018.35 ±0.12
0–864	864 032.1 ±0.2

Table 6.24 *Computation of lengths (mm) between users' markers on the height level of users' marker 0.*

Interval	Underground	Proj. corr.	Height corr.	Users' markers
0–24	24 017.00	–4.45	+0.01	24 012.56
0–216	216 018.66	+6.65	+0.07	216 025.38
0–432	432 018.35	+3.66	+0.15	432 022.16
0–864	864 032.12	+9.73	+0.29	864 042.14

Table 6.25 *Final results. Lengths of baseline sections between users' markers at the height level of users' marker 0, with expanded uncertainties.*

Interval	Length (mm)
0–24	24 012.6 ±0.2
0–216	216 025.4 ±0.2
0–432	432 022.2 ±0.2
0–864	864 042.1 ±0.2

Table 6.26 *Gödöllő Standard Baseline, comparison of final results (mm-part). In the second column, a scale correction only, based on frequency calibration, has been applied. In the third–sixth columns, the scale is determined from the interference measurements performed in 1987 or 1999. The measurements and results from 1987 were reported in Kääriäinen et al. (1988).*

Interval	ME5000 1999	Väisälä & ME5000 1999	Väisälä & ME3000 1987	Users' markers 1999	Users' markers 1987
0–24	–	17.00	17.06	12.56	12.61
0–216	18.57	18.66	18.76	25.38	25.74
0–432	18.19	18.35	18.40	22.16	22.60
0–864	31.80	32.12	32.16	42.14	42.18
216–432	99.62	(99.69)	(99.64)	(96.78)	(96.86)
432–864	13.61	(13.77)	13.76	(19.98)	(19.58)

7 The HUT Väisälä Baseline

A 75-m-long calibration baseline was measured with the Väisälä interference comparator as a joint project between the Finnish Geodetic Institute (FGI) and the, then, Laboratory of Geodesy and Cartography of the Helsinki University of Technology (HUT). In addition to determining the length of the baseline, the purpose was to examine the usability of the Väisälä baseline measurement method indoors and to improve comparability between this method and other high-precision geodetic distance measurement methods. The results and experience gained from the project are presented here.

7.1 Baseline design

The HUT Väisälä Baseline (Figs. 7.2–7.3) was located in the basement of the main building of the Helsinki University of Technology in Otaniemi. The 82-m-long, 3 m to 5 m wide and 2.1 m to 2.6 m high room was designed for various purposes related to calibration measurements in metrology. It met the requirements of a proper calibration laboratory quite well. Several doors, but no windows, opened to the room. Temperature differences of up to 1 °C occurred along the baseline, but the air conditioning kept the variations small. The observation personnel and lighting caused minor changes in temperature.

The observation pillars had been mechanically insulated, being built upon the bedrock, to lessen vibrations from the surrounding floor. For the mirrors, as many as 11 pillars could be used: at 0, 1, 5, 6, 24, 25, 30, 48, 50, 72 and 75 m. All of the pillars were equipped with both Kern forced-centring plates and studs for the Väisälä interference comparator instruments. Thus, there were as many as six possible ways to measure a Väisälä baseline: $1 \times 5 \times 5 \times 3$ m = 75 m, $1 \times 6 \times 4 \times 3$ m = 72 m, $1 \times 5 \times 5 \times 2$ m = 50 m, $1 \times 6 \times 4 \times 2$ m = 48 m and $1 \times 6 \times 5$ m or $1 \times 5 \times 6$ m = 30 m. The observers, Jorma Jokela and Markku Poutanen, chose the longest option and conducted the measurement with the interference comparator using the pillars at 0, 1, 5, 25 and 75 m.

7.2 Measurement procedure

The measurement method was mostly identical with the other interference measurements, which can be found in other parts of this thesis and is not repeated here.

The entire measurement required about three weeks in January–February 1998. During the first week, the observers installed the instruments on the pillars. Since the baseline was originally designed for the Väisälä interference comparator, no major difficulties were encountered. The heavy calibration rail between the observation pillars and the wall would have caused a lack of space if using the conventional measurement geometry. The problem was solved by installing the instruments as a mirror image of the method usually used for such purposes. Slight modifications and adjustments were needed for the observation telescope, and the support for the quartz gauge had to be reconstructed.

Another week was needed for doing the interference observations and projection measurements, and the third week was used for doing computations and research work. The observers measured the 75-m baseline six times; every measurement consisted of ten interference observations. On 2 February three measurements were made using quartz gauge no. 49, and on 4 February three measurements were made using quartz gauge no. 51. A nice coincidence was that 3 February was the 100th anniversary of Alvar Aalto's birth (1898–1976), the famous architect who had designed the university building with the geodetic baseline, now defunct in the university named after him.

7.3 Quartz gauges

According to the calibration certificates offered by the PTB in Braunschweig, Germany (1996), the lengths of the quartz gauges were as follows:

no. 49: 1 000 032.35 μm ± 0.06 μm, at epoch 1995.86;
no. 51: 1 000 018.38 μm ± 0.06 μm, at epoch 1995.85.

After making corrections for the estimated lengthening of 5 nm a^{-1}, the lengths were:

no. 49: 1 000 032.36 μm ± 0.06 μm, at epoch 1998.1;
no. 51: 1 000 018.39 μm ± 0.06 μm, at epoch 1998.1.

The lengths stated above were valid at a temperature of 20°C. The air temperature and pressure affecting the length of the quartz gauge during the measurement in Otaniemi are listed in Table 7.6. The thermometers no. 3867 and no. 3868 from the FGI were used for the quartz gauge temperature simulations. The air pressure was measured using an aneroid Thommen 3B4.01.1 no. 164610, which was placed on the telescope pillar. A correction of +0.2 kPa, determined via comparisons with the mercury barometer Fuess 794 from the FGI, was added to the observed values. For the computation, the coefficients of formulas listed by Poutanen (1995) and Jokela (1996) were used. The lengths of the quartz gauges, expressed in temperature t (°C) and pressure p (mmHg), were as follows:

no. 49:

$$l_{49} = 1\ \text{m} + [\ 32.36 + 0.394 \times (t - 20) + 0.00155 \times (t - 20)^2 - 0.00099 \times (p - 760.)\ ]\ \mu\text{m};$$

(Eq. 7.1)

no. 51:

$$l_{51} = 1\ \text{m} + [\ 18.39 + 0.394 \times (t - 20) + 0.00172 \times (t - 20)^2 - 0.00099 \times (p - 760.)\ ]\ \mu\text{m}.$$

(Eq. 7.2)

The results are presented in Table 7.6.

The method and equipment used to measure the gap between the quartz gauge and mirror 1 were equal to those used in the other interference measurements listed in this thesis.

7.4 Light source, collimator, mirrors and compensators

In Otaniemi, the same instruments were used as in Nummela. The mirrors and the resulting corrections are listed in Tables 7.1–7.3.

Table 7.1 *Mirrors.*

Pillar ν	Mirror no.	Thickness (mm)
0	40	19.985
1	36	20.001
5	38	19.932
25	37	19.983
75	53	19.981

Table 7.2 *Corrections due to thicknesses of mirror bodies.*

Distance	Correction (mm)
0–5	–0.026
0–25	–0.001
0–75	–0.002

Table 7.3 *Corrections due to thicknesses of mirror coatings.*

Distance	Correction (mm)
0 – 1	– 0.000
0 – 5	– 0.002
0 – 25	– 0.010
0 – 75	– 0.030

7.5 Refraction

The same thermometer placement, observation procedure and computing formulas were used as when measuring distances of 72 m and less in Nummela. Thermometers with small instrument corrections were selected, and only the values listed in Table 7.4 were needed.

The temperature profiles of the average temperatures at the HUT Väisälä Baseline are presented in Fig. 7.1. Local maxima were caused by the observation personnel (near 0) and the door to a warmer corridor (near 20). The back part of the line from 50 m to 75 m ran into a narrower and distinctly warmer room. Temperature differences caused refraction corrections ranging from 4 μm to 8 μm for the 75-m distance.

7.6 Heights

The height differences between the levelled objects on the pillars are listed in Table 7.5. *T* is the height benchmark, except at 75 m, where it is the front stud under the mirror rail. The observers first made the precise levellings between the *T*'s. *P* is the forced-centring plate, and all of the heights were presented relative to the height of the plate at 0, which is also the level of the final lengths. *K* is the auxiliary benchmark in the centre of a pillar; the heights of the *K*'s refer to the hair-crossed benchmark screw, which was removed to make way for the fixing screws of the mirror rails. All heights refer to the uppermost surfaces that could be reached with a short levelling rod suitable for indoor measurements. Using these heights, the observers adjusted the parts of the Väisälä interference

comparator on the same horizontal line. The height of the line through the mirror centres was +166 mm.

Table 7.4 *Corrections to the thermometers.*

Thermometer at (m)	no.	Correction (°C) at +20°C	Thermometer at (m)	no.	Correction (°C) at +20°C
t_o	3868	+0.02	17	7938	0.00
t_i	3867	+0.02	24	7933	–0.01
0	7935	–0.02	36	7937	+0.01
1	7932	–0.01	48	7936	0.00
4	7939	–0.02	60	7929	–0.03
10	4480	+0.04	72	7931	–0.02

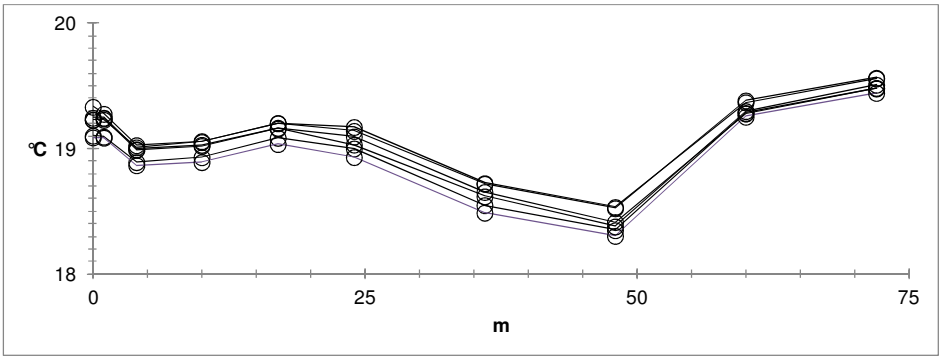

Figure 7.1 *Temperature profiles in the six interference measurements.*

Table 7.5 *Height differences (mm).*

Pillar	*T*	***P***	*K*
0	– 46.05	**0.00**	– 26.25
5	– 47.59	– 1.46	– 25.93
25	– 45.81	– 0.05	– 25.75
75	– 09.43	– 2.16	– 25.25

7.7 Interference observations

Jorma Jokela and Markku Poutanen performed the interference observations at the HUT Väisälä Baseline in Otaniemi; the measurement procedure was done identically as the one for the three shortest distances at Nummela by simply replacing 6 with 5, 24 with 25 and 72 with 75. One measurement with ten interferences lasted for approximately two hours (75–25–0, 25–5–0, 5–1–0, turn of quartz gauge, 0–1–5, 0–5–25, change of observer, 25–5–0, 5–1–0, turn of quartz gauge, 0–1–5, 0–5–25, 0–25–75). The results are listed in Tables 7.7–7.9. Using the interference observations and the transfer readings between the mirror surfaces and the transferring bars, the distances between transferring bars were computed (Table 7.10).

The author thanks Prof. Teuvo Parm and Dr Jaakko Santala for making the arrangements in Otaniemi. The author also thanks Mr Veli-Matti Salminen, who solved many practical problems in developing the equipment, and Messrs Janne Filpus, Quanwei Liu, Tapio Poutanen and Mauri Väisänen, who assisted in the projection measurements and temperature observations.

Table 7.6 *Length of quartz gauges in the ambient temperature, t (°C), and pressure, p (mmHg).*

Quartz gauge no. 49					Quartz gauge no. 51				
Date and time		*t*	*p*	µm + 1 m	Date and time		*t*	*p*	µm + 1 m
1998-02-02	10:12	19.08	753.6	32.01	1998-02-04	10:30	18.99	754.9	18.00
	10:27	19.15	753.6	32.03		10:42	19.08	754.9	18.03
	10:59	19.17	753.2	32.04		11:14	19.07	754.9	18.03
	11:11	19.19	753.2	32.05		11:25	19.11	754.9	18.05
	13:17	19.23	751.6	32.07		13:18	19.15	755.1	18.06
	13:47	19.25	751.6	32.07		13:27	19.23	755.1	18.09
	14:29	19.23	751.2	32.06		13:53	19.24	755.1	18.10
	14:45	19.30	751.2	32.09		14:03	19.27	755.1	18.11
	16:31	19.23	750.0	32.07		15:03	19.18	755.1	18.07
	16:42	19.28	750.0	32.09		15:20	19.19	755.2	18.08
	17:13	19.27	749.5	32.08		15:47	19.22	755.2	18.09
	17:25	19.35	749.5	32.11		15:57	19.27	755.2	18.11

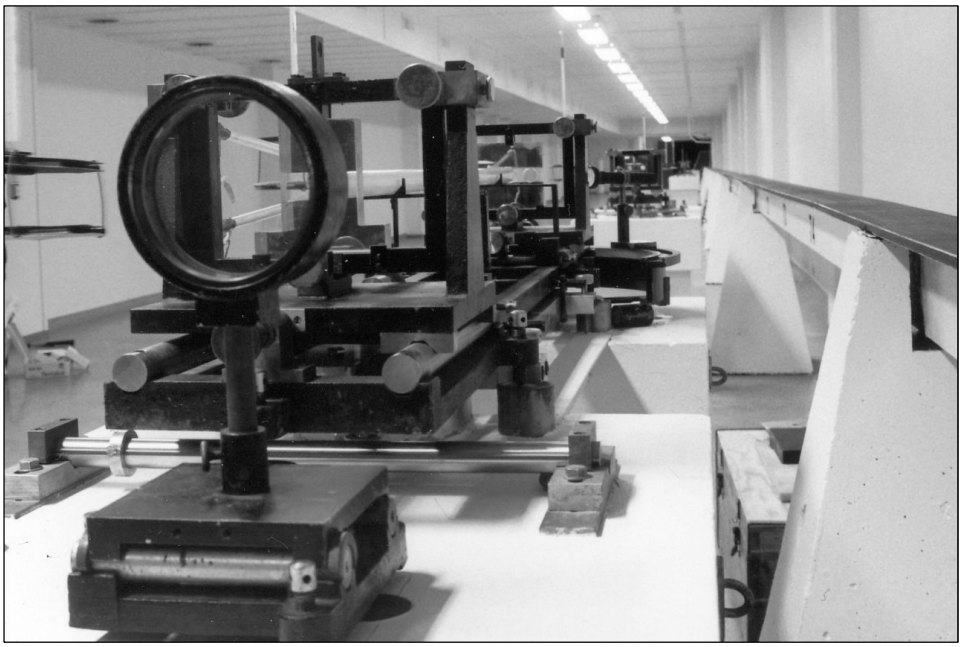

Figure 7.2 *The HUT Väisälä Baseline in Otaniemi, seen from 0 to 75.*

Figure 7.3 *The 0 end of the HUT Väisälä Baseline.*

Table 7.7 *Computation of interference 0 – 1 – 5. The distance [0 – 1] is the sum of the quartz gauge length (from Table 7.6) and the gap between the quartz gauge and mirror 1. The distance [0 – 5] is five times the distance [0 – 1], corrected with compensator and refraction corrections.*

Date and time 1998	Obs.	Q. g. no.	Gap (μm)	[0–1] μm + 1 m	Comp. corr. (μm)	Refr. corr. (μm)	[0–5] μm + 5 m
2 Feb. 10:12	JJ	49	2.84	34.85	–10.19	–0.85	163.21
10:27	JJ	49	1.48	33.51	–1.97	–1.07	164.51
10:59	MP	49	1.48	33.52	+0.04	–1.01	166.63
11:11	MP	49	1.86	33.91	–4.18	–1.09	164.28
							164.66
							±0.72
2 Feb. 13:17	JJ	49	2.84	34.91	–6.50	–0.96	167.09
13:47	JJ	49	2.33	34.40	–2.46	–1.08	168.46
14:29	MP	49	1.49	33.55	+2.15	–1.09	168.81
14:45	MP	49	2.31	34.40	–2.05	–1.17	168.78
							168.28
							±0.41
2 Feb. 16:31	JJ	49	1.94	34.01	–6.20	–1.12	162.73
16:42	JJ	49	1.10	33.19	–2.99	–1.27	161.69
17:13	MP	49	1.86	33.94	–5.58	–1.14	162.98
17:25	MP	49	1.07	33.18	–1.83	–1.24	163.83
							162.81
							±0.44
4 Feb. 10:30	JJ	51	1.77	19.77	+5.90	–0.84	103.91
10:42	JJ	51	1.07	19.10	+9.44	–1.23	103.71
11:14	MP	51	1.27	19.30	+8.22	–0.97	103.75
11:25	MP	51	2.02	20.07	+5.10	–1.08	104.37
							103.94
							±0.15
4 Feb. 13:18	JJ	51	1.01	19.07	–3.45	–1.03	90.87
13:27	JJ	51	1.01	19.10	–3.17	–1.26	91.07
13:53	MP	51	2.02	20.12	–7.17	–0.98	92.45
14:03	MP	51	1.88	19.99	–7.17	–1.25	91.53
							91.48
							±0.35
4 Feb. 15:03	JJ	51	2.10	20.17	–3.42	–0.95	96.48
15:20	JJ	51	0.96	19.04	+3.84	–1.17	97.87
15:47	MP	51	1.43	19.52	+1.88	–1.05	98.43
15:57	MP	51	2.45	20.56	–4.29	–1.24	97.27
							97.51
							±0.42

Table 7.8 *Computation of interference 0 – 5 – 25. The distance [0 – 25] is five times the distance [0 – 5] (from Table 7.7), corrected with compensator and refraction corrections.*

Date and time 1998	5 × [0–5] µm + 25 m	Comp. corr. (µm)	Refr. corr. (µm)	[0–25] µm + 25 m
2 Feb. 09:50	816.05	+53.94	+1.80	871.79
10:38	822.55	+52.77	+1.40	876.72
10:46	833.15	+53.07	+1.60	887.82
11:20	821.40	+52.08	+0.60	874.08
				877.60
				±3.55
2 Feb. 12:59	835.45	+50.03	+1.48	888.96
14:04	842.30	+35.98	+1.71	879.99
14:11	844.05	+35.95	+1.59	881.59
15:01	843.90	+35.60	+1.48	880.98
				882.38
				±1.56
2 Feb. 16:16	813.65	+59.00	+0.93	873.58
16:53	808.45	+58.30	+1.01	867.76
16:59	814.90	+57.67	+1.05	873.62
17:32	819.15	+57.62	–0.49	876.28
				872.81
				±1.80
4 Feb. 10:13	519.55	+6.40	+0.60	526.55
10:51	518.55	+5.08	+0.79	524.42
11:00	518.75	+4.95	+1.31	525.01
11:32	521.85	+4.78	+0.07	526.70
				525.67
				±0.57
4 Feb. 13:04	454.35	+70.33	+1.02	525.70
13:35	455.35	+68.48	+0.58	524.41
13:40	462.25	+67.98	+0.79	531.02
14:11	457.65	+67.00	–0.03	524.62
				526.44
				±1.55
4 Feb. 14:49	482.40	+40.10	+0.89	523.39
15:28	489.35	+39.58	+0.24	529.17
15:35	492.15	+39.25	+0.64	532.04
16:06	486.35	+39.21	–0.20	525.36
				527.49
				±1.93

Table 7.9 *Computation of interference 0 – 25 – 75. The distance [0 – 75] is three times the distance [0 – 25] (from Table 7.8), corrected with compensator and refraction corrections.*

Date and time 1998	**3 × [0–25] μm + 75 m**	**Comp. corr. (μm)**	**Refr. corr. (μm)**	**[0–75] μm + 75 m**
2 Feb. 09:31	2 632.81	+28.43	–4.47	2 656.77
11:29	2 632.81	+29.30	–6.30	2 655.81
				2 656.29
				±0.48
2 Feb. 12:43	2 647.14	+31.12	–4.03	2 674.23
15:12	2 647.14	+23.02	–4.40	2 665.76
				2 670.00
				±4.24
2 Feb. 16:04	2 618.43	+33.38	–3.64	2 648.17
17:41	2 618.43	+35.98	–6.43	2 647.98
				2 648.08
				±0.10
4 Feb. 09:50	1 577.01	+30.58	–4.35	1 603.24
11:41	1 577.01	+29.51	–6.56	1 599.96
				1 601.60
				±1.64
4 Feb. 12:52	1 579.31	+29.29	–4.15	1 604.45
14:19	1 579.31	+29.55	–8.43	1 600.43
				1 602.44
				±2.01
4 Feb. 14:40	1 582.47	+31.68	–6.57	1 607.58
16:15	1 582.47	+30.76	–7.81	1 605.42
				1 606.50
				±1.08

Table 7.10 *Distances B from the transferring bar at 0 to the transferring bars at other pillars (mm, metres for I and B not displayed). The difference in transfer readings L and the thickness of mirror 0, D_0 = 19.985 mm, are added to the interference observations I (from Tables 7.7–7.9): $B_\nu = I_\nu - L_\nu + L_0 + D_0$. $s(\bar{q})$ is the experimental standard deviation of the mean $\bar{q}$.*

Date 1998		I_5	L_5	L_0	B_5
2 Feb.	I	0.165	11.866	12.452	20.736
	II	0.168	11.861	12.448	20.740
	III	0.163	11.862	12.452	20.738
4 Feb.	IV	0.104	11.808	12.450	20.731
	V	0.091	11.793	12.451	20.734
	VI	0.098	11.800	12.450	20.733
	$\bar{q}$				20.735
	$s(\bar{q})$				±0.001
Date 1998		I_{25}	L_{25}	L_0	B_{25}
2 Feb.	I	0.878	12.932	12.452	20.383
	II	0.882	12.932	12.448	20.383
	III	0.873	12.933	12.452	20.377
4 Feb.	IV	0.526	12.583	12.450	20.378
	V	0.526	12.583	12.451	20.379
	VI	0.527	12.584	12.450	20.378
	$\bar{q}$				20.380
	$s(\bar{q})$				±0.001
Date 1998		I_{75}	L_{75}	L_0	B_{75}
2 Feb.	I	2.656	16.315	12.452	18.778
	II	2.670	16.314	12.448	18.789
	III	2.648	16.318	12.452	18.767
4 Feb.	IV	1.602	15.266	12.450	18.771
	V	1.602	15.266	12.451	18.772
	VI	1.606	15.266	12.450	18.775
	$\bar{q}$				18.775
	$s(\bar{q})$				±0.003

7.8 Replacing the traditional projection method by developing transferring methods

The observations between the mirror surfaces can easily be transferred to the distances between the transferring bars with the transferring device, without causing much uncertainty. On the other hand, the projections from this point onwards are not easy to do and not extremely accurate. At outdoor baselines, the length is usually projected onto a line between the underground reference markers. This time, however, the observers made the projections on a line between the permanently fixed, forced-centring plates on the pillars.

For the projection measurements, theodolites Wild T1600 no. 335322 and Wild T2000 no. 314345 were used in January and Wild T2000 no. 309806 in February, as well as Metri and Richter steel tapes no. VJ6675 and VJ6837. The Wild T1600 was used to align the mirrors. A low, Wild GST03 tripod was used under the instruments. the height determinations were performed using the Karl Zeiss Jena Ni002 precise levelling instrument no. 423196 and a 1-m-long Kern rod.

One problem that was encountered was that the forced-centring plates were under the mirror rails and were not visible during the interference measurement period; this forced the observers to make the projection measurements in two parts (Fig. 7.4). First, on 19 and 21 January, before installing the instruments measurements between the forced-centring plates and auxiliary benchmarks on the pillars were performed. Then, on 9 February, soon after making the interference observations, measurements between the same auxiliary benchmarks and the mirrors (and transferring bars) were performed. The auxiliary benchmarks consisted of permanently installed screw bases, to which indices for wire or tape measurements are normally affixed and to which mirror rails were attached now. A small, cone-shaped target was used to visualize the centre of the forced-centring plate and a mirror index to locate the centre of the mirror.

The results obtained with the traditional projection method are listed in Table 7.11. A projection from a transferring bar to the centre of a mirror is the sum of the transfer reading to the mirror surface and half of the mirror's thickness.

One additional disadvantage when doing the projection measurements was the unfavourable geometry. The forced-centring plates were between 153 mm and 158 mm apart from the mirrors in the baseline direction (and between 0 mm and 7 mm in the perpendicular direction). The angles to be measured should be near-zero or right angles, but now this was not possible. At the pillar at 75 m, even an accessory front lens (Wild GVO7) was needed for focusing the theodolite, as it was not possible to place the theodolite further than 1 m from the targets.

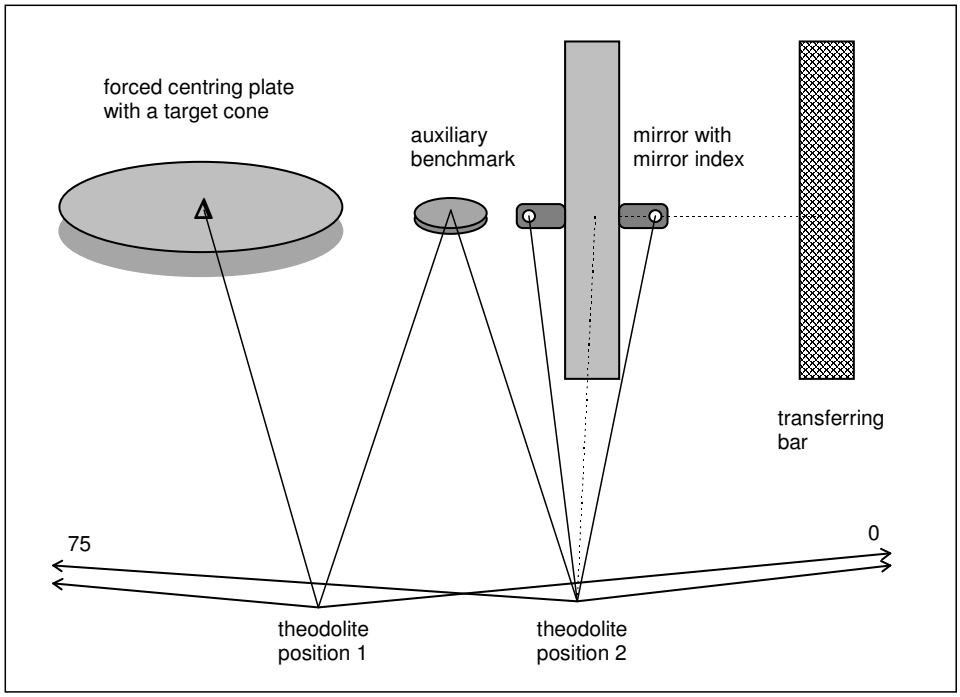

Figure 7.4 *The two-step projection method.*

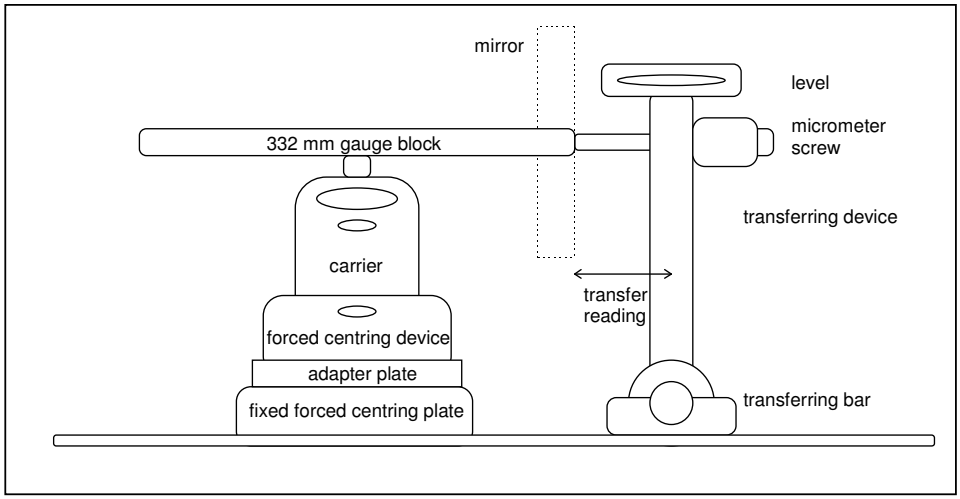

Figure 7.5 *The transferring method.*

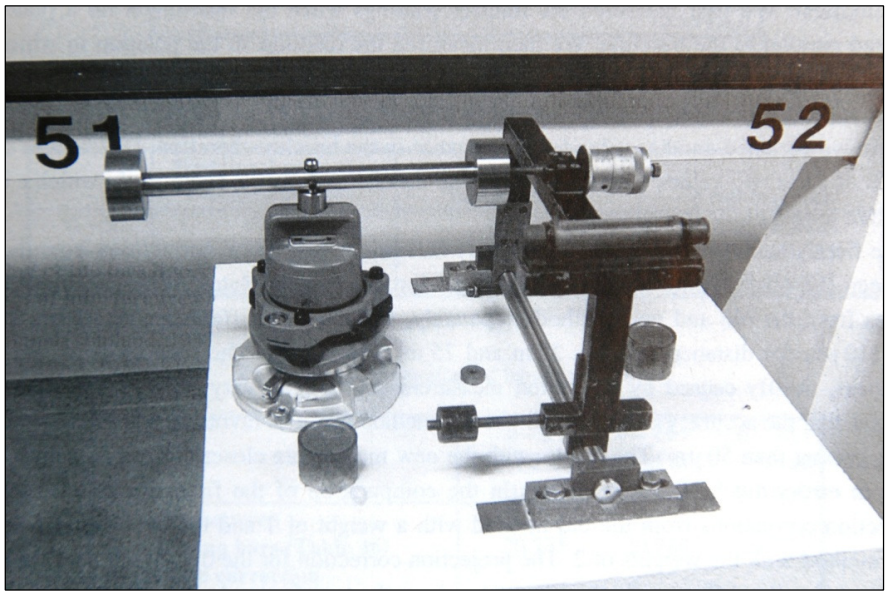

Figure 7.6 *A transferring measurement.*

The problems in applying the traditional projection method prompted new developments. Would it be possible to replace the theodolite and tape measurements with the transferring measurements? The solution was looked for by constructing a new accessory instrument, a gauge block, which could be attached to the forced-centring plate with the aid of a carrier, a forced-centring device and an adapter (Figs. 7.5–7.6). By removing the mirror equipment after making the interference observations, it was possible to make transfer measurements to the new instrument with the same transferring device that was used to measure the mirror positions. Instead of distances between the transferring bars and mirror surfaces, one could now obtain distances between the transferring bars and the new instrument. If the instrument could be placed in the same manner on every forced-centring plate, it was not even necessary to know its length.

The repeatability of forced-centring is quite good, up to ±20 μm, based on observations in Otaniemi. This is valid when using a single piece of equipment only and under laboratory conditions. When the instrument was rotated along the vertical axis and along the axis in the baseline direction, the observers could take transfer readings in four positions and obtain symmetry in the measurements. The dimensions of the instrument were such that the transferring point of the instrument was at about the same location as the mirror centre had been. The transferring bars on the pillars remained in the same position throughout the measurement procedure. The transferring device could be placed on it in the same manner every time, both when measuring to the mirror's surface and to the gauge block. The repeatability at this end is up to a few micrometres.

The line through the mirror centres and the line through the forced-centring plates were not congruent and not exactly parallel, and, to be precise, the latter was not even a line but a traverse. This did not cause any harm, but it did provide the observers with the possibility for one additional checking measurement. At first, the transfer readings were measured when the instrument on a plate was directed parallel to the baseline. Then the readings were measured at the position in which the distance between the instrument and the transferring device (and the mirror centre) was shortest. As it was known how far the forced-centring plate was from the line between the mirrors (from 0 mm to 3 mm), another value for the distance in the baseline direction was obtained. Differences in the means of these two values were from 2 μm to 12 μm. The means are listed in Table 7.12, in which c is the constant length of the instrument.

Finally, two independently determined projection corrections from the line between the mirrors onto the line between the forced-centring plates were obtained. When the values from the old and new methods were applied separately, differences of 80 μm, 20 μm and 120 μm were obtained for the distances of 5 m, 25 m and 75 m, respectively. Usually the standard uncertainties, mostly caused by projection measurements, for such distances are from 30 μm to 50 μm. It is now obvious that the accuracy obtained with the old method is not as favourable; with the old method the standard uncertainties were larger than 50 μm. The results with the new method are closer to true values, with standard uncertainties being much less than 50 μm. When computing the final results, the projection corrections from the old method were used with a weight of 1 and the two values from the new method with weights of 2.

The projection correction for the distance $0 - \nu$ (Table 7.13) was obtained as the difference in the projections from the transferring bars to the forced-centring plates, $P_\nu - P_0$.

7.9 Length of the baseline

Starting with the distances between the transferring bars, all of the necessary corrections were added to reduce these distances to the line through the forced-centring plates on the level of plate 0 (Table 7.14).

7.10 Uncertainty of the measurement

In Otaniemi there were no underground benchmarks like in Nummela, but both the primary markers (forced-centring plates) and secondary markers (transferring bars) were placed on the observation pillars. It was thus not possible to monitor the pillar movements via projection measurements; the only possibility for doing this was to examine the differences between the interference measurements. During the measurement period, no evidence of pillar movements was found. If the equipment was left properly adjusted for interference observations in the evening, one could still see the interference fringes without needing to adjust the lamp, mirrors or compensators on the following day, even after a weekend.

Table 7.11 *Results of projection measurements.*

	Projection (mm) in the baseline direction			
Pillar	**from transferring bar to mirror centre**	**from mirror centre to auxiliary marker**	**from auxiliary marker to forced-centring plate**	**from transferring bar to forced-centring plate**
0	+22.442	+4.566	+148.789	+175.797
5	+21.770	+4.092	+150.107	+175.969
25	+22.576	+5.025	+149.614	+177.215
75	+25.258	+5.775	+151.779	+182.812

Table 7.12 *Results of transfer measurements.*

	Projection (mm) in the baseline direction from transferring bar to forced-centring plate	
Pillar	**"Extreme value method"**	**"Parallelism method"**
0	9.717 + c	9.714 + c
5	9.967 + c	9.969 + c
25	11.152 + c	11.164 + c
75	16.619 + c	16.614 + c

Table 7.13 *Projection corrections (mm).*

Pillar interval	**Traditional projection measurements**	**New transfer measurements**	**Weighted mean**
0–5	+0.172	+0.252	+0.236 ±0.023
0–25	+1.418	+1.442	+1.438 ±0.008
0–75	+7.015	+6.901	+6.924 ±0.032

Table 7.14 *Computation of length of baseline.*

	0–5: mm + 5 m	**0–25: mm + 25 m**	**0–75: mm + 75 m**
Length between transferring bars (Table 7.10)	+20.735	+20.380	+18.775
Projection correction (Table 7.13)	+0.236	+1.438	+6.924
Mirror-body correction (Table 7.2)	–0.026	–0.001	–0.002
Mirror-coating correction (Table 7.3)	–0.002	–0.010	–0.030
Correction to the level of the forced-centring plate 0 (Section 7.6)	–0.000	–0.001	–0.002
Final length	+20.943	+21.806	+25.665

The stability of the pillars and the adequate repeatability of the transferring measurements also resulted in the fact that the uncertainties of distances between the transferring bars, u_B, compare favourably with the uncertainties of distances between the mirror surfaces, u_M; $u_B \geq u_M$. This could be verified with the same kind of uncertainty examination as has been done with the other interference measurements (Table 7.15).

Table 7.15 *Uncertainty of distances between mirror surfaces or transferring bars.*

	0–5	**0–25**	**0–75**
n_s	6	6	6
n_{obs}	4	4	2
u_I (μm)	< 1	2	2
u_I^{acc} (μm)	< 1	2	6
u_M (μm)	< 1	1	2
u_B (μm)	1	1	3

Finally, distances were reduced onto the baseline through the forced-centring plates on the level of plate 0. When estimating the total uncertainty budget, Table 7.16, the values u_B (Table 7.10) were used for the uncertainty of interference observations and transfer readings and the values u_P (Table 7.13) for the uncertainty of projection measurements. For the uncertainties due to the length standard and mirror surfaces the same estimates were used as in the previous measurement in Nummela. The geometrical corrections (<1 μm) due to horizontal non-parallelism were neglected.

Table 7.16 *Total uncertainty budget (μm).*

	0–5	**0–25**	**0–75**
Uncertainty in interference observations and transfer readings	1	1	3
Uncertainty in projection measurements	23	8	32
Uncertainty in determination of the absolute length of the quartz gauge	0	1	3
Uncertainty in thicknesses of mirror coatings	0	1	3
Total standard uncertainty	23	8	32

Since the samples are rather small, and since the observers did not consider the shorter distances to be significantly more accurate than the longest one, generally applicable values of standard uncertainty, 0.03 mm, and expanded uncertainty, 0.06 mm, were chosen to be presented in connection with the final results.

7.11 Final results

The length of the HUT Väisälä Baseline with its sections at the level of the forced-centring plate on pillar 0 is presented in Table 7.17.

Table 7.17 *The HUT Väisälä Baseline section lengths, with expanded uncertainties.*

Interval	**Length (mm)**
0–5	5 020.94 ±0.06
0–25	25 021.81 ±0.06
0–75	75 025.66 ±0.06

7.12 Conclusion regarding indoor measurements

At the HUT Väisälä Baseline, the observers obtained the accuracy expected in the interference observations. A well-designed calibration room provides more stable circumstances than field conditions but, if not every detail is considered, it may make projections for the final distances more laborious and inaccurate. Adapting a Väisälä baseline to other geodetic distance measurements, or using an existing baseline for interference observations, has always been a problem that increases uncertainty of measurement. Developing transferring methods is one method for maintaining a favourable level of uncertainty.

8 Summary of experiences with Väisälä baseline measurements

8.1 Nummela Standard Baseline

The interference measurements for the Nummela Standard Baseline are presented in Chapter 4. In addition to presenting the latest results in numbers, the chapter presents a comprehensive description of the present state of the baseline and an in-depth compilation of instructions for interference measurements, many of which have not previously been published. A few improvements to the measurement procedure are presented as well.

According to GUM, a measurement result is a "*set of quantity values being attributed to a measurand together with any other available relevant information*" (BIPM 2008a, Section 2.9), and "*generally expressed as a single measured quantity value and a measurement uncertainty*". The final measurement results for the Nummela Standard Baseline include values and uncertainties for five baseline sections, with the longer sections being multiples of the shorter sections (Table 4.32). These results constitute the essential link when transferring the traceable scale from laboratories to outdoor applications.

It has been customary to use standard uncertainty as a measure of uncertainty throughout the history of doing standard baseline measurements; the computation method for our past measurement projects was an analogue method and it is comparable with the method used in our present project and with the one suggested by GUM. Actually, the values of standard uncertainty are needed more often as a component of combined uncertainty when the scale of the standard baseline is transferred further. However, following GUM again, in this thesis most of the final results are now expressed with expanded uncertainties.

The recent results from 2005 and 2007 are equal to the previous results from 1996; even the largest difference of –0.19 mm obtained for the shortest distance of 24 m is fully acceptable in the long-time series. The length of the entire baseline, 864 122.86 mm, with a standard uncertainty of 0.07 mm, as well as the results for the shorter baseline sections are still outstanding for an outdoor, long-distance measurement standard. The FGI has successfully used the recent results in its latest international and national scale transfer projects, which are summarized in Chapter 9. They also provide a new verified set of traceable true distances for EDM calibrations and for testing and validating novel ADM instruments.

The new office and store building and the fences, roofs and cages sheltering the baseline structures were built in 2004, and the observation pillars were refurbished in 2007, including the addition of a drainage system around underground marker 0. The contractors had to perform the construction works with extreme caution to preserve the underground benchmarks of the baseline. The work was quite successful, which was confirmed in repeated projection measurements during the time that the construction work was going on, and finally in the interference measurements done in 2005 and 2007. At the 0 end of the baseline, the drainage system now keeps the soil dryer than before,

preventing suspected instability due to ground frost. The refurbished baseline structures and indoor premises together enable metrological research and development in excellent conditions.

In addition to the aforementioned new numbers for the Nummela Standard Baseline, a few remarks – significant or insignificant, but things present in the latest measurements – are listed here. When it comes to the weather, the most recent years have shown both the difficulty and the ease of doing interference measurements. In autumn 2005, no observations were possible until 864 m, but in 2007 up to eight measurements were performed. This is consistent with experiences at other standard baselines. It is not possible to adjust the comparator in unfavourable conditions, with any such attempts often being more detrimental than beneficial. In favourable conditions, the measurement must proceed without delay. Any sort of carelessness or lack of precision when making the preparations for or adjustments will likely cause difficulties later on. Since a team of observers may only make a few complete series of interference measurements during their career, this fact cannot be overemphasized.

When searching for the interference fringes for the first time, the approximate positions of the mirrors need to be adjusted with the help of high-precision EDM equipment. This accessory measurement gives reasonable results only when using a suitable reflector prism with the EDM equipment. If the mirrors are not covered, the reflecting surfaces of the comparator equipment could produce extraneous reflections, resulting in incorrect distances.

When searching for the interference fringes for the first time at a previously measured standard baseline, another precise method is available. The observers developed it and successfully applied it during the interference measurement done in 2007 and in 2013. The method presumes that the baseline is stable enough, so the older results are still for the most part valid. By comparing projection measurements for the previous interference measurements from several years ago with the new measurements currently being taken, the most probable positions of the mirrors for a successful interference observation can be computed. The positions of the mirrors for shorter distances, for which the observers have already found the interference fringes, determine the distance that must be multiplied to find the interference fringes for the longer distances.

The smooth performance of the projection measurements requires regular maintenance of the mechanical parts: the tripod setup, screws, slides, bars and levels. Daily control of the transferring device diminishes the influences of possible damages to it; a special self-made calibration tool for this is available. Of course, all parts must be cleaned and all possible broken and missing parts must be replaced before installing the comparator; this may be difficult later during the measurements.

Work with the quartz gauge in the Väisälä comparator can also be facilitated by avoiding large temperature changes when storing the quartz gauge between measurements. The observers found this out the hard way, as difficulties occasionally arose when measuring the gap between the quartz gauge

and mirror 1. The quartz gauge was kept in the new warm house between measurements, and it was suspected that a cooling down period of a few hours may not be enough during the cool autumn nights. Long-term storing of the quartz gauge at a temperature close to the prevailing outdoor temperature is therefore necessary to improve the stability of the measurement standard and to decrease the uncertainty of measurement. This phenomenon was closely studied during the interference measurements in autumn 2013. The result was that when keeping the quartz gauge outdoors all autumn the 10 nm-level deformations could still not be avoided, and the behaviour depended on outdoor conditions only. Uncertainty due to the temperature of the quartz gauge is included in the combined uncertainty of measurement with a value of 20 nm/m.

As presented in Chapters 4–7, the maximum values of (relative) refractive correction between the two baseline sections (the one to be multiplied and the multiplied one) at the four locations discussed in this thesis reach: 46 µm for 864 m at Nummela in 2007, 99 µm for 384 m at Chengdu, 83 µm for 432 m at Gödöllő and 8 µm for 75 m at the HUT. A noteworthy detail is that at Nummela in 2005, when the measurements up to 864 m failed due to unfavourable weather conditions, the maximum value was 66 µm for 432 m. It seems that about a 100 µm correction is close a limit, when observations still are possible; otherwise the two parts of the baseline are under significantly different temperature conditions. Due to the relative nature of the correction, the influence of recomputation using newer formulas, other than Kukkamäki's, would be negligible. Also the lack of inclusive pressure and humidity data prevents this.

8.1.1 True values for the scale transfer

For the scale transfer measurements, calibrations of the transfer standards made use of the results from the interference measurements done in 1996 as true values until 2005. Twice the amount of calibrations done in 2006 and 2007 used the results from the interference measurements done in 2005, but only for the first half of the baseline, up to 432 m. Calibrations done since 2008 have used the results from the interference measurements done in 2007. Since the results from the interference measurements are practically identical, there is no use to interpolate values for the intermediate years. The final computation of interference measurements done in 2013 will produce a new set of true distances.

8.1.2 Stability of the transfer standard

Most of the scale transfer measurements from the Nummela Standard Baseline presented in this thesis (Chapter 9) utilized the same EDM equipment, the Kern Mekometer ME5000 no. 357094 with prism reflector no. 374414, as a transfer standard. Table 8.1 shows an example of the calibration results for this equipment from autumn 2008, and Fig. 8.1 depicts the calibration results from a 16-year period, 1997–2012. Use of the first half of the baseline only and old worn-out adapter plates on the observation pillars caused the large uncertainties

in 2006–2007. Fig. 8.2 depicts the dependency on environmental conditions for calibrations done during the ten-year period 2003–2012. No results have been omitted.

Table 8.1 *Additive constant (mm) and scale correction (mm/km) from the eight calibrations for the scale transfer measurements in autumn 2008. The uncertainty values are experimental standard deviations of the mean from the adjustment computations.*

	Additive constant	**Scale correction**
28–29 August	+0.081 ±0.048	+0.011 ±0.048
1 September	+0.052 ±0.051	+0.423 ±0.054
2 September	+0.082 ±0.066	+0.251 ±0.075
3 September	+0.044 ±0.063	+0.180 ±0.075
average "before", equal weights	+0.065 ±0.010	+0.216 ±0.085
average "before", weighted	+0.065 ±0.010	+0.200 ±0.099
31 October	+0.077 ±0.086	+0.151 ±0.096
3 November	+0.101 ±0.083	+0.134 ±0.094
5 November	+0.096 ±0.045	+0.125 ±0.048
6 November	+0.091 ±0.052	+0.056 ±0.049
average "after", equal weights	+0.091 ±0.005	+0.117 ±0.021
average "after", weighted	+0.093 ±0.004	+0.102 ±0.022

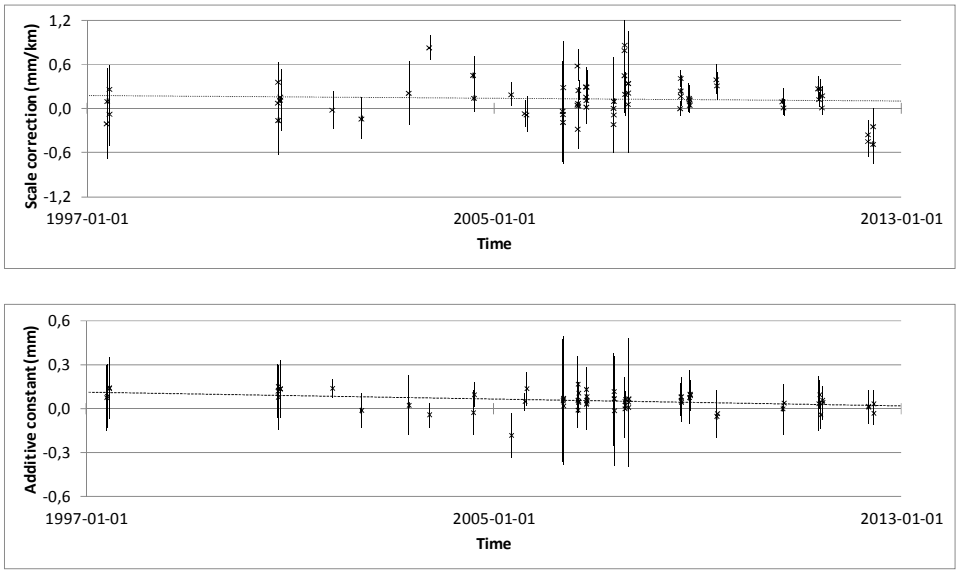

Figure 8.1 *Calibration results of the transfer standard Kern ME5000 no. 357094 and prism reflector no. 374414, instrument corrections with expanded uncertainties.*

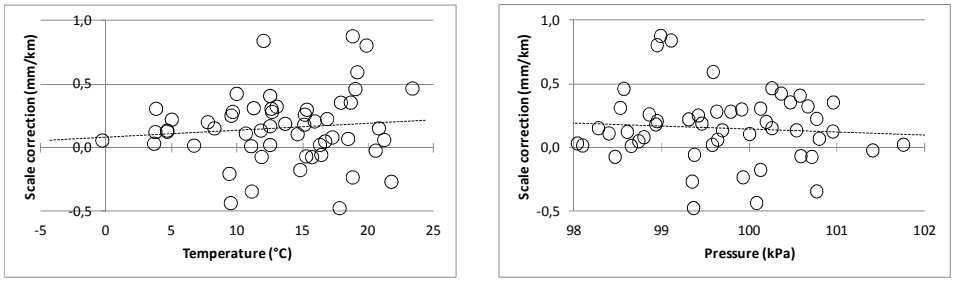

Figure 8.2 *Calibration history of the transfer standard Kern ME5000 no. 357094 and prism reflector no. 374414, dependency on environmental conditions.*

After making the appropriate corrections, the dependence on weather conditions is obvious only in the uncertainty of measurement, but not in the average quantity values. The long-term history shows an insignificant 10^{-7} level or smaller trends or dependencies in scale, and also the minor drift in the additive constant is insignificant. There are few outliers. However, the small degree of variation in the results does not contest the need for repeated calibrations.

8.2 Experiences at the Chengdu Standard Baseline

The work done on the Chengdu Standard Baseline is presented in Chapter 5. The design of the baseline was interesting and exceptional. The SBSM had established facilities for the Väisälä interference comparator in the middle of the 1.5 km baseline, and it would have been possible to conduct interference observations in both directions, even though this would have required major efforts. Even the possibility to extend the baseline immediately using high-precision EDM equipment was excellent. An even greater advantage was offered by the possibility to do geodetic satellite positioning on the roofs of several pillar shelters, right above the central benchmarks of the observation pillars and, if desired, even simultaneously with the EDM observations. Satellite positioning was not yet included in the documented measurement project, but the baseline design and multi-purpose structure could be utilized in some later works.

The tall structure used for the observation pillars, 2 to 3 metres above the ground, was obviously favourable with respect to refraction outside of the sheltering structures. At the same time, the concrete walls around approximately 50 metres of the middle part of the baseline were disadvantageous, causing mixed temperature gradients around them when warming occurred during the days and cooling during the nights. The thermal effects were different depending on the amount and direction of the sunshine, but they could be seen in the changing temperatures even at the smaller structures at the intermediate pillars. Turbulence affected the propagation of the measurement beam especially strongly close to the components of the Väisälä comparator. The behaviour was unpredictable and not clearly detected before the interference measurements.

The lack of underground benchmarks was not important, and a geodetic standard baseline can easily be maintained without them. Actually, the connection between the equipment used with the Väisälä interference comparator and the reference points for the surveying instruments is often more accurate and easier to carry out with mechanical probing than with an inconvenient optical projection measurement method. Some modified instrumentation may be needed to reach the reference points with the transferring instrument as well as the "ortho-truncated cone forced-centring" plate used at the Chengdu Standard Baseline. A large number of observation pillars is a good basis for regular stability control with high-precision EDM.

In autumn 1998, the weather conditions were far from optimal in Chengdu. The observers successfully measured a distance of 384 m with the Väisälä interference measurements, which they extended using the preceding and successive EDM observations up to a rather long distance of 1 488 m. The results from the two methods were compatible and eligible for a geodetic baseline either alone or together, but the processing phase also immediately raised some doubts about the stability of the results. The published final result made use of a combination of interference measurements and EDMs, with a tolerable estimate of the uncertainty of measurement.

8.3 Experiences at the Gödöllő Standard Baseline

The work done at the Gödöllő Standard Baseline is presented in Chapter 6. In addition to Nummela, this is another successfully remeasured stable standard baseline. The observers in 1999, Jokela and Poutanen, obtained – within the expanded uncertainties of measurement – the same results as the observers in 1987, Kääriäinen and Konttinen (Kääriäinen et al. 1988). Since the observers have to reconstruct the comparator for every interference measurement period, this is again excellent evidence of the reproducibility of the Väisälä method. It is also noteworthy that the projection measurement procedure was different than the one used at Nummela, since the underground markers are under the observation pillars; this challenging part of the measurement procedure was also successful.

The experiences from 1999 are an example of both the arduousness and ease of using interference measurements. Clear October nights caused a 29-day delay in the observations, but after that the observers made five measurements in one week, with the last ones being done in pouring rain. The weather conditions are not a major source of uncertainty – as long as they allow for successful observations. The slight variation in the five measurements seems to be dependent on the scale, possibly indicating the difficulties or deficiencies in working with a quartz gauge.

In the continuation from 432 m to 864 m, the observers used a Kern Mekometer model ME3000 in 1987 and model ME5000 in 1999. The preeminent improvements in the instrument were convenient for making the observations, but they can hardly be noticed in terms of the results. The

connection between the interference measurements and the EDM equipment was smooth, since the mirror equipment of the comparator was replaced with the EDM equipment using the same installation rails on the observation pillars.

In addition to immediately being able to use the results from the interference measurements, two frequency calibration results were also available for computing the measurements made in 1999. Leica Geosystems performed one determination in Switzerland in 1997, and an accredited calibration laboratory in Hungary performed another one with equal results in 2000. When calibrating the EDM equipment at an outdoor geodetic baseline, the circumstances are often close to what prevails when using the equipment under other circumstances, and actually a complete measurement system can be calibrated instead of just part of one. One advantage of a frequency calibration is that it is effortless to perform – where a metrological service is available for just this purpose. Though the data set compiled in Gödöllő was scarce, a comparison of the scale corrections obtained when using the two completely different methods was interesting. A scale difference of 0.37 mm/km is quite large, but compatible when regarded together with the EDM time series.

As a remarkable resource in European length metrology, the Gödöllő Standard Baseline is worthy of all necessary care and maintenance. It is one of the few geodetic baselines where a remeasurement with the Väisälä interference comparator could be considered. Based on recent information from the FÖMI, the baseline would need some refurbishment. However, there is a lack of resources for maintaining regular control of it with high-precision EDM.

8.4 Experiences at the HUT Väisälä Baseline

The work done at the HUT Väisälä Baseline is presented in Chapter 7. The laboratory room was originally planned for interference measurements with the Väisälä method, and it had already been used for a long time to calibrate surveying instruments. Thus, the location was quite optimal for reproducing the interference measurement method indoors once again. The observers chose the longest distance, $3 \times 5 \times 5 \times 1$ m = 75 m, to be measured with the interference comparator.

As expected, the measurements confirmed that the Väisälä method can be reproduced effortlessly under stable conditions. The complete procedure took only three weeks, including installations, measurements and computations. The significant, but small and regular, temperature changes along the baseline caused no problems. The only major challenge was to transfer the good results from the different parts of the comparator – mirrors and transferring bars – to the distances between the forced-centring plates, which would be of use in further research and calibrations. As a solution to this problem, the observers implemented the connection between the interference measurements and applications both with mechanical probing – an advanced transferring method – and with two-step, theodolite-based projection measurements. The transferring

method was quite similar to what was later applied at the Chengdu Standard Baseline.

As long as the transfer and projection measurements remain major sources of uncertainty of measurement, the total standard or expanded uncertainties in indoor measurements are quite equal to those under field conditions, especially for short distances. With the good repeatability of the Kern-type forced-centring the baseline still provided known lengths with less than 50 µm in total standard uncertainties, which can be used in various applications. Analyses of the Väisälä interference comparator results and the laser interferometer measurements (which HUT performed) have not been published, but HUT reported that no changes in the previously applied baseline section lengths were necessary due the new interference measurements, indicating the sufficient stability and good usability of the baseline. Justifying with confidentiality, the HUT couldn't response to the author's request for a more detailed data.

With more abundant resources, a more inclusive measurement project would have been possible. The dense layout of the observation pillars would have allowed a different multiplication up to 72 m, or also to shorter distances, which would have yielded a large set of different distances from 1 m to 75 m. The only technical requirement for this would be to have enough mirror equipment to place on the intermediate pillars and to be able to temporarily remove the extra mirrors as the measurement proceeds. The measurement beam directed between the optical elements under different geometric conditions could easily be adjusted. Comparable measurement facilities for fundamental research work on surveying instruments utilizing interference measurements have not been established elsewhere in the world, which makes the recent closure of the premises regrettable.

8.5 Traceability and uncertainty for incompatible measurement methods

The traceability chain described in this thesis includes use of several measurement methods utilizing different fixing, centring and adjusting principles of instruments. Especially critical is the change from Väisälä interference comparator equipment to forced-centring devices of common EDM and other surveying instruments. As presented in Chapters 4–7, mechanical probing in transferring measurements and optimal arrangements for projection measurements help maintaining traceability and 0.1 mm-level or better uncertainty.

Comparisons of quartz gauges at the Tuorla Observatory do not increase the uncertainty of lengths of the quartz gauges. On the contrary, they provide a possibility to utilize a larger set of results of absolute calibrations, instead of results for only one or two quartz gauges, which are used in single standard baseline measurements with the Väisälä interference comparator. The lengths are compared in identical conditions; after careful adjusting of the quartz gauges in the comparator box the main source of uncertainty are temperature changes, which remain at the 0.01 °C-level.

Use of transferring bars is the solution for reliable maintenance of traceability and for achieving small uncertainty in measurements with the Väisälä interference comparator. The transferring bars are permanently installed on the observation pillars. With the transferring device distances between the permanent transferring bars and adjustable mirror surfaces can easily be measured with a few μm uncertainty. The most accurate results in interference measurements, distances between mirror surfaces and distances between transferring bars, are obtained with a similar uncertainty. Always both observers take the transfer readings; no difference larger than 3 μm is allowed between their observations. During a measurement period, condition and operation of the transferring device is checked daily. In the uncertainty computations the uncertainty of transfer readings is included in the standard uncertainty values of interference observations, which typically range between 0.01 mm and 0.05 mm.

The transferring bars on the observation pillars can be used also, if results of interference measurements with the Väisälä interference comparator have to be transferred to distances between forced-centring plates at a baseline with no underground benchmarks. Some precision mechanical gauges may be needed as auxiliary instruments when taking transfer readings; examples are presented in Sections 5.4 and 7.8. Transfer readings can be used also, if forced-centring plates are attached on robust iron stands which can be placed on the same rails as the Väisälä comparator mirrors (though not simultaneously); an example is presented in Section 6.3. Again, the uncertainties due to transfer readings are only a few μm.

When a geodetic standard baseline has a line of underground benchmarks next to the line of observation pillars, repeated projection measurements create the connection between interference measurements and EDM. In projections from observation pillars to underground benchmarks during an interference measurement period no exact location is needed for the angle measurement instrument. Though much more inconvenient in use, traditional high-precision theodolites seem to be more precise in angle observations than the modern tacheometers. Symmetrical observations (to the different positions of the plumbing rod and to the sides of the mirror) and optimal measurement geometry (right horizontal angles and small vertical angles) keep measurement uncertainties decent, though the typical standard uncertainty values between 0.01 mm and 0.06 mm for projection corrections remain as a major source of uncertainty in the estimation of total uncertainty. Subdividing the uncertainty of projections in components is difficult, and the variation in results seems to be random. Two projections are needed for a projection correction of one distance. It is advisable to measure all projections with the same angle measurement instrument. Two observers perform the measurements. Working with the plumbing rod needs special caution, but possible faulty centrings are easily detected in the on-site check computations. More details are presented in Chapter 4.

In projections from underground benchmarks back to observation pillars the angle measurement instrument is placed on the observation pillar to be projected. At every pillar a forced-centring device attached on a robust iron stand is fixed on the pillar, not on the rails for Väisälä comparator mirrors (which are removed soon after the interference measurements) but separately. The measurement principle remains the same, with optimal geometry and symmetrical observations to the plumbing rod in different positions and to the two baseline directions. Repeated projection measurement periods during a field work season should produce smaller than 0.1 mm standard uncertainties.

The centring and adjusting methods of EDM discussed in this thesis are limited to the most common methods used with surveying instruments. More advanced centring apparatus is used in applications of industrial metrology, and they may help decreasing the uncertainty of centrings also in geodetic measurements. The principle of an auxiliary instrument is often simple, such as a prism reflector installed in a precisely spherical shell which is placed directly on an inset at a measurement point, or pinned or furrowed structures of fixing plates allowing adjusting of an instrument in one way only. Producing such instruments may need machining with methods of precision mechanics; some commercial solutions are available, too. The usability of these instruments in more practical surveying applications may be limited.

9 Summary of scale transfer measurements

Metrologically traceable scale transfer measurements from the Nummela Standard Baseline have been a widely utilized service during the last twenty years (Table 9.1). The results and special features of several interesting scale transfer projects are briefly presented here; they have also been introduced and summarized by Jokela et al. (2009a). More details are available in the other scientific articles (referred to later), which the author of this thesis has written.

The projects utilized the results from interference measurements done at the Nummela Standard Baseline in 1996, 2005 and 2007 for the calibration of other geodetic baselines and test fields. Kern Mekometer ME5000 high-precision EDM equipment, repeatedly calibrated at the Nummela Standard Baseline, was used as a transfer standard (Figs. 9.1–9.2). The results of the interference measurements were practically identical, allowing for an equal, traceable scale that could be transferred without ambiguity. Also, the operation of the EDM transfer standard has been stable, with little variation in the scale factor (see Section 8.1.2). Computing the group refractive index of air for the first velocity correction is an essential part of processing the observations. Unless otherwise stated, weather observation data for scale transfer measurements were processed using a computation method first proposed by Ciddor (1996), as recommended in Resolution no. 3 of the 1999 IAG General Assembly (IAG 2000).

Table 9.1 *Recent scale transfer measurements using the quartz gauge system and Väisälä interference comparator and/or Nummela Standard Baseline for other geodetic baselines.*

1997, 2001, 2007, 2008, 2014	Kyviškės, Lithuania, 1 320 m
1997	Hsinchu, Taiwan, 432 m
1998	Otaniemi, Finland, 75 m
1998	Chengdu, China, 1 488 m
1999	Gödöllő, Hungary, 864 m
2000, 2008	Vääna, Estonia, 1 728 m, 1 344 m
2002	Eggemoen, Norway, 960 m
2002	Novobërdë, Serbia (Kosovo), 1 831 m
2002–2012	Olkiluoto, Finland 511 m
2003	Tsukuba, Japan, 204 m
2006	Daejeon, South Korea, 280 m
2008–2011, 2013–	Participation in European Metrology Research Programme (EMRP) Joint Research Projects
2008	Innsbruck, Austria, 1 080 m
2009	Beijing and Zhengzhou, China
2011, 2014	Braunschweig, Germany, 600 m
2012	Valencia, Spain, 330 m

Figure 9.1 *Measuring for calibration of the Kern Mekometer ME5000 at the 0 pillar of the Nummela Standard Baseline, with two Thommen aneroids, bottom left, and a suspended Assmann psychrometer, top right.*

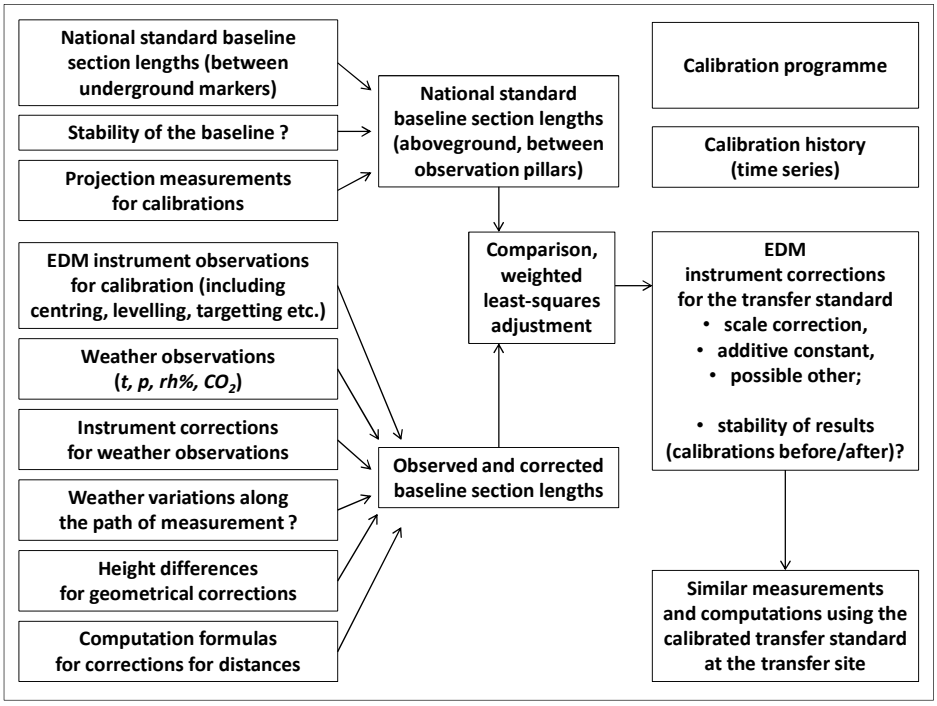

Figure 9.2 *Overview of calibration of transfer standard for scale transfer .*

9.1 Kyviškės Calibration Baseline in Lithuania

The project to establish a calibration baseline in Lithuania was started as a joint project between the VGTU and the FGI. In 1996, the Kyviškės Calibration Baseline was established. Repeated calibrations in 1997, 2001, 2007 and (in connection with a GNSS measurement experiment, Fig. 9.7) in 2008 have proved that the baseline is accurate and stable. They make it possible to maintain a national calibration service and serve as a remarkable resource for geodetic metrology, even at the international level (Jokela et al. 1999, 2002; Koivula et al. 2012a). A summary of the first ten years has been presented by Būga et al. (2008).

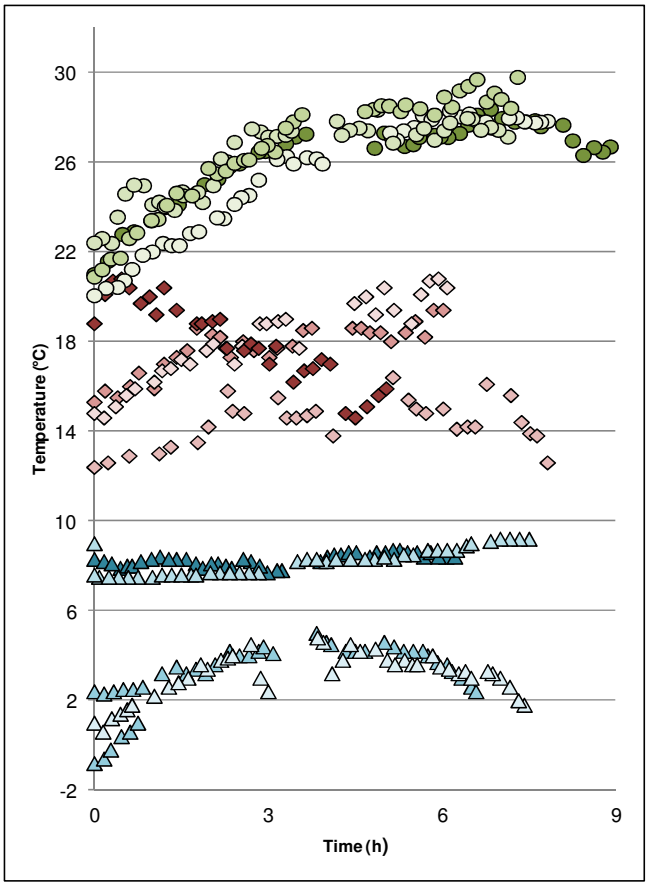

Figure 9.3 *The repeated calibration of the Kyviškės Calibration Baseline and test field covers an impressive variety of measurement temperatures. With the establishing measurement done in June 1997 (quadrangles), large temperature fluctuations prevailed, whereas a warm August 2007 (circles) and chilly October 2001 (triangles) offered more stable measurement conditions. The different colour tones of the symbols indicate the four different measurement days for each year. The calibration results are presented in Fig. 9.4.*

Calibrations of the Kyviškės Calibration Baseline are a prominent example of repeated scale transfer measurements under very different weather conditions. Three measurement projects under distinct, but internally rather homogeneous, temperature conditions can be compared, covering temperatures from 0°C to 30°C (Fig. 9.3). The difficulties in making the temperature observations and in determining the resulting uncertainty of measurement were recognized when processing the observations; there is a small correlation of corrected lengths along with temperatures (Būga et al. 2014). The determined uncertainty values obviously were reasonable from the beginning, and the results from the later calibrations fit well together with the first result (Fig. 9.4). Our later experiments have confirmed the good reliability of classical weather observation instruments when properly used.

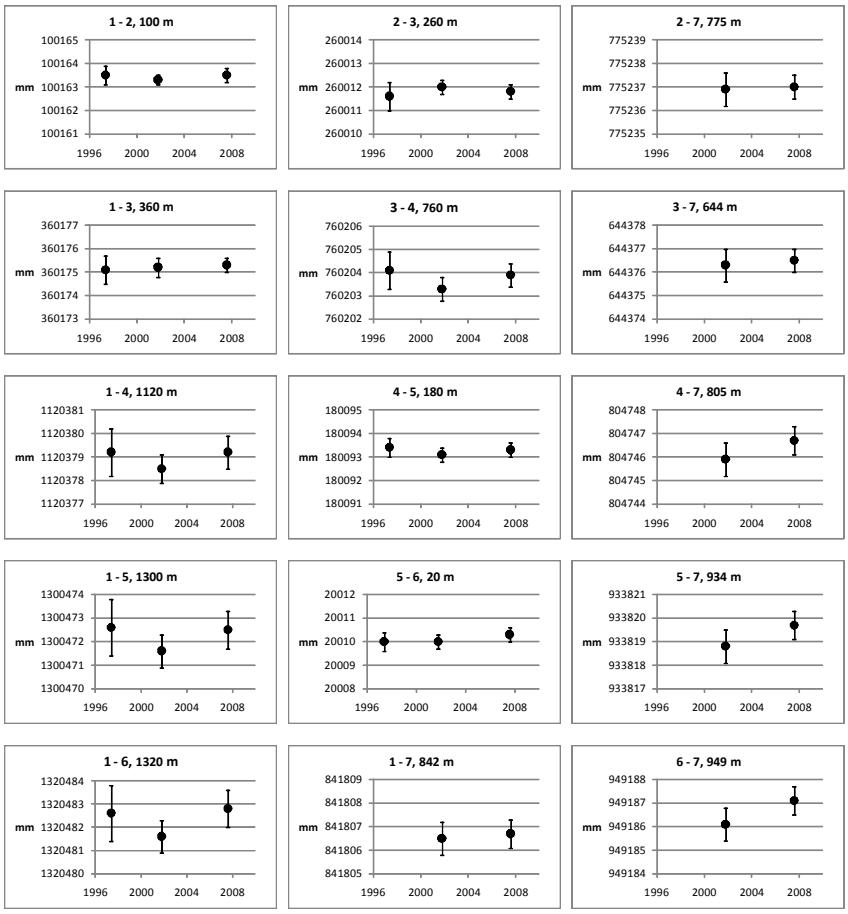

Figure 9.4 *Results from the three calibration periods at the Kyviškės Calibration Baseline and test field (at epochs 1997.4, 2001.8 and 2007.6), showing lengths with expanded (95%) uncertainties. The figure is a reprint from Būga et al. (2008).*

The expanded total uncertainties of the distances between pillars ranged from 0.4 mm to 1.2 mm for distances between 20 m and 1 320 m in 1997. In 2001 and 2007, the values were smaller, from 0.2 mm to 0.8 mm, due to more favourable weather conditions. The measurements made in 2008 continue the compatible time series. Our experiences show that the scale transfer method is quite effective when the objective is to obtain sub-millimetre uncertainties.

The usability of the GNSS measurements is an indisputable advantage at Kyviškės. The observation pillars are suitable for antennas, and the visibility is open almost down to the horizon at most of the pillars. The surrounding grassland is favourable both for terrestrial and satellite geodetic measurements. The facilities and our first experiences are a topical example of how to advance GNSS metrology.

There is common interest in continuing the co-operation related to the Kyviškės Calibration Baseline. A new remeasurement was performed in July 2014, among with some other international scale transfer measurements.

9.2 Vääna Calibration Baseline in Estonia

Calibrations of the Vääna Calibration Baseline are another example of a successful co-operative project carried out in the Baltic countries. The FGI calibrated the baseline for the first time in October 2000 and again in October 2008. Many of the original baseline constructions from the late Soviet period were still in use in 2000. Before the remeasurement in 2008, *Maa-Amet* performed an elaborate refurbishment of the baseline.

The new special baseline design, 13 observation pillars in a line at intervals from 2 m to 374 m, makes it possible to measure a large set of distances up to 1 344 m (Fig. 9.8). As another advantage, the elevations of the pillar tops are equal to within 3 mm. For the calibration done in 2008, the observers measured all distances ranging from 24 m to 1 344 m from nine different observation pillars. They measured distances longer than 20 m from the four other observation pillars; the transfer standard is not capable of measuring distances shorter than 20 m without additional software. Altogether, 144 observation sets compiled during the course of four days in proper measurement conditions created an abundant data set to be adjusted.

With the precise new centring method, the centre plug of a high-quality steel adapter plate is placed in the centre hole of another steel plate, which is permanently fixed to the top of an observation pillar. The thread on the top of the adapter plate, which also determines the reference point of a pillar, fixes the measurement instrument precisely and firmly. The centring method contributes to the good repeatability of measurements and to the small degree of uncertainties achieved during the measurements; a distribution of residuals is illustrated in Fig. 9.5.

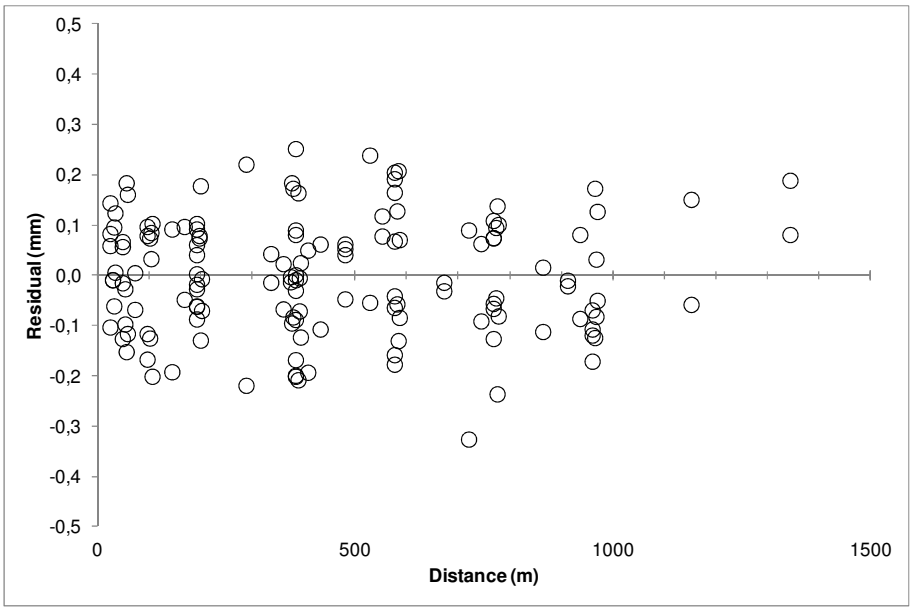

Figure 9.5 *Residuals from a least-squares adjustment of 144 Kern ME5000 observations at the Vääna Calibrations Baseline for the scale transfer done in October 2008; they demonstrate an achievable level of accuracy under proper conditions. No scale dependency is discernible.*

Estimating the uncertainty of measurement included taking into account uncertainties due to well-known components, uncertainties that did not have such well-known numerical values. These included (Table 9.2) the scale transfer from the definition of the metre to the interference measurements, the projection measurements, the calibration of the EDM transfer standard, temperature measurements, air pressure measurements, the determination of the relative humidity, and experimental standard deviations based on the adjustments made for the additive constant and for single pillar intervals. Under favourable weather conditions, uncertainty due to weather instruments and weather observations was not treated separately. The similarity of the measurement conditions and environs of Nummela and Vääna contributed to the stability and reliability of the transfer standard.

The estimated expanded total uncertainty ranged from 0.16 mm to 0.22 mm for the 12 sequential pillar intervals between 2 m and 374 m (and to 0.60 mm or 0.45 mm/km for the entire 1 344 m). This result is probably close to the best that can be achieved with the present method. Regardless of the established guides, such as GUM, estimating the uncertainty components under field conditions remains challenging, and whether or not the measurements are successful depends on the researcher's experience and views. Therefore, slightly different results (smaller or larger uncertainty values) are possible and acceptable.

Table 9.2 *Estimation of uncertainty of measurement at the Vääna Calibration Baseline.*

GUM type of uncer-tainty	**Description**	**Quantity x_i**	**Standard uncertainty $u(x_i)$**	**Sensitivity coefficient c_i**	**Standard uncertainty, fixed component (mm)**	**Standard uncertainty, proportional component (mm × L, L in km)**
A	12 distances from the adjustments (including centring and levelling)	from 2 m to 374 m	from 0.033 mm to 0.040 mm	1	from 0.033 to 0.040	0.000
B	scale at Nummela	1.000000000	0.000000086	L	0.000	0.086
B	projection measurements	0 mm	0.070 mm	1	0.070	0.000
B	EDM scale correction	1.000000151	0.000000049	L	0.000	0.049
B	EDM additive constant	0.035 mm	0.020 mm	1	0.020	0.000
B	temperature observations	from 278.2 K to 285.6 K	0.15 K	1×10^{-6} K^{-1} L	0.000	0.150
B	pressure observations	from 99.84 kPa to 102.07 kPa	23 Pa	3×10^{-9} Pa^{-1} L	0.000	0.070
B	humidity observations	from 67 % to 98 %	2 %	1×10^{-8} %$^{-1}$ L	0.000	0.020
	Total standard uncertainty				from 0.080 to 0.083	0.194

In addition to the pillar intervals, the observers measured five old benchmarks built in the ground along the baseline. Robust wooden tripods and a precise optical nadir plummet Wild NL were an essential help and guaranteed good accuracy during the centrings. Two pillar intervals of up to 360 m were fixed in the adjustment computation of 15 observed distances between the pillars and benchmarks. The expanded total uncertainties were smaller than 0.3 mm for the adjusted distances between 24 m and 96 m; for such short distances, the random variation when setting up the instruments is the main source of uncertainty. In general, installations on tripods cause additional sources of uncertainty, depending on the miscellaneous instruments and users, and should be avoided in measurements done at geodetic baselines.

The Estonian specialists have carried out the refurbishment and development work done at the Vääna Geodetic Baseline with consideration and care. The environment is constant and quiet. The site is quite suitable for EDM equipment, probably also for ADM equipment, and worthy of further maintenance and development work, even that done for it to serve as an international metrological resource.

9.3 BEV Geodetic Baseline in Innsbruck, Austria

When presented in numbers, the results of calibration done at the BEV Geodetic Baseline are completely acceptable (Jokela et al. 2010). Temperature conditions were quite equal both in Nummela and in Innsbruck, ranging from 6°C to 16°C. The expanded uncertainties ranged from 0.21 mm to 0.81 mm for the 21 different baseline sections between 30 m and 1 080 m. A previous measurement done with a similar – but not the same – instrument makes it possible to compare the two results from 2006 (1 x 42 measured distances) and 2008 (4 x 42 measured distances), showing good short-term stability and an equal scale (Fig. 9.6).

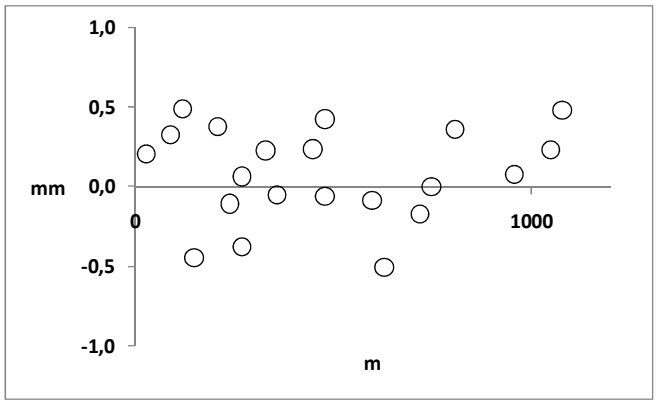

Figure 9.6 *Differences between the distances at the BEV Geodetic Baseline, based on the measurements made in September 2006 to September 2008.*

For routine calibrations of surveyors' EDM instruments, the location of the baseline is serviceable, though not pleasant for the observers. The baseline is easy to access and the measurement conditions are, though challenging, close to what the observers may encounter in their practical work (Fig. 9.9). For the scientific purposes of the EMRP, which were planned as the main application of the baseline, the choice of location for the baseline could have been much better. The change from the controlled laboratory conditions to the turbulent chaos next to the baseline – busy motorway, icy river, sunny mountainside – was too much for a serviceable testing of the new instruments.

9.4 PTB Geodetic Baseline in Braunschweig, Germany

The design of the PTB Geodetic Baseline makes it possible to measure all distances between 50 m and 600 m at 50 m intervals (Fig. 9.10). A major advantage of the baseline is its location next to, and inside the fences of, a large metrology institute with all the necessary and useful infrastructure located in the immediate vicinity. Pollinger et al. (2012) give a thorough description of the refurbishment of the baseline and of the first research efforts using the new weather sensor system. The other recent description examines possible differences in the weather data obtained using a few classical instruments and the inclusive sensor system; the data were recorded in connection with the calibration of the baseline in June 2010 (Figs. 9.12–9.13; Jokela et al. 2012b). The classical instruments included just two calibrated Assmann psychrometers for measuring the dry and wet air temperature and one or two calibrated Thommen aneroids for measuring the air pressure. Through velocity corrections, possible differences would have an influence on the resulting baseline section lengths.

When comparing the few classical weather observation instruments and the sensor system, the average difference between 168 dry temperature observation sets compiled during five observation days was +0.27 K, with a standard deviation of 0.53 K. On the only day with favourable conditions, the average difference was just −0.01 K, with a standard deviation of 0.22 K. In unfavourable weather conditions, local variations along the measurement beam path are multiple and it is difficult to determine what temperatures are true; significant systematic differences may occur. The few classical instruments cannot reveal the variations along the measurement beam at all, but variations of up to several Kelvins will remain as a disturbance and will also increase the level of uncertainty in the sensor system data, with the differently shaded and open sections of the baseline causing most of the variation.

The average difference in air pressure for the 168 observation sets was +8 Pa, with a standard deviation of 30 Pa. The average difference in relative humidity for the 168 observation sets was −3 percentage points, with a standard deviation of 3 percentage points. Under stable conditions with high humidity, the difference was just −1 percentage point, with a standard deviation of 2 percentage points.

As a result of the weather data analysis, practically equal average values in the weather data sets resulted in equal velocity corrections and equal corrected baseline section lengths. When using psychrometers and aneroids for the weather observations, after making adjustment computations the expanded uncertainties for the final seven distances between 50 m and 600 m were from 0.20 mm to 0.47 mm. Using the sensor network data instead, changes for the same final distances between 50 m and 600 m ranged from –0.07 mm to +0.12 mm and from –0.07 mm to +0.09 mm for the seven sequential pillar intervals between 50 m and 150 m.

Figure 9.7 *VGTU's Kyviškės Calibration Baseline and test field in Lithuania.*

Figure 9.8 *Maa-amet's Vääna Calibration Baseline in Estonia.*

Figure 9.9 *BEV's Geodetic Baseline in Innsbruck, Austria, next to a busy motorway. Outside the picture, a slope drops to the river Inn next to the track on the left and high mountains rise just behind the river.*

Figure 9.10 *PTB's Geodetic Baseline with environmental sensors in Braunschweig, Germany. The fence on the left is for safety when measuring with lasers.*

Figure 9.11 *UPV's Geodetic Baseline and test field in Valencia, Spain.*

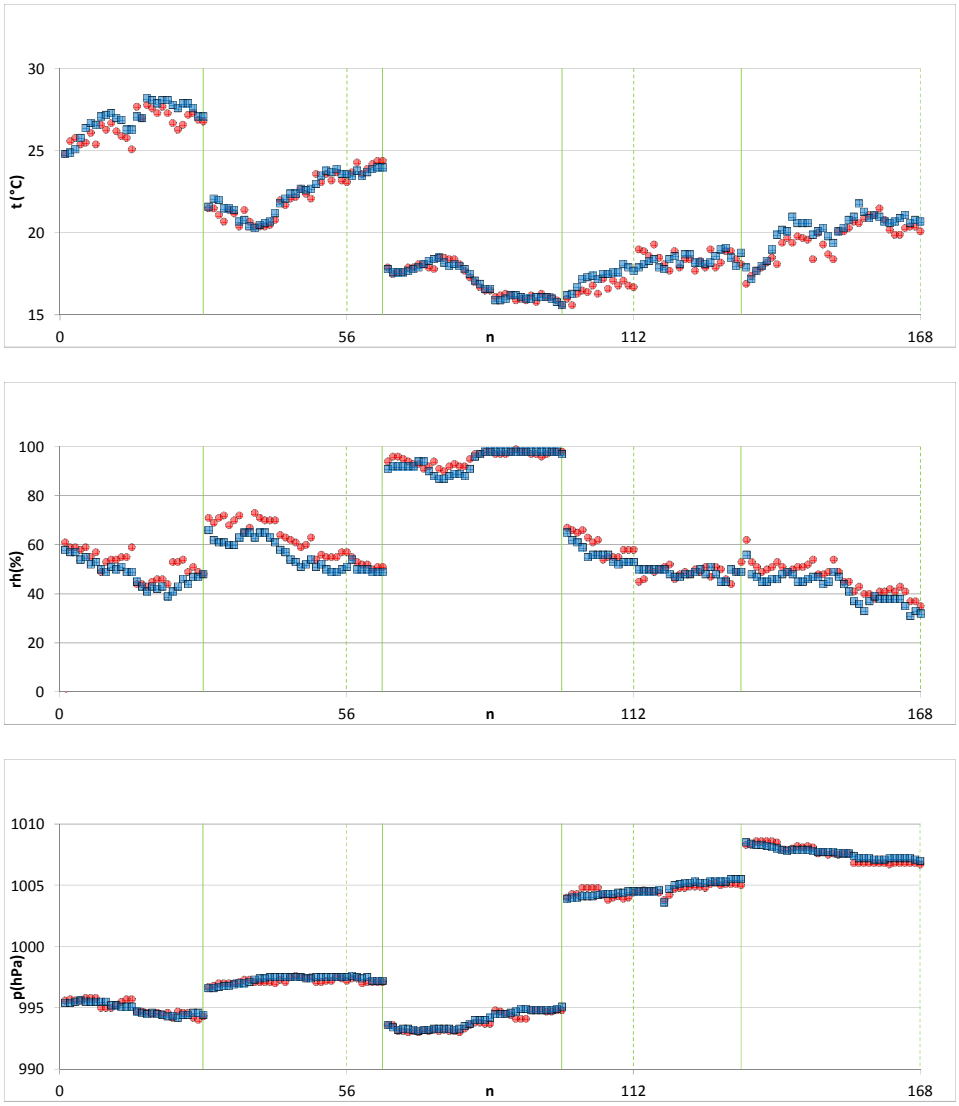

Figure 9.12 *On the top, average temperature during the 168 distance measurements at the PTB Geodetic Baseline. The red circles depict the data obtained with the FGI weather instruments, while the blue squares depict the data obtained with the PTB sensor system. The dashed green lines separate the data for the three calibrations, while the solid green lines separate the five measurement days (on 6–10 June 2011) with different weather conditions. The third day was the most favourable (mostly cloudy and rainy), whereas the other days were mostly clear or partly cloudy. The two other plots show the average relative humidities and average air pressures, respectively.*

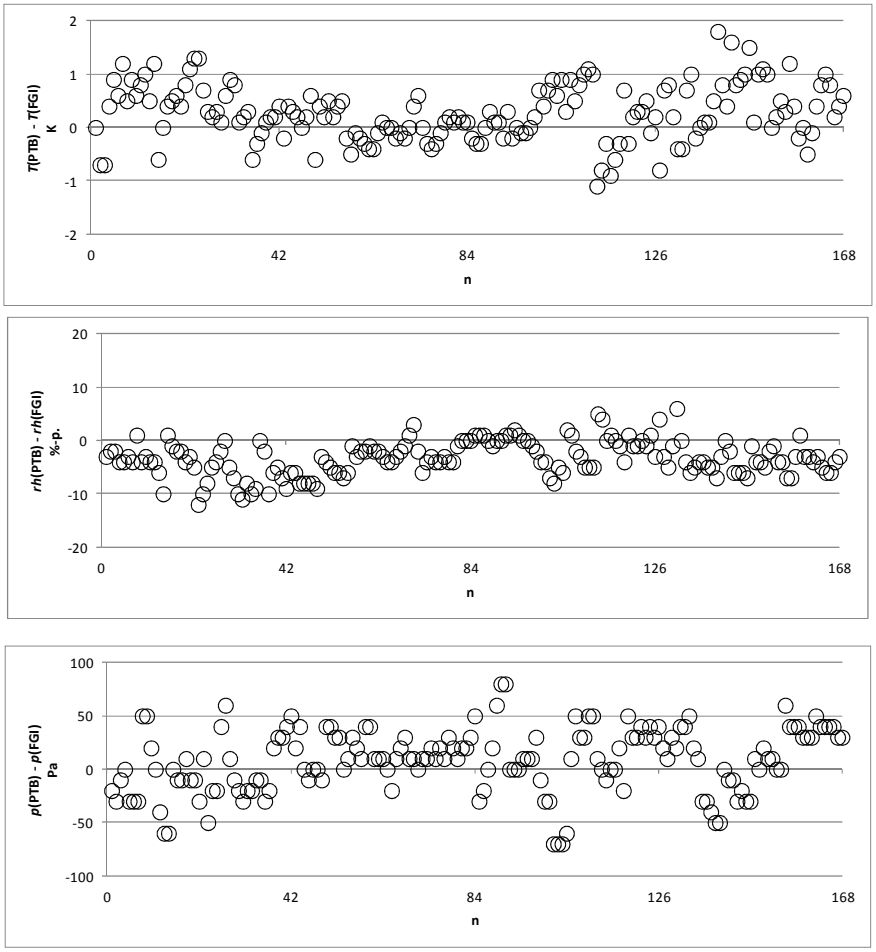

Figure 9.13 *Average temperature differences, relative humidity differences and air pressure differences during the 168 distance measurements at the PTB Geodetic Baseline on 6–10 June 2011.*

The PTB Geodetic Baseline, with its new environmental sensor system, is a good place for outdoor testing, validation and calibration of long-distance measurement instruments. In real field work, when laboratory-level equipment is not available, a few good-quality weather observation instruments with skilled observers are adequate for compiling reliable data for making velocity corrections. Since neither of the methods removes the difficulties caused by outdoor conditions, favourable weather conditions should be preferred when possible.

The impressive installation of weather data sensors prompted the FGI to make the decision to modernize its weather observation instruments. Tests with

the new Vaisala PTU307 weather station, which is specially equipped for field work use, and comparisons with the classical instruments were started in 2012.

9.5 UPV Geodetic Baseline and Test Field in Valencia, Spain

The calibration of the UPV Geodetic Baseline (Fig. 9.11) is another example of a recent successful scale transfer measurement. The sky was mostly clear during the five measurement days in Valencia. A constant wind from the nearby Mediterranean Sea kept the measurement conditions surprisingly favourable, and the variations in temperatures were smooth and within seven degrees (from 21°C to 28°C). Large sturdy sunshades protected the instruments sufficiently well.

For the six-pillar baseline, the observers measured four times from every pillar to every other pillar, altogether 120 distances. Adjustment computations resulted in experimental standard deviations of the mean ranging from 0.009 mm to 0.040 mm. Combining them with other uncertainty components in the traceability chain resulted in expanded uncertainties ranging from 0.20 mm to 0.33 mm for the distances between 28 m and 330 m. For the seventh pillar, only four distances between 67 m and 190 m were visible and thus measured, with expanded uncertainties ranging from 0.19 mm to 0.24 mm.

9.6 EDM comparisons at NMIJ and KRISS

The best advantage of the comparison done at the NMIJ was that the participants could familiarize themselves with completely different calibration facilities and methods. In Tsukuba, the impressive rail structure with laser interferometers and reflector conveyors and controlled measurement conditions create an excellent indoor environment for research on geodetic length metrology (Fig. 9.14). The arrangements allow for a much larger set of different distances to be measured, in contrast to the 15 different distances in Nummela.

When determining the scale correction, observation pillars at 99 m, 153 m and 206 m made it possible to measure and compare distances ranging from 6 m to 204 m with the distances measured using laser interferometers. As Table 9.3 shows, the calibration results obtained when using the different sections of the Tsukuba baseline were significantly different. The reason for this remains an unsolved mystery and would require further measurements and investigations. The average values of the scale corrections determined at the Nummela Standard Baseline before and after the comparison were (with experimental standard deviations) +1.46 mm/km ±0.09 mm/km for the DI2002 and +1.43 mm/km ±0.20 mm/km for the TC2003. For the latter instrument, compatibility with the results in Tsukuba is not what was expected.

Using the shortest (< 100 m) distances only, some tenths of millimetre differences naturally led to corrections of several mm/km. One conclusion is that the scale corrections made for short distances cannot be safely used to correct longer distances; the use of longer baselines is therefore justified.

.

Table 9.3 *Determination of scale correction (mm/km) at the Tsukuba baseline using different observation distances: measurements at intervals of 1.0714 m (1) from "99 m", distances between 6 m and 97 m (2) from "153 m", distances between 60 m and 151 m and (3) from "206 m", distances between 113 m and 204 m.*

Date, Year 2003	NMIJ TCA2003	FGI DI2002	FGI TC2003
July 15	(99) +1.97 ±0.55 (153) +2.62 ±0.34 (206) +1.94 ±0.37		
July 16		(99) +1.75 ±0.33 (153) +2.21 ±0.37 (206) +1.18 ±0.33	(99) +4.02 ±0.30 (153) +2.02 ±0.29 (206) +1.33 ±0.30
July 17	(99) +2.03 ±0.39	(99) +3.36 ±0.33 (153) +1.02 ±0.39 (206) +1.44 ±0.42	(99) +4.42 ±0.30 (153) +2.65 ±0.29 (206) +1.97 ±0.29
July 18		(99) +2.49 ±0.32 (153) +0.42 ±0.36 (206) +1.83 ±0.43	
July 22		(99) +1.30 ±0.43 (153) +1.38 ±0.36 (206) +1.05 ±0.30	(99) +4.75 ±0.29 (153) +1.99 ±0.26 (206) +2.13 ±0.26
July 23			(99) +4.82 ±0.32 (153) +2.60 ±0.27 (206) +1.47 ±0.24
Extreme values	+1.94 … +2.62	+0.42 … +3.36	+1.33 … +4.82

The main results of the APMP EDM comparison done at KRISS in Daejeon (Fig. 9.14) are summarized in Fig. 9.15 (Suh 2010). It shows the differences in the final values obtained from the five participants compared with the weighted average values obtained from all the participants. The weighting was based on standard uncertainties, which the participants reported for their methods. Results with small uncertainties from the laser comb distance meter (proportional component 0.33 µm/m) dominated in this determination of reference values, whereas the uncertainties obtained from the other participants were quite similar with each other (from 0.40 µm/m to 0.46 µm/m).

Statistical analyses (E_n values, Birge ratio test) confirmed the rather good consistency of the results. Without the more heavily weighted laser comb distance measurements, the average value would change, and the level of consistency between the FGI and CMS Mekometers and the NMIJ and KRISS tacheometers would be even better. The scale of the NMIJ tacheometer needed further checking. The FGI transferred the scale of the Nummela Standard Baseline, whereas the other participants used frequency calibration of EDM instruments. In addition, in a check with the KRISS rubidium frequency standard, the scale of the Finnish Mekometer proved to be equal at the level of 10^{-7}, as expected.

Figure 9.14 *EDM comparisons in Asia. Left: tacheometer reflector on a pillar and rail constructions at the NMIJ laboratory tunnel in Tsukuba, Japan. Right: Mekometer measurements on pillar "s" at the KRISS geodetic baseline in Daejeon, Republic of Korea. The seven monuments have the names and contain definitions for the seven SI base units.*

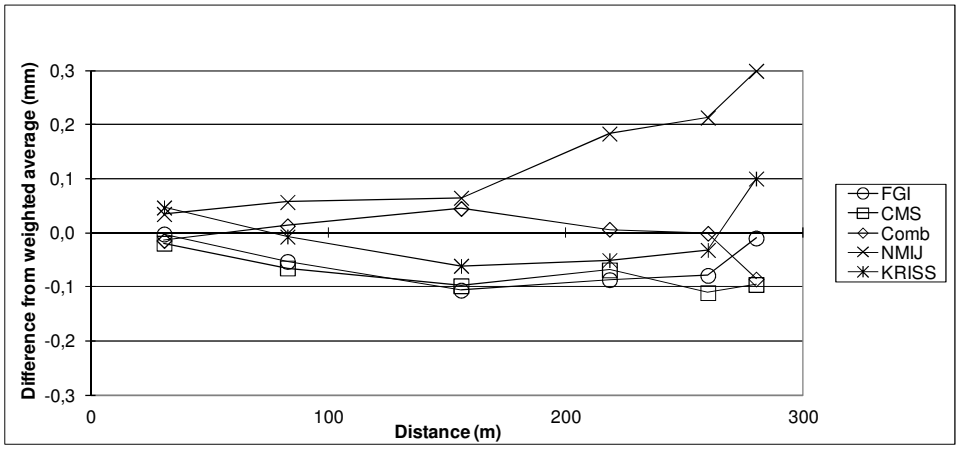

Figure 9.15 *Results from the five participants in the APMP EDM comparison, compared with the weighted average values, which were accepted as reference values. Picture: KRISS.*

Changing temperatures along the relatively cool last 20 m of the baseline may largely explain the variation at 280 m. Overall, the determination and compensation of temperature gradients remained a major source of uncertainty of measurement – a perpetual concern with EDM equipment used in field conditions. Dry and wet lawns, hot asphalt lanes and shaded sections along the baseline created challenging measurement conditions, in which all of the participants were still quite successful. The comparison was a successful beginning in a new field of geodetic metrology.

9.7 Contribution of the European Metrology Research Programme

The work done as part of the EMRP Joint Research Project "Absolute Long-distance Measurement in Air" at the Nummela Standard Baseline in autumn 2010 was rather successful. Both the CNAM and PTB could control the paths of the measurement beams of their different synthetic wavelength interferometry ADM equipments up to 864 m and back during the first tests done in moderate field conditions. MIKES tested improved spectroscopic methods for determining atmospheric refraction up to 72 m. Operational reliability still needs to be improved and uncertainty diminished. The large sizes of the installations also still hinder practical measurements. Overall, the results were encouraging. A new EMRP Joint Research Project, "Metrology for long distance surveying", is making it possible to continue the work until the year 2016.

9.8 Some applications in local geodynamics

At the Metsähovi fundamental geodetic station, control measurements between the observation sites have continued on an infrequent basis for the last four decades. The first measurements connected new instruments and observations for Doppler measurements to the existing national first-order triangulation network. Developing geodetic satellite positioning methods, SLR first and later GPS, created the need to connect new observation sites to the global networks of fundamental geodetic stations and modern international and national networks. Stability control of the observation sites is an essential reason for repeated measurements. The first measurement projects conducted at Metsähovi towards what nowadays is known as "local ties" are presented in a paper by Jokela et al. (2009b) and in preceding papers by Vermeer and Paunonen (1994) and Jokela (1997). The extensive renovation and new instruments (VLBI, SLR, GNSS and others) developed since 2011 requires the continuation and further development of control measurements. Common to such measurements, both then and now, is the use of calibrated (terrestrial) instruments with a metrologically traceable scale. GPS measurement networks around the observations sites and even the antennas installed in the instruments (VLBI) have been widely used in the latest experiments.

Repeated tacheometer measurements show that a 1-mm-level reproducibility with 1-mm-level uncertainties is achievable with our method, which is based on conventional terrestrial angle and distance measurements. This goes for both the horizontal and vertical position. Use of the best available instruments, exact definitions of the reference points that need to be observed, well-planned observation geometry, a sufficient number of observations, skilled observers and favourable weather conditions greatly contribute to a successful measurement result. Calibrated instruments bring metrological traceability and reliability to the measurements, albeit the calibration corrections done in small networks often are insignificant. To retain traceability even when processing the results, the use of mathematical adjusting methods must be considered with care. Comparisons of different measurement methods may produce interesting information about the accuracy of the GPS measurements compared with the "true" reference from the traceable terrestrial measurements. For a reliable scale determination of an entire network, the number of known traceable distances should be close to the number of GPS vectors in the network – a feature to be considered when developing our networks. A new test field for GNSS metrology is being built at Metsähovi in summer 2014.

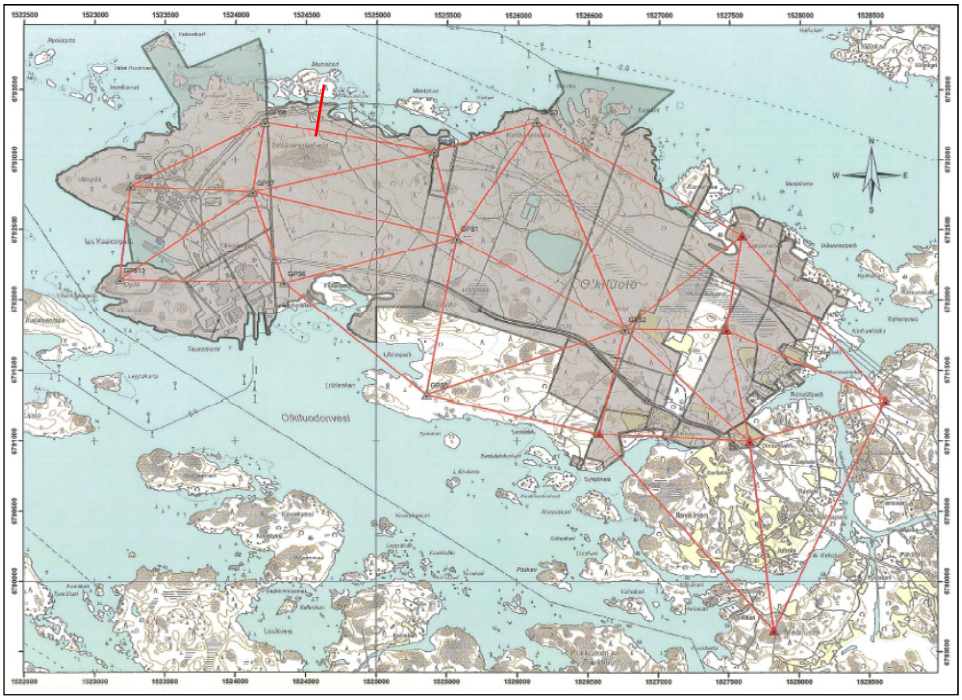

Figure 9.16 *A sketch of an extended deformation monitoring network at Olkiluoto. The 511-m geodetic baseline is in the oldest part, on the left. Picture: Posiva.*

In the original Olkiluoto deformation monitoring network, the length of only one vector in a small network (a few km^2) was monitored with both GPS and EDM equipment in the years 2002–2012. This example of a traceable scale transferred to a local geodynamical measurement is briefly discussed, together with the background, by Jokela et al. (2012a). The monitoring effort has recently ended due to new construction works, which will prevent further measurements. A way to process the accumulated data again using a uniform and somewhat improved method is currently under preparation, but it seems that it will just confirm the previous results. The project has repeatedly produced expected good EDM results, which slightly, but systematically, differ from the GPS results. The equal trend in both measurements confirms the sub-millimetre shortening of the vector over the years (Koivula et al. 2012b). Due to new construction works, causing new obstructions in visibility, monitoring is now being developed and will be continued in the future without EDM (Fig. 9.16).

Finally, the Metsähovi precise levelling test field (Lehmuskoski et al. 2006; not to be confused with the network for local ties) and two local geodynamical networks in Pasmajärvi (Takalo et al. 2004) are examples of other applications. The FGI has brought reliability and traceability to the site using calibrated high-precision instruments (tacheometers and levelling equipment) in repeated control measurements. Again, total uncertainties of less than 1 mm have been achieved there. Together with proper documentations, the measurements enable reasonable deformation analyses in the long term (during several decades or more), regardless of new measurement instruments and methods.

10 Concluding discussion

Recent research and developments relating to novel distance measurement instruments and efforts to improve the traceability of long distances have aroused interest in geodetic baselines once again. This publication describes in extensive detail the history and the present status of the Nummela Standard Baseline. Also, it discusses three other alternative standard baseline designs and how they were put into practice. The new interference measurements at Nummela in autumn 2013 have updated the traceable length data of the measurement standard that will be used in various measurement projects during the next few years. In addition to the conventional use of calibrations, these projects will again include scale transfer measurements using high-precision EDM equipment of several geodetic baselines and test fields and participation in international research and development efforts in geodetic metrology.

Reproduction of the Väisälä interference comparator using present-day techniques would be a fascinating undertaking. The light source could be moved and directed and the mirrors adjusted smoothly with motorized remote-controlled carriers. Reflecting beams could be tracked and interference fringes searched using digital image processing. An automated weather data recording system would replace the thermometer readers. Completely redesigned interfaces on observation pillars would adapt all of the necessary components in turn on the same bench: mirrors, EDM and ADM instruments, and reflectors, even projection measurement accessories, if still needed. In a measurement situation, necessary adjustments of instruments could be computed in real time and controlled electronically and mechanically, instead of the present tuning by eyes and hands.

Attempts to commercialize the Väisälä interference comparator were not successful half a century ago. Now it would undoubtedly be possible to reproduce the work of the comparator, but demands for such improvements are few and funding is a problem. Carrying out the necessary experiments would require an enclosed space with electric mains and communications. Outdoor problems due to weather conditions would remain; a sufficiently spacious and stable indoor environment would probably be impossible to find. The need to reproduce the work of the comparator also holds true for the image producing and processing system in the quartz gauge comparisons at Tuorla; there, only minor investments are required and a modernization is ongoing in 2013–2014.

Metrological experts nowadays rely increasingly upon laser techniques. A remarkable single improvement in the Väisälä interference comparator would be to replace the use of the quartz gauge in such a way that some of the shortest intervals could be traceably measured with an ADM instrument. Probably this would be reasonable only if the ADM instrument would be capable of handling such short distances, but not up to 1 km under field conditions. A safe conclusion at the moment is that the FGI will continue conducting measurements with the present version of the Väisälä interference method at the Nummela Standard Baseline as long as there is a need for them. Since it is still the most

accurate method and the most stable baseline in the world, the end is not on the horizon. Using the method at standard baselines other than Nummela is becoming increasingly unlikely both on the part of the FGI as well as other experts.

Uncertainty of measurement has remained similar during every standard baseline measurement. Expanded uncertainties ranging from 0.04 mm to 0.14 mm for baseline section lengths between 5 m and 864 m were obtained during the five interference measurement projects included in this publication (Chapters 4–7). Success in working with the quartz gauge and in performing the projection measurements determines much of the obtainable accuracy for the baseline. Without major improvements during these stages of the process, smaller uncertainty values are not probable for the coming measurements.

In the 11 scale transfer projects included in this publication (Chapters 5–6 and Sections 9.1–9.5), expanded uncertainties ranging from 0.1 mm to 1.2 mm for baseline section lengths between 2 m and 1 488 m were obtained. When a baseline is calibrated using scale transfer measurements with a single EDM instrument and without on-site interference observations, an expanded uncertainty of 0.5 mm/km (as in Vääna) is close to the best achievable result under favourable conditions. With a set of novel ADM instruments and methods (as in Munich, Heunecke 2012) or with on-site interference observations (as in Gödöllő), one can achieve an expanded uncertainty of 0.2 mm/km.

The reasons for the unwillingness to measure new baselines with the existing Väisälä interference comparator are obvious. A location's suitability for interference measurements is difficult to assess with the reconnaissance work done beforehand, and the measurements are extremely laborious even under favourable conditions. The stability of the baseline should be ensured with regular, high-precision monitoring for several years before the interference observations. Even the neighbourhood of a baseline should be ensured against disturbing factors, such as new construction work, for several decades. These prerequisites for stability and permanence unfortunately can rarely be fulfilled, and the risks of engaging in unsuccessful measurement efforts are increasing. The same risks hold true even for EDM and ADM instruments, but with smaller possible economical losses.

At the time of this publication in 2014, a new three-year joint research project, "Metrology for long distance surveying", is ongoing as part of the European Metrology Research Programme (EMRP). Nine European metrology institutes and three universities are participating in the project, with the FGI being one of them. The project was selected as part of the EMRP's call for "SI Broader Scope", one purpose of which is to make measurement excellence available outside of the traditional metrological community. New EDM and (long distance) ADM instruments and measurement methods will be developed, tested and validated under the subheading "Tracing the kilometre to the SI metre". The project includes comparisons of geodetic baselines using different measurement methods. Among a larger set of measurements, the FGI will

perform scale transfer measurements from the Nummela Standard Baseline to two German baselines in 2014, and the CNAM in France and the PTB in Germany will use their new ADM instruments to carry out measurements in Nummela in 2015. The different measurement methods will result in a traceable scale to several baselines based on different traceability chains, making it possible to examine similarity in scale. Other tasks in the new project include topical research for GNSS metrology and local tie measurements at fundamental stations for global geodesy and geodynamics. This will require improved monitoring networks with a traceable scale.

If the work for new ADM instruments leads to practicable results, as is expected, a shortening of the traceability chain and facilitation of the measurements will be most welcome. The need for geodetic baselines will remain, since well-kept, stable establishments at proper locations are still necessary for testing and maintenance of the instruments. Ensuring the operability of the new instruments in real field conditions, in addition to user-friendly baselines, is a major challenge. The influence of atmospheric phenomena along the measurement beam probably still needs to be researched more.

With the shortened traceability chain, the measurand may get its value, uncertainty and traceability in a more straightforward manner from the ADM instruments than it does now in the scale transfer with EDM. The price of the possible new commercial ADM instruments will determine if ordinary customers can afford them, or whether they will settle for less expensive choices, which may need regular calibrations at baselines just like before. Probably the new instruments will first be utilized by existing metrological services. There may also be quality problems ahead if various operators produce traceable distances without basic competence in metrology.

Whether or not the calibration of geodetic instruments is a profitable business will depend on the legislation passed by a particular country and on the policy of a particular institute. Operation of the National Standards Laboratories at the FGI is based on legislation; it is funded almost completely by the government and must not yield profits as a result of customer service. Since surveying operators have no obligations to calibrate their instruments, they often neglect to do so if not required by a quality management system. The small clientele in need of calibrations consists of, in addition to scientists, quality-aware experts, who need to show their competence. With the present resources, the situation at the FGI is satisfactory, and the numerous international contacts enhance its effectiveness in the special field of geodetic metrology.

For the next scale transfer projects, the FGI plans to for the most part use the same Kern Mekometer ME5000 transfer standard as before. Some planned activities include calibrating customers' transfer standards, a small set of precise EDM instruments or tacheometers and FGI's instruments that will be used for scale transfer. The projects include repeated calibrations, which will help maintain calibration services and quality at the customers' baselines and test

fields. Concerning permanence, the locations of most of the recently calibrated objects have been better selected than the locations of many standard baselines.

The possibility to test GNSS-based distance measurements at a traceable geodetic baseline is an advantage, which unfortunately few locations can provide at the moment. Separate test fields will need to be established for this burgeoning branch of length measurements. The FGI's Metsähovi will be one location for such tests.

The two planned scale transfer measurements to Germany will serve in a comparison of European baselines, that is, they will be a part of the EMRP's pioneering effort to trace the kilometre to the SI metre. One of the German baselines is particularly suitable for GNSS measurements. To obtain comparable results, consistent measurement practices and procedures are required; various experiences at different institutes will benefit this work when preparing an applicable measurement protocol. The comparison may also produce updates for the existing international standards, which guide field procedures when making calibrations.

In the coming comparison of baselines, the participants will need to pay attention to improved ways to determine air temperature, pressure and humidity for reducing the EDM and ADM observations. Observers may need more observation instruments or sensor systems for more observations along the measurement beam. All weather observation instruments need to be calibrated. In addition to a more abundant set of weather observations, they will produce data to calculate estimates of the horizontal and vertical gradients. Based on the FGI's experience, the work will not be easy: it is almost impossible to model unfavourable weather conditions, whereas modelling favourable weather conditions is rather insignificant for the results. Nonetheless, possible advantages will appear in the reduced uncertainty of measurement.

This work has shown that even a simple set of traditional weather observation instruments may produce good quality weather data when properly used. Regardless of the apparent accuracy in calibrations under laboratory conditions, many thermometers and weather stations have only a limited capability in changing outdoor conditions; the displayed values do not always reliably represent the prevailing temperatures along the observation beam at the moment of measurement. Computation formulas for how to determine the group refractive index based on weather observation data for the purposes of velocity correction may need some redefining, but differences from the present set of a few recommended formulas (e.g. IAG 2000; Ciddor 1996; Owens 1967) will be on the level of 10^{-7} at maximum.

The FGI's unique service for traceable scale transfer is based on the availability of the most stable standard baseline and the most precise EDM equipment as a transfer standard. The same constant set of reliable weather observation instruments is used in most measurements. Regular calibrations of the Nummela Standard Baseline with the Väisälä interference comparator, complemented with calibrations of the quartz gauges, keep the baseline in top

condition, and regular calibrations of the EDM equipment enable the reliable transfer of a traceable scale. Still, at the moment the Kern Mekometer ME5000 is the most precise EDM instrument for distances ranging from tens of metres to a few kilometres under field conditions. Several such instruments are still in operation in Europe, but maintaining the ageing instrument is difficult, since no repair service has been available for years. This fact keeps hopes alive for a new instrument to replace it; makes and models of the existing tacheometers are not the most appropriate for metrological applications. Capability of laser trackers is now considerable at short distances and improving. The FGI will keep up with developments and improve its metrological procedures when new innovations give cause for it.

References

Bell, B. (1992). ME5000 Operation. In Bell, B. (Ed.) The Use and Calibration of the Kern ME5000 Mekometer. Proceedings of the Workshop, Jun 18–19, 1992, Stanford Linear Accelerator Center, Stanford University, Stanford, California, USA, p. 9–16.

Bell, B. (ed., 1992a). The Use and Calibration of the Kern ME5000 Mekometer. Proceedings of the Workshop, Jun 18–19, 1992, Stanford Linear Accelerator Center, Stanford University, Stanford, California, USA.

BIPM (2008a). International vocabulary of metrology – Basic and general concepts and associated terms (VIM). *JCGM* **200:2008**. Joint Committee for Guides in Metrology. 90 p. http://www.bipm.org/

BIPM (2008b). Evaluation of measurement data – Guide to the expression of uncertainty in measurement (GUM). *JGCM* **100:2008**. Joint Committee for Guides in Metrology. 120 p. http://www.bipm.org/

Brunner, F. K. and J. M. Rüeger (1992). Theory of the local scale parameter method for EDM. *B. Géod.* **66:4**, 355–364.

Būga, A., J. Jokela and R. Putrimas (2008). Traceability, stability and use of the Kyviškės Calibration Baseline – the first 10 years. In Cygas, D. and K.D. Froehner (Eds.) The 7th International Conference Environmental Engineering, Selected Papers, Vol. 3, p. 1274–1280. Vilnius, Lithuania, May 22–23, 2008, http://www.vgtu.lt/upload/leid_konf/buga_et_al_traceability.pdf

Būga, A., R. Putrimas, D. Slikas and J. Jokela (2014). Kyviškės Calibration Baseline: measurements and improvements analysis. The 9th International Conference "Environmental Engineering", 22–23 May 2014, Vilnius, Lithuania, Selected papers. 5 p.
http://enviro.vgtu.lt

Ciddor, P. E. (1996). Refractive index of air: New equations for the visible and near infrared", *Appl. Opt.* **35:9**, 1566–1573.

Curtis, C. J. (1992). Calibration and use of the Mekometer ME5000 in the survey of the Channel tunnel. In Bell, B. (Ed.) The Use and Calibration of the Kern ME5000 Mekometer. Proceedings of the Workshop, Jun 18–19, 1992, Stanford Linear Accelerator Center, Stanford University, Stanford, California, USA, p. 67–82.

EMRP (2014). Internet page for the European Metrology Research Programme. Programme of EURAMET. Maintained at http://www.emrponline.eu/.

EMRP-SIB60 (2014). Internet page for the European Metrology Research Programme Joint Research Project SIB60 "Metrology for long distance surveying". Maintained at http://www.ptb.de/emrp/sib60-home.html.

Engelhard, E. (1959). Interferometrische Kalibrierung von Endmassstäben aus Quartz. *Z. Instrumentenkd.* **67,** 59–65.

Heunecke, O. (2012). Auswertung des Ringversuchs auf der neuen Kalibrierbasis der UniBW München zur Bestimmung der Sollstrecken. *Allgemeine Vermessungs-Nachrichten* **119**, 380–385.

Honkasalo, T. (1950). Measuring of the 864 m-long Nummela standard base line with the Väisälä light interference comparator and some investigations into invar wires. *Publ. Finn. Geod. Inst.* **37**. 88 p.

IAG (1951). Motions et Vœux adoptés. Comptes Rendus d'ensemble de la IX Assemblée Générale, Bruxelles, Août 1951. *B. Géod.* **22**, 469.

IAG (1955). Texte *in extenso* des Vœux et Résolutions adoptés. Comptes Rendus d'ensemble de la X Assemblée Générale, Rome, Septembre 1954. *B. Géod.* **35**, 96–97.

IAG (2000). IAG Resolution 3 adopted at the XXIIth General Assembly in Birmingham. *J. Geodesy* **74:1**, 66–67.

Ikonen, E. and K. Riski (1993). Gauge-block interferometer based on one stabilized laser and a white-light source. *Metrologia* **30,** 95–104.

İnai, C., İ. Şanlıoğlu and C. Ö. Yiğit (2008). Scaling of EDM calibration baselines by GPS and controlling of EDM parameters. *Survey Review* **40**, 309: 304–312.

ISO (2001). ISO 17123-3:2001 International Standard. Optics and optical instruments – Field procedures for testing geodetic and surveying instruments – Part 3: Theodolites.

ISO (2005). ISO/IEC 17025:2005 International Standard. General requirements for the competence of testing and calibration laboratories.

ISO (2008). ISO 9001:2008 International Standard. Quality management systems – Requirements.

ISO (2012a). ISO 17123-4:2012 International Standard. Optics and optical instruments – Field procedures for testing geodetic and surveying instruments – Part 4: Electro-optical distance meters (EDM measurements to reflectors).

ISO (2012b). ISO 17123-5:2012 International Standard. Optics and optical instruments – Field procedures for testing geodetic and surveying instruments – Part 5: Total stations.

Jokela, J. (1994). The 1993 adjustment of the Finnish First-Order Terrestrial Triangulation. *Publ. Finn. Geod. Inst.* **119**. 137 p.

Jokela, J. (1996). Interference measurements of the Chang Yang Standard Baseline in 1994. *Publ. Finn. Geod. Inst.* **121**. 32 p.

Jokela, J. (1997). Vectors connecting the geodetic points at Metsähovi and Sjökulla. In Brunner, F. K. (Ed.) Advances in Positioning and Reference Frames. *IAG Symposia* **118**, 131–136.

Jokela, J., A. Būga, R. Putrimas and V. Tulevičius (2002). Analysis of repeated calibration of Kyviškės baseline. *Geodezija ir kartografija* **XXVIII:4**, 125–130.

Jokela, J. and P. Häkli (2010). Interference measurements of the Nummela Standard Baseline in 2005 and 2007. *Publ. Finn. Geod. Inst.* **144**. 85 p.

Jokela, J., P. Häkli, J. Ahola, A. Būga and R. Putrimas (2009a). On traceability of long distances. Proceedings of the XIX IMEKO World Congress "Fundamental and Applied Metrology", September 6–11, 2009, Lisbon, Portugal, pp. 1882–1887.
http://www.imeko2009.it.pt/Papers/FP_100.pdf

Jokela, J., P. Häkli, R. Kugler, H. Skorpil, M. Matus and M. Poutanen (2010). Calibration of the BEV Geodetic Baseline. FIG Congress 2010 "Facing the Challenges – Building the Capacity", Sydney, Australia, April 11–16, 2010. 15 p.
http://www.fig.net/pub/fig2010/papers/ts05c/ts05c_jokela_hakli_et_al_3873.pdf

Jokela, J., P. Häkli, M. Poutanen, U. Kallio and J. Ahola (2012a). Improving length and scale traceability in local geodynamical measurements. In Kenyon, S., M. C. Pacino and U. Marti (Eds.) Proceedings of the 2009 IAG Symposium "Geodesy for Planet Earth", Buenos Aires, Argentina, August 31 – September 4, 2009. International Association of Geodesy Symposia **136**, 59–66.

Jokela, J., P. Häkli, J. Uusitalo, J. Piironen and M. Poutanen (2009b). Control Measurements between the Geodetic Observation Sites at Metsähovi. In Drewes,

H. (Ed.) Geodetic Reference Frames. IAG Symposium, Munich, Germany, October 9–14, 2006. International Association of Geodesy Symposia **134**, 101–106. Springer.

Jokela, J., P. Petroškevičius and V. Tulevičius (1999). Kyviškės Calibration Baseline. *Rep. Finn. Geod. Inst.* **99:3**. 15 p.

Jokela, J., F. Pollinger, N. R. Doloca and K. Meiners-Hagen (2012b). A comparison of two weather data acquisition methods for the calibration of the PTB geodetic baseline. Proceedings of the XX IMEKO World Congress "Metrology for Green Growth" (paper no. TC14-O-18), September 9–14, 2012, Busan, Republic of Korea.
http://www.imeko.org/publications/wc-2012/IMEKO-WC-2012-TC14-O18.pdf

Jokela, J. and M. Poutanen (1998). The Väisälä baselines in Finland. *Publ. Finn. Geod. Inst.* **127**. 61 p.

Jokela, J., M. Poutanen, Zs. Németh and G. Virág (2001). Remeasurement of the Gödöllő Standard Baseline. *Publ. Finn. Geod. Inst.* **131**. 37 p.

Jokela, J., M., Poutanen, J.Z. Zhao, W.L. Pei, Z.Y. Hu and S.S. Zhang (2000). The Chengdu Standard Baseline. *Publ. Finn. Geod. Inst.* **130**. 46 p.

Jordan, Eggert, Kneissl (1958). Handbuch der Vermessungskunde, Band IV. J.B. Metzlersche Verlagsbuchhandlung, Stuttgart, p. 482–501.

Kääriäinen, J. (1984). Baseline measurements with invar wires in Finland in 1958–1970. *Publ. Finn. Geod. Inst.* **100**. 74 p.

Kääriäinen, J., R. Konttinen and Zs. Németh (1988). The Gödöllő Standard Baseline. *Publ. Finn. Geod. Inst.* **109**. 66 p.

Kääriäinen, J., R. Konttinen, Q. Lu and Z.Y. Du (1986). The Chang Yang Standard Baseline. *Publ. Finn. Geod. Inst.* **105**. 36 p.

Kääriäinen, J., R. Konttinen and M. Poutanen (1992). Interference measurements of the Nummela Standard Baseline in 1997, 1983, 1984 and 1991. *Publ. Finn. Geod. Inst.* **114**. 78 p.

Kallio, U. and M. Poutanen (2012). Can we really promise a mm-accuracy for the local ties on a geo-VLBI antenna? In Kenyon, S., M. C. Pacino and U. Marti (Eds.) Proceedings of the 2009 IAG Symposium "Geodesy for Planet Earth", Buenos Aires, Argentina, August 31 – September 4, 2009. International Association of Geodesy Symposia **136**, 35–42.

Kallio, U. and M. Poutanen (2013). Local ties at fundamental stations. In Altamimi, Z. and X. Collilieux (Eds.) Reference Frames for Applications in Geosciences. International Association of Geodesy Symposia **138**, 147–152.

Kern (1986). Operating instructions Mekometer ME5000 Precision Distance Meter.

Kiviniemi, A. (1970). Niinisalo calibration baseline. *Publ. Finn. Geod. Inst.* **69**. 36 p.

Koivula, H., P. Häkli, J. Jokela, A. Būga and R. Putrimas (2012a). GPS metrology – Bringing traceable scale to local crustal deformation GPS network. In Kenyon, S., M. C. Pacino and U. Marti (Eds.) Proceedings of the 2009 IAG Symposium "Geodesy for Planet Earth", Buenos Aires, Argentina, August 31 – September 4, 2009. International Association of Geodesy Symposia **136**, 105–112.

Koivula, H., U. Kallio, S. Nyberg, J. Jokela and M. Poutanen (2012b). GPS operations at Olkiluoto in 2011. Posiva Working Report 2012-36. POSIVA Oy, Olkiluoto. 57 p. http://www.posiva.fi/en/databank/working_reports

Konttinen, R. (1981). Measurements in the Garm network, U.S.S.R., established for deformation studies of the Earth's surface, using the Kern Mekometer ME3000. In Kakkuri, J., A. Kiviniemi and R. Konttinen (Eds.) Contributions from the Finnish Geodetic Institute to the tectonic plate motion studies in the area between the Pamirs and Tien-Shan mountains. *Publ. Finn. Geod. Inst.* **81**, 17–34.

Konttinen, R. (1985). Plate motion studies in Central Asia. *Publ. Finn. Geod. Inst.* **101**. 31 p.

Konttinen, R. (1988). Baseline multiplication using the Kern Mekometer ME3000. *Rep. Finn. Geod. Inst.* **88:1**. 10 p.

Konttinen, R. (1994). Observation results. Geodimeter observations in 1971–72, 1974–80 and 1984–85. *Publ. Finn. Geod. Inst.* **117**. 58 p.

Konttinen, R., J. Jokela and Q. Li (1991). The remeasurement of the Chang Yang Standard Baseline. *Publ. Finn. Geod. Inst.* **113**. 40 p.

Kukkamäki, T. J. (1933). Untersuchungen über die Meterendmasse aus geschmolzenem Quartz nach lichinterferometrischen Methoden. Uuden Auran osakeyhtiön kirjapaino, Turku. 83 p.

Kukkamäki, T. J. (1969). Ohio Standard Baseline. *Ann. Acad. Sci. Fenn.* **Series A. III. 102.** 59 p.

Kukkamäki, T. J. (1978). Väisälä interference comparator. *Publ. Finn. Geod. Inst.* **87**. 49 p.

Lassila, A., J. Jokela, M. Poutanen and J. Xu (2003). Absolute calibration of quartz bars of Väisälä interferometer by white light gauge block interferometer. *Proc. XVII IMEKO World Congress,* June 22–27, 2003, Dubrovnik, Croatia, p. 1886–1890.

Lechner, J., L. Cervinka and I. Umnov (2008). Geodetic surveying tasks for establishing a national long length standard baseline. FIG Working Week, Stockholm, Sweden, June 14–19, 2008. 9 p.

Lehmuskoski, P., P. Rouhiainen, V. Saaranen, M. Takalo and H. Virtanen (2006). Seasonal Change of Bedrock Elevation at the Metsähovi Levelling Test Field. *Nordic Journal of Surveying and Real Estate Research,* **3:1**, 58–68.

Matsui, S. and H. Kimura (2008). Survey comparison using GNSS and ME5000 for one kilometer range. The 10th International Workshop on Accelerator Alignment, KEK, Tsukuba, Japan, February 11–15, 2008. 6 p.

Matsumoto, H., X. Wang and K. Takamasu (2012). Absolute measurement of base lines up to 400 m using temporal coherence heterodyne interferometer of optical frequency comb. Proceedings of the XX IMEKO World Congress "Metrology for Green Growth" (paper no. TC14-O-12), September 9–14, 2012, Busan, Republic of Korea.
http://www.nanolab.t.u-tokyo.ac.jp/pdffiles/2012-3I05.pdf

Meier, D. and R. Loser (1986). Das Mekometer ME 5000 – Ein neuer Präzisionsdistanzmesser. *Allgemeine Vermessungs-Nachrichten* **93**, 182–190.

MIKES (2000). Certificates of Calibration, no. M-L 74, M-L 75, M-L 76, M-L 78.

Minoshima, K. and H. Matsumoto (2000). High-accuracy measurement of 240-m distance in an optical tunnel by use of a compact femtosecond laser. *Appl. Opt.* **39:30**, 5512–5517.

Neumann, I. (2012). Messunsicherheit bei elektrooptisch bestimmten Strecken. *Allgemeine Vermessungs-Nachrichten* **119**, 369–379.

Niemi, A. (2001). Metrin vertaus. Manuscript for a manual for comparisons of quartz metres at Tuorla.

Niemi, A. (2005). Metrikomparaattorin käyttö. Manuscript for a manual for the comparator of quartz metres at Tuorla.

Owens, J. C. (1967). Optical refractive index of air: dependence on pressure, temperature and composition. *Appl. Opt.* **6**, 51–59.

Parm, T. (1976). High precision traverse of Finland. *Publ. Finn. Geod. Inst.* **79**. 108 p.

Parm, T. (ed., 1980). Proceedings of the IAG-Symposium "High precision geodetic length measurements", June 19–22, 1978, Helsinki, Finland. *Rep. Finn. Geod. Inst.* **80:1**. 364 p.

Pollinger, F., T. Meyer, J. Beyer, N. R. Doloca, W. Schellin, W. Niemeier, J. Jokela, P. Häkli, A. Abou-Zeid and K. Meiners-Hagen (2012). The upgraded PTB 600 m baseline: a high-accuracy reference for the calibration and the development of long distance measurement devices. *Meas. Sci. Tech.* **23** (2012) 094018, 11 p. doi:10.1088/0957-0233/23/9/094018.
http://stacks.iop.org/MST/23/094018

Poutanen, M. (ed., 1995). Interference measurements of the Taoyuan Standard Baseline. *Publ. Finn. Geod. Inst.* **120**. 35 p.

PTB (1996). Calibration certificate, Ref. No. 4.31-23912/95.

Rüeger, J. M. (1996). Electronic Distance Measurement. 4th ed. 276 p. Springer.

Saaranen, V., P. Rouhiainen and H. Suurmäki (2014). Monitoring bedrock deformation in Olkiluoto using precise leveling data. Paper in prep., pres. at the 2nd Joint International Symposium on Deformation Monitoring (JISDM), September 9–11, 2013, Nottingham, UK.

Suh, H. (2010). Asia-Pacific Metrology Programme Pilot Study, Calibration of Electro-optical Distance Meter, Comparison Results. Manuscript 2010-08-13. KRISS.

Takalo, M., P. Rouhiainen, J. Jokela, H. Ruotsalainen, J. Ahola and H. Suurmäki (2004). Geodetic measurements at the Pasmajärvi and Nuottavaara faults. *Rep. Finn. Geod. Inst.* **2004:1**. 44 p.

Väisälä, Y. (1923). Die Anwendung der Lichtinterferenz zu Längenmessungen auf grösseren Distanzen. *Publ. Finn. Geod. Inst.* **2**. 47 p.

Väisälä, Y. (1930). Anwendung der Lichtinterferenz bei Basismessungen. *Publ. Finn. Geod. Inst.* **14**. 22 p.

Väisälä, Y. (1956). Zur Theorie der Kompensatoren. *Annales Universitatis Turkuensis* A I 24.

Väisälä, Y. and L. Oterma (1967). System of quartzmetres and the absolute length of its gauges. *Metrologia*, **3:2**, 37–41.

Vermeer, M. and M. Paunonen (1994). The vector connecting the fundamental points Metsähovi and Sjökulla. In Gubler, E. and H. Hornik (Eds.) Report on the Symposium of the IAG Subcommission for the European Reference Frame (EUREF) held in Warsaw 8–11 June 1994. *Veröff. Bayer. Komm. Int. Erdmess.* **54**, 210–215.

Whitten, C. A. and E. Schmidt (ed., 1960). International Symposium on Electronic Distance Measurement Techniques. *J. Geophys. Res.* **65:2**, 385–528.

Suomen Geodeettisen laitoksen julkaisut:
Veröffentlichungen des Finnischen Geodätischen Institutes:
Publications of the Finnish Geodetic Institute:

1. Y. VÄISÄLÄ: Tafeln für geodätische Berechnungen nach den Erddimensionen von Hayford. Helsinki 1923. 30 S.
2. Y. VÄISÄLÄ: Die Anwendung der Lichtinterferenz zu Längenmessungen auf grösseren Distanzen. Helsinki 1923. 22 S.
3. ILMARI BONSDORFF, Y. LEINBERG, W. HEISKANEN: Die Beobachtungsergebnisse der südfinnischen Triangulation in den Jahren 1920-1923. Helsinki 1924. 235 S.
4. W. HEISKANEN: Untersuchungen über Schwerkraft und Isostasie. Helsinki 1924. 96 S. 1 Karte.
5. W. HEISKANEN: Schwerkraft und isostatische Kompensation in Norwegen. Helsinki 1926. 33 S. 1 Karte.
6. W. HEISKANEN: Die Erddimensionen nach den europäischen Gradmessungen. Helsinki 1926. 26 S.
7. ILMARI BONSDORFF, V.R. ÖLANDER, Y. LEINBERG: Die Beobachtungsergebnisse der südfinnischen Triangulation in den Jahren 1924-1926. Helsinki 1927. 164 S. 1 Karte.
8. V.R. ÖLANDER: Ausgleichung einer Dreieckskette mit Laplaceschen Punkten. Helsinki 1927. 49 S. 1 Karte.
9. U. PESONEN: Relative Bestimmungen der Schwerkraft auf den Dreieckspunkten der südfinnischen Triangulation in den Jahren 1924-1925. Helsinki 1927. 129 S.
10. ILMARI BONSDORFF: Das Theorem von Clairaut und die Massenverteilung im Erdinnern. Helsinki 1929. 10 S.
11. ILMARI BONSDORFF, V.R. ÖLANDER, W. HEISKANEN, U. PESONEN: Die Beobachtungsergebnisse der Triangulationen in den Jahren 1926-1928. Helsinki 1929. 139 S. 1 Karte.
12. W. HEISKANEN: Über die Elliptizität des Erdäquators. Helsinki 1929. 18 S.
13. U. PESONEN: Relative Bestimmungen der Schwerkraft in Finnland in den Jahren 1926-1929. Helsinki 1930. 168 S. 1 Karte.
14. Y. VÄISÄLÄ: Anwendung der Lichtinterferenz bei Basismessungen. Helsinki 1930. 47 S.
15. M. FRANSSILA: Der Einfluss der den Pendel umgebenden Luft auf die Schwingungszeit beim v. Sterneckschen Pendelapparat. Helsinki 1931. 23 S.
16. Y. LEINBERG: Ergebnisse der astronomischen Ortsbestimmungen auf den finnischen Dreieckspunkten. Helsinki 1931. 162 S.
17. V.R. ÖLANDER: Über die Beziehung zwischen Lotabweichungen und Schwereanomalien sowie über das Lotabweichungssystem in Süd-Finnland. Helsinki 1931. 23 S.
18. PENTTI KALAJA, UUNO PESONEN, V.R. ÖLANDER, Y. LEINBERG: Beobachtungsergebnisse. Helsinki 1933. 240 S. 1 Karte.
19. R.A. HIRVONEN: The continental undulations of the geoid. Helsinki 1934. 89 pages. 1 map.
20. ILMARI BONSDORFF: Die Länge der Versuchsbasis von Helsinki und Längenveränderungen der Invardrähte 634-637. Helsinki 1934. 41 S.
21. V.R. ÖLANDER: Zwei Ausgleichungen des grossen südfinnischen Dreieckskranzes. Helsinki 1935. 66 S. 1 Karte.
22. U. PESONEN, V.R. ÖLANDER: Beobachtungsergebnisse. Winkelmessungen in den Jahren 1932-1935. Helsinki 1936. 148 S. 1 Karte.
23. R.A. HIRVONEN: Relative Bestimmungen der Schwerkraft in Finnland in den Jahren 1931, 1933 und 1935. Helsinki 1937. 151 S.
24. R.A. HIRVONEN: Bestimmung des Schwereunterschiedes Helsinki-Potsdam im Jahre 1935 und Katalog der finnischen Schwerestationen. Helsinki 1937. 36 S. 1 Karte.
25. T.J. KUKKAMÄKI: Über die nivellitische Refraktion. Helsinki 1938. 48 S.
26. Finnisches Geodätisches Institut 1918-1938. Helsinki 1939. 126 S. 2 Karten.
27. T.J. KUKKAMÄKI: Formeln und Tabellen zur Berechnung der nivellitischen Refraktion. Helsinki 1939. 18 S.
28. T.J. KUKKAMÄKI: Verbesserung der horizontalen Winkelmessungen wegen der Seitenrefraktion. Helsinki 1939. 18 S.
29. ILMARI BONSDORFF: Ergebnisse der astronomischen Ortsbestimmungen im Jahre 1933. Helsinki 1939. 47 S.
30. T. HONKASALO: Relative Bestimmungen der Schwerkraft in Finnland im Jahre 1937. Helsinki 1941. 78 S.
31. PENTTI KALAJA: Die Grundlinienmessungen des Geodätischen Institutes in den Jahren 1933-1939 nebst Untersuchungen über die Verwendung der Invardrähte. Helsinki 1942. 149 S.
32. U. PESONEN, V.R. ÖLANDER: Beobachtungsergebnisse. Winkelmessungen in den Jahren 1936-1940. Helsinki 1942. 165 S. 1 Karte.
33. PENTTI KALAJA: Astronomische Ortsbestimmungen in den Jahren 1935-1938. Helsinki 1944. 142 S.
34. V.R. ÖLANDER: Astronomische Azimutbestimmungen auf den Dreieckspunkten in den Jahren 1932-1938; Lotabweichungen und Geoidhöhen. Helsinki 1944. 107 S. 1 Karte.
35. U. PESONEN: Beobachtungsergebnisse. Winkelmessungen in den Jahren 1940-1947. Helsinki 1948. 165 S. 1 Karte.
36. Professori Ilmari Bonsdorffille hänen 70-vuotispäivänään omistettu juhlajulkaisu. Publication dedicated to Ilmari Bonsdorff on the occasion of his 70th anniversary. Helsinki 1949. 262 pages. 13 maps.
37. TAUNO HONKASALO: Measuring of the 864 m-long Nummela standard base line with the Väisälä light interference comparator and some investigations into invar wires. Helsinki 1950. 88 pages.
38. V.R. ÖLANDER: On the geoid in the Baltic area and the orientation of the Baltic Ring. Helsinki 1950. 26 pages.
39. W. HEISKANEN: On the world geodetic system. Helsinki 1951. 25 pages.
40. R.A. HIRVONEN: The motions of Moon and Sun at the solar eclipse of 1947 May 20th. Helsinki 1951. 36 pages.
41. PENTTI KALAJA: Catalogue of star pairs for northern latitudes from 55° to 70°for astronomic determination of latitudes by the Horrebow-Talcott method. Helsinki 1952. 191 pages.
42. ERKKI KÄÄRIÄINEN: On the recent uplift of the Earth's crust in Finland. Helsinki 1953. 106 pages. 1 map.
43. PENTTI KALAJA: Astronomische Ortsbestimmungen in den Jahren 1946-1948. Helsinki 1953. 146 S.
44. T.J. KUKKAMÄKI, R.A. HIRVONEN: The Finnish solar eclipse expeditions to the Gold Coast and Brazil 1947. Helsinki 1954. 71 pages.
45. JORMA KORHONEN: Einige Untersuchungen über die Einwirkung der Abrundungsfehler bei Gross-Ausgleichungen. Neu-Ausgleichung des südfinnischen Dreieckskranzes. Helsinki 1954. 138 S. 3 Karten.

46. Professori Weikko A. Heiskaselle hänen 60-vuotispäivänään omistettu juhlajulkaisu. Publication dedicated to Weikko A. Heiskanen on the occasion of his 60th anniversary. Helsinki 1955. 214 pages.
47. Y. VÄISÄLÄ: Bemerkungen zur Methode der Basismessung mit Hilfe der Lichtinterferenz. Helsinki 1955. 12 S.
48. U. PESONEN, TAUNO HONKASALO: Beobachtungsergebnisse der finnischen Triangulationen in den Jahren 1947-1952. Helsinki 1957. 91 S.
49. PENTTI KALAJA: Die Zeiten von Sonnenschein, Dämmerung und Dunkelheit in verschiedenen Breiten. Helsinki 1958. 63 S.
50. V.R. ÖLANDER: Astronomische Azimutbestimmungen auf den Dreieckspunkten in den Jahren 1938-1952. Helsinki 1958. 90 S. 1 Karte.
51. JORMA KORHONEN, V.R. ÖLANDER, ERKKI HYTÖNEN: The results of the base extension nets of the Finnish primary triangulation. Helsinki 1959. 57 pages. 5 appendices. 1 map.
52. V.R. ÖLANDER: Vergleichende Azimutbeobachtungen mit vier Instrumenten. Helsinki 1960. 48 pages.
53. Y. VÄISÄLÄ, L. OTERMA: Anwendung der astronomischen Triangulationsmethode. Helsinki 1960. 18 S.
54. V.R. ÖLANDER: Astronomical azimuth determinations on trigonometrical stations in the years 1955-1959. Helsinki 1961. 15 pages.
55. TAUNO HONKASALO: Gravity survey of Finland in years 1945-1960. Helsinki 1962. 35 pages. 3 maps.
56. ERKKI HYTÖNEN: Beobachtungsergebnisse der finnischen Triangulationen in den Jahren 1953-1962. Helsinki 1963. 59 S.
57. ERKKI KÄÄRIÄINEN: Suomen toisen tarkkavaaituksen kiintopisteluettelo I. Bench mark list I of the Second Levelling of Finland. Helsinki 1963. 164 pages. 2 maps.
58. ERKKI HYTÖNEN: Beobachtungsergebnisse der finnischen Triangulationen in den Jahren 1961-1962. Helsinki 1963. 32 S.
59. AIMO KIVINIEMI: The first order gravity net of Finland. Helsinki 1964. 45 pages.
60. V.R. ÖLANDER: General list of astronomical azimuths observed in 1920-1959 in the primary triangulation net. Helsinki 1965. 47 pages. 1 map.
61. ERKKI KÄÄRIÄINEN: The second levelling of Finland in 1935-1955. Helsinki 1966. 313 pages. 1 map.
62. JORMA KORHONEN: Horizontal angles in the first order triangulation of Finland in 1920-1962. Helsinki 1966. 112 pages. 1 map.
63. ERKKI HYTÖNEN: Measuring of the refraction in the Second Levelling of Finland. Helsinki 1967. 18 pages.
64. JORMA KORHONEN: Coordinates of the stations in the first order triangulation of Finland. Helsinki 1967. 42 pages. 1 map.
65. Geodeettinen laitos - The Finnish Geodetic Institute 1918-1968. Helsinki 1969. 147 pages. 4 maps.
66. JUHANI KAKKURI: Errors in the reduction of photographic plates for the stellar triangulation. Helsinki 1969. 14 pages.
67. PENTTI KALAJA, V.R. ÖLANDER: Astronomical determinations of latitude and longitude in 1949-1958. Helsinki 1970. 242 pages. 1 map.
68. ERKKI KÄÄRIÄINEN: Astronomical determinations of latitude and longitude in 1954-1960. Helsinki 1970. 95 pages. 1 map.
69. AIMO KIVINIEMI: Niinisalo calibration base line. Helsinki 1970. 36 pages. 1 sketch appendix.
70. TEUVO PARM: Zero-corrections for tellurometers of the Finnish Geodetic Institute. Helsinki 1970. 18 pages.
71. ERKKI KÄÄRIÄINEN: Astronomical determinations of latitude and longitude in 1961-1966. Helsinki 1971. 102 pages. 1 map.
72. JUHANI KAKKURI: Plate reduction for the stellar triangulation. Helsinki 1971. 38 pages.
73. V.R. ÖLANDER: Reduction of astronomical latitudes and longitudes 1922-1948 into FK4 and CIO systems. Helsinki 1972. 40 pages.
74. JUHANI KAKKURI AND KALEVI KALLIOMÄKI: Photoelectric time micrometer. Helsinki 1972. 53 pages.
75. ERKKI HYTÖNEN: Absolute gravity measurement with long wire pendulum. Helsinki 1972. 142 pages.
76. JUHANI KAKKURI: Stellar triangulation with balloon-borne beacons. Helsinki 1973. 48 pages.
77. JUSSI KÄÄRIÄINEN: Beobachtungsergebnisse der finnischen Winkelmessungen in den Jahren 1969-70. Helsinki 1974. 40 S.
78. AIMO KIVINIEMI: High precision measurements for studying the secular variation in gravity in Finland. Helsinki 1974. 64 pages.
79. TEUVO PARM: High precision traverse of Finland. Helsinki 1976. 64 pages.
80. R.A. HIRVONEN: Precise computation of the precession. Helsinki 1976. 25 pages.
81. MATTI OLLIKAINEN: Astronomical determinations of latitude and longitude in 1972-1975. Helsinki 1977. 90 pages. 1 map.
82. JUHANI KAKKURI AND JUSSI KÄÄRIÄINEN: The Second Levelling of Finland for the Aland archipelago. Helsinki 1977. 55 pages.
83. MIKKO TAKALO: Suomen Toisen tarkkavaaituksen kiintopisteluettelo II. Bench mark list II of the Second Levelling of Finland. Helsinki 1977. 150 sivua.
84. MATTI OLLIKAINEN: Astronomical azimuth determinations on triangulation stations in 1962-1970. Helsinki 1977. 47 pages. 1 map.
85. MARKKU HEIKKINEN: On the tide-generating forces. Helsinki 1978. 150 pages.
86. PEKKA LEHMUSKOSKI AND JAAKKO MÄKINEN: Gravity measurements on the ice of Bothnian Bay. Helsinki 1978. 27 pages.
87. T.J. KUKKAMÄKI: Väisälä interference comparator. Helsinki 1978. 49 pages.
88. JUSSI KÄÄRIÄINEN: Observing the Earth Tides with a long water-tube tiltmeter. Helsinki 1979. 74 pages.
89. Publication dedicated to T.J. Kukkamäki on the occasion of his 70th anniversary. Helsinki 1979. 184 pages.
90. B. DUCARME AND J. KÄÄRIÄINEN: The Finnish Tidal Gravity Registrations in Fennoscandia. Helsinki 1980. 43 pages.
91. AIMO KIVINIEMI: Gravity measurements in 1961-1978 and the results of the gravity survey of Finland in 1945-1978. Helsinki 1980. 18 pages. 3 maps.
92. LIISI OTERMA: Programme de latitude du tube zénithal visuel de l'observatoire Turku-Tuorla systéme amélioré de 1976. Helsinki 1981. 18 pages.
93. JUHANI KAKKURI, AIMO KIVINIEMI AND RAIMO KONTTINEN: Contributions from the Finnish Geodetic Institute to the Tectonic Plate Motion Studies in the Area between the Pamirs and Tien-Shan Mountains. Helsinki 1981. 34 pages.
94. JUSSI KÄÄRIÄINEN: Measurement of the Ekeberg baseline with invar wires. Helsinki 1981. 17 pages.
95. MATTI OLLIKAINEN: Astronomical determinations of latitude and longitude in 1976-1980. Helsinki 1982. 90 pages. 1 map.
96. RAIMO KONTTINEN: Observation results. Angle measurements in 1977-1978. Helsinki 1982. 29 pages.

97. G.P. ARNAUTOV, YE N. KALISH, A. KIVINIEMI, YU F. STUS, V.G. TARASIUK, S.N. SCHEGLOV: Determination of absolute gravity values in Finland using laser ballistic gravimeter. Helsinki 1982. 18 pages.
98. LEENA MIKKOLA (EDITOR): Mean height map of Finland. Helsinki 1983. 3 pages. 1 map.
99. MIKKO TAKALO AND JAAKKO MÄKINEN: The Second Levelling of Finland for Lapland. Helsinki 1983. 144 pages.
100. JUSSI KÄÄRIÄINEN: Baseline Measurements with invar wires in Finland 1958-1970. Helsinki 1984. 78 pages.
101. RAIMO KONTTINEN: Plate motion studies in Central Asia. Helsinki 1985. 31 pages.
102. RAIMO KONTTINEN: Observation results. Angle measurements in 1979-1983. Helsinki 1985. 30 pages.
103. J. KAKKURI, T.J. KUKKAMÄKI, J.-J. LEVALLOIS ET H. MORITZ: Le 250^{e} anniversaire de la mesure de l'arc du meridien en Laponie. Helsinki 1986. 60 pages.
104. G. ASCH, T. JAHR, G. JENTZSCH, A. KIVINIEMI AND J. KÄÄRIÄINEN: Measurements of Gravity Tides along the "Blue Road Geotraverse" in Fennoscandia. Helsinki 1987. 57 pages.
105. JUSSI KÄÄRIÄINEN, RAIMO KONTTINEN, LU QIANKUN AND DU ZONG YU: The Chang Yang Standard Baseline. Helsinki 1986. 36 pages.
106. E.W. GRAFAREND, H. KREMERS, J. KAKKURI AND M. VERMEER: Adjusting the SW Finland Triangular Network with the TAGNET 3-D operational geodesy software. Helsinki 1987. 60 pages.
107. MATTI OLLIKAINEN: Astronomical determinations of latitude and longitude in 1981-1983. Helsinki 1988. 37 pages.
108. MARKKU POUTANEN: Observation results. Angle measurements in 1967-1973. Helsinki 1988. 35 pages.
109. JUSSI KÄÄRIÄINEN, RAIMO KONTTINEN AND ZSUZSANNA NÉMETH: The Gödöllö Standard Baseline. Helsinki 1988. 66 pages.
110. JUSSI KÄÄRIÄINEN AND HANNU RUOTSALAINEN: Tilt measurements in the underground laboratory Lohja 2, Finland, in 1977-1987. Helsinki 1989. 37 pages.
111. MIKKO TAKALO: Lisäyksiä ja korjauksia Suomen tarkkavaaitusten linjastoon 1977-1989. Helsinki 1991. 98 sivua.
112. RAIMO KONTTINEN: Observation results. Angle measurements in the Pudasjärvi loop in 1973-1976. Helsinki 1991. 42 pages.
113. RAIMO KONTTINEN, JORMA JOKELA AND LI QUAN: The remeasurement of the Chang Yang Standard Baseline. Helsinki 1991. 40 pages.
114. JUSSI KÄÄRIÄINEN, RAIMO KONTTINEN AND MARKKU POUTANEN: Interference measurements of the Nummela Standard Baseline in 1977, 1983, 1984 and 1991. Helsinki 1992. 78 pages.
115. JUHANI KAKKURI (EDITOR): Geodesy and geophysics. Helsinki 1993. 200 pages.
116. JAAKKO MÄKINEN, HEIKKI VIRTANEN, QIU QI-XIAN AND GU LIANG-RONG: The Sino-Finnish absolute gravity campaign in 1990. Helsinki 1993. 49 pages.
117. RAIMO KONTTINEN: Observation results. Geodimeter observations in 1971-72, 1974-80 and 1984-85. Helsinki 1994. 58 pages.
118. RAIMO KONTTINEN: Observation results. Angle measurements in 1964-65, 1971, 1984 and 1986-87. Helsinki 1994. 67 pages.
119. JORMA JOKELA: The 1993 adjustment of the Finnish First-Order Terrestrial Triangulation. Helsinki 1994. 137 pages.
120. MARKKU POUTANEN (EDITOR): Interference measurements of the Taoyuan Standard Baseline. Helsinki 1995. 35 pages.
121. JORMA JOKELA: Interference measurements of the Chang Yang Standard Baseline in 1994. Kirkkonummi 1996. 32 pages.
122. OLLI JAAKKOLA: Quality and automatic generalization of land cover data. Kirkkonummi 1996. 39 pages.
123. MATTI OLLIKAINEN: Determination of orthometric heights using GPS levelling. Kirkkonummi 1997. 143 pages.
124. TIINA KILPELÄINEN: Multiple Representation and Generalization of Geo-Databases for Topographic Maps. Kirkkonummi 1997. 229 pages.
125. JUSSI KÄÄRIÄINEN AND JAAKKO MÄKINEN: The 1979-1996 gravity survey and the results of the gravity survey of Finland 1945-1996. Kirkkonummi 1997. 24 pages. 1 map.
126. ZHITONG WANG: Geoid and crustal structure in Fennoscandia. Kirkkonummi 1998. 118 pages.
127. JORMA JOKELA AND MARKKU POUTANEN: The Väisälä baselines in Finland. Kirkkonummi 1998. 61 pages.
128. MARKKU POUTANEN: Sea surface topography and vertical datums using space geodetic techniques. Kirkkonummi 2000. 158 pages
129. MATTI OLLIKAINEN, HANNU KOIVULA AND MARKKU POUTANEN: The Densification of the EUREF Network in Finland. Kirkkonummi 2000. 61 pages.
130. JORMA JOKELA, MARKKU POUTANEN, ZHAO JINGZHAN, PEI WEILI, HU ZHENYUAN AND ZHANG SHENGSHU: The Chengdu Standard Baseline. Kirkkonummi 2000. 46 pages.
131. JORMA JOKELA, MARKKU POUTANEN, ZSUZSANNA NÉMETH AND GÁBOR VIRÁG: Remeasurement of the Gödöllö Standard Baseline. Kirkkonummi 2001. 37 pages.
132. ANDRES RÜDJA: Geodetic Datums, Reference Systems and Geodetic Networks in Estonia. Kirkkonummi 2004. 311 pages.
133. HEIKKI VIRTANEN: Studies of Earth Dynamics with the Superconducting Gravimeter. Kirkkonummi 2006. 130 pages.
134. JUHA OKSANEN: Digital elevation model error in terrain analysis. Kirkkonummi 2006. 142 pages. 2 maps.
135. MATTI OLLIKAINEN: The EUVN-DA GPS campaign in Finland. Kirkkonummi 2006. 42 pages.
136. ANNU-MAARIA NIVALA: Usability perspectives for the design of interactive maps. Kirkkonummi 2007. 157 pages.
137. XIAOWEI YU: Methods and techniques for forest change detection and growth estimation using airborne laser scanning data. Kirkkonummi 2007. 132 pages.
138. LASSI LEHTO: Real-time content transformations in a WEB service-based delivery architecture for geographic information. Kirkkonummi 2007. 150 pages.
139. PEKKA LEHMUSKOSKI, VEIKKO SAARANEN, MIKKO TAKALO AND PAAVO ROUHIAINEN: Suomen Kolmannen tarkkavaaituksen kiintopisteluettelo. Bench Mark List of the Third Levelling of Finland. Kirkkonummi 2008. 220 pages.
140. EIJA HONKAVAARA: Calibrating digital photogrammetric airborne imaging systems using a test field. Kirkkonummi 2008. 139 pages.
141. MARKKU POUTANEN, EERO AHOKAS, YUWEI CHEN, JUHA OKSANEN, MARITA PORTIN, SARI RUUHELA, HELI SUURMÄKI (EDITORS): Geodeettinen laitos – Geodetiska Institutet – Finnish Geodetic Institute 1918–2008. Kirkkonummi 2008. 173 pages.

142. MIKA KARJALAINEN: Multidimensional SAR Satellite Images – a Mapping Perspective. Kirkkonummi 2010. 132 pages.
143. MAARIA NORDMAN: Improving GPS time series for geodynamic studies. Kirkkonummi 2010. 116 pages.
144. JORMA JOKELA AND PASI HÄKLI: Interference measurements of the Nummela Standard Baseline in 2005 and 2007. Kirkkonummi 2010. 85 pages.
145. EETU PUTTONEN: Tree Species Classification with Multiple Source Remote Sensing Data. Kirkkonummi 2012. 162 pages.
146. JUHA SUOMALAINEN: Empirical Studies on Multiangular, Hyperspectral, and Polarimetric Reflectance of Natural Surfaces. Kirkkonummi 2012. 144 pages.
147. LEENA MATIKAINEN: Object-based interpretation methods for mapping built-up areas. Kirkkonummi 2012. 210 pages.
148. LAURI MARKELIN: Radiometric calibration, validation and correction of multispectral photogrammetric imagery. Kirkkonummi 2013. 160 pages.
149. XINLIAN LIANG: Feasibility of Terrestrial Laser Scanning for Plotwise Forest Inventories. Kirkkonummi 2013. 150 pages.
150. EERO AHOKAS: Aspects of accuracy, scanning angle optimization, and intensity calibration related to nationwide laser scanning. Kirkkonummi 2013. 124 pages.
151. LAURA RUOTSALAINEN: Vision-Aided Pedestrian Navigation for Challenging GNSS Environments. Kirkkonummi 2013. 180 pages.
152. HARRI KAARTINEN: Benchmarking of airborne laser scanning based feature extraction methods and mobile laser scanning system performance based on high-quality test fields. Kirkkonummi 2013. 346 pages.
153. ANTERO KUKKO: Mobile Laser Scanning – System development, performance and applications. Kirkkonummi 2013. 247 pages.
154. JORMA JOKELA: Length in Geodesy – On Metrological Traceability of a Geospatial Measurand. Kirkkonummi 2014. 240 pages.

Finnish Geodetic Institute
P.O. Box 15
FI-02431 Masala
Finland
http://www.fgi.fi